

# Microbial Electrosynthesis of Biochemicals

*Innovations on biocatalysts, electrodes and ion-exchange  
for CO<sub>2</sub> supply, chemicals production and separation*



Suman Bajracharya



# **Microbial Electrosynthesis of Biochemicals**

*Innovations on biocatalysts, electrodes and ion-exchange for  
CO<sub>2</sub> supply, chemicals production and separation*

**Suman Bajracharya**

## **Thesis committee**

### **Promotor**

Prof. Dr C.J.N. Buisman

Professor of Biological Recovery and Re-use Technology

Wageningen University

### **Co-promotors**

Dr D.P.B.T.B. Strik

Assistant professor, Sub-department of Environmental Technology

Wageningen University

Dr D. Pant

Senior Researcher, Separation and conversion Technology Unit

Flemish Institute for Technological Research (VITO), Mol, Belgium

### **Other members**

Prof. Dr J.H. Bitter, Wageningen University

Dr C. Picioreanu, Delft University of Technology

Dr A.W. Jeremiasse, Magneto Special Anodes B.V., Schiedam

Prof. Dr S. Puig Broch, University of Girona, Spain

This research was conducted under the auspices of the Research school for Socio-Economic and Natural Sciences of the Environment (SENSE).

# **Microbial Electrosynthesis of Biochemicals**

*Innovations on biocatalysts, electrodes and ion-exchange for  
CO<sub>2</sub> supply, chemicals production and separation*

**Suman Bajracharya**

## **Thesis**

submitted in fulfilment of the requirements for the degree of doctor

at Wageningen University

by the authority of the Rector Magnificus

Prof. Dr A.P.J. Mol,

in the presence of the

Thesis Committee appointed by the Academic Board

to be defended in public

on Friday 23 September 2016

at 4 p.m. in the Aula.

Suman Bajracharya

Microbial Electrosynthesis of Biochemicals

Innovations on biocatalysts, electrodes and ion-exchange for CO<sub>2</sub> supply, chemicals production and separation

184 pages.

PhD thesis, Wageningen University, Wageningen, NL (2016)

With references, with summary in English

ISBN 978-94-6257-853-1

DOI <http://dx.doi.org/10.18174/385426>

*For my Mother*





## Table of contents

|   |           |  |     |
|---|-----------|--|-----|
| 1 | Chapter 1 | Introduction   | 9   |
| 2 | Chapter 2 | Carbon dioxide reduction by mixed and pure cultures in microbial electrosynthesis using an assembly of graphite-felt and stainless steel as a cathode              | 21  |
| 3 | Chapter 3 | Application of gas diffusion biocathode in microbial electrosynthesis from carbon dioxide  | 45  |
| 4 | Chapter 4 | Long-term operation of bioelectrochemical reduction of CO <sub>2</sub> from mixed culture avoiding methanogenesis  | 71  |
| 5 | Chapter 5 | <i>In situ</i> acetate separation in microbial electrosynthesis (MES) using ion-exchange resins  | 91  |
| 6 | Chapter 6 | An overview on emerging bioelectrochemical systems (BESs): Technology for sustainable energy, waste remediation, resource recovery, chemical production and beyond | 105 |
| 7 | Chapter 7 | Syntheses, discussion and perspectives   | 141 |
|   |           | Summary  | 161 |
|   |           | Supplementary information  | 165 |



---

C  
H  
A  
P  
T  
E  
R

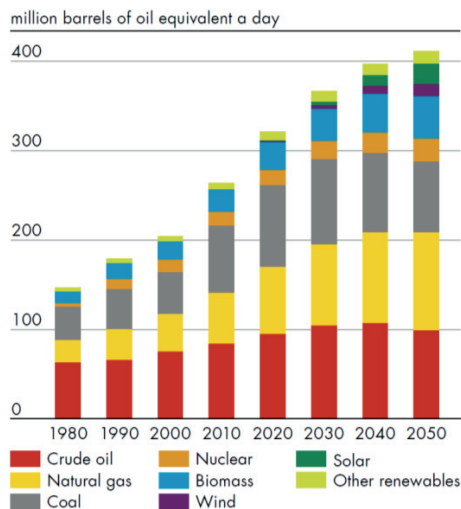


**Introduction**

---

## 1.1 Humans impact the planet

Mankind has been effectively manipulating the natural world to the remarkable extent for our needs on food, water, fuels, other chemicals, building materials and more. This intervention has resulted in rapid economic growth and a population boom in the last few centuries. The world population grew from 2 billions in 1990 to 7.3 billions in 2015 [1]. A large amount of fossil fuel based energy and raw materials consumption is supporting the current global economy. The worldwide energy use has increased from 256 EJ (Exajoule,  $10^{18}$  J) per year in 1973 to 567 EJ per year in 2013 and is projected to reach 623-710 EJ per year in 2035 [2]. In the current scenario, fossil fuels contribute to 80% of the world's energy demands and will continue to dominate the energy consumption pattern in coming years. As per the predictions, the fossil fuels would still account for 75% of global energy demand in [3, 4]. As per the projections made for 2050, energy derived from fossil fuels will continue to be a major part of global energy consumption, reaching up to 65% (Figure 1.1) [5]. The economic growth and increasing energy consumption have imposed accelerating loads on the ecological goods and services. Earth's climate, its terrestrial surface, and the functioning of its ecosystems are all in a state of change. The ecosphere—land surface, atmosphere, freshwater, and oceans—is under threat by anthropogenic activities. The current and predicted change to Earth's climate, its terrestrial surface, and the functioning of its ecosystems is destructing our current and future access to the basic requirements of life—safe water, clean air, adequate nutrition, and protection from infectious disease and natural disasters.



**Figure 1.1** : Global energy demand projected to 2050 [5].

## 1.2 Fossil resource use causes environmental pollutions and affects human health

The use of fossil resources (coal, oil, and natural gases) results in pollution and greenhouse gas (GHG) emissions. During the harvest of oil, spills are made [e.g. Deepwater horizon oil spill [6]] and large polluted water fractions are produced [e.g. by tar sands mining [7]] which affect the local environment. The combustion of fossil-based fuels without appropriate filters further pollutes the environment emitting NO<sub>x</sub>, SO<sub>x</sub> and particulate matters which create detrimental effects on the environment and the human health. Also during the production of chemicals using fossil resources, pollutants—for instance, acid waste gases and chlorinated organics—are often released. A link to this

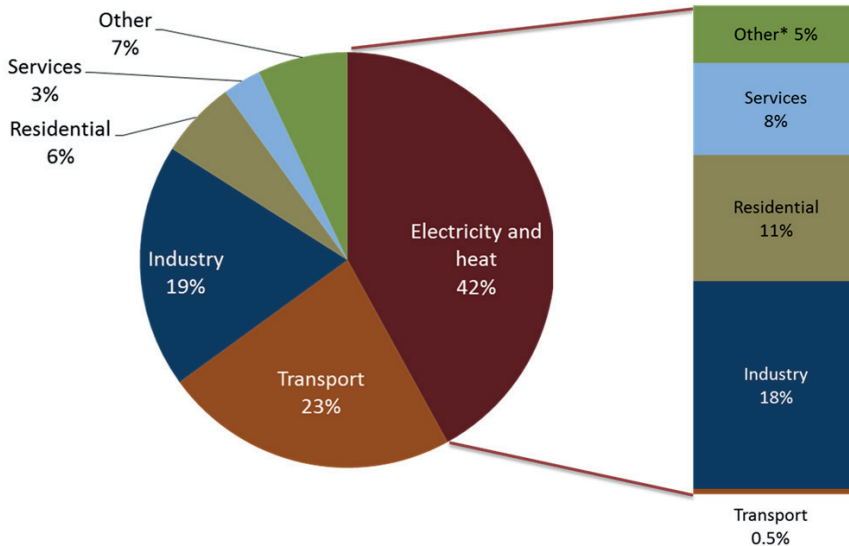
threatening effect is supported by the estimation of World Health Organization (WHO) reporting 7 million deaths attributed by air pollution in 2012 [8].

### ***1.3 Carbon dioxide release and fossil resource use are ongoing global concerns***

Carbon dioxide (CO<sub>2</sub>) is naturally available in earth's atmosphere and it balances the ecosystem via series of processes in the carbon cycle. However, growing population and increasing energy demand have been attributing to the alteration of the natural cycles of greenhouse gases (GHGs) including CO<sub>2</sub>.

A steadily increasing concentration of atmospheric CO<sub>2</sub> was observed from 315 ppm in 1957 to 390.5 ppm in 2011 [9]. The CO<sub>2</sub> levels in the air have increased by about 40%, as industries ramped up the emissions (preindustrial level, ~280 ppm) [10]. While a sustained rise of 80 ppm was seen between 11,000 and 17,000 years ago, the rise in CO<sub>2</sub> revealed the biggest leap just recently, showing 200 times faster CO<sub>2</sub> rise [10, 11]. In fact, very recently on 8 March 2016, the National Oceanic and Atmospheric Administration (NOAA) recorded the highest levels of CO<sub>2</sub> at 403.94 ppm, ever since the records are being kept [10]. The accumulation of CO<sub>2</sub> causes absorption and re-emission of heat, which attributes to the additional warming of the planet. The consequences of CO<sub>2</sub> rise in global warming was marked by the record-breaking temperatures in 2015, the hottest year on record till date [11].

The actual increase in fossil fuel use results in the rise of CO<sub>2</sub> concentration in the earth's atmosphere. Also contributing to this are the changes in land-use practices (predominantly deforestation and increasing agricultural lands) [12]. Intergovernmental Panel on Climate Change (IPCC) revealed the significant rise in the trend of global emissions of CO<sub>2</sub> from fossil fuels since 1900 [13]. The report shows that fossil fuel combustion and industrial processes associated CO<sub>2</sub> emissions accounted for 78% of the increase in total GHG emissions from 1970 to 2010. The global fossil fuel based carbon emission estimation in 2013 was 9,776 million metric tons of carbon. From 1751 to 2013, approximately 392 billion metric tons of CO<sub>2</sub>-C have been contributed to the atmosphere from the fossil fuels consumption and cement production, half of which are added after the 1980s [14]. Fossil fuel use for electricity and heat production, and in transport sector emits nearly two-third of global CO<sub>2</sub> emission in 2013 (Figure 1.2) [15].



\* Other includes agriculture/forestry, fishing, energy industries other than electricity and heat generation, and other emissions not specified elsewhere

**Figure 1.2:** Sector-wise distribution of world CO<sub>2</sub> emission (32.2 Gt CO<sub>2</sub>) in 2013 [source: IEA [15]]. Column (on right) shows the allocation of electricity and heat to end-use sectors.

Due to the further depletion and uneven distribution of fossil fuel resources, energy insecurity and economic instability will likely continue in some of the crude oil producing and importing countries [16, 17]. The observed environmental destructions and reported social threats underline that developments are needed to make a sustainable planet feasible.

#### **1.4 Renewable resource use is environmentally and human-friendly**

For the reasons including environmental destructions, alternatives resources for energy and fuel supply are being used in increasing trend. The concept of biorefinery has been put forward to promote “biobased economy” that utilizes renewable biomass resources to produce fuels, power, heat, and value-added chemicals in a circular economy model fostering reuse and recycling of materials.

Biomass feedstock, mainly comprising dedicated energy crops and biomass wastes, is a readily available source that can partly replace the current dependency on fossil resources by supplying a renewable feedstock for chemicals and fuel. Besides these conventional sugar based crops, the unstable organic wastes including sewage sludge, municipal solid waste, industrial and agricultural wastes hold a large stock of biomass resources. Additionally, CO<sub>2</sub> is also a potential source for renewable resource generation, although energy intensive processes are required to make it a useful energy carrier.

Renewable sources can provide secure and sustainable energy & fuel, being readily available and constantly replenished. Renewable energy and materials are environmentally/human-friendly, potentially without any environmental damage and support the prospects for socio-economic development, secure supplies and climate

---

change mitigation. The renewable sources also attribute to negate the environmental and health impacts, since the utilization does not result in pollution and GHG emissions. Recent advancements in renewable energy harvesting technologies such as photovoltaic, wind turbine, hydro and biomass have made it technically possible to harvest 1.9 -6.3 times more energy than the global energy demand from the renewable sources [18]. The prediction reveals that the share of renewable electricity will rise from 19% in 2009 to 50-60% in 2050 [19].

### **1.5 Biomass usage encounters huge challenges**

Biomass is a renewable resource produced via photosynthesis which already provides food and many other services to our society, including biochemicals and biofuels. Currently, a yearly production of 50 million tons of biochemicals (excluding biofuels) that represents 10% of the global chemical production [20]. It is targeted to replace 25-30 % of petroleum-based production of chemicals by bioenergy alternatives by the year 2030 in China, USA, Canada and The Netherlands [20, 21]. However, an extensive use of biomass is required to meet these relatively ambitious expectations.

The global biomass used for renewable energy currently accounts for 50 EJ yr<sup>-1</sup>, while that for food, fodder and feed amounts to 219 EJ yr<sup>-1</sup>. For the transition of energy supply to renewable resources by 2050, the deployment level of biomass to 100-300 EJ yr<sup>-1</sup> is predicted [18]. This bioenergy goal is technically possible once developments are made on plant productivity improvement, use of marginal/degraded lands, use of surplus forestry resources and increase on the usage of residues of agriculture and organic wastes. Furthermore, future policy schemes should adopt the practices of good land use governance and improved agricultural management, considering water limitations, biodiversity protection, soil degradation and competition with food.

The biggest challenge of using biomass as a supply for renewable energy is related to increased food price. The primary source of biomass (first generation feed such as maize and edible oil seeds) is not, in consensus, seen as a sustainable option, while it intrinsically competes with the food chain provisions. Even more, as it is expected that the food prices will rise due to more renewable fuels and chemicals, only fewer people may have access to the affordable food. Nowadays, already an uneven distribution of food exists; so it is of ethical concern whether food should be used as a resource for fuels and other chemicals or that it should support those who do not have access to sufficient food.

Also, the requirement of more arable land and huge amount of water and nutrients for the biomass-based production processes creates all kinds of controversies on the sustainability of biofuels and biochemicals [22]. While corn plantation for bioethanol production is associated with increased food/feed prices [23], the palm oil (for biodiesel production) is linked with deforestation. Deforestation is associated with the addition of CO<sub>2</sub> and GHG, global warming, threats to biodiversity and often spread of infectious diseases. According to the Roundtable on Sustainable Palm Oil (RSPO), 3.5 million hectares of forest land loss was observed during large-scale oil palm expansion between 1990 and 2010 in Indonesia, Malaysia, and Papua New Guinea [24, 25]. The current developments within the biobased sector embrace the avoidance of primary land use, valorization of residues and utilization of abandoned lands.

Lignocellulosic biomass and inedible oilseed crops or algal oil and even CO<sub>2</sub> could provide alternative feedstock for the production of drop-in fuel and commodity chemicals. Different strategies are proposed to convert the lignocellulosic biomass mixture into valuable products. Several routes are explored at the moment. Thermochemical (pyrolysis/thermal cracking) and biochemical (fermentation/anaerobic digestion) conversions are the foundations of the so-called 'syngas', 'ethanol' and 'carboxylate platform' which are the building block for further processing.

---

Evidently, Agro-forest based biomass can contribute to more clean fuel and other chemical productions. But, it will not probably be the only way to build the renewable feedstocks. The quest for a technology that can efficiently transfer CO<sub>2</sub> into biofuels and biochemicals is crucial for the bioeconomy. The green electricity-driven bioproduction is a promising technology to address the shortcomings of agriculture driven biofuel technologies, for instance, issues regarding land use [26, 27], threats to biodiversity [28], increasing food prices [29] and increased pressure on scarce water resources. Unlike the production of organics from agricultural technology that requires large quantities of water [30], the green electricity-driven bioproduction uses limited amount of fresh water and therefore, is a hopeful technology over agriculture to produce organics.

### ***1.6 Renewable electricity as a driving force enables new opportunities to produce fuels and chemicals***

The declining cost of equipment and installation for renewable energy harvesting is a major driver for its continued growth. Moreover, financing sectors have offered low-interest rates on renewable energy investment. Global investments in renewable energy set highest record of approximately \$286 billion in 2015 (more than six times as compared in 2004), especially with solar photovoltaics (PV) and wind turbines [31, 32]. Today, several renewable electricity technologies are among the most cost-competitive options for power generation. Furthermore, the doubling of shares of renewables on the global energy supply (from 18 % in 2014 to 36 % in 2030) is sought to meet the climate-change targets and sustainable development goals of the countries [32].

Electricity is a common energy carrier from renewable sources. Hence, renewable electricity production is foreseen to be abundant in near future. In such scenario, the whole energy system requires a transition to electricity as the main energy carrier. Nonetheless, renewable electricity is produced intermittently by most of the renewable sources. As a consequence electricity needs to be stored when the production is more than the demand and this storage should be supplied back when there is no or insufficient production. Additionally, electricity cannot be integrated directly into the current fuel/chemical based system. Currently, biomass is the only source of renewable fuels/chemicals but still the production of fuel from biomass is limited due to lower efficiencies and competition with food/feed. Thus, a technology is required that converts electricity directly to fuel and chemicals.

### ***1.7 Microbial Electrosynthesis allows biocatalyst and electrode to utilize CO<sub>2</sub> and electricity***

Bioelectrochemical system (BES) is a bioreactor technology originally developed for the concurrent wastewater treatment and electricity production using the ability of electrochemically active microorganisms to transport electron to/from the solid electrode. Research in recent years has broadened the utility of BESs to much more complex processes such as chemical synthesis, bioremediation, and resource recovery. Uniquely, BESs have also been able to produce value-added fuels and chemicals from low-value waste or CO<sub>2</sub> with a small input of electrical power. Such a production system is also known as Microbial Electrosynthesis (MES) in which cathodic biocatalysts reduce the available terminal electron acceptor to produce value-added products [33].

In the present scenario of renewable energy development, renewable electricity from solar photovoltaics and wind-turbines has become prudently available but due to the intermittent nature of sun and wind energy, the storage of electricity is required during the off-hours. BES provides a way to store the electricity as chemicals, based on the innate ability of electroactive microbes to incorporate electricity into the bioproduction of organic compounds, also known as bioelectrosynthesis. The process of bioelectrosynthesis can be highly specific, depending on the biocatalyst catalyzing the redox reaction and the terminal electron acceptor involved in the process, along with the



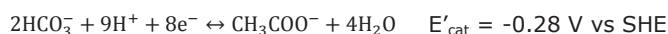
electrochemically active redox mediators or suitable reducing equivalents. Bioelectrochemical reduction of CO<sub>2</sub> is a specific application of autotrophic bioproduction technology which is electricity-driven, CO<sub>2</sub> negative and independent of biomass [33].

As such, MES is prospected as an alternative strategy to capture electrical energy in the covalent chemical bonds of organic products. Several studies have reviewed and highlighted different aspects of MES including microbiology, technology, and economics as well as understanding the metabolic routes involved, electron transfer mechanisms and practical considerations [33–35].

### **1.8 Principles of Microbial electrosynthesis from CO<sub>2</sub>**

The discovery of microbial ability to catalyze reduction reactions by accepting the electron from cathode has developed an emerging research on the application of biocathode based BES. The MES is one of the exciting application of biocathode based BES for the bioproduction of organics powered by the electricity [33]. The electrons at the cathode serve as the energy source for microbial reduction. Anaerobic metabolisms of homoacetogenic bacteria are known for the metabolic conversion of CO<sub>2</sub> and H<sub>2</sub> to acetate and other multi-carbon compounds.

As such, homoacetogenic biocatalysts are employed in MES to reduce CO<sub>2</sub> to multi-carbon organic compounds using the electrons or reductants derived from the cathode. Nevin et al. [36] presented the first proof of concept of MES as a microbial catalysis of CO<sub>2</sub> electro-reduction to multi-carbon organic compounds. An oxidation reaction at the anode produces protons and electrons for the cathodic reduction and an electric power source drives the electrons from anode to cathode through an external circuit (Figure 1.3). The electrons and proton produced at the anode are transported to the cathode by applying external electrical energy. At the cathode, bioelectrochemical reduction of CO<sub>2</sub> takes place through the microbial electrocatalysis. Under the homoacetogenic microbial electrocatalysis, acetate is produced from CO<sub>2</sub> (here HCO<sub>3</sub><sup>-</sup>) reduction at the biological condition.

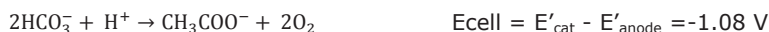


(versus standard hydrogen electrode)

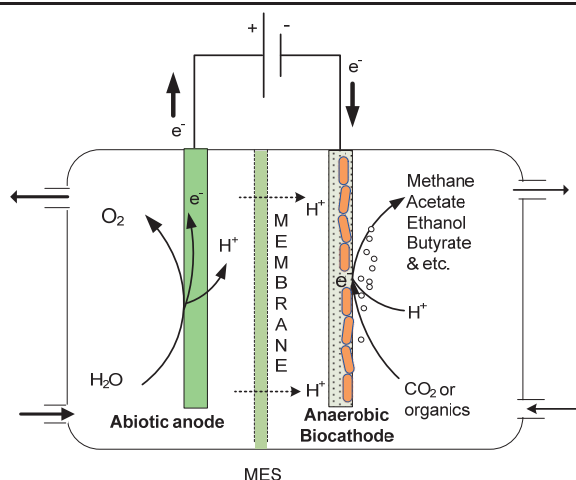
In case, water oxidation at the anode is considered producing proton and electrons according to



Overall reaction of



which is the minimum voltage required. The negative cell voltage for the reactions means energy needs to be applied.



**Figure 1.3:** Principle of microbial electrosynthesis at the cathode.

Several lithoautotrophs are reported for the metabolic reduction of  $\text{CO}_2$  to acetate and other multi-carbon compounds with hydrogen as an energy source [37, 38]. The anaerobic conversion of  $\text{CO}_2$  &  $\text{H}_2$  to acetate by acetogens follows the Wood/Ljungdahl or acetyl-CoA pathway [39, 40]. In case of bioelectrochemical reduction, there is no need for the external supply of hydrogen as the microbe can either directly get the protons from electrolyte and electrons from the cathode or the reaction could be mediated via hydrogen produced in-situ. When homoacetogenic bacteria catalyze the  $\text{CO}_2$  reduction reaction, the major product of  $\text{CO}_2$  reduction is mainly acetate. However, the products can extend to alcohols and other carboxylates. In another case, if methanogens are present then methane ( $\text{CH}_4$ ) is produced ultimately.

### 1.9 Objectives and outline of this thesis

At present the concept of MES is nascent and the production of biochemicals in MES from  $\text{CO}_2$  is at the proof of concept stage. In this regard, understanding of the reaction mechanisms of microbial electrocatalysis and decrypting key features responsible for the observed efficiency should be beneficial. Systematic investigations are required in order to design more efficient biocatalysts and compatible electrodes for  $\text{CO}_2$  utilization.

This thesis aims to bring innovation and insights on microbial electrosynthesis biocatalysts, electrodes and ion exchange resins for the supply of  $\text{CO}_2$ , the production of chemicals and the eventual extraction of products. A pure and mixed bacterial culture has been used as biocatalysts for  $\text{CO}_2$  reduction. Specifically, an enriched mixed culture has been developed from the biological sources which could reduce  $\text{CO}_2$  effectively. An exploration on  $\text{CO}_2$  based MES and its emerging prospects have been presented in this thesis. Adjustment on biocatalyst and electrodes has been sought for the establishment of a complete MES system for production and separation of organics from  $\text{CO}_2$ .

The chapters of the thesis are outlined (Figure 1.4) according to the objectives in various chapters:

#### To develop MES from $\text{CO}_2$ using pure and mixed culture

Chapter 2 elucidates the concept of bioelectrochemical  $\text{CO}_2$  reduction using a mixed culture from a biological source and also using a pure culture of homoacetogen. The

concept of acetate/ethanol production from CO<sub>2</sub> with a specific interest to the impact of hydrogen production with carbon felt-stainless steel mesh assembly as a cathode was presented. Competitive side reactions including CH<sub>4</sub> production was described as one of the main reasons behind the lower efficiency of acetate production from CO<sub>2</sub>.

**To develop biocompatible electrode capable of CO<sub>2</sub> capturing and reduction**

Chapter 3 deals with the way of supplying gaseous CO<sub>2</sub> to the MES system for an effective microbial catalysis. Gas diffusion electrode (GDE) was applied as CO<sub>2</sub> diffusing biocathode. The distinguishing performances and compatibility of GDE over the conventional submerged technology for the biocathodic CO<sub>2</sub> reduction have been described.

**To develop stable CO<sub>2</sub> reducing biocatalyst avoiding methanogen from mixed culture**

Chapter 4 deals with the shaping of the cathodic microbiome towards multi-carbon biochemical production. It involved upgrading and development of a stable and robust biocathode using mixed culture isolated from an anaerobic biological source. Suppression of methanogenesis and selective enrichment for acetogenesis to improve acetate production was described to allow solely production of liquid chemicals.

**To demonstrate an MES system comprising production and separation of organic compounds from CO<sub>2</sub>**

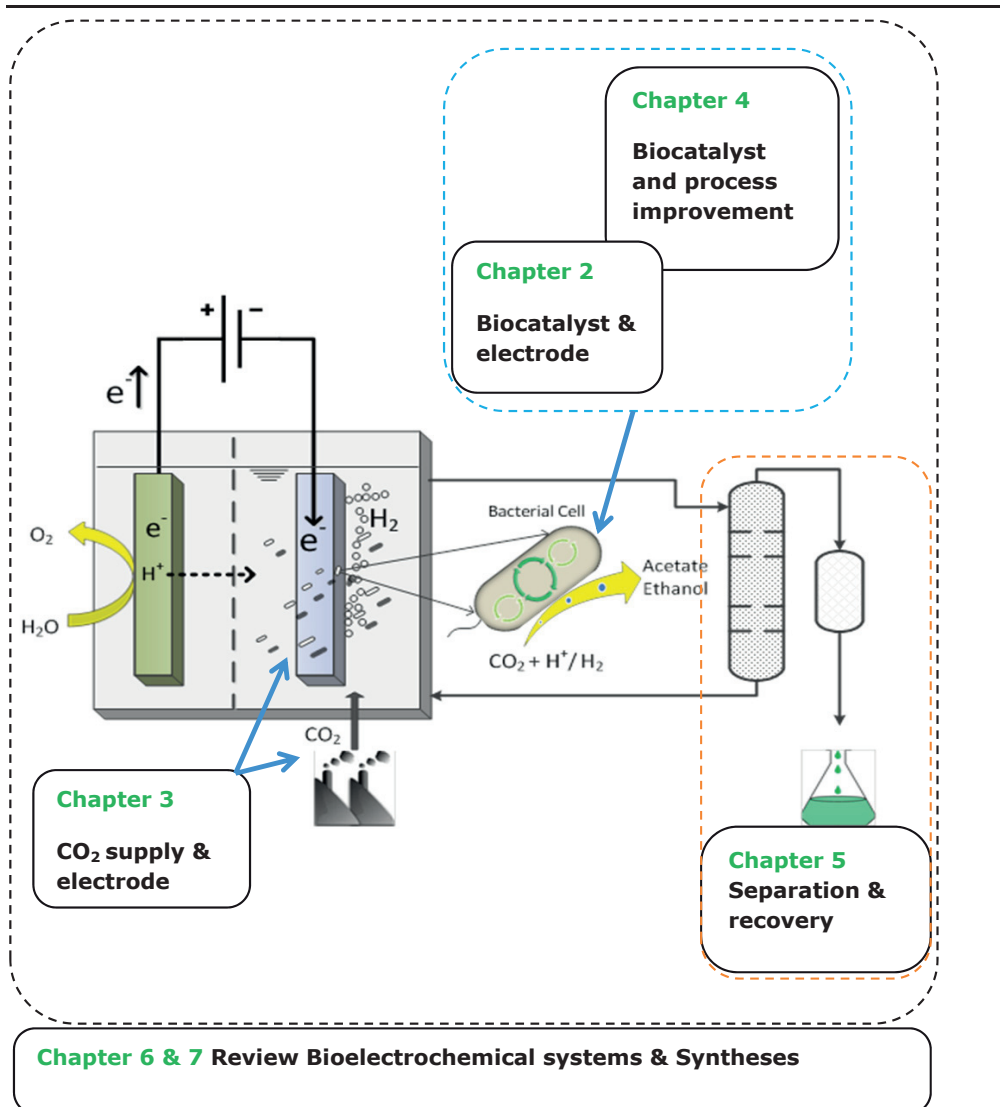
Chapter 5 deals with the research challenges regarding the product recovery. Construction of a continuous reactor with an integrated anion exchange resins extraction system was demonstrated for the substantial production and recovery of acetate from CO<sub>2</sub> reduction.

**To provide overview on potential application of BES with new development in MES**

Chapter 6 discusses the recent developments that have been made in BESs in the light of newer MES concept and emphasizes on the potential applications of BES beyond electricity generation.

**To provide a state-of-art on MES and its needed developments as well as its future applications**

Finally, Chapter 7 synthesizes the thesis work and envisions a full-scale technology for CO<sub>2</sub> reduction in Microbial Electrosynthesis. Furthermore, it provides discussions of all the results presented in this thesis. On the basis of the outcome, future applications and new perspectives of MES are presented.



**Figure 1.4:** Schematic outline of the thesis.

## References

1. United Nations Department of Economic and Social Affairs Population Division (2015) World Population Prospects: The 2015 Revision, Key Findings and Advance Tables. Working Paper No. ESA/P/W.P.241. New York
2. IEA (2015) Key World Energy Statistics 2015. doi: 10.1787/9789264039537-en
3. IEA (2013) World Energy Outlook 2013. Paris Cedex, France
4. Global CCS Institute (2014) The global Status of CCS | 2014. Melbourne, Australia
5. Royal Dutch Shell (2012) Sustainability Report 2012.
6. Schrope M (2011) Oil spill: Deep wounds. *Nature* 472:152–4. doi: 10.1038/472152a
7. Schindler D (2010) Tar sands need solid science. *Nature* 468:499–501. doi: 10.1038/468499a
8. WHO (2014) 7 million premature deaths annually linked to air pollution. In: News Release. <http://www.who.int/mediacentre/news/releases/2014/air-pollution/en/>. Accessed 5 May 2016
9. Ciais P, Sabine C, Bala G, et al (2013) Carbon and Other Biogeochemical Cycles. In: Stocker TF, D. Qin, G.-K. Plattner, M. Tignor, S.K. Allen, J. Boschung, A. Nauels, Y. Xia, V. Bex and P.M. MiddleStocker, T.F., D. Qin, G.-K. Plattner, M. Tignor, S.K. Allen, J. Boschung, A. Nauels, Y. Xia VB and PMM (eds) *Clim. Chang. 2013 - Phys. Sci. Basis. Contrib. Work. Gr. I to Fifth Assess. Rep. Intergov. Panel Clim. Chang.* Cambridge University Press, Cambridge, United Kingdom and New York, NY, USA, pp 465–570
10. Dlugokencky E, Tans P (2016) Trends in Atmospheric Carbon Dioxide. In: NOAA/ESRL. [www.esrl.noaa.gov/gmd/ccgg/trends/global.html](http://www.esrl.noaa.gov/gmd/ccgg/trends/global.html). Accessed 5 May 2016
11. Pashley A (2016) CO<sub>2</sub> levels make largest recorded annual leap, NOAA data shows. *Guard*.
12. National Research Council (2010) *Advancing the Science of Climate Change*. National Research Council. The National Academies Press, Washington, DC, USA
13. IPCC (2014) *Climate Change 2014: Synthesis Report. Contribution of Working Groups I, II and III to the Fifth Assessment Report of the Intergovernmental Panel on Climate Change*. IPCC, Geneva, Switzerland
14. Boden TA, Marland G, Andres RJ (2016) Global, Regional, and National Fossil-Fuel CO<sub>2</sub> Emissions. Carbon Dioxide Information Analysis Center, Oak Ridge National Laboratory, U.S. Department of Energy. doi: 10.3334/CDIAC/00001\_V2016
15. IEA (2015) Key Trends in CO<sub>2</sub> Emissions: Excerpt from CO<sub>2</sub> Emissions Fuel Combustion.
16. Khatib H, Barnes A, Chalabi I, et al (2000) Energy Security. In: *World Energy Assess. Energy Chall. Sustain.* pp 111–131
17. Van de Graaf T, Verbruggen A (2015) The oil endgame: Strategies of oil exporters in a carbon-constrained world. *Environ Sci Policy* 54:456–462. doi: 10.1016/j.envsci.2015.08.004
18. IPCC (2011) *Renewable Energy Sources and Climate Change Mitigation. Special Report of the Intergovernmental Panel on Climate Change*.
19. IEA (2012) *Technology Roadmap Bioenergy for Heat and Power*. Paris Cedex, France
20. IEA Bioenergy (2012) *Bio-based Chemicals, Value Added Products from Biorefineries*.
21. Patel M, Manuela K, Dornburg V, et al (2006) Medium and Long-term Opportunities and Risks of the Biotechnological Production of Bulk Chemicals from Renewable Resources - The Potential of White Biotechnology The BREW Project. Final report Prepared under the European Commission's GROWTH Programme (DG . doi: 10.1111/j.1442-8903.2004.00172.x
22. Naik SN, Goud V V., Rout PK, Dalai AK (2010) Production of first and second generation biofuels: A comprehensive review. *Renew Sustain Energy Rev* 14:578–597.
23. Peplow M (2014) Cellulosic ethanol fights for life. *Nature* 507:152–153.
24. Schouten G, Glasbergen P (2011) Creating legitimacy in global private governance: The case of the Roundtable on Sustainable Palm Oil. *Ecol Econ* 70:1891–1899. doi: 10.1016/j.ecolecon.2011.03.012
25. World Wide Fund for Nature (2016) Palm oil and deforestation. [http://www.wwf.org.au/our\\_work/saving\\_the\\_natural\\_world/forests/palm\\_oil/palm\\_oil\\_and\\_deforestation/](http://www.wwf.org.au/our_work/saving_the_natural_world/forests/palm_oil/palm_oil_and_deforestation/). Accessed 12 May 2016
26. Larson D (2008) Biofuel production technologies: status, prospects and implications for trade and development. *United Nations Conf Trade Dev* 1–41.
27. FAO (2008) *Soaring Food Prices: Facts, Perspectives, Impacts and Actions Required*. Information document (HLC/08/INF/1) prepared for the High-Level Conference on World Food Security: the

- Challenges of Climate Change and Bioenergy, Rome, 3-5 June 2008. doi: 10.1525/jer.2008.3.1.toc
28. Fargione J, Hill J, Tilman D, et al (2008) Land clearing and the biofuel carbon debt. *Science* (80- ) 319:1235–8. doi: 10.1126/science.1152747
  29. OECD-FAO (2008) OECD-FAO Agricultural Outlook 2008-2017, Summary in English.
  30. FAO (2008) Opportunities and challenges of biofuel production for food security and the environment in Latin America and the Caribbean. Document prepared for the 30th Session of the FAO Regional Conference for Latin America and the Caribbean, held in Brasilia, Brazil.
  31. Frankfurt School-UNEP Centre/BNEF (2016) Global Trends in Renewable Energy Investment 2016.
  32. IRENA (2016) REmap: Roadmap for a Renewable Energy Future. Abu Dhabi
  33. Rabaey K, Rozendal RA (2010) Microbial electrosynthesis — revisiting the electrical route for microbial production.pdf. *Nat Rev Microbiol* 8:706–16. doi: 10.1038/nrmicro2422
  34. Desloover J, Arends JB a, Hennebel T, Rabaey K (2012) Operational and technical considerations for microbial electrosynthesis. *Biochem Soc Trans* 40:1233–8. doi: 10.1042/BST20120111
  35. Rabaey K, Girguis P, Nielsen LK (2011) Metabolic and practical considerations on microbial electrosynthesis. *Curr Opin Biotechnol* 22:371–7. doi: 10.1016/j.copbio.2011.01.010
  36. Nevin KP, Woodard TL, Franks AE, et al (2010) Microbial Electrosynthesis: Feeding Microbes Electricity To Convert Carbon Dioxide and Water to Multicarbon Extracellular Organic. *MBio* 1:e00103–10–. doi: 10.1128/mBio.00103-10.Editor
  37. Wood HG (1991) Life with CO or CO<sub>2</sub> and H<sub>2</sub> as a source of carbon. *FASEB* 5:156–163.
  38. Berg I a, Kockelkorn D, Ramos-Vera WH, et al (2010) Autotrophic carbon fixation in archaea. *Nat Rev Microbiol* 8:447–60. doi: 10.1038/nrmicro2365
  39. Drake HL, Daniel SL (2004) Physiology of the thermophilic acetogen *Moorella thermoacetica*. *Res Microbiol* 155:422–36. doi: 10.1016/j.resmic.2004.03.003
  40. Ljungdahl LG (1986) The autotrophic pathway of acetate synthesis in acetogenic bacteria. *Annu Rev Microbiol* 40:415–450.

---

C  
H  
A  
P  
T  
E  
R

2

**Carbon dioxide Reduction by Mixed and Pure Cultures  
in Microbial Electrosynthesis Using an Assembly of  
Graphite-felt and Stainless Steel Mesh as a Cathode**

This chapter is *published as*

Bajracharya, S., ter Heijne, A., Dominguez, X., Strik, D.P.B.T.B., Vanbroekhoven, K., Buisman, C.J.N., Pant, D. (2015). *CO<sub>2</sub> reduction by mixed and pure cultures in microbial electrosynthesis using an assembly of graphite felt and stainless steel as a cathode*. *Bioresour. Technol.* doi:10.1016/j.biortech.2015.05.081

---

**Abstract**

Carbon dioxide (CO<sub>2</sub>) reduction to multi-carbon compounds at the cathode using chemolithoautotrophs is an emerging application of microbial electrosynthesis (MES). In this study, CO<sub>2</sub> reduction in MES was investigated at hydrogen evolving potentials, separately by a mixed-culture and *Clostridium ljungdahlii*, using a graphite felt and stainless steel mesh assembly as a cathode. The mixed-culture reactor produced acetate at the maximum rate of 1.3 mM.d<sup>-1</sup>, along with methane and hydrogen at -1.1 V<sub>Ag/AgCl</sub>. Over 160 days of run-time in four fed-batches, 26% of bicarbonate was converted to acetate between day 28 to 41, whereas in the late batches, methane production prevailed. Out of 45 days of run-time in the *C. ljungdahlii* reactor, 2.4 mM.d<sup>-1</sup> acetate production was achieved at -0.9 V<sub>Ag/AgCl</sub> in batch 1. Simultaneous product degradation occurred when the mixed culture was not selectively enriched. Hydrogen evolution is potentially the rapid way of transferring electrons to the biocatalysts for higher bioproduction rates.

**Keywords:** Microbial electrosynthesis, CO<sub>2</sub> reduction, Biocathode, Hydrogen evolution, Bioproduction



---

## 2.1 Introduction

Bioelectrochemical systems (BESs) offer unique possibilities for the clean and efficient production of high-value chemicals and fuels from low-value wastes or even carbon dioxide (CO<sub>2</sub>) using microorganisms as biocatalysts [1, 2], such systems are referred to as microbial electrosynthesis (MES). CO<sub>2</sub> can be metabolically reduced to multi-carbon organic compounds by microbes using electrons or reducing equivalents derived from the cathode in MES. An oxidation reaction at the anode produces protons and electrons for the cathodic reduction and an electric power source drives the electrons from anode to cathode through an external circuit.

Several lithoautotrophs have been reported for the metabolic reduction of CO<sub>2</sub> and carbon monoxide (CO) to acetate and other multi-carbon compounds with hydrogen (H<sub>2</sub>) as an energy source [3]. The anaerobic conversion of CO<sub>2</sub> and H<sub>2</sub> to acetate by acetogenic bacteria has been described to follow the reductive acetyl-CoA pathway [4]. In the case of MES, reduction at the biocathode occurs with the application of electric energy without the external supply of reductants such as hydrogen. The microbes involved in the biocathode can receive the electrons either directly from the cathode or indirectly via mediators or via H<sub>2</sub> produced by water electrolysis [2, 5]. Nevin et al. [1] described the first proof of principle of CO<sub>2</sub> reduction in microbial electrosynthesis using the acetogen *Sporomusa ovata*, which can use electrons directly from solid graphite electrodes for the reduction of CO<sub>2</sub> to produce acetate and small amounts of 2-oxobutyrate at -0.6 V<sub>Ag/AgCl</sub> cathode potential. In a succeeding study, a number of pure acetogenic cultures namely, *Sporomusa*, *Clostridia* and *Moorella* spp demonstrated microbial electrosynthesis by reducing CO<sub>2</sub> directly using electrons from the electrode at -0.6 V<sub>Ag/AgCl</sub> cathode potential [6]. Mixed microbial consortia from different sources have also been used in MES for CO<sub>2</sub> reduction to acetate [7–10]. In addition to the acetate, methane was also produced as a by-product when mixed culture inoculum was used without pre-enrichment [7, 8].

Thermodynamically, the threshold potential for hydrogen evolution at a cathode is -0.6 V<sub>Ag/AgCl</sub> at pH 7 under biological conditions but the threshold potential shifts further to more negative magnitudes due to the electrode overpotentials. When the bacteria reduce CO<sub>2</sub> at less negative cathode potential than that required for hydrogen evolution, direct electron uptake from electrode could potentially occur. Direct electron transfer at less negative cathode potential is interesting and ideally energy-efficient in bioelectrocatalysis [5] but the volumetric production rates and yields reported in such studies were fairly low. In particular, Nevin et al. [1] reported only ca. 0.17 mM.d<sup>-1</sup> acetate production with *S. ovata* at -0.6 V<sub>Ag/AgCl</sub> with ~1 L of catholyte spent under the continuous operation and Zaybak et al. [9] reported only 0.05 mM.d<sup>-1</sup> acetate production with enriched mixed culture at -0.6 V<sub>Ag/AgCl</sub>. Nickel nanoparticles coating on carbon based cathode improved the surface-based production rates in *S. ovata* MES systems [11, 12]. Projected surface area based acetate production was increased 2.3 times over untreated graphite cathode using Ni nanowire coating on graphite stick at -0.6 V<sub>Ag/AgCl</sub> [12]. However, the volumetric production rate remained only 1.13 mM.d<sup>-1</sup> even with the surface modifications.

For the upscaling of MES, an increase in the electrode/electrolyte ratio and a better acclimated biocathode can consequently increase the production rates. Indeed, application of a slightly more negative cathode potential for bioelectrochemical CO<sub>2</sub> reduction seemed to be favorable for higher conversion rates and titers [13]. Improvements in acetate production from CO<sub>2</sub> reduction were shown using mixed microbial communities at more negative cathode potentials along with H<sub>2</sub> and methane (CH<sub>4</sub>) production [7, 8]. At more negative potentials, proton reduction is favored producing H<sub>2</sub> which mediates the electron transfer to CO<sub>2</sub>. But, the evolved H<sub>2</sub> (in the gaseous phase) might not be completely available for biological CO<sub>2</sub> reduction and ultimately, escapes from the reactor, lowering the current and energy-input efficiencies

---

of the process. An optimization among the production rates, H<sub>2</sub> availability in the catholyte and efficiencies could be achieved by using a highly adsorbing cathode materials with lower H<sub>2</sub> evolution overpotential. Using granular carbon bed cathode, Marshall et al. [13] achieved highest acetate production rate of 17.25 mM.d<sup>-1</sup> at -0.79 V<sub>/Ag/AgCl</sub> along with H<sub>2</sub> production from methanogenesis suppressed autotrophic microbiomes when acclimated for long time in MES mode. Recently, Jourdin et al. [14] reported highest surface area based acetate production rate (1.3±0.2 mM.cm<sup>-2</sup>.d<sup>-1</sup>) with nanoweb reticulated vitreous carbon cathode at -1.05 V<sub>/Ag/AgCl</sub> but still the volumetric production rate remained only ~0.5 mM.d<sup>-1</sup>.

Generally, anaerobic biofilm development at negatively polarized biocathode, feeding only bicarbonate (HCO<sub>3</sub><sup>-</sup>) is difficult without the addition of H<sub>2</sub> and/or organic compounds [15]. Autotrophic growth of acetogens is occurring at the theoretical thermodynamic microbial metabolic limits [16]. Thus, electrochemical H<sub>2</sub> production at more negative cathode potential in an MES appears to hold the key for the stimulation of autotrophic metabolism of hydrogenotrophic acetogens in the biocathode [2]. Moreover, H<sub>2</sub> adsorbed on the electrode surface or dissolved in the electrolyte serves as electron shuttle in microbial CO<sub>2</sub> reduction. Most recently, the electrochemically produced H<sub>2</sub> driven MES has also been reported for producing high-value products such as butyrate from CO<sub>2</sub> reduction [17].

The main goal of this study is to investigate the application of lower H<sub>2</sub> evolution overpotential material like stainless steel in an assembly with graphite felt as cathodes in CO<sub>2</sub> reduction in MES using mixed and pure microbial cultures. The study also provides a comparative scenario of MES using mixed and pure bacterial cultures with respect to the competing biological processes involved and their response to the electrochemical H<sub>2</sub> evolution. The MES performances in long-term batch operations are evaluated based on current efficiencies, production rates, and current densities.

## **2.2 Materials and methods**

### **2.2.1 Bacterial cultivation**

For the pure culture experiments, a homoacetogenic bacterial strain *Clostridium ljungdahlii* DSM 13528 was purchased from the German Collection of Microorganisms and Cell Cultures DSMZ (Germany). *C. ljungdahlii* cells were cultivated anaerobically in serum bottles at 37 °C in DSMZ 879 medium for at least two weeks. Bacterial growth was attained with an optical density at 600 nm (OD<sub>600</sub>) reached 0.3–0.4 and the cultured strain was verified by microscopic tests. The bacterial strain was maintained viable by sub-culturing in every 2–3 months until the MES reactors were inoculated. The sub-culturing was done up to four batches.

The inoculum for mixed culture MES was obtained from an anaerobic culture of carboxydophilic actinomycete *Streptomyces thermospinisporus* DSM 41779 in serum bottles in Nutrient Buffer Acetate-Fumarate (NBAF) medium [18], which was mixed with the wastewater sludge available in the laboratory during the anaerobic sub-culturing. The mixed culture community was undefined but when cultivated on mineral medium (DSMZ 879 medium without fructose) with H<sub>2</sub>:CO<sub>2</sub> (80:20 v/v) gas in headspace at 1.5 bar, it grew to an OD<sub>600</sub> of 0.2 indicating the presence of CO<sub>2</sub> fixing strains. After two anaerobic sub-culturing in mineral media with H<sub>2</sub>:CO<sub>2</sub> (80:20) gas in headspace, the mixed culture was inoculated into the catholyte of MES reactor.

---

### 2.2.2 Bioelectrochemical reactor setups

#### a) Setup for mixed culture

For the experiments with mixed cultures, a double chambered bioelectrochemical cell was assembled using two circular cylindrical polyvinylidene difluoride (PVDF) rings each of which formed a compartment that can hold 16 ml electrolyte. The anode and cathode compartments were separated by a Fumasep FKB CEM PEEK<sup>®</sup> reinforced membrane. The counter electrode (anode) was a circular platinum sheet (10 cm<sup>2</sup>) laser-welded to a Titanium (Ti) plate current collector. The cathode was a 10 cm<sup>2</sup> circular piece of graphite felt with stainless steel mesh as a current collector (Supplementary information-Chapter 2 Figure SI-1). An assembly of graphite felt and stainless steel mesh was used because stainless steel worked not only as a current collector but also as a hydrogen evolving cathode. The cathode materials and membrane were first boiled to 70 °C for 1 hour in phosphate buffer solution (PBS) before using in the cell. Each compartment was connected to a separate electrolyte bottle by polyvinyl chloride (PVC) tubes (Ø 6/8) making a loop and a peristaltic pump (Watson Marlow 323U/D) was used for the recirculation of electrolyte in the loop. The recirculation rate was 90 mL·min<sup>-1</sup>. Anaerobic condition in the catholyte bottle was maintained by Nitrogen (N<sub>2</sub>) gas flushing and stirring with a magnetic stirrer (400 –500 rpm). An Ag/AgCl (3 M KCl, +205 mV vs SHE) reference electrode (REF321, Radiometer-Analytical) was connected in the cathode chamber and kept near the cathode. For the electrochemical measurement, the electrodes were connected to a Potentiostat (VMP3, Biologic Science Instruments, France) in the three-electrode setup; cathode as a working electrode, anode as a counter electrode and Ag/AgCl reference electrode. All potentials are reported with respect to Ag/AgCl throughout this paper unless stated otherwise.

#### b) Setup for pure culture

Due to the sterility issues, PVDF cell could not be used for pure culture experiments. A fully autoclavable and hermetically closed H-type glass reactor was fabricated by joining two 250 mL glass bottles (Supplementary information-Chapter 2 Figure SI-2). Pretreated Nafion 117<sup>®</sup> proton exchange membrane (Sigma-Aldrich) was used to separate the two compartments in this cell. As Nafion 117<sup>®</sup> proton exchange membrane is heat-resistant, it was used in this autoclavable reactor. The cathode was an assembly of two pieces of 5×3 cm<sup>2</sup> graphite felts with a stainless steel mesh sandwiched between them. A 9×3.5 cm<sup>2</sup> rectangular piece of Titanium with an Iridium coated dimensionally stable anode (DSA) (Magneto special anodes B. V.) was used as an anode. Each chamber was isolated and hermetically closed by using butyl rubber stoppers. For the electrical power source connection, the electrodes were provided with a short platinum wire extruded through a butyl rubber cap on the upper openings of both chambers. Catholyte was continuously stirred by using a magnetic stirrer revolving at 400 –500 rpm (revolutions per minute). For the electrochemical measurement, the cell was connected to a Potentiostat (VMP3, Biologic Science Instruments, France) in the three-electrode setup with an Ag/AgCl (3 M KCl, +205 mV vs SHE) reference electrode in the cathode chamber.

### 2.2.3 Electrolytes

The media used for the growth phase in the study was a phosphate buffer solution (PBS) composed of (g·L<sup>-1</sup>): 0.33 KH<sub>2</sub>PO<sub>4</sub>, 0.45 K<sub>2</sub>HPO<sub>4</sub>, 1 NH<sub>4</sub>Cl, 0.1 KCl, 0.8 NaCl, 0.2 MgSO<sub>4</sub>·7H<sub>2</sub>O, and 1 yeast extract, which was later supplemented with 20 mL·L<sup>-1</sup> vitamin solution (DSMZ 141), 20 mL·L<sup>-1</sup> trace element solution (DSMZ 141) and 4 g·L<sup>-1</sup> sodium bicarbonate (NaHCO<sub>3</sub>) prior to operation. The media was prepared anaerobically by heating it just to boil and then immediately cooled on ice under N<sub>2</sub> gas purging. This media is named mineral media henceforward. During the bacterial growth/start-up phase, 20 mM additional fructose as substrate and 2 mL·L<sup>-1</sup> of 1 M Na<sub>2</sub>S·9H<sub>2</sub>O solution (as an oxygen scavenger to maintain anaerobic condition) were injected. In the production

---

phase, fructose was removed and the 4 g.L<sup>-1</sup> bicarbonate mineral media was used as the catholyte. The anolyte was constituted by the phosphate buffer solution which was kept acidic (pH between 3–4) during the operation by 1 M HCl addition. pH was measured using a purpose-built multimeter (wtw 340i, Germany). The pH of the catholyte was adjusted to 7 at the beginning and temperature was maintained at 30 °C by using a thermocouple controlled heater.

## **2.2.4 Start up and operation of MES**

### *2.2.4.1 Mixed culture MES in cylindrical cell*

MES experiments were initiated with heterotrophic bacterial growth at the cathode using 20 mM fructose in 500 mL catholyte with 10% (v/v) of mixed culture inoculum. The reactor was started-up in batch mode at -0.6 V/<sub>Ag/AgCl</sub> cathode potential. The cathode potential was applied through potentiostat using Chronoamperometry (CA), an electrochemical technique to measure the current at constant applied potential. The catholyte became turbid during the biocatalyst growing phase which was ~ 30 days. Afterward, a number of preliminary polarization tests at potentials -0.6 V to -1 V were performed randomly. The intention was to allow sufficient time to completely degrade the fructose as well as to acclimate the bacteria in the electrochemical cell (in the study, 20 days). Then, the catholyte was replaced by 500 mL of fresh catholyte, while keeping around 50–70 mL of the previous electrolyte as inoculum. The subsequent semi-batch operations of MES with only HCO<sub>3</sub><sup>-</sup> as carbon source was hereafter, termed as Batch 1, Batch 2, Batch 3 and so on. In the experiments, electrochemically produced H<sub>2</sub> served as an additional electron source other than the electric current. Batch 1 was conducted in a fed-batch mode for 95 days fixing the cathode potential at -1.1 V in order to acclimate autotrophic bacteria in the cathode. A 10–30 mL of 5% (w/v) NaHCO<sub>3</sub> solution was added as a replacement of sampling volume whenever bicarbonate concentrations were lower than 200 mg.L<sup>-1</sup>, otherwise the sampling volume was replaced by the same amount of phosphate buffer solution. The headspace of the catholyte container was intermittently flushed by N<sub>2</sub> gas, particularly after sampling and the addition of HCO<sub>3</sub><sup>-</sup> or phosphate buffer solution, in order to avoid oxygen.

After 95 days operation of MES in Batch 1, subsequent batches of MES namely, Batch 2, 3 and 4 were repeated by replacing the previous catholyte with 400 ml of fresh catholyte, while retaining around 50 mL of the previous catholyte as inoculum. Batch 2 was operated at -1.1 V while Batch 3 and 4 were operated at -1 V cathode potential. The cathode potential was shifted toward less negative values so as to lower the electrochemical H<sub>2</sub> supply and to promote direct electron uptake. The start-up and batches of mixed culture MES are outlined in Table 1.1. The pH of catholyte was continuously monitored in the reactor. Whenever pH rose above 7.5, 1–2 mL of 1 M HCl was added to maintain the pH between 6.5–7.5.

**Table 2.1:** Operation scheme of mixed and pure culture MESSs.

|                            | Mixed culture   | Pure culture                    |
|----------------------------|---|---------------------------------|
| <b>Cultivation</b>         | <u>Batch cultures in serum bottles</u>                |                                 |
|                            | Media: NBAF [18]                                      | DSMZ 879                        |
|                            | Duration: 2 weeks                                     | 2 weeks                         |
| <b>Growth phase in BES</b> | <u>Growing with 20 mM fructose</u>                    |                                 |
|                            | Media: Fructose based                                 | Fructose based                  |
|                            | Process: Bacterial growth / acclimation               | Fermentation / acclimation      |
|                            | Cathode potential: -0.6 V                             | -0.6 V                          |
|                            | Duration: 1 month                                     | 1 week                          |
| <b>Production phase</b>    | <u>Bicarbonate as carbon source</u>                   |                                 |
|                            | <b>Batch 1</b>  |                                 |
|                            | Operation mode: Semi-batch mode: $\text{HCO}_3^-$ fed | Semi-batch mode                 |
|                            | Process: Acclimation to $\text{HCO}_3^-$              | Acclimation to $\text{HCO}_3^-$ |
|                            | Catholyte volume: 500 ml                              | 200 ml                          |
|                            | Cathode potential: -1.1 V                             | -0.9 V                          |
|                            | Duration: 95 days                                     | 1.5 week                        |
|                            | <b>Batch 2</b>  |                                 |
|                            | Operation mode: Semi-batch mode                       | Semi-batch                      |
|                            | Catholyte volume: 400 ml                              | 200 ml                          |
|                            | Cathode potential: -1.1 V                             | -0.9 V                          |
|                            | Duration: 3 weeks                                     | 2 weeks                         |
|                            | <b>Batch 3</b>  |                                 |
|                            | Operation mode: Batch mode                            | Batch mode                      |
|                            | Catholyte volume: 400 ml                              | 200 ml                          |
|                            | Cathode potential: -1.1 V                             | -0.9 V                          |
|                            | Duration: 2 weeks                                     | 2 weeks                         |
|                            | <b>Batch 4</b>  |                                 |
|                            | Operation mode: Batch mode                            | not done                        |
|                            | Catholyte volume: 400 ml                              |                                 |
|                            | Cathode potential: -1.1 V                             |                                 |
|                            | Duration: 4 weeks                                     |                                 |

#### 2.2.4.2 Pure culture H-type cell

The whole set up was first, autoclaved with the phosphate buffer solutions in both anode and cathode compartments. Filter-sterilized vitamin solution, trace element solution, and  $\text{HCO}_3^-$  solutions were later injected thereby maintaining sterility. 200 mL of electrolytes in the cathode and the anode chambers were continuously stirred at 400-500 rpm. In order to grow bacterial cells at the cathode, the operation was started up in heterotrophic growth mode with 20 mM fructose in the catholyte as mentioned in electrolyte section. The reactor was inoculated by 10% (v/v) of *C. ljungdahlii* sub-culture originally purchased from DSMZ. Cathode potential of -0.6 V vs Ag/AgCl was applied during the

growing phase. When the catholyte became turbid, almost 70% of it was replaced by a fresh anaerobic catholyte. Three sequential batches of MES were performed with *C. ljungdahlii* at -0.9 V cathode potential, feeding  $\text{HCO}_3^-$  solution as a carbon source. The start-up and subsequent semi-batch operations of *C. ljungdahlii* MES in H-type cell were schemed as in Table 1. During the operation, the catholyte was frequently flushed with filter sterilized  $\text{N}_2:\text{CO}_2$  (80:20 v/v) gas, mainly after sampling and after the addition of  $\text{HCO}_3^-$  or phosphate buffer solution, in order to avoid oxygen.

### 2.2.5 Chemical Analysis

Samples of the catholytes (5-10 mL) were taken for inorganic carbon ( $\text{HCO}_3^-$ ), volatile fatty acids (VFAs) and alcohols analysis, taking care of the moment of  $\text{HCO}_3^-$  addition. To maintain a constant catholyte volume, the sampled volume was replaced by the same volume of either 5%  $\text{NaHCO}_3$  solution whenever the pH was 6–6.5 or by acidified phosphate buffer (pH 5) whenever the catholyte pH was above 7.5.  $\text{HCO}_3^-$  was measured by a Total Inorganic Carbon (TIC) analyzer (TOC 5050A, Shimadzu).

For analysis of VFAs, samples were filtered through a 0.45  $\mu\text{m}$  Acrodisc syringe filters and acidified with 0.5 mL of 1:1 (v/v)  $\text{H}_2\text{SO}_4$  solution. 80  $\mu\text{L}$  of 2-methylhexanoic acid (6  $\text{mg}\cdot\text{L}^{-1}$ ) was added as internal standard solution followed by 1-2 mg of NaCl. Subsequently, 2 mL of diethyl ether was added for extraction of the VFAs. The sample was vortexed for 2 minutes and afterward centrifuged for 3 minutes at 1900 g (5810R centrifuge, Eppendorf, Hamburg, Germany). The supernatant was transferred to a vial for Gas Chromatography (GC) analysis (Focus GC, Thermo Fischer Scientific) equipped with an AT<sup>M</sup>-1000 capillary column (15 m  $\times$  0.53 mm; 1.20  $\mu\text{m}$  film thickness) with flame ionization detection. During the measurement, temperatures were conditioned as: injector temperature 145 °C, detector temperature 200 °C, column temperature linearly rising from 40 to 100 °C at 3 °C $\cdot\text{min}^{-1}$ . Helium was used as the carrier gas at a constant flow of 6  $\text{mL}\cdot\text{min}^{-1}$ .

The concentrations of acetone, ethanol, propanol and butanol were analyzed by gas chromatography using an AT-WAX capillary column (60 m  $\times$  0.32 mm; 1.00  $\mu\text{m}$  film thickness) with flame ionization detection (FID). D6-ethanol was used as an internal standard. The analysis was carried out under the same temperature conditions as indicated above: helium flow rate, 1.6  $\text{mL}\cdot\text{min}^{-1}$ ;  $\text{H}_2$  flow rate, 35  $\text{mL}\cdot\text{min}^{-1}$ ; air flow rate, 350  $\text{mL}\cdot\text{min}^{-1}$ .

Gas samples were collected by using a gas-tight plastic syringe and analyzed in a GC (Trace GC Ultra, Thermo Scientific) equipped with a thermal conductivity detector (TCD).  $\text{H}_2$  content was analyzed with a 2 m stainless steel column packed with a molecular sieve 5A (80/100 mesh) using nitrogen as carrier gas at a flow rate of 20  $\text{mL}\cdot\text{min}^{-1}$ .  $\text{CO}_2$ ,  $\text{O}_2$ ,  $\text{N}_2$  and  $\text{CH}_4$  gases were analyzed with a 2 m stainless steel HayeSep Q (80/100 mesh) and molecular sieve 5A (80/100 mesh) columns. Helium was used as carrier gas at 15  $\text{mL}\cdot\text{min}^{-1}$  flow rate.

### 2.2.6 Calculations

In the batch mode operation of MES, production of acetate (in mol) at any time  $t$  was calculated as per equation 1.2:

$$n_{\text{acetate},t} = \frac{V_{\text{cat}} \times (C_{\text{acetate},t} - C_{\text{acetate},t_0})}{M_{\text{acetate}}} \quad (2.1)$$

Subscripts  $t_0$  and  $t$  refer to two subsequent samples,  $n$  is the number of moles of acetate produced,  $V_{\text{cat}}$  is total volume of the catholyte,  $C$  is the concentration of acetate ( $\text{mg}\cdot\text{L}^{-1}$ ), whereas  $M_{\text{acetate}}$  is its molecular weight. The rate of production of acetate in  $\text{mg}\cdot\text{L}^{-1}\cdot\text{d}^{-1}$  is given by equation 2.2:

$$P_{\text{acetate},t} = \frac{(C_{\text{acetate},t} - C_{\text{acetate},t_0})}{t - t_0} \quad (2.2)$$

$t - t_0$  being the time difference in days (d) between sample at time  $t$  and previous sample at time  $t_0$ .

Cathodic electron efficiency, also named current efficiency (CE), is the efficiency of capturing the electron from the electric currents to the product (related to product selectivity). In this study, only the acetate production was considered for electron efficiency calculations and was calculated using equation 2.3:

$$\text{CE in } \%, \eta_e = \frac{n_{\text{acetate},t} \times f_{e,\text{acetate}} \times F}{\int_{t_0}^t I dt} \times 100 \quad (2.3)$$

Where  $n_{\text{acetate},t}$  is the moles of acetate analyzed at time  $t$ ,  $f_{e,\text{acetate}}$  represents the molar conversion factor (8 electron equivalent per mol for acetate),  $F$  is Faraday constant (96,485 C.mol<sup>-1</sup> of electron) and  $I$  is the current.

The carbon fixing or recovery efficiency ( $\eta_c$ ) indicates to what extent carbon from  $\text{HCO}_3^-$  was recovered in reduced organics. In this study, only the acetate production in mixed culture MES was considered for calculation. Carbon recovery (CR) in % was calculated according to equation 2.4:

$$\eta_{C,t} = \frac{n_{\text{acetate},t} \times f_{C,\text{acetate}}}{n_{\text{bic},t_0}} \times 100 \quad (2.4)$$

$\eta_{C,t}$  refers to carbon efficiency at a time  $t$ ,  $n_{\text{acetate},t}$  is the number of moles of acetate produced at time  $t$ ,  $f_{C,\text{acetate}}$  is the number of moles of carbon in a mole of acetate (=2) and  $n_{\text{bic},t_0}$  is the number of moles of  $\text{HCO}_3^-$  present in a sample analyzed at previous time  $t_0$ .

The energy efficiency of a production system is typically calculated as the amount of energy invested (kWh) per unit of product. The increasingly available electricity at low cost supports MES to attain high production rate rather than the current efficiency since providing just enough reducing power might limit the thermodynamic driving force [19]. The electrical energy input required for the production of acetate from  $\text{CO}_2$  reduction in MES ( $J_{\text{acetate}}$  in kWh.mol<sup>-1</sup> acetate) was calculated from the actual cell voltage given by ( $E_{\text{cathode}} - E_{\text{anode}}$ ) values measured during the operation of MES in CA, according to equation 2.5:

$$J_{\text{acetate},t} = \frac{(E_{\text{cathode},t} - E_{\text{anode},t}) \times \int_{t_0}^t I dt}{n_{\text{acetate},t}} \quad (2.5)$$

## 2.7 Scanning electron microscopy (SEM) analyses

The bacterial adhesion on the graphite felt cathode and membrane was analyzed by using a SEM. Approximately 0.25 cm<sup>2</sup> of the graphite felt and 0.25 cm<sup>2</sup> of Nafion proton exchange membrane (PEM) were cut from the *C. ljungdahlii* MES cell at batch 3 operation. The specimens were fixed in 4% glutaraldehyde in sterile phosphate buffer solution (PBS) for 1 hour at room temperature and subsequently rinsed three times in PBS. The samples were then stored at 4 °C overnight and dehydrated using graded ethanol series (20%, 30%, 50%, 70%, 90% and 100%; 10 min at each stage). The electrode pieces were finally dried at  $\text{CO}_2$ -critical point for 3 h and gold coated before the micrographs were taken.

---

## 2.3 Results and discussion

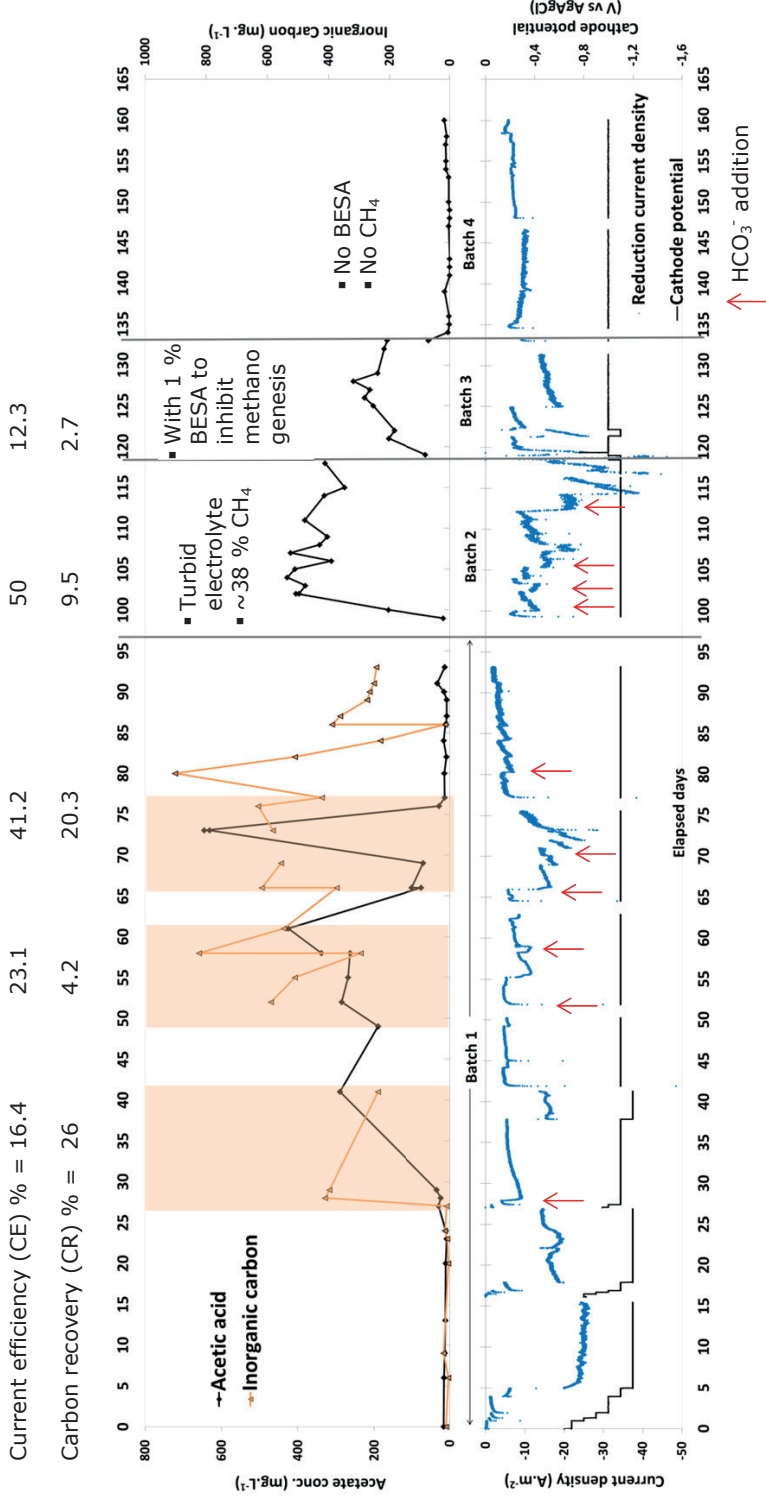
### 2.3.1 H<sub>2</sub> evolution in carbon felt and stainless steel mesh assembly cathode

Thermodynamically, proton reduction in aqueous electrolyte occurs at more negative cathode potentials than  $-0.6 V_{/Ag/AgCl}$  under standard biological conditions, producing H<sub>2</sub>, which can eventually mediate the electron transfer in CO<sub>2</sub> reduction carried out by the bacteria at the cathode. But due to the overpotential of electrode material for H<sub>2</sub> evolution, more negative potential has to be applied. In addition, the evolved gaseous H<sub>2</sub> has limited dissolution and mass transfer in aqueous electrolyte, so it might not be completely available for the biological CO<sub>2</sub> reduction. A lower H<sub>2</sub> evolution overpotential material and also highly adsorbing nature of cathode was necessary for the effective CO<sub>2</sub> reduction in MES. An assembly of graphite felt and stainless steel mesh was a direct solution for the CO<sub>2</sub> reducing MES cathode because stainless steel is an effective H<sub>2</sub> evolving cathode and graphite felt can adhere the evolved H<sub>2</sub>. Furthermore, graphite felt provided larger surfaces for bacterial attachment as well as. The photographs of cathodes used in mixed and pure culture reactors are provided in the supplementary information-Chapter 2 Figure SI-1 and SI-2.

In the mixed culture MES reactor, stainless steel mesh (SS316L) was kept in between the graphite felt (on the catholyte side) and a piece of Teflon layer (at the closing end). In order to set the cathode at H<sub>2</sub> evolution potential in the mixed culture reactor, a number of polarization tests were performed by applying a series of chronoamperometry technique. The polarization test was started by setting cathode potential from  $-0.6$  to  $-1.2 V_{/Ag/AgCl}$  with a step of  $-0.1 V$  until a phase of consistent current densities were recorded at each potential. The current densities were relatively low (below  $1 A.m^{-2}$ ) at more positive cathode potential than  $-1 V_{/Ag/AgCl}$ . An increments in reduction current densities from  $5$  to  $20 A.m^{-2}$  at  $-1.1 V$  and  $-1.2 V V_{/Ag/AgCl}$  (Figure 2.1) indicated electrochemical H<sub>2</sub> evolution. Cyclic voltammetry performed on mixed culture reactor during the operational phase also displayed electrochemical H<sub>2</sub> evolution at  $-1.1 V_{/Ag/AgCl}$  (Supplementary information-Chapter 2 Figure SI-3). The cathode potential of  $-1.1 V_{/Ag/AgCl}$  was selected for further operation of mixed culture MES where H<sub>2</sub> evolution was clear from higher current density.

In the H-type reactor, an assembly of two pieces of  $5 \times 3 cm^2$  graphite felts with a stainless steel mesh in between, as a cathode, was dipped in the catholyte. H<sub>2</sub> bubbles were visible at  $-0.9 V_{/Ag/AgCl}$  during a short polarization test. Cyclic voltammetry performed on H-type reactor after the growth phase of *C. ljungdahlii* also showed H<sub>2</sub> evolution starting from  $-0.9 V_{/Ag/AgCl}$  (Supplementary information-Chapter 2 Figure SI-4). Furthermore, 7% (v/v) H<sub>2</sub> was found in the analysis of headspace gas from the H-type reactor. It is expected that due to the differences in reactor design and also due to the acidifying effect of CO<sub>2</sub> gas from N<sub>2</sub>:CO<sub>2</sub> (80:20) flushing in the cathode chamber of the pure culture reactor, H<sub>2</sub> evolution occurred at a more positive potential than in the mixed culture reactor.





**Figure 2.1:** Long-term  $\text{CO}_2$  reduction experiment with mixed culture. Acetate production profile and bicarbonate concentration profile (Top), current density and cathode potential (Bottom). Batch 1:- first autotrophic phase after the bacterial growth at the cathode in fed-batch mode. Shaded boxes are periods of acetate production. Batches 2, 3 and 4:- Subsequent batch operations. 1% (w/v) sodium 2-bromoethanesulfonate was included in the Batch 3 catholyte. Red arrows indicate the points of bicarbonate addition from 8% stock solution. Abrupt spikes in the current density profile (in the lower graph) are due to pH adjustments, bicarbonate additions and change of cathode potentials.

---

### **2.3.2 Acetate production from bicarbonate reduction catalyzed by mixed bacterial culture**

CO<sub>2</sub> reduction experiments at the cathode of BES were conducted under the potentiometric control of cathode potential with water oxidation at the anode serving as the electrons and protons source. In order to make the reducing equivalents or H<sub>2</sub> available for the HCO<sub>3</sub><sup>-</sup> reduction, cathode potential was fixed to -1.1 V. The experiments were conducted in a fed-batch mode with the intermittent addition of NaHCO<sub>3</sub> solution as a carbon source. NaHCO<sub>3</sub> will dissociate into HCO<sub>3</sub><sup>-</sup> and CO<sub>3</sub><sup>2-</sup> which serve as dissolved inorganic carbon sources. At acidic pH, the HCO<sub>3</sub><sup>-</sup> forms carbonic acid (dissolved form of CO<sub>2</sub>) which ultimately equilibrates with gaseous CO<sub>2</sub>. When pH was maintained between 6 to 8 in the experiment, the majority of dissolved inorganic carbon remained as HCO<sub>3</sub><sup>-</sup>.

During the first 25 days of operation, no production of acetate was observed, but noticeably the amount of inorganic carbon was also below 50 mg.L<sup>-1</sup> in that period. One can expect acetate production from the degradation of yeast extract present in the catholyte since yeast extract was used as a source of trace nutrients. At least 0.01% of yeast extract is necessary for acetogens to maintain structural integrity [20]. But during the first 25 days of the experiment when the HCO<sub>3</sub><sup>-</sup> concentrations were low, there was no production. This confirmed that yeast extract did not serve as a carbon source in this process. From day 28 to 41, after the addition of 30 ml of 5% (w/v) NaHCO<sub>3</sub> solution, an increase in acetate concentration was observed along with an increase in reduction current. Once HCO<sub>3</sub><sup>-</sup> was added, acetate concentration increased with a corresponding decrease in the HCO<sub>3</sub><sup>-</sup> concentration. This trend of rising acetate concentration and usage of inorganic carbon was repetitively observed in Batch 1. The shaded parts in Batch 1 of Figure 2.1 indicate the periods where the reduction of HCO<sub>3</sub><sup>-</sup> resulted in the production of acetate repetitively. These observations explain that acetate was produced from the reduction of inorganic carbon, more precisely between day 28 to 41, day 58 to 61 and day 66 to 73 of Batch 1. Apparently, the current densities also increased with the addition of HCO<sub>3</sub><sup>-</sup>.

Notably, as observed in Batch 1 of Figure 2.1, acetate was not accumulated continuously. Drops in acetate concentration were as seen in the periods after the shaded parts in Figure 2.1. These observations indicated that once acetate concentration reached a certain level, it was converted to other products. Though acetate was repetitively produced and consumed, no substantial amounts of alcohols or other higher VFAs were found in the electrolyte. A possible explanation could be the conversion of acetate to CH<sub>4</sub> by acetoclastic methanogens or oxidized by sulfate reducers which are normally present in culture from wastewaters [21]. Methane was detected up to 10% (v/v) in a number of headspace gas analysis during Batch 1 even though the system was not completely gas tight and irregularly flushed with N<sub>2</sub>. Detection of methane in headspace explains that the microbial population in mixed culture MES consisted not only the acetogens, but also the methanogens. A number of studies on MES with the mixed culture at hydrogen evolving potentials have also reported methane production along with acetate and hydrogen [7, 8]. However, the presence of sulfate reducers cannot be neglected since sulfate salts were also present in the catholyte and sulfide was also used to maintain anaerobic condition.

While the acetate concentrations were lower than the preceding concentrations, 10–30 mL of NaHCO<sub>3</sub> solution was added and the reduction of bicarbonate to acetate resumed again. The highest concentration of acetate accumulated in the catholyte was 10.5 mM on the 73<sup>rd</sup> day of Batch 1 operation and this production encompasses the highest production rate of 1.26 mM.d<sup>-1</sup>. Thereafter, acetate concentration abruptly dropped to 20 mg.L<sup>-1</sup> and did not increase even though the inorganic carbon was likely sufficiently available. Furthermore, Figure 2.1 showed that the inorganic carbon in the catholyte also gradually decreased from 900 mg.L<sup>-1</sup> to 10 mg.L<sup>-1</sup> and continued decreasing even after the addition of bicarbonate in the last 20 days of Batch 1. Eventually, the acetate concentration did not rise but methane was detected up to 10% (v/v) in the headspace

---

during that period. CH<sub>4</sub> production is characteristic in an anaerobic mixed culture system with syntrophic acetate degradation [22]. Acetate is a principal precursor for CH<sub>4</sub> productions. Acetoclastic methanogens are primarily responsible for CH<sub>4</sub> production than hydrogenotrophic methanogens in anaerobic digestion [23, 24]. Several research have described acetate and hydrogen as electron donor for CH<sub>4</sub> production in bioelectrochemical systems operated at -0.9 to -1.1 V vs Ag/AgCl cathode potential [25–27]. Hence, it is most likely that in Batch 1 operation, methane production took place once acetate was accumulated to a certain concentration.

Batch 2 of the CO<sub>2</sub> reduction experiment was conducted in the same cell by replacing Batch 1 catholyte with 400 ml of fresh catholyte. Approximately 50 mL of the previous electrolyte was retained as an inoculation source. The cell was operated in a semi-batch mode with an intermittent addition of 10-20 ml of NaHCO<sub>3</sub> solution mostly during the sampling of catholyte in order to compensate for the sampling volume. Simultaneous production of acetate and CH<sub>4</sub> recurred in this batch within a short period of operation. The acetate production rate during the first three days of the 2<sup>nd</sup> batch operation was 1.35 mM.d<sup>-1</sup>, the highest rate in the entire mixed culture experiment. However, the maximum concentration of acetate accumulated in the electrolyte was only 6.7 mM, which was lower than in the first batch. A similar study by Jiang et al. [8] reported 6.57 mM d<sup>-1</sup> acetate production along with CH<sub>4</sub> at -1.15 V. The production rate in our study was five times lower than the rate reported by Jiang et al. [8] but, the cathode size was also five times smaller. Besides, the catholyte volume, operating methods, and inoculum were also different.

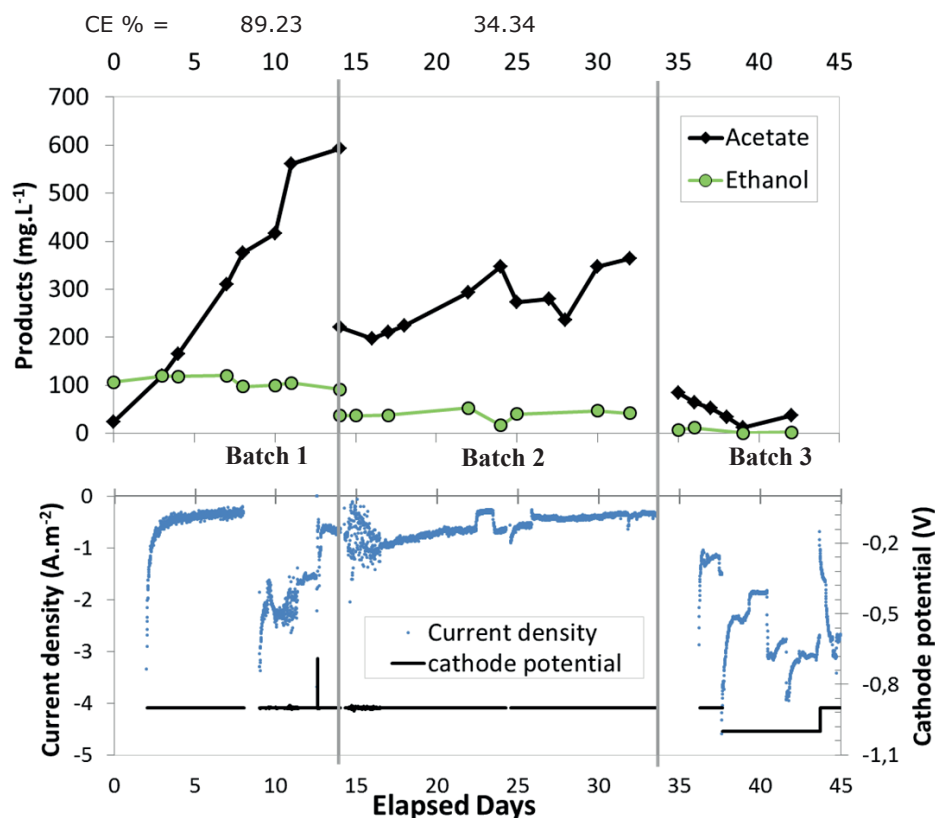
Furthermore, from day 102 in Batch 2, the acetate concentration varied between 300 and 450 mg.L<sup>-1</sup> (Figure 2.1). These fluctuations of acetate concentration, even at the ample supply of bicarbonate, infer that there were simultaneous production and degradation of acetate. CH<sub>4</sub> concentration measured in the headspace was also higher in this batch than previous batches, reaching 38% (v/v). In order to remove methanogens, the catholyte was replaced after ~10 days of Batch 2 operation and additionally, 1% (w/v) sodium 2-bromosulfonate, a well-known methanogenesis inhibitor [28], was included in the catholyte of Batch 3. Acetate production was again observed but the concentrations were even lower than in the Batch 2.

Notably, the Batch 3 was operated without any bicarbonate addition to the catholyte during the operation and the set cathode potential was -1 V. Less negative cathode potential was set to achieve CO<sub>2</sub> reduction with a smaller amount of electrochemically produced hydrogen. During the sampling, only acidified phosphate buffer (pH 5) was added to balance the sampling volume. The reduction current density still remained higher than 10 A.m<sup>-2</sup>. No CH<sub>4</sub> was found in the headspace in this batch. However, the concentration of acetate declined slightly at the later stage of Batch 3, possibly due to other biodegradation processes such as acetate oxidation to CO<sub>2</sub> by sulfate reducers [21]. In the Batch 4 operation, acetate production was not restored and most likely, this might be due to the large portion of bacterial biomass removal during the catholyte replacement between the batches. Visually, the catholyte appeared less turbid than the previous batches. Lower concentrations of acetate in successive batches might be due to the continued removal of bacteria during the replacement of catholyte as well as due to the absence of CO<sub>2</sub> reduction by direct electron up-taking microorganisms.

The acetogenic CO<sub>2</sub> reduction using mixed cultures in MES had to compete with methanogenic CO<sub>2</sub> reduction, since acetogens and methanogens usually cohabit the same environment and both can utilize CO<sub>2</sub> with H<sub>2</sub> as the energy source. This elucidates that operating MES without methane production using mixed bacterial inocula from wastewater as biocatalyst is another challenge.

### 2.3.3 Acetate production in *C. ljungdahlii* reactor under electrochemically produced $H_2$

Acetate production from  $CO_2$  reduction with *C. ljungdahlii* was observed when  $-0.9$  V (instead of  $-1.1$  V) cathode potential was applied in the H-type bioelectrochemical cell with  $50$  mM  $NaHCO_3$  buffer catholyte (Figure 2.2). The headspace had  $7\%$  of  $H_2$  (v/v) at the beginning of Batch 1 operation with  $-0.9$  V cathode potential and it continuously accumulated along the operation as the cell was hermetically sealed. In this H-type cell at  $-0.9$  V cathode potential, the current density stabilized around  $-1$  A  $m^{-2}$  (Figure 2.2). In the first batch operation after the bacterial growth, acetate was produced at an average rate of  $1$  mM  $d^{-1}$  and the product was continuously accumulating without degradation. Microbial electrosynthesis of acetate with traces of 2-oxobutyrate and formate from  $CO_2$  reduction using *C. ljungdahlii* in bioelectrochemical system was previously reported by Nevin et al. [6]. However, the acetate production rate was only  $\sim 0.013$  mM  $d^{-1}$  (based on  $110$   $\mu$ moles acetate produced in 7 days from  $1.21$  L catholyte) at  $-0.6$  V<sub>Ag/AgCl</sub> [6]. In our study, the acetate production rate has been increased by  $60$ – $70$  times by shifting the cathode potential to  $-0.9$  V.



**Figure 2.2:** Acetate production from bicarbonate reduction in H-type cell with *C. ljungdahlii* in Batch 1, 2 and 3. Acetate production profile (Top), current density and cathode potential (Bottom). Current fluctuations are due to pH adjustments and bicarbonate addition.

---

When the production rate was calculated from day 10 to 11 of Batch 1, the rate of production reached a maximum of  $2.4 \text{ mM}\cdot\text{d}^{-1}$ . Moreover, ethanol was also detected in the catholyte but it was not increasing like the acetate concentrations. Ethanol was found in the catholyte from the beginning of the experiment which indicated that it was most likely the residual ethanol from the growth phase where fructose was used as the substrate. So far ethanol production from the reduction of  $\text{CO}_2$  was not sufficiently evident in our experiment. Nevertheless, a number of studies on *C. ljungdahlii* have already reported the production of ethanol from syngas fermentation and also from  $\text{CO}_2$  and  $\text{H}_2$  [29]. Interestingly, despite the slight fluctuations in concentration, ethanol was present in the catholyte throughout the experiment. That means no considerable (net) ethanol or acetate degrading processes were involved. The absence of the ethanol degradation also shows that the acetate production was not resulting from the product degradation but due to  $\text{CO}_2$  or  $\text{HCO}_3^-$  fixation. In this sense, the pure culture of an acetogen can acclimate faster and produce acetate at higher rates when hydrogen is available. Based on the literature reporting biochemical ethanol production from  $\text{CO}_2$  and  $\text{H}_2$  by *C. ljungdallii*, it can be postulated that *C. ljungdahlii* could potentially produce ethanol through  $\text{CO}_2$  reduction with the hydrogen evolving cathodes.

In order to observe the reproduction of the process, Batch 2 was started replacing 70% of the previous catholyte with the new electrolyte. In the 2<sup>nd</sup> batch, the production of acetate was repeated but slower than the first batch. After 10 days of operation, a slight drop in acetate concentration was noted, though the concentration increased afterward. Overall, the first 10 days of Batch 2 resulted in an acetate production rate of  $0.2 \text{ mM}\cdot\text{d}^{-1}$  which was at least around 20 times higher than the acetate production rates reported by Nevin et al. [6] for *C. ljungdahlii*. However, the production rate in Batch 2 was five times slower than the average rate of production in Batch 1.

When the reactor was operated in Batch 3, the production of acetate did not recur, rather both the residual acetate and ethanol concentrations declined to undetectable levels. Probably, due to the removal of bacteria during catholyte replacement, the production declined in each transfer of batch. In contrast, Nevin et al. [1, 6] reported that periodic removal of planktonic cells during the growth with  $\text{N}_2:\text{CO}_2:\text{H}_2$  (80:13:7) bubbling promoted biofilm growth on cathode surface and the acetate production was resumed in the subsequent batch. In our experiment, the removal of planktonic cells after Batch 2 stopped the acetate production indicating that there was no acetogenic bacterial attachment or biofilm formed on the cathode. Here, it is noteworthy that hydrogen evolving stainless steel cathodes were used in our experiments. Concisely, acetate production from  $\text{CO}_2$  reduction in the successive batch operations of MES with *C. ljungdahlii* was observed repetitively using hydrogen evolving cathode. However, the production rate declined in the subsequent batches due to the removal of planktonic bacterial cells.

### **2.3.4 Comparative overview of performances**

Operations of MES with mixed culture and *C. ljungdahlii* at the hydrogen evolving cathode potential resulted in the synthesis of organic compounds from  $\text{CO}_2$  reduction, repeatedly. The products of the mixed culture MES were primarily acetate and  $\text{CH}_4$ , whereas the MES with the *C. ljungdahlii* produced mainly acetate. MES using mixed culture biocathode involved a number of competitive bioelectrochemical processes and the profile of acetate concentrations exhibited several fluctuations. Whereas in pure culture biocathode, the production profile was consistent, which indicated that there were no/very few competing processes going on. Based on the production of acetate in different batches, several performance parameters have been calculated in order to provide a comparative overview of both MES experiments (Table 2.2). Maximum production rate achieved by the mixed culture biocathode was  $1.35 \text{ mM}\cdot\text{d}^{-1}$  which corresponds to  $\sim 50\%$  current efficiency whereas in the case of pure culture biocathode the maximum rate of production was  $2.4 \text{ mM}\cdot\text{d}^{-1}$  with 89% current recovered between

day 11–12. When considered for a whole Batch 1, the pure culture produced acetate at  $\sim 1 \text{ mM}\cdot\text{d}^{-1}$  with ca. 40% current efficiency. The average acetate production rates achieved by utilizing electrochemically produced hydrogen as the energy source in both the MES experiments were almost similar. As the area of the cathode used in the pure culture MES was larger than the cathode area of the mixed culture MES, the projected surface area based production rate of acetate was higher in mixed culture biocathode reaching ca.  $40 \text{ g}\cdot\text{m}^{-2}\cdot\text{d}^{-1}$  with  $10 \text{ cm}^2$  projected cathode area.

**Table 2.2:** Overview of acetate production from CO<sub>2</sub> reduction by mixed and pure culture

| Phases                    | Operation duration | Max. conc. (mM) | Acetate production rate (mM d <sup>-1</sup> ) | CE (%) | Production rate (g m <sup>-2</sup> d <sup>-1</sup> ) | Energy requirement (kWh mol <sup>-1</sup> ) | Average Voltage | Cell                                     |
|---------------------------|--------------------|-----------------|---|--------|--|---|-----------------|--|
|                           |                    |                 |   |        |  |   |                 | E <sub>cat</sub> - E <sub>an</sub>   (V) |
| <b>Mixed culture MES</b>  |                    |                 |   |        |  |   |                 |  |
| <b>Batch 1</b>            | Day 28 to 41       | 4.81            | 0.34  | 16.38  | 10.19  | 4.52  | 3.3             | 3.3                                      |
|                           | Day 58 to 61       | 7.08            | 0.48  | 23.12  | 14.46  | 2.41  | 3.1             | 3.1                                      |
|                           | Day 66 to 73       | 10.50           | 1.26  | 41.25  | 37.89  | 1.35  | 3.4             | 3.4                                      |
| <b>Batch 2</b>            | Day 99 to 102      | 6.74            | 1.35  | 49.91  | 32.37  | 1.12  | 3.3             | 3.3                                      |
| <b>Batch 3</b>            | Day 119 to 128     | 4.24            | 0.35  | 12.27  | 8.49   | 4.54  | 2.9             | 2.9                                      |
| <b>C. ljungdahlii MES</b> |                    |                 |   |        |  |   |                 |  |
| <b>Batch 1</b>            | Day 4 to 11        | 9.33            | 0.94  | 39.15  | 7.51   | 0.20  | 2.15            | 2.15                                     |
|                           | Day 10 to 11       | 9.33            | 2.40  | 89.23  | 19.19  | 0.36  | 2.14            | 2.14                                     |
| <b>Batch 2</b>            | day 14 to 24       | 5.77            | 0.21  | 34.34  | 1.67   | 1.29  | 2.05            | 2.05                                     |

Max. conc.: Maximum concentration; CE: Current efficiency; E<sub>cat</sub>: Cathode potential; E<sub>an</sub>: Anode potential; |E<sub>cat</sub> - E<sub>an</sub>|: absolute voltage

---

For the electricity driven bioproduction, energy consumption per unit mass of product is an important performance indicator. Energy consumptions in the electrosynthesis are proportional to the applied cathode potentials when the anode reactions remain the same. The calculations of the energy requirement for our experiments were based on the measured cell voltages by the potentiostat. On this basis, the performance was better with the pure culture biocathode which was operated at  $-0.9$  V with the minimum electrical energy input being  $0.2 - 0.4$  kWh.mol<sup>-1</sup> of acetate produced, whereas in the mixed culture experiments, the minimum electrical energy requirement was  $1.1 - 1.3$  kWh.mol<sup>-1</sup> of acetate produced at  $-1.1$  V (Table 2.2). These values are only an indication of how an MES effectively utilize electric energy in bioproduction and are completely based on the power inputs at the preliminary stages of investigation. There were plenty of rooms for optimization with better acclimated electroactive biofilms and systems design. Electric energy demand calculations clearly illustrate that the production achieved at less negative cathode potential is more beneficial in terms of operating cost involved.

A summarized scenario of CO<sub>2</sub> reduction in MES from different literature and a comparison with this study are presented in Table 2.3, including a number of insightful production parameters. Marshall et al. [7] and Jiang et al. [8] reported autotrophic production of acetate and CH<sub>4</sub> along with H<sub>2</sub> evolution which were the same products as in our mixed culture biocathode study. These two studies presented the most comparable MES systems to our mixed culture MES experiments. The volumetric production rate of acetate achieved in our study ( $1.3$  mM.d<sup>-1</sup>) was less than that reported in the mentioned literature [ $4$  mM.d<sup>-1</sup> Marshall et al. [7] and Jiang et al.  $6.57$  mM.d<sup>-1</sup> [8]], but current efficiency in our study [50%] was higher than the efficiency reported by Jiang et al. [8] [28.4%] and slightly lower than that of Marshall et al. [7] [67%].

There were several differences in the operational mode and the reactor design between our study and those in the literature. Most strikingly, our study used electrodes with a stainless steel current collector which is a well-known non-noble hydrogen evolving cathode material. Hence, the bacterial response to the stainless steel electrodes was different than with the non-metal carbon electrodes reported in the literature. The stainless steel current collector itself could support higher H<sub>2</sub> production, especially in the presence of weak acids [30, 31].

In the case of MES with a pure culture biocathode, this study achieved 60-70 times higher volumetric acetate production rate [ $0.94$  mM.d<sup>-1</sup>] and 10 times higher titer ( $0.6$  g.L<sup>-1</sup>) than Nevin et al. [1] reported rate [ $0.17$  mM.d<sup>-1</sup>] and titer [ $0.063$  g.L<sup>-1</sup>] with *S. Ovata* biocathode. The acetate production rate achieved [ $0.2$  mM.d<sup>-1</sup>] in Batch 2 operation of *C. ljundahlii* reactor with hydrogen producing cathode was at least 20 times higher than Nevin et al. [6] reported rate [ $0.013$  mM.d<sup>-1</sup>] with the direct electron accepting *C. ljundahlii*. The energy input for the MES at  $-0.9$  V cathode potential would be higher than that operated at  $-0.6$  V when the anodic reaction remained the same. However, the studies reporting direct electron uptake at less negative potential with cathode modifications have also not yet succeeded to produce significant titer [acetate concentration attained in catholyte:  $0.09$  g.L<sup>-1</sup> in Nie et al. [12] with nanowire coated graphite stick;  $0.6$  g.L<sup>-1</sup> in this study].

Mixed-culture MES can be preferred for scaling up of the technology due to the difficulties in maintaining growth and sterility, as well as the higher operation costs involved with the pure cultures. However, enrichment of the acetogenic mixed population and the suppression of methanogens are necessary. In the mixed culture biocathodes, specific enrichment and long-term acclimation can facilitate to attain higher production rates, i.e.  $1$  g.L<sup>-1</sup>.d<sup>-1</sup> being the highest reported till now [13]. Furthermore, pre-enrichment procedures have established electrochemically active biofilms that produce a number of organic metabolites by CO<sub>2</sub> reduction at  $-0.6$  V or at hydrogen evolving potential [9, 17].



**Table 2.3:** Comparative overview of autotrophic acetate production in microbial electrosynthesis (this study and a few selected studies)

| References           | Electrode material                 | Cathode potential<br>$V_{/Ag/AgCl}$ | Biocatalyst                                   | Product(s)                             | Acetate Production rate<br>( $\text{mM}\cdot\text{d}^{-1}$ ) | Current density<br>( $\text{A}\cdot\text{m}^{-2}$ ) | Projected area based acetate production<br>( $\text{g}\cdot\text{m}^{-2}\cdot\text{d}^{-1}$ ) | CE for acetate<br>% | Max. product titer<br>( $\text{g}\cdot\text{L}^{-1}$ ) |
|----------------------|------------------------------------|-------------------------------------|---|--|--|---|---|---------------------|--|
| This Chapter         | Carbon felt with Stainless steel   | -1.1                                | Mixed culture WW                              | $\text{H}_2$ , Acetate & $\text{CH}_4$ | 1.3  | 10  | 40  | 40-50               | 0.6  |
| This Chapter         | Carbon felt with Stainless steel   | -0.9                                | <i>C. ljungdahlii</i>                         | $\text{H}_2$ , Acetate & Ethanol       | 0.94   | ~1  | 7.51  | 40                  | 0.6  |
| Nevin et al. [1]     | Unpolished graphite sticks         | -0.6                                | <i>Sporomusa Ovata</i>                        | Acetate and Oxybutyrate                | 0.17 *   | n.g.  | 7.3   | 86±21               | 0.063 <sup>f</sup>                                     |
| Nevin et al. [6]     | graphite stick                     | -0.6                                | <i>C. ljungdahlii</i>                         | Acetate, Oxobutyrate & Formate         | 0.013*   | n.g.  | 0.1   | 88±2                | 0.005 <sup>f</sup>                                     |
| Nevin et al. [6]     | graphite stick                     | -0.6                                | <i>Moorella thermoacetica</i>                 | Acetate                                | 0.01*  | n.g.  | 0.1   | 84                  | 0.003 <sup>f</sup>                                     |
| Nie et al. [12]      | Ni-nanowire coated graphite stick  | -0.6                                | <i>Sporomusa Ovata</i>                        | Acetate                                | 1.13   | 0.63  | 3.38  | 82±14               | 0.094 <sup>f</sup>                                     |
| Marshall et al. [7]  | Graphite granules and graphite rod | -0.79                               | Brewery WW sludge                             | $\text{H}_2$ , $\text{CH}_4$ & Acetate | 4  | n.g.  | n.g.  | 67 <sup>s</sup>     | 1.71   |
| Jiang et al. [8]     | Carbon felt                        | -1 to -1.15                         | Mixed culture WWTP sludge                     | $\text{H}_2$ , $\text{CH}_4$ & Acetate | 6.57 (@-0.95 V)  | ~19   | 19  | 28.4 (@-0.85 V)     | ~0.1   |
| Marshall et al. [13] | Graphite granules and graphite rod | -0.79                               | adapted mixed acetogen from brewery WW sludge | $\text{H}_2$ & Acetate                 | 17.25  | n.g.  | n.g.  | 69                  | 10.5   |
| Su et al. [10]       | Carbon felt                        | -0.9 to -1.1                        | Mixed culture domestic WWTP sludge            | $\text{H}_2$ & Acetate                 | 15.67 (@ -0.9 V)   | 2.96  | 10  | 89.5 (@ -0.9 V)     | 4.7  |

| References          | Electrode material                  | Cathode potential<br>$V_{/Ag/AgCl}$ | Biocatalyst                        | Product(s) | Acetate Production rate<br>( $mM \cdot d^{-1}$ ) | Current density<br>( $A \cdot m^{-2}$ ) | Projected area based acetate production<br>( $g \cdot m^{-2} \cdot d^{-1}$ ) | CE for acetate<br>% | Max. product titer<br>( $g \cdot L^{-1}$ ) |
|---------------------|-------------------------------------|-------------------------------------|------------------------------------|------------|--|---|--|---------------------|--|
| Zaybak et al. [9]   | Carbon fiber rod                    | -0.6                                | Enriched culture from bog sediment | Acetate    | 0.05   | 0.03                                    | $0.063 \pm 0.008$  | $35.2 \pm 4.4$      | 0.02                                       |
| Jourdin et al. [14] | NanoWeb reticulated vitreous carbon | -1.05                               | Pond sediments and WWTP sludge     | Acetate    | $0.47 \pm 0.07$                                  | $37 \pm 3$                              | $195 \pm 30$   | 78.5                | n.g.                                       |

WW- Wastewater; n.g.- Not given or cannot be deduced; WWTP- Wastewater treatment plant; \* derived on the basis of total catholyte spent on reported days of operation; <sup>f</sup>calculated based on linear production rate and reported flow rate; <sup>g</sup>including H<sub>2</sub>

---

### 2.3.5 Hydrogen evolving cathode limits biofilm formation

CO<sub>2</sub> reduction in a bioelectrochemical system with mixed culture as a biocatalyst was shown repeatedly in successive batches from Batch 1 to 4. The profile of acetate concentration in all those batches showed that the accumulated concentration of acetate in subsequent batches decreased in each transfer. Moreover, the turbidity of the catholyte also decreased. These observations can be explained as an effect of the removal of active bacteria while substituting the electrolytes.

A periodic removal of planktonic cells promotes biofilm formation on the cathode of MES [1, 13]. Methanogens can also be removed by a reduction of the hydraulic retention time (so as to facilitate wash out). However, our observation indicated that acetogens were also washed out during catholyte substitutions. Likewise, acetate production in successive batches was observed with electrochemically generated hydrogen using *C. ljungdahlii* biocathode, but the concentrations decreased in each transfer. Also as explained above, it could be due to the removal of a fraction of the active bacterial population during the catholyte replacement. This implies that the active bacteria rather remained suspended in the solution rather than attached on the cathode surface or forming biofilm. A scanning electron microscope image of carbon felt from *C. ljungdahlii* biocathode at the end of Batch 3 operation shows only a few bacterial cells attached on the carbon felt whereas more bacterial adhesion is visible on the Nafion 117 membrane (Supplementary information-Chapter 2, Figure SI-5).

Carbon felts are typically used in bioelectrochemical systems as porous carbon electrode for the development of electroactive biofilms. In this study, carbon felt was used together with stainless steel mesh. Stainless steel electrodes have already been reported in use for a *Geobacter* spp biocathode [32, 33]. Soussan et al. [32] reported CO<sub>2</sub> reduction with a stainless steel cathode by developing *Geobacter* spp biofilms. However, the cathode potentials were more positive than the hydrogen evolution potential in all those stainless steel biocathode studies. The overpotential for hydrogen evolution on stainless steel is lower than that of the carbon felt and at the set cathode potential of -0.9 V, a large amount of hydrogen can evolve from the cathode when phosphates and weak acids are present in the catholyte [30]. Hydrogen accumulation up to 45% was found in the headspace of H-type cell during Batch 1 experiment. From these findings, it can be expected that H<sub>2</sub> evolution has limited the attachment of bacteria on the cathode surface and the bacterial biomass remained in suspension. Hydrogen bubbles evolved from the stainless steel cathode might have disturbed the biofilm formation on the carbon felt [34].

Yet another reason of limited bacterial attachment pertains to the issue of pH. The pH at the immediate cathode surroundings is expected to increase substantially as the protons are consumed for hydrogen evolution [35]. High pH near the cathode could potentially limit the bacterial attachment and growth. But, further confirmatory experiments need to be done to explain the phenomenon. In conclusion, limitation on biofilm formation on hydrogen evolving cathode was indicative in our MES experiments. When biofilm development was limited, the suspended bacteria were prevented for direct electron uptake from the solid cathode. Thus, in case an optimized microbial electrosynthesis has to be developed with H<sub>2</sub> evolving cathode, a mechanism to retain the bacterial biomass should be incorporated in order to recover the washed out biomass in a continuous operation mode.

## 2.4 Conclusions

CO<sub>2</sub> reduction primarily to acetate was repeatedly demonstrated with electrochemically produced hydrogen serving as an energy source using mixed culture and *C. ljungdahlii* in the cathode compartment. Higher volumetric production rates were achieved with electrochemically evolved H<sub>2</sub> than with the direct electron uptake although the current efficiencies remained low. Electrochemical H<sub>2</sub> evolution at cathode could attain

---

considerable production rates but might impede the development of biofilm. Methane production and other interfering processes need to be inhibited in order to improvement the production of other multi-carbon compounds.

### **Acknowledgements**

The work was supported by a PhD grant to Suman Bajracharya from VITO's strategic research funds.

### **References**

1. Nevin KP, Woodard TL, Franks AE, et al (2010) Microbial Electrosynthesis: Feeding Microbes Electricity To Convert Carbon Dioxide and Water to Multicarbon Extracellular Organic. *MBio* 1:e00103-10-. doi: 10.1128/mBio.00103-10.Editor
2. Rabaey K, Rozendal RA (2010) Microbial electrosynthesis — revisiting the electrical route for microbial production.pdf. *Nat Rev Microbiol* 8:706–16. doi: 10.1038/nrmicro2422
3. Amils R (2011) Chemolithoautotroph. In: Gargaud M, Amils R, Quintanilla JC, et al (eds) *Encycl. Astrobiol.* Springer Berlin Heidelberg, p 289
4. Ljungdahl LG (1986) The autotrophic pathway of acetate synthesis in acetogenic bacteria. *Annu Rev Microbiol* 40:415–450.
5. Lovley DR (2011) Powering microbes with electricity: direct electron transfer from electrodes to microbes. *Environ Microbiol Rep* 3:27–35. doi: 10.1111/j.1758-2229.2010.00211.x
6. Nevin KP, Hensley SA, Franks AE, et al (2011) Electrosynthesis of organic compounds from carbon dioxide is catalyzed by a diversity of acetogenic microorganisms. *Appl Environ Microbiol* 77:2882–6. doi: 10.1128/AEM.02642-10
7. Marshall CW, Ross DE, Fichot EB, et al (2012) Electrosynthesis of commodity chemicals by an autotrophic microbial community. *Appl Environ Microbiol* 78:8412–20. doi: 10.1128/AEM.02401-12
8. Jiang Y, Su M, Zhang Y, et al (2013) Bioelectrochemical systems for simultaneously production of methane and acetate from carbon dioxide at relatively high rate. *Int J Hydrogen Energy* 38:3497–3502. doi: 10.1016/j.ijhydene.2012.12.107
9. Zaybak Z, Pisciotta JM, Tokash JC, Logan BE (2013) Enhanced start-up of anaerobic facultatively autotrophic biocathodes in bioelectrochemical systems. *J Biotechnol* 168:478–485. doi: 10.1016/j.jbiotec.2013.10.001
10. Su M, Jiang Y, Li D (2013) Production of acetate from carbon dioxide in bioelectrochemical systems based on autotrophic mixed culture. *J Microbiol Biotechnol* 23:1140–6.
11. Zhang T, Nie H, Bain TS, et al (2013) Improved cathode materials for microbial electrosynthesis. *Energy Environ Sci* 6:217. doi: 10.1039/c2ee23350a
12. Nie H, Zhang T, Cui M, et al (2013) Improved cathode for high efficient microbial-catalyzed reduction in microbial electrosynthesis cells. *Phys Chem Chem Phys* 15:14290–4. doi: 10.1039/c3cp52697f
13. Marshall CW, Ross DE, Fichot EB, et al (2013) Long-term operation of microbial electrosynthesis systems improves acetate production by autotrophic microbiomes. *Environ Sci Technol* 47:6023–9. doi: 10.1021/es400341b
14. Jourdin L, Freguia S, Donose BC, et al (2014) A novel carbon nanotube modified scaffold as an efficient biocathode material for improved microbial electrosynthesis. *J Mater Chem A* 2:13093–13102. doi: 10.1039/C4TA03101F
15. Gregory KB, Bond DR, Lovley DR (2004) Graphite electrodes as electron donors for anaerobic respiration. *Environ Microbiol* 6:596–604. doi: 10.1111/j.1462-2920.2004.00593.x
16. Schuchmann K, Müller V (2014) Autotrophy at the thermodynamic limit of life: a model for energy conservation in acetogenic bacteria. *Nat Rev Microbiol* 12:809–821. doi: 10.1038/nrmicro3365
17. Ganigué R, Puig S, Batlle-Vilanova P, et al (2015) Microbial electrosynthesis of butyrate from carbon dioxide. *Chem Commun* 51:3235–3238. doi: 10.1039/C4CC10121A
18. Coppi M V, Leang C, Sandler SJ, Lovley DR (2001) Development of a Genetic System for *Geobacter sulfurreducens*. *Appl Environ Microbiol* 67:3180–3187. doi: 10.1128/AEM.67.7.3180
19. Sharma M, Bajracharya S, Gildemyn S, et al (2014) A critical revisit of the key parameters used to describe microbial electrochemical systems. *Electrochim Acta* 140:191–208. doi: 10.1016/j.electacta.2014.02.111
20. Vega JL, Prieto S, Elmore BB, et al (1989) The Biological production of ethanol from synthesis gas. *Appl*

- 
- Biochem Biotechnol 20-21:781–797. doi: 10.1007/BF02936525
21. Stams AJM, Plugge CM, De Bok FAM, et al (2005) Metabolic interactions in methanogenic and sulfate-reducing bioreactors. *Water Sci Technol* 52:13–20.
  22. Stams AJM (1994) Metabolic interactions between anaerobic bacteria in methanogenic environments. *Antonie Van Leeuwenhoek* 66:271–294.
  23. Avery Jr GB, Shannon RD, Jeffrey R, et al (2003) Controls on methane production in a tidal freshwater estuary and a peatland : methane production via acetate fermentation and CO<sub>2</sub> reduction. *Biogeochemistry* 62:19–37.
  24. Zamanzadeh M, Parker WJ, Verastegui Y, Neufeld JD (2013) Biokinetic and molecular studies of methanogens in phased anaerobic digestion systems. *Bioresour Technol* 149:318–326. doi: <http://dx.doi.org/10.1016/j.biortech.2013.09.058>
  25. van Eerten-Jansen MCAA, Jansen NC, Plugge CM, et al (2015) Analysis of the mechanisms of bioelectrochemical methane production by mixed cultures. *J Chem Technol Biotechnol* 90:963–970. doi: 10.1002/jctb.4413
  26. Clauwaert P, Tolêdo R, van der Ha D, et al (2008) Combining biocatalyzed electrolysis with anaerobic digestion. *Water Sci Technol* 57:575–9. doi: 10.2166/wst.2008.084
  27. Villano M, Aulenta F, Ciucci C, et al (2010) Bioelectrochemical reduction of CO(2) to CH(4) via direct and indirect extracellular electron transfer by a hydrogenophilic methanogenic culture. *Bioresour Technol* 101:3085–90. doi: 10.1016/j.biortech.2009.12.077
  28. Zinder SH, Anguish T, Cardwell SC (1984) Selective Inhibition by 2-Bromoethanesulfonate of Methanogenesis from Acetate in a Thermophilic Anaerobic Digester. *Appl Environ Microbiol* 47 :1343–1345.
  29. Liew FM, Köpke M, Simpson SD (2013) Gas Fermentation for Commercial Biofuels Production.
  30. De Silva Munoz L, Erable B, Etcheverry L, et al (2010) Combining phosphate species and stainless steel cathode to enhance hydrogen evolution in microbial electrolysis cell (MEC). *Electrochem commun* 12:183–186.
  31. Da Silva S, Basséguy R, Bergel A (2004) Electrochemical deprotonation of phosphate on stainless steel. *Electrochim Acta* 49:4553–4561. doi: <http://dx.doi.org/10.1016/j.electacta.2004.04.039>
  32. Soussan L, Riess J, Erable B, et al (2013) Electrochemical reduction of CO<sub>2</sub> catalysed by *Geobacter sulfurreducens* grown on polarized stainless steel cathodes. *Electrochem commun* 28:27–30. doi: 10.1016/j.elecom.2012.11.033
  33. Dumas C, Basseguy R, Bergel A (2008) Microbial electrocatalysis with *Geobacter sulfurreducens* biofilm on stainless steel cathodes. *Electrochim Acta* 53:2494–2500. doi: 10.1016/j.electacta.2007.10.018
  34. Parini MR, Pitt WG (2005) Removal of oral biofilms by bubbles: The effect of bubble impingement angle and sonic waves. *J Am Dent Assoc* 136:1688–1693. doi: 10.14219/jada.archive.2005.0112
  35. Honda T, Murase K, Hirato T, Awakura Y (1998) pH measurement in the vicinity of a cathode evolving hydrogen gas using an antimony microelectrode. *J Appl Electrochem* 28:617–622. doi: 10.1023/A:1003254219905
-



---

C  
H  
A  
P  
T  
E  
R

3

**Application of Gas Diffusion Biocathode in  
Microbial Electrosynthesis from Carbon dioxide**

This chapter is *published as*

Bajracharya S, Vanbroekhoven K, Buisman CJN, Pant D, Strik DPBTB (2016). *Application of Gas Diffusion Biocathode in Microbial Electrosynthesis from Carbon dioxide*. Environ. Sci. Pollut. Res. doi:10.1007/s11356-016-7196-x

---

---

## **Abstract**

Microbial catalysis of carbon dioxide (CO<sub>2</sub>) reduction to multi-carbon compounds at the cathode is a highly attractive application of microbial electrosynthesis (MES). The microbes reduce CO<sub>2</sub> either taking the electrons or the reducing equivalents produced at the cathode. While using gaseous CO<sub>2</sub> as the carbon source, the biological reduction process depends on the dissolution and mass-transfer of CO<sub>2</sub> in the electrolyte. In order to deal with this issue, a gas diffusion electrode (GDE) was investigated by feeding CO<sub>2</sub> through the GDE into the MES reactor for its reduction at the biocathode. A combination of the catalyst layer (porous activated carbon and Teflon binder) and hydrophobic gas diffusion layer (GDL) creates a three-phase interface at the electrode. So, CO<sub>2</sub> and reducing equivalents will be available to the biocatalyst on the cathode surface. An enriched inoculum consisting of acetogenic bacteria, prepared from an anaerobic sludge was used as biocatalyst. The cathode potential was maintained a -1.1 V vs Ag/AgCl to facilitate direct and/or hydrogen mediated CO<sub>2</sub> reduction. Bioelectrochemical CO<sub>2</sub> reduction mainly produced acetate but also extended the products to ethanol and butyrate. Average acetate production rates of 32 mg L<sup>-1</sup>d<sup>-1</sup> and 61 mg L<sup>-1</sup>d<sup>-1</sup> respectively with 20% and 80% CO<sub>2</sub> gas mixture feed were achieved with 10 cm<sup>2</sup> of GDE. The maximum acetate production rate remained 238 mg L<sup>-1</sup>d<sup>-1</sup> for 20% CO<sub>2</sub> gas mixture. In conclusion, gas diffusion biocathode supported bioelectrochemical CO<sub>2</sub> reduction with enhanced mass-transfer rate at the continuous supply of gaseous CO<sub>2</sub>.

**Keywords:** Microbial electrosynthesis, CO<sub>2</sub> reduction, Gas diffusion electrode, Biocathode, Autotrophic Bioproduction



---

### 3.1 Introduction

The accumulation of CO<sub>2</sub> and other greenhouse gases (GHGs) in the atmosphere from the anthropogenic activities in the last two centuries is contributing to global warming and climate change [1, 2]. The atmospheric CO<sub>2</sub> level is projected to increase in the near future as fossil fuels are still supplying the major global energy demand [2]. A sequestration and control of the CO<sub>2</sub> emission can contribute to the mitigation of climate change and its detrimental environmental effects [3]. A shift from fossil resources towards renewable energy and sustainable forms of fuels and chemicals is an urgent need. Renewable energy sources such as wind and sun offer alternatives for electricity, whereas biomass is the main source that supplies a renewable feedstock for chemicals and fuels. Sugars obtained from crops can create debatable competition with priority commodities such as food [4–6]. Meanwhile, the land, water, and fertilizers required to cultivate biomass are scarce. Yet, CO<sub>2</sub> is also a potential carbon resource for biomass available on the earth. In such circumstances, technologies that can convert low-grade lignocellulosic biomass or recycle carbon dioxide (CO<sub>2</sub>) into fuels and chemicals are becoming more attractive. A recent development of bioelectrochemical system known as microbial electrosynthesis (MES) can address the necessity to produce biofuels and bulk to fine chemicals from low-value wastes and even from CO<sub>2</sub> exhausts, for example, from steel industry or biogas or wood heating systems [7, 8]. At the same time, MES converts the excess electricity generated from renewable sources into a storable form.

Bioelectrochemical reduction of CO<sub>2</sub> to multi-carbon organic compounds at the cathode by applying electrical power has become highly attractive in the scientific community. Homoacetogens like *Sporomusa ovata*, *Clostridium ljungdahlii* etc. have been shown to reduce CO<sub>2</sub> to acetate and other multi-carbon compounds accepting the electrons directly from the cathode [9, 10]. Acetate was the primary product, while 2-oxobutyrate, formate [9] and butyrate [11] were also reported. Applied electric energy drives the electrons and protons from anode towards the cathode. The bioelectrochemical reduction of CO<sub>2</sub> can also occur indirectly via electrochemically produced hydrogen when the applied cathode potential is more negative than -0.414 V versus standard hydrogen electrode (vs SHE) [7, 12]. Under anaerobic and highly reductive conditions, acetogenic bacteria utilize CO<sub>2</sub> as a terminal electron-acceptor via the Wood-Ljungdahl pathway, fixing CO<sub>2</sub> mainly into acetate as well as other products such as ethanol, butyrate and butanol etc. [13].

In most of the MES studies that reported acetate production from CO<sub>2</sub>, 2–2.5 g L<sup>-1</sup> sodium bicarbonate as well as 10–100% (v/v) CO<sub>2</sub> gas mixture with N<sub>2</sub> were used as carbon source [11, 14–16] whereas only the bicarbonate (HCO<sub>3</sub><sup>-</sup>) solutions were used as carbon source in few studies [17–19]. However, in order to take the MES system to the real practical application, utilization of CO<sub>2</sub> from exhaust gases would be the target. In this sense, CO<sub>2</sub> capture from diluted exhaust streams and faster dissolution in the electrolyte must be achieved for the application of MES using real waste CO<sub>2</sub>. So far, the process for biological CO<sub>2</sub> reduction with the supply of gaseous CO<sub>2</sub> encompasses lower CO<sub>2</sub> capture since most of the CO<sub>2</sub> supplied by continuous bubbling escapes due to the limited solubility in aqueous medium and low mass-transfer of CO<sub>2</sub> [20]. In order to reduce the escaping of CO<sub>2</sub> from the reactor, gaseous CO<sub>2</sub> feed can be recycled. However, conversion/fixation rates should be increased to maximize CO<sub>2</sub> utilization from the gaseous feeding the MES system. Continuous bubbling using sparger or on-demand injection of CO<sub>2</sub> on aqueous solution is carried out to feed gaseous CO<sub>2</sub> in a system. CO<sub>2</sub> fixation in algal photobioreactors also comprises CO<sub>2</sub> capture in aqueous medium. The maximum CO<sub>2</sub> capture efficiency of only 8.1% was reported for continuous bubbling of 10% CO<sub>2</sub>-air mixture in microalgal culture [21, 22] whereas by on-demand injection of flue gas 32.8% of CO<sub>2</sub> utilization efficiency was reported at optimum microalgal growth condition [23]. A process of capturing CO<sub>2</sub> efficiently from flue gas and also transferring it to microbial culture is necessary to make CO<sub>2</sub> conversion systems efficient.

Capturing of up to 80% of supplied CO<sub>2</sub> from flue gases has been reported by Fernández et al. [24] and González-López et al. [20] using carbonate-bicarbonate buffers of pH 8–10 based on the dynamic equilibrium of bicarbonates with CO<sub>2</sub>. However, CO<sub>2</sub> capture from flue gas based on carbonate-bicarbonate equilibrium is slower than other chemical adsorption processes. Yet, the bicarbonate solution has been the most used aqueous system for CO<sub>2</sub> supply in order to avoid chemical influences to biological systems. Also, in microbial fuel cells (MFCs), slightly alkaline HCO<sub>3</sub><sup>-</sup> solutions were used due to the buffering of pH near the electrode surfaces with CO<sub>2</sub> dissolution [25, 26]. Gas diffusion electrodes (GDEs) were used in the MFCs and electrochemical systems where the gas phase reactant had to react effectively with the liquid phase reactants, also interacting with the solid electrode [27–29]. The combination of hydrophobic and hydrophilic micro-pores in GDE creates a three phase interface (gas–liquid–solid), which ensures abundant availability of the gaseous reactants on the electrode surface [29]. The GDE is a porous composite electrode, usually consisting of a hydrophobic gas diffusion layer (GDL), a current collector (CC) and a catalyst layer (CL) [29, 30]. In MFCs, GDEs were originally used as air cathodes for oxygen reduction [31]. The GDL has a dual function of gas delivery and waterproofing in electrochemical fuel cells. The current density of CO<sub>2</sub> electro-reduction was reported to increase by one to two orders of magnitude using GDEs [30]. In electrochemical CO<sub>2</sub> reduction, GDE with Sn electrocatalyst produced formate attaining up to 2 kA/m<sup>2</sup> with ~90% faradaic efficiency [32].

It can be expected that a GDE as biocathode will help to provide CO<sub>2</sub> to the electrochemically active bacteria attached on the electrode directly on-site at controlled rates minimizing/avoiding the CO<sub>2</sub> mass transfer limitations from solution to the electrode and also within the electrode. At the same time, the wastage of CO<sub>2</sub> will be minimized due to its immediate adsorption and availability to microbes for assimilation. As such, the gas diffusion electrode is expected to fit in MES. Moreover, the size of the micro-pores in GDE can be controlled to maintain appropriate CO<sub>2</sub> diffusion flux depending on bioelectrochemical CO<sub>2</sub> reduction rate.

In this work, investigations on the effect of gaseous CO<sub>2</sub> supply via VITO-CoRE<sup>®</sup> gas diffusion electrode were carried out to address the key question of CO<sub>2</sub> availability at the biocatalytic surface of the cathode. VITO-CoRE<sup>®</sup> GDEs have been shown effective for oxygen reduction when used as air cathode as a low-cost alternative for platinum in microbial fuel cell [33]. Microbial electrosynthesis was studied for the first time with the gas diffusion biocathode and the performance was assessed and compared based on production rates and efficiencies with earlier CO<sub>2</sub> reducing MES studies using submerged electrodes to advocate gas diffusion biocathode as a platform for the electrosynthetic production of fuels and chemicals.

## **3.2 Materials and methods**

### **3.2.1 Determination of gas-liquid mass transfer coefficients**

CO<sub>2</sub> and O<sub>2</sub> dissolution experiments were done to compare the effectiveness of gas supply into the aqueous electrolyte used in MES reactor-(1) by using a conventional gas sparger and (2) by supplying through a gas diffusion electrode. Gas-liquid mass-transfer coefficients ( $k_L a$ ) are used to compare the effectiveness of gas supplies. The pH and dissolved gas concentrations in aqueous solutions were recorded to determine the values of  $k_L a$  for the two methods of gas feeding. The experimental setups and procedures are detailed in the following sub-sections.

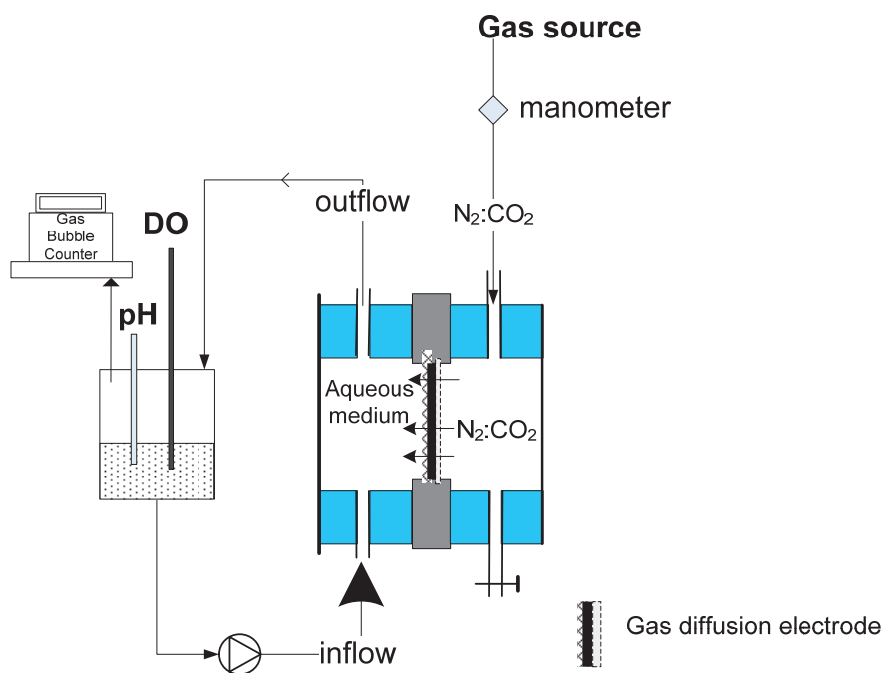
#### *3.2.1.1 Experimental Setup*

A circular shaped flow-cell was assembled keeping a gas diffusion electrode in between two 16 mL compartments created by two rings made of poly-vinylidene difluoride (PVDF), one of which was filled with CO<sub>2</sub> or compressed air and the another was filled with

aqueous solution. CO<sub>2</sub>/compressed air was supplied to the gas chamber of the circular cell at a constant flow rate (50 mL min<sup>-1</sup>).

The aqueous solution used for the gas dissolving experiments contained (g L<sup>-1</sup>): 0.33 KH<sub>2</sub>PO<sub>4</sub>, 0.45 K<sub>2</sub>HPO<sub>4</sub>, 1 NH<sub>4</sub>Cl, 0.1 KCl, 0.8 NaCl, 0.2 MgCl<sub>2</sub>·7H<sub>2</sub>O. A peristaltic pump was used to recirculate 500 mL of aqueous solution between the cell and a recirculation vessel at 180 mL min<sup>-1</sup>. A pressure gauge (manometer) was connected at the gas inlet of the cell. A milli-gas counter was connected at the gas outlet of the recirculation vessel in order to measure the outflow of gas from the recirculation bottle. In the experiment, the dissolved oxygen (DO) and pH probes were inserted into the recirculation bottle containing the aqueous solution. A schematic diagram of the experimental setup is shown in Figure 3.1.

For the comparison purposes, a direct CO<sub>2</sub>/air bubbling test was also carried out using a fish-tank sparger. The flow-cell unit with the GDE was disconnected in this test. The gas feed was maintained at 50 mL min<sup>-1</sup> and the solution was stirred using a magnetic stirrer at 250 rpm.



**Figure 3.1** Schematic of the flow-cell set up used for air/CO<sub>2</sub> dissolution measurement.

### 3.2.1.2 Reaeration test for gaseous mass-transfer rate determination

Determination of CO<sub>2</sub> mass-transfer in the aqueous medium required online measurement of dissolved CO<sub>2</sub>. However, the instrument for dissolved CO<sub>2</sub> measurement was not available during the experiment. Estimations of CO<sub>2</sub> concentration based on pH related models can be possible but the errors in estimation could be large. In contrast, an online measurement device for dissolved oxygen was available with high accuracy of measurement. In addition, the gas-liquid mass-transfer coefficient ( $k_L a$ ) of oxygen (O<sub>2</sub>) can be used to estimate  $k_L a$  of CO<sub>2</sub> based on the diffusivity of the gases. Hence,

reaeration tests were carried out to calculate the mass transfer coefficient ( $k_{La}$ ) of  $O_2$  from air to the aqueous medium using GDE as well as using fish-tank sparger. Previously,  $N_2$  was sparged into the medium to make it deoxygenated. The outflow of gas using milligas counter, DO, pH were recorded at every minute for one hour. Translation of mass transfer coefficients of oxygen to that for  $CO_2$  was carried out using equation (3.4) described in calculation section. Similar method was also reported in several studies such as in Doucha et al. [23] and Hu et al.[34].

### **3.2.2 MES experiments for $CO_2$ reduction using gas diffusion biocathode**

MES experiments were performed to investigate  $CO_2$  reduction using gas diffusion biocathode in a specifically designed reactor (as described in the following sub-sections). At first, inocula for  $CO_2$  reduction were selectively prepared from anaerobic sludge and applied in the MES reactor for the experiments.

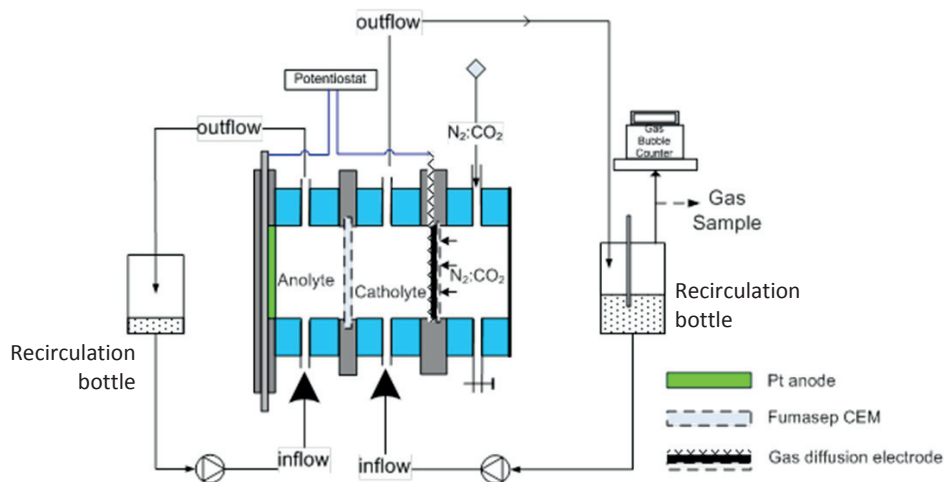
#### *3.2.2.1 Preparing the inoculum: homoacetogenic activity enrichment from wastewater sludge*

The granular sludge from the anaerobic digester was collected. Details about the sludge are available in Mohanakrishna et al. [35]. A four stage selective enrichment methodology (schematized in Supplementary information-Chapter 3 Figure SI-1) was applied to enrich the homoacetogenic activity in the culture. In the first stage, 200 mL of wet sludge in a glass bottle was heated over a thermocouple-controlled hot plate to 90 °C for 1 hour in order to eliminate heat-intolerant methanogens [35, 36]. Only the spore-forming/heat-tolerant bacteria were expected to remain after this heat shock. In the second stage, the heat treated sludge was subjected to heterotrophic growth in a sealed glass bottle using 20 mM glucose as a substrate in the pH 6.0 mineral medium (DSMZ 879) with 2 mM of Sodium 2-bromoethanesulfonate (NaBES-an inhibitor for methanogenesis) under 37 °C to reactivate the whole consortia. The heterotrophically grown culture was shifted to the autotrophic mode by transferring to DSMZ 879 mineral medium providing a gas mixture of  $CO_2$  (20%) and  $H_2$  (80%) which proliferated the homoacetogenic activity under the repeated transferring and growing under  $H_2:CO_2$  (80:20) for four times. Methane production was absent in all the sub-cultures. The culture after four transfers was used as an inoculum for the bioelectrochemical  $CO_2$  reduction in the cathode chamber of the reactor.

#### *3.2.2.2 MES reactor setup*

For the MES experiments, a double chambered microbial electrosynthesis reactor was assembled using three circular cylindrical PVDF rings each of which forms a 16 mL compartment. The first and second ring formed anode and cathode compartments whereas the third ring created a gas supply chamber. A schematic representation of reactor is available in Figure 3.2. The anode and cathode compartments were separated by a Fumasep FKB CEM PEEK<sup>®</sup> reinforced membrane. The counter electrode (anode) was a circular platinum sheet (10 cm<sup>2</sup>) laser-welded to a Titanium (Ti) plate current collector. A VITO-Core<sup>®</sup> GDE (projected surface area of 10 cm<sup>2</sup>) as a cathode [also used in MFC study by [37]] was placed between the second and third compartment with Polytetrafluoroethylene (PTFE) GDL facing the gas compartment and a CL facing the catholyte side. Before placing in the reactor, the GDE and the membrane were boiled at 70 °C for 1 hour in phosphate buffer solution (PBS). Polyvinyl chloride (PVC) tubes (Ø 6/8) connected each compartment to a separate electrolyte bottle for recirculation. A peristaltic pump (Watson Marlow 323U/D) was used for the recirculation. The recirculation rate was 180 mL min<sup>-1</sup>. At the start, the catholyte in the recirculation bottle was maintained anaerobic by flushing with  $N_2$  gas and stirring with a magnetic stirrer (250 rpm). During the experiment,  $CO_2:N_2$  gas mixture fed through GDE maintained the anaerobicity as well as supply  $CO_2$ . An Ag/AgCl (3 M KCl, +205 mV vs SHE) reference electrode (REF321, Radiometer-Analytical) was placed near the cathode. For the

electrochemical measurement, the electrodes were connected to a Potentiostat (VMP3, Biologic Science Instruments, France) in the three-electrode setup; cathode as a working electrode, anode as a counter electrode and Ag/AgCl reference electrode. All potentials are reported with respect to Ag/AgCl throughout this paper unless stated otherwise.



**Figure 3.2:** Experimental setup for MES reactor with gas diffusion biocathode.

### 3.2.2.3 Electrolytes

The medium used for the start-up phase of the study was a phosphate buffer solution (PBS) composed of ( $\text{g L}^{-1}$ ): 0.33  $\text{KH}_2\text{PO}_4$ , 0.45  $\text{K}_2\text{HPO}_4$ , 1  $\text{NH}_4\text{Cl}$ , 0.1  $\text{KCl}$ , 0.8  $\text{NaCl}$ , 0.2  $\text{MgSO}_4 \cdot 7\text{H}_2\text{O}$ , and 1 yeast extract, which was supplemented with 20  $\text{mL L}^{-1}$  vitamin solution (DSMZ 141), 20  $\text{mL L}^{-1}$  trace element solution (DSMZ 141) and 4  $\text{g L}^{-1}$  sodium bicarbonate prior to operation. The media was prepared anaerobically by purging  $\text{N}_2$  gas. During the MES from  $\text{CO}_2$  experiments, yeast extract was removed from the medium due to its possible contribution in redox mediating and electron donating properties [38]. The media not containing yeast extract, henceforward, is called mineral media. During the start-up phase, 5 mM additional fructose was added as substrate. In the microbial electrosynthesis phase, fructose was removed and only the mineral media was used as the catholyte. The anolyte was constituted by the acidified mineral medium of pH 3–4 maintained by adding 1 M HCl. pH was measured using a purpose-built multi-meter (wtw 340i, Germany). The pH of the catholyte was adjusted to 7 at the start of the experiment and the reactor temperature was maintained at 30 °C by heating the electrolyte in recirculation bottle on a thermocouple-controlled hot plate.

### 3.2.2.4 Start-up and operation of $\text{CO}_2$ reduction in MES reactor

After setting up, the MES reactor with GDE as a cathode was started with 500 mL of catholyte recirculated at  $120 \text{ mL min}^{-1}$  between the reactor and a glass container. The reactor was inoculated with 10% V/V enriched bacterial culture from the wastewater sludge as mentioned previously. In the cathode chamber, at first bacterial growth with 5 mM fructose was carried out and then the catholyte was replenished with new catholyte to follow an acclimation batch for 28 days with  $\text{N}_2:\text{CO}_2:\text{H}_2$  (80:13:7) feed at the cathode potential from -0.7 to -0.8 V vs Ag/AgCl using the Chronoamperometry (CA) technique.

---

This batch was intended for the adaptation for autotrophic growth and microbial electrochemical activity. The steps followed for MES reactor start-up and operation are schematized in Supplementary information-Chapter 3 Figure SI-2. After day 28, tests for acetate production by CO<sub>2</sub> reduction at -0.8 and -1 V vs Ag/AgCl cathode potentials were carried out by supplying CO<sub>2</sub>:N<sub>2</sub> (20:80). However, in order to avoid the limitations due to reduction potentials, a cathode potential of -1.1 V vs Ag/AgCl was chosen for next batches.

After the start-up/acclimation phase of 58 days, the catholyte was replaced by 450 mL of fresh catholyte, retaining around 50 mL of the previous electrolyte as inoculum. MES operation with CO<sub>2</sub>:N<sub>2</sub> (20:80) gas feeding through the GDE was carried out by polarizing the cathode at -1.1 V vs Ag/AgCl. Sufficiently low cathode potential of -1.1 V vs Ag/AgCl was maintained in order to allow H<sub>2</sub> evolution. Since bioelectrochemical CO<sub>2</sub> reduction in MES by using mixed culture are reported mainly at lower cathode potential than H<sub>2</sub> evolution-onset potential and H<sub>2</sub> was reported to mediate CO<sub>2</sub> reduction [14, 18, 39]. An overpressure of 100-150 mbar was maintained in the CO<sub>2</sub> gas supply chamber in order to pass the gas through the GDE to the cathode chamber. The reduction current was recorded every 10 minutes. Two batches termed as Batch 1 (day 58 -199 500 mL catholyte) and Batch 2 (day 199-240 with 600 mL catholyte) of MES operation were carried out with CO<sub>2</sub> and N<sub>2</sub> gas mixture feed through the GDE. In the Batch 1, from day 58 to day 120, a gas mixture of CO<sub>2</sub> and N<sub>2</sub> (20:80) was fed and for the rest of the operation (80:20) CO<sub>2</sub>:N<sub>2</sub> was fed.

#### 3.2.2.5 Samplings and chemical analyses

The 3-5 mL of catholyte was sampled in every 2-3 day for the analysis of short-chained volatile fatty acids (VFAs) and ethanol. To maintain a constant catholyte volume, the sampled volume was replaced by the same volume of the mineral medium described earlier in the electrolyte section. The pH of the sample was measured and whenever it increased above 7.5, 1 M HCl was added to lower it.

For the analysis of formic acid, acetic acid, propionic acid, butyric acid and ethanol, the cell-free supernatants were analyzed in Agilent 1200 series HPLC with an Agilent Hi-Plex H column and an Agilent 1260 infinity refractive index detector. The column eluted at 60 °C with 0.01 M sulfuric acid as the mobile phase with the flow rate of 1 mL min<sup>-1</sup>. The detector temperature was 55 °C.

Gas samples were collected by using a gas-tight plastic syringe and analyzed in a GC (Trace GC Ultra, Thermo Scientific) equipped with a thermal conductivity detector (TCD). H<sub>2</sub> content was analyzed with a 2 m stainless steel column packed with a molecular sieve 5A (80/100 mesh) using nitrogen as carrier gas at a flow rate of 20 mL min<sup>-1</sup>. The CO<sub>2</sub>, O<sub>2</sub>, N<sub>2</sub> and CH<sub>4</sub> gases were analyzed with a 2 m stainless steel HayeSep Q (80/100 mesh) and molecular sieve 5A (80/100 mesh) columns. Helium was used as carrier gas at 15 mL min<sup>-1</sup> flow rate.

## 3.3 Calculations

### 3.3.1 Mass transfer coefficient determination

The mass transfer of gas into aqueous medium is proportional to the interfacial area and the concentration difference. Hence,

$$\text{Rate of mass transferred per unit time} = k (\text{interfacial area}) (\text{concentration difference}) \quad (3.1)$$

Where  $k$  is the proportionality constant and is the mass transfer coefficient in  $\text{m}^3$  per hour per  $\text{m}^2$ . When divided both sides of the equation by interface area and volume of liquid, the equation can be written as

$$\text{Mass transfer rate per unit area per unit volume } (R) = k_L a (C^* - C_t) \quad (3.2)$$

Where  $k_L a$  is the mass transfer coefficient independent of the interface area and volume of the aqueous medium;  $C^*$  is saturation concentration of the particular dissolved gas at the interface and  $C_t$  is the dissolved gas concentration in bulk at any time 't'. At the interface, the aqueous medium can be considered at saturation.

From the mass balance,

Rate of gas accumulation = Mass transfer rate from gas phase - consumption rate

When there is no consumption, accumulation is equal to mass transfer rate

$$d(V C_t)/dt = k_L a (C^* - C_t) V$$

For a constant volume of aqueous solution, the  $dC/dt$  equation can be written as

$$dC_t/dt = k_L a (C^* - C_t)$$

where  $k_L a$  is volumetric mass transfer coefficient.

$$\int dC_t/(C^* - C_t) = k_L a \int dt$$

After integration over time from start 0 to  $t$ ,

$$\ln(C^* - C_t) - \ln(C^* - C_0) = -k_L a t$$

$$\ln(C^* - C_t) = -k_L a t + \ln(C^* - C_0) \quad (3.3)$$

The plot of  $\ln(C^* - C_t)$  versus time gives a straight line, the slope of the line provides the  $k_L a$  value for a gas in aqueous solution. Mass transfer coefficient  $O_2$  from air was determined from the aeration experiment on deoxygenated buffer solution.  $k_L a$  for oxygen (air) can be determined from the plot of DO values in equation (3.3). For deoxygenated buffer initial DO ( $C_0$ ) = 0  $\text{mg L}^{-1}$  and at 25°C and 1 atm pressure, DO saturation concentration ( $C^*$ ) = 8  $\text{mg L}^{-1}$ .

### **CO<sub>2</sub> mass transfer coefficient**

The  $k_L a$  value for  $CO_2$  can be obtained from the  $k_L a$  value of air using the following equation,

$$\frac{(k_L a)^{CO_2}}{(k_L a)^{air}} = \left( \frac{D_L^{CO_2}}{D_L^{air}} \right)^{0.5} \quad [23, 34, 40] \quad (3.4)$$

Where  $D_L$  denotes the diffusion coefficient of respective gas.  $D_L^{CO_2}$  at 25 °C = 0.0000177  $\text{cm}^2 \text{s}^{-1}$  and  $D_L^{air}$  at 25 °C = 0.00002  $\text{cm}^2 \text{s}^{-1}$  [41]

### 3.3.2 MES experiments for CO<sub>2</sub> reduction

#### 3.3.2.1 Rate of production

Various reduction products i.e. hydrogen, acetate, propionate, butyrate, methane and ethanol are possible in MES. In batch mode, production of any reduced compound  $i$  (in mol) at any time  $t$  was calculated as per equation 3.5:

$$n_{i,t} = V_{cat} \times (C_{i,t} - C_{i,t-1}) / M_i \quad (3.5)$$

subscripts  $i$  refer to any reduced compound, subscripts  $t$  and  $t-1$  refer to two subsequent samples,  $n$  is the number of moles of the reduced compound produced,  $V_{cat}$  is the total volume of the catholyte (L),  $C$  is the concentration of the compound (mg L<sup>-1</sup>), whereas  $M$  is its molecular weight (mg mol<sup>-1</sup>).

The rate of production of reduced compound in mg L<sup>-1</sup> d<sup>-1</sup> is given by equation 3.6:

$$P_{i,t} = (C_{i,t} - C_{i,t-1}) / \Delta t \quad (3.6)$$

$\Delta t$  being the time difference (in d) between sample time  $t$  and previous sample time  $t-1$

#### 3.3.2.2 Coulombic efficiency

Coulombic efficiency (CE), also named current efficiency, is the efficiency of capturing the electron from the electric current to the product(s) and was calculated using equation 3.7 based on [42]:

$$\text{Current efficiency in } \%, \eta_e = \frac{n_{i,t} \times f_{e,i} \times F}{\int_{t-1}^t I dt} \times 100 \quad (3.7)$$

Where  $n_{i,t}$  is the moles of the product  $i$  analysed at time  $t$ ,  $f_{e,i}$  represent the molar conversion factor (8 electron equivalent per mol for acetate),  $F$  is faraday constant (96,485 C mol<sup>-1</sup> of electron) and  $I$  is the current (A). In this study, mainly the acetate production was considered for coulombic efficiency calculations. Coulombic efficiencies at every measurement point of acetate concentration were calculated based on the accumulating product (acetate) concentrations. Additionally, CE was calculated for instantaneous time interval based on the difference of acetate concentrations between two consecutive measurements within a batch operation.

#### 3.3.2.3 CO<sub>2</sub> transfer rates

Based on the  $k_L a$  values, CO<sub>2</sub> mass-transfer rate in grams of CO<sub>2</sub> per unit time can be expressed as

$$R_{CO_2} = k_L a (f \times C^* - C_t) V \quad (3.8)$$

Where  $R_{CO_2}$  is the mass-transfer rate of CO<sub>2</sub> (in g CO<sub>2</sub> per unit time,  $f$  is the fraction of CO<sub>2</sub> in the supplied gas mixture,  $C^*$  is the saturation concentration of CO<sub>2</sub> in g L<sup>-1</sup> at the experimental condition,  $C_t$  is the dissolved concentration of CO<sub>2</sub> in g L<sup>-1</sup> at any given time  $t$ , and  $V$  is the working volume of the liquid phase. A maximum CO<sub>2</sub> mass-transfer rate occurs when the liquid phase is completely deficient of dissolved CO<sub>2</sub> ( $C_t = 0$ ) and the process becomes mass-transfer limited. Hence, the gas to liquid mass transfer rate per unit volume of liquid phases can be calculated given by

$$R_{CO_2, max} = k_L a \times f \times C^* \quad (3.9)$$

Where  $R_{CO_2, max}$  has the unit of g CO<sub>2</sub> L<sup>-1</sup> per unit time.



### 3.3.2.4 CO<sub>2</sub> consumption rates in acetate and biomass production

On the basis of the organic compounds production rate in the MES reactor, CO<sub>2</sub> fixation rate can be calculated. Mainly acetate was produced from bioelectrochemical CO<sub>2</sub> reduction. A mole of acetic acid (C<sub>2</sub>H<sub>5</sub>O<sub>2</sub>, molecular weight 60 g mol<sup>-1</sup>) production is equivalent to 2 moles of CO<sub>2</sub> fixation. Additionally, in the case of chemolithoautotrophic microbes producing acetate from CO<sub>2</sub> and H<sub>2</sub>, 5% of the carbon flux was considered to account the cell biomass [43]. One mole of cell biomass CH<sub>2.08</sub>O<sub>0.53</sub>N<sub>0.24</sub> (molecular weight = 26 g mol<sup>-1</sup>) [44] is equivalent to a mole of CO<sub>2</sub> fixation.

Hence, CO<sub>2</sub> consumption rate in g L<sup>-1</sup> per unit time = 1.05 \* acetate production rate in g L<sup>-1</sup> per unit time x 2/60 x 44  
(3.10)

The maximum electron available in the MES reactor provided from the electrical current can be compared to the moles of electron recovered in the cell biomass and acetate produced. One mole of acetic acid is equivalent to 8 moles of electron. Using a molecular formula for cell biomass of CH<sub>2.08</sub>O<sub>0.53</sub>N<sub>0.24</sub>, one mole of cell biomass will be equivalent to 4.3 moles of electron [43, 44],

The optical density (OD) of a cell culture medium is generally used as an equivalent parameter for the dry cell concentration in the medium. Taking a model anaerobic acetogenic bacterium *Moorella thermoacetica* culture, for which 1 OD was found to be equivalent to ~0.46 g dry cell L<sup>-1</sup> [45], the total electron moles captured in cell biomass in terms of OD will be 4.3 x OD x 0.46/26. Thus, the total amount of electron moles captured in cell biomass and acetate can be expressed as

$$\text{Moles } e^- \text{ equivalent assimilated} = (4.3 \times \text{OD} \times 0.46/26 + 8 \times C_{\text{acetic acid}}/60) \times V \quad (3.11)$$

## 3.4 Results and discussion

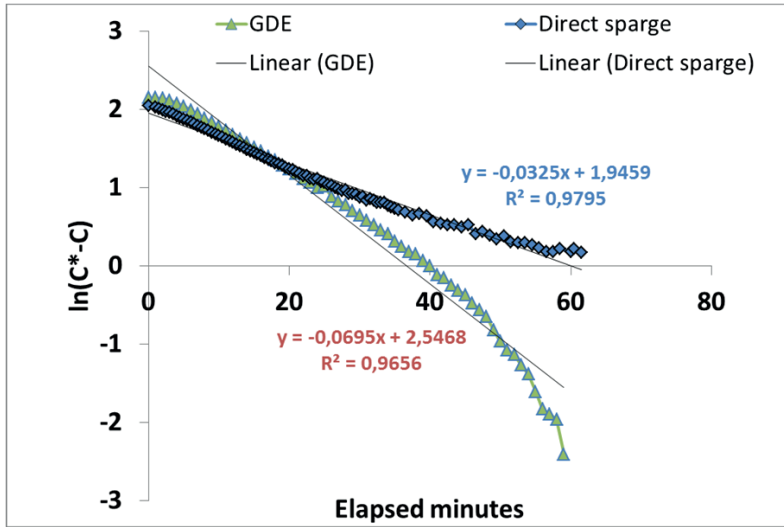
### 3.4.1 Gas diffusion electrode enhanced gas-liquid mass transfer over conventional spargers

To assess the  $k_{La}$  for O<sub>2</sub> dissolution from air, reaeration tests were performed on anaerobic aqueous buffer solution at ambient pressure and temperature; the dissolved oxygen concentrations were monitored every minute.  $k_{La}$  for direct air sparging by using conventional sparger and  $k_{La}$  for air supply by using the gas diffusion electrode in the circular test flow-cell were separately determined. The plots of  $\ln(C^*-C)$  versus time for both the tests are shown in Figure 3.3. The slopes of the fitted straight lines estimate the  $k_{La}$  values (given in Table 3.1).

**Table 3.1:** Comparative estimates of  $k_{La}$  values for conventional sparger and GDE at same gas feed rate

| Parameters  | Conventional sparger | GDE    |
|---|----------------------|--------|
| $k_{La}$ for O <sub>2</sub> from aeration experiment (h <sup>-1</sup> )             | 1.95                 | 4.17   |
| Estimated $k_{La}$ for CO <sub>2</sub> (h <sup>-1</sup> )                           | 1.81                 | 3.92   |
| Max. CO <sub>2</sub> transfer rate at 25 °C (mg L <sup>-1</sup> min <sup>-1</sup> ) | 42.14*               | 91.53* |

\*Calculated from [46] considering  $1.4 \text{ g L}^{-1}$  saturation concentration at  $25 \text{ }^\circ\text{C}$  with 100%  $\text{CO}_2$  feed at normal pressure



**Figure 3.3:** Plot of  $\ln(C^*-C_t)$  vs time for  $\text{O}_2$  dissolution from aeration in phosphate buffer using conventional sparger (diamonds) and using GDE (triangles). The slopes of trend lines give the  $k_L a$  values for the corresponding gas supply method. Therefore,  $k_L a$  for GDE =  $0.069 \text{ min}^{-1}$  and  $k_L a$  for sparger =  $0.0325 \text{ min}^{-1}$ .

Reaeration experiment showed that the  $k_L a$  for  $\text{O}_2$  (air) in GDE setup was  $4.17 \text{ h}^{-1}$ . When this  $k_L a$  was interpolated for  $\text{CO}_2$  on the basis of diffusivities of  $\text{O}_2$  and  $\text{CO}_2$  molecules [23, 46, 47],  $k_L a$  for  $\text{CO}_2$  using GDE was estimated to be  $\sim 4 \text{ h}^{-1}$  which was at least double than the  $k_L a$  with conventional sparger ( $1.8 \text{ h}^{-1}$  for  $\text{CO}_2$ ).

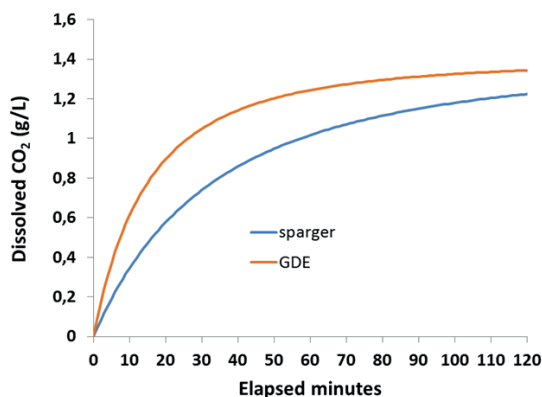
Based on the  $k_L a$  value determined for GDE, the mass transfer rate of  $\text{CO}_2$  can reach the maximum value of  $91.53 \text{ mg L}^{-1} \text{ min}^{-1}$  (Table 3.1) given that the initial dissolved  $\text{CO}_2$  concentration in the solution is zero and the saturation concentration at  $25 \text{ }^\circ\text{C}$  with 1 atm  $\text{CO}_2$  partial pressure is  $1.4 \text{ g L}^{-1}$ . Furthermore, using the estimated values of  $k_L a$ , the concentration of dissolved  $\text{CO}_2$  in the aqueous solution during the feeding can be modeled according to the equation

$$[\text{CO}_2]_t = [\text{CO}_2]_0 + V_{MTR, t} \times t \quad (3.12)$$

where,  $V_{MTR, t}$  is the rate of mass transfer at any time  $t$  given by the relation based on [46]

$$V_{MTR, t} = k_L a ([\text{CO}_2]^* - [\text{CO}_2]_t) / [(k_L a \times t / 2) + 1] \quad (3.13)$$

The plot of equation (3.12) gives the modeled trends of dissolved  $\text{CO}_2$  in the aqueous solution during the supply of  $\text{CO}_2$  via a conventional sparger and via a GDE as shown in Figure 3.4. It can be observed from the plot that with GDE the saturation concentration can be attained faster than using the sparger.



**Figure 3.4:** Modeled profiles (based on equation 3.12) of dissolved  $\text{CO}_2$  in aqueous solution from the time of start of 100%  $\text{CO}_2$  supply. The calculated  $k_{L,a}$  values for conventional sparger and GDE were used to estimate the dissolved  $\text{CO}_2$ . Saturation level can be quickly attained in GDE than in conventional sparger.

When the gas feed rate remains fixed, the gas-liquid interface area plays an important role in the mass transfer of gas to liquid. The interfacial surface area is related to the mean gas bubble size when the gas is bubbled into the aqueous medium [48]. The hydrophobic micropores in the GDE can create smaller bubbles or formed larger interfacial surface area than the conventional sparger, which gave high  $k_{L,a}$  for GDE. However, it should also be considered that the stirring of aqueous medium increases the mass transfer rate since fast stirring prolongs the gas contact time in the aqueous medium [47]. In case of the conventional sparging experiment, the solution was mixed by stirring at 250 rpm using magnetic stirrer and in the case of GDE setup the mixing was carried out with the recirculation of solution at 180 mL  $\text{min}^{-1}$ . Additionally, the recirculation of the aqueous solution in GDE setup also refreshed the gas-liquid interface at the GDE introducing more turbulence. Hence, the gas feed through GDE appeared more effective for gas-liquid mass transfer rate.

### 3.4.2 Volatile Fatty Acids and alcohols production via bioelectrochemical $\text{CO}_2$ reduction with GDE

#### 3.4.2.1 Acclimation to bioelectrochemical $\text{CO}_2$ reduction

During the batch operation with  $\text{N}_2:\text{CO}_2:\text{H}_2$  feed in the start-up phase at -0.7 to -0.8 V vs Ag/AgCl, the OD of catholyte reached 0.314 and the total chemical oxygen demand (COD) increased from 1.58  $\text{g L}^{-1}$  initially to 2.18  $\text{g L}^{-1}$  on day 28. The increase in COD was used to indicate that the organic compounds produced solely from  $\text{CO}_2$ , not a conversion from other organic products. That means, the bioproduction of organic compounds from  $\text{CO}_2$  accounted to 0.6  $\text{g L}^{-1}$  of COD during that period. The measured VFAs ( $\text{C}_1\text{-C}_4$ ) and ethanol in the catholyte on day 28 is equivalent to the COD of 1.11  $\text{g L}^{-1}$ . Thus, the remaining COD (2.18-1.11 = 1.07  $\text{g L}^{-1}$ ) most likely corresponds to the cell-biomass present in the reactor on day 28 which will be equivalent to 0.87  $\text{g biomass L}^{-1}$  [biomass =  $\text{CH}_{2.08}\text{O}_{0.53}\text{N}_{0.24}$  [43]]. The change in acetate concentration from 0.52  $\text{g L}^{-1}$  to 0.98  $\text{g L}^{-1}$  was observed during these 28 days long adaptation batch. The acetate production rates were slower although  $\text{H}_2$  containing gas mixture [ $\text{N}_2:\text{CO}_2:\text{H}_2$  (80:13:7)] was fed.

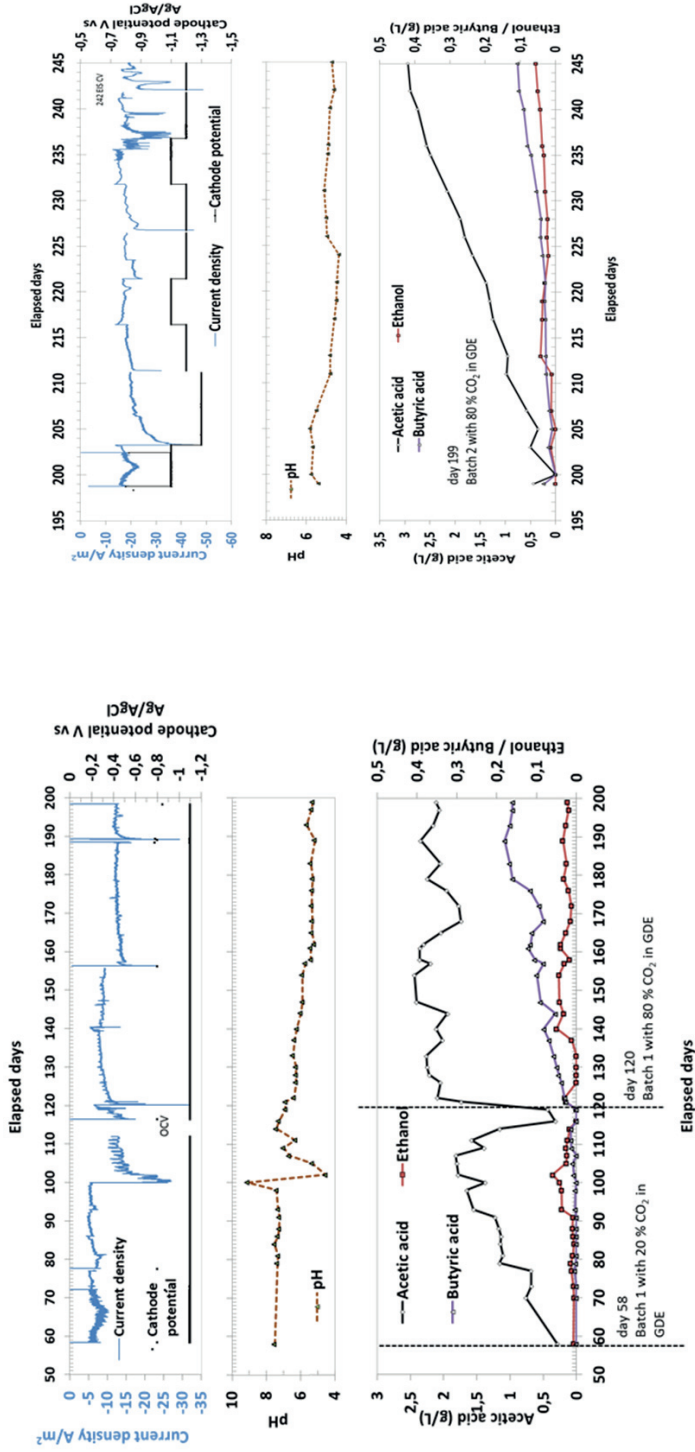
---

After day 28, electricity-driven acetate production was tested in MES at -0.8 and -1 V vs Ag/AgCl cathode potentials by supplying CO<sub>2</sub>:N<sub>2</sub> (20:80) over the GDE. During -0.8 V cathode polarization, acetate was produced in some period but degraded in subsequent period. A clear accumulating trend was not observed. Acetate production was observed significantly accumulating to 2.2 g L<sup>-1</sup> only after the cathode polarized to -1 V vs Ag/AgCl.

#### 3.4.2.2 Production batches from bioelectrochemical CO<sub>2</sub> reduction

After 58 days of start-up/acclimation phase, the MES reactor was operated in Batch 1 with a fresh new catholyte fed with a CO<sub>2</sub>:N<sub>2</sub> (20:80) gas mixture. Since bioelectrochemical CO<sub>2</sub> reduction in MES has been reported consistently at hydrogen evolving potential [14, 15, 18], a sufficiently low cathode potential of -1.1 V vs Ag/AgCl was maintained in order to allow hydrogen evolution. Since it was aimed to assess GDE as effective biocathode on the basis of improvement in CO<sub>2</sub> transfer and acetate production rates, the limiting effects of cathode potential were minimized by polarizing cathode to -1.1 V vs Ag/AgCl. Furthermore, the recent literature on CO<sub>2</sub> reduction in MES emphasized the requirement of hydrogen for CO<sub>2</sub> reduction and also showed that hydrogen mediation is the only way to achieve higher acetate production rates from bioelectrochemical CO<sub>2</sub> reduction [49, 50]

The regular analysis of catholyte samples showed a gradual increase of acetate concentration. The current, pH and identified organic products formed at the cathode along the operation can be seen in Figure 3.5. Under the potentiometric control of cathode potential at -1.1 V vs Ag/AgCl, the current recorded remained between -6 to -10 A m<sup>-2</sup> around neutral pH. This current was partly assimilated into hydrogen and partly into acetate via CO<sub>2</sub> reduction. Under the feed of (20 : 80) CO<sub>2</sub>:N<sub>2</sub>, the instantaneous acetate production rate reached the highest rate of 238 mg L<sup>-1</sup> d<sup>-1</sup> (119 g m<sup>-2</sup> d<sup>-1</sup>) and the acetate accumulated in the catholyte up to 2 g L<sup>-1</sup> on day 109. The average rate of acetate accumulation from the start of the 20% CO<sub>2</sub> feed to the day of maximum concentration was 32 mg L<sup>-1</sup> d<sup>-1</sup> (16 g m<sup>-2</sup> d<sup>-1</sup> surface area based). Besides acetate, ethanol and butyrate were, also detected in the catholyte samples. The concentrations were lower (< 50 mg L) compared to acetate, though when the catholyte pH went accidentally to 4.5, the ethanol concentration increased up to 59 mg L<sup>-1</sup> (day 102).



**Figure 3.5:** Operation of CO<sub>2</sub> reduction in MES with gas diffusion cathode in Batch 1(Left) and Batch 2 (Right). Bioelectrochemical reduction of CO<sub>2</sub> produced acetic acid along with ethanol and butyrate (Bottom) in the catholyte. Current densities at respective cathode potentials (Top) and resulting pH of catholyte (Middle) are associated to the MES operation.

From day 112 to 117, there was no applied potential on the cathode as the run-time of electrochemical technique programmed in the potentiostat finished and the reactor went on to open circuit voltage (OCV). At OCV, the reducing equivalents were not available from the cathode, however, the gas mixture of 20% CO<sub>2</sub> was still fed into the reactor. In the products graph from Figure 3.5, a decline in the concentration of acetate during the OCV can be observed. This means that when there were not enough reducing equivalents available, the products of CO<sub>2</sub> reduction started to be degraded or converted to other non-measured forms. Indeed, the heat-treated mixed culture from wastewater might contain syntrophic acetate-oxidizing species or even sulfate reducers which can oxidize acetate [51]. Remarkably, methane was not detected in the headspace of the reactor (Table 3.2). Methanogenic activities might have been inhibited in our case due to the heat shock and higher dose of Na-BES treatment during the selection procedures for acetogens. Patil et al. [16] also mentioned that the selection pressure (H<sub>2</sub>:CO<sub>2</sub>) for acetogenic activity during the pre-enrichment was effective in avoiding methanogenic activity at least for two month of MES operation producing acetate from CO<sub>2</sub> and electric current.

**Table 3.2:** *Headspace gas composition on different days of whole MES experiment with GDE*

| Measurement day | Operation stage | Supplied CO <sub>2</sub> :N <sub>2</sub> composition | % (v/v) in headspace |                |                |                 |                |
|-----------------|-----------------|--|----------------------|----------------|----------------|-----------------|----------------|
|                 |                 |  | CO <sub>2</sub>      | O <sub>2</sub> | N <sub>2</sub> | CH <sub>4</sub> | H <sub>2</sub> |
| <b>92</b>       | Batch 1         | 20:80  | 19                   | 1              | 79             | nd              | 0.18           |
| <b>109</b>      | Batch 1         | 20:80  | 19                   | 0              | 78             | nd              | 1              |
| <b>171</b>      | Batch 1         | 80:20  | 62                   | 4              | 32             | nd              | 2              |
| <b>200</b>      | Batch 2         | 80:20  | 72                   | 1              | 22             | nd              | 3              |
| <b>221</b>      | Batch 2         | 80:20  | 73                   | 1              | 23             | nd              | 3              |

nd: not detected (detection limit 0.01 %)

After the product concentration declined, from the day 118 cathode potential was retained to -1.1 V vs Ag/AgCl and the 20% CO<sub>2</sub> gas feed was replaced by 80% CO<sub>2</sub> feed. As soon as the 80% CO<sub>2</sub> mixture was fed to the reactor, acetate concentration increased to 2.09 g L<sup>-1</sup> in 2 days. At this stage, the fastest acetate production rate of 650 mg L<sup>-1</sup> d<sup>-1</sup> was achieved. But the increase in electron equivalents from the electric current between day 121 to day 122 were lower than the increase in electron equivalents in the accumulated acetate during that period (Figure 3.6 day 121-122). That means the electron equivalents might be supplemented from the unknown source or cell biomass degradation. Thus, the acetate production rate of 650 mg L<sup>-1</sup> d<sup>-1</sup> was most likely contributed from the reappearance of the acetate that was lost/converted to the unknown compounds or cell biomass during the open circuit period. Moreover, the calculated instantaneous coulombic efficiency at this time was higher than 100% (data not shown). Further on, the acetate concentration slowly increased to reach 2.5 g L<sup>-1</sup> with 80% CO<sub>2</sub> feed. The average acetate production rate during 80% CO<sub>2</sub> feed reached 21 mg L<sup>-1</sup> d<sup>-1</sup> (equivalently to 10.5 g m<sup>-2</sup> d<sup>-1</sup>) which was lower than the average acetate production rate during 20% CO<sub>2</sub> feed (32 mg L<sup>-1</sup> d<sup>-1</sup>). For 80% CO<sub>2</sub> supply, higher production of acetate could be expected with more CO<sub>2</sub> availability for reduction but was not observed during the first operation phase with 80% CO<sub>2</sub> at -1.1 V cathode potential.

Additionally, the acetate production was not continuously occurring even at high CO<sub>2</sub> partial pressure (80% CO<sub>2</sub>). However, the production of ethanol and butyrate was more prominent in this period of MES operation. This indicates that the accumulation of acetate in the long run of MES can shift the production pattern and the process parameters other than CO<sub>2</sub> partial pressure in the reactor become limiting in acetate production. Notably, the headspace gas analysis showed up to 4% of oxygen on day 171 due to accidental air intrusion into the reactor, which might be unfavorable for the strict anaerobes and hence, the acetate concentration declined.

The pH of the catholyte during the Batch 1 operation with 80% CO<sub>2</sub> feed decreased from 7 to 5.5 on day 160 due to the higher partial pressure of supplied CO<sub>2</sub>. At the same time, the decreasing pH could enhance the hydrogen evolution. It was observed from the production graph in Figure 3.5 that butyrate and ethanol were formed while pH was decreasing. The fastest rate of butyrate production reached 22 mg L<sup>-1</sup> d<sup>-1</sup> and the average rate was 2-3 mg L<sup>-1</sup> d<sup>-1</sup> when the pH remained 5.5. As mentioned in the literature, pH values of catholyte substantially affect the production rates and product distribution from CO<sub>2</sub> reduction electrochemically [52] as well as bioelectrochemically [11, 53]. This decrease in the pH of the catholyte might be due to CO<sub>2</sub> dissolution effect as well as the accumulation of a large fraction of undissociated acetic acid. Due to the inhibitory effect of the undissociated acetic acid, the bacterial metabolism could have shifted to the production of butyrate and ethanol from acetic acid. Thus, solventogenesis [45, 54, 55] and subsequent chain elongation [11, 56] mechanisms could be responsible for the production of ethanol and butyrate in the MES from CO<sub>2</sub>. Hence, in the mixed culture microbial community, the metabolism and the dominant species might differ with varying conditions like pH and dissolved CO<sub>2</sub> availability.

On day 199, the catholyte was replaced by fresh minimal medium not containing bicarbonate and Batch 2 operation of the MES started with 80% CO<sub>2</sub> feed through GDE. Acetate and butyrate production was repeated in this batch with pH slowly decreasing from 6 to 5. Figure 3.5 (right) shows the trends of products, electric current, and pH in this batch operation. Maximum acetate concentration of 2.89 g L<sup>-1</sup> was accumulated in about 45 days of operation during this batch which corresponded to acetate production rate of 61 mg L<sup>-1</sup> d<sup>-1</sup> (36.6 g m<sup>-2</sup> d<sup>-1</sup>). The maximum measured rate was 166 mg L<sup>-1</sup> d<sup>-1</sup> (99.6 g m<sup>-2</sup> d<sup>-1</sup>) on day 203. Acetate production trend in this batch can be considered as uniformly rising when the cathode potential was maintained mostly at -1.1 to -1.2 V to create sufficient cathode potential for hydrogen evolution. The stable currents density remained around -20 A m<sup>-2</sup> in Batch 2 which was double than the current densities in Batch 1. Most probably, due to the inactive bacterial biomass deposition on the cathode surface, overpotential might increase in the GDE which limits the stabilization current at -20 A m<sup>-2</sup> even at -1.3 V cathode potential and decreasing pH. The acetate production rate in batch 2 with 80% CO<sub>2</sub> feeding was almost double than the rate attained with 20% CO<sub>2</sub>. Although the CO<sub>2</sub> feed in batch 2 was four times concentrated, the acetate production rates did not increase proportionally. The rate of acetate production did not only depend on the CO<sub>2</sub> supply, but also on the cathode potential which was more negative in batch 2 that can enhance the bioelectrochemical CO<sub>2</sub> reduction. On the contrary, when the cathode potential was -1.1 V in the batch 1 operation, the acetate production rate was lower even at 80% CO<sub>2</sub> gas mixture feed than at 20% CO<sub>2</sub> mixture feed. Hence, under these findings, it can be speculated that the bioelectrochemical CO<sub>2</sub> reduction was not yet limited by CO<sub>2</sub> partial pressures for this MES system with the prevailing microbial activity. Based on the mass transfer coefficients, Supplementary information-Chapter 3 Table SI-3 is provided with the estimations of maximum CO<sub>2</sub> assimilation rates and corresponding acetate production rates under 10, 20 and 80% CO<sub>2</sub> gas mixtures feed to MES with GDE. These CO<sub>2</sub> transfer rates can be supported only when CO<sub>2</sub> is a limiting condition and other factors including reducing equivalents and bacterial activity are non-limiting. The dissolved CO<sub>2</sub> concentration under continuous 20% CO<sub>2</sub> supply still provide sufficient dissolved CO<sub>2</sub> to support a maximum acetate production rate of 8.98 g acetate L<sup>-1</sup> d<sup>-1</sup> even if 50% of supplied CO<sub>2</sub> used in biomass

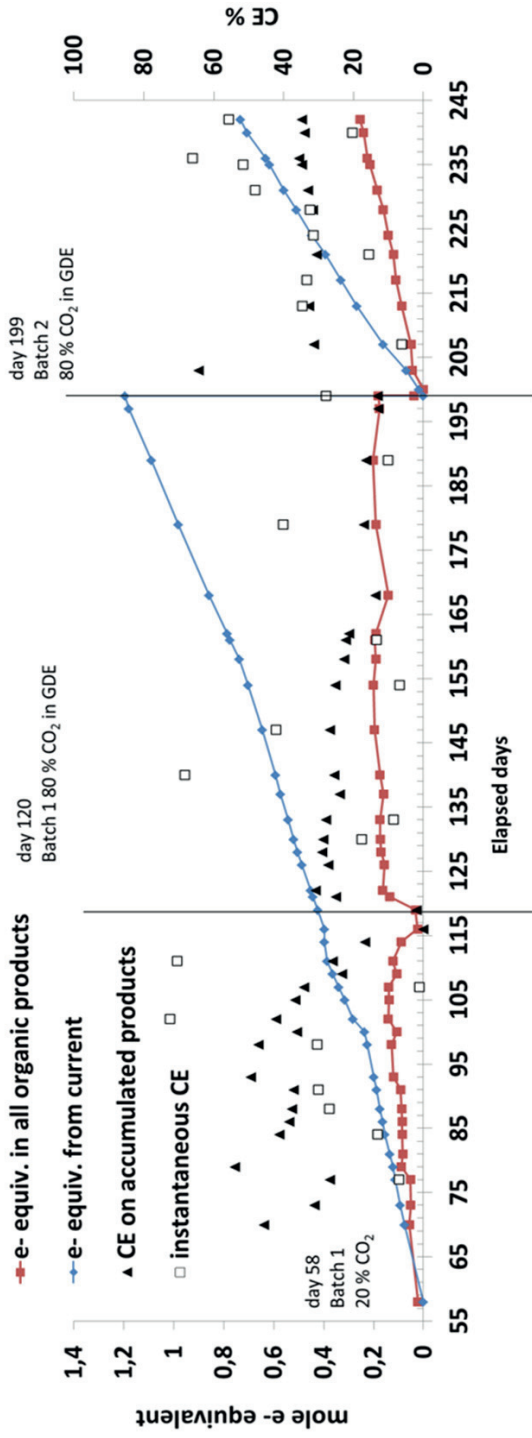
---

production. Thus, under the continuous feed of CO<sub>2</sub> gas mixture in MES reactor through GDE, CO<sub>2</sub> limitation may not be likely. But, the availability of reducing equivalents most likely pose a limitation for the CO<sub>2</sub> reduction.

#### *3.4.2.3 Coulombic efficiencies associated with acetate production in Batch 1 and Batch 2*

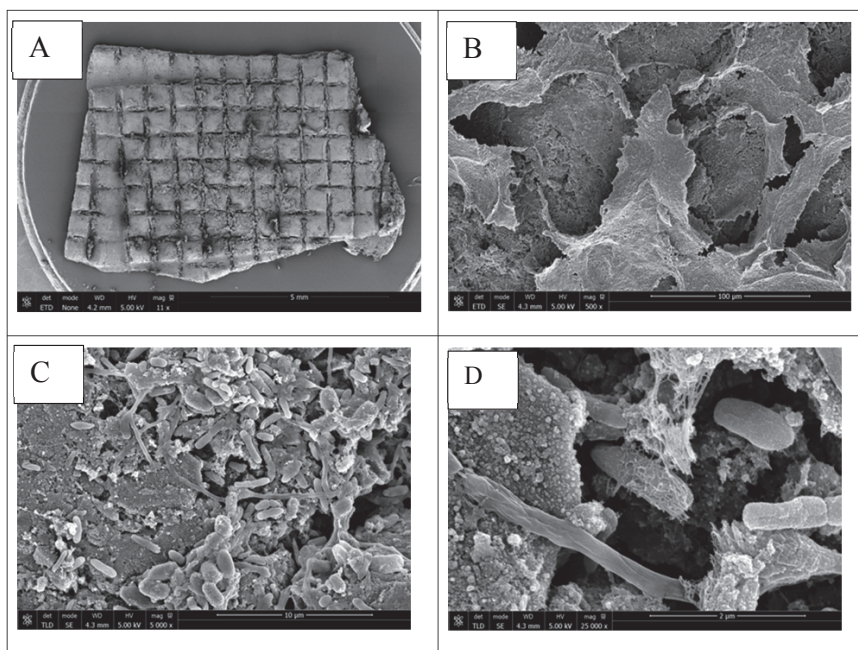
Almost 95% of the products from bioelectrochemical CO<sub>2</sub> reduction in this MES operation, in all batches, was acetate. The coulombic efficiencies of acetate production in each batch were calculated from the amount of accumulated acetate during the batch operation as well as from every two successive acetate measurements, instantaneously. The number of moles of electron equivalent available from electric current, mole of electron equivalent in products and respective coulombic efficiencies for the batches of MES operation can be found in Figure 3.6. The net acetate accumulation of 1 g L<sup>-1</sup> in the first 21 days of batch 1 operation with 20% CO<sub>2</sub> feed resembles the coulombic efficiency of 52% whereas on day 109 (late phase) with highest acetate accumulation of 1.8 g L<sup>-1</sup> accounted coulombic efficiency of 42%. This means 42% of electrons from the current were assimilated into acetic acid. The rest of the electrons obtained from the current might be assimilated in hydrogen which remained unreacted or escaped from the reactor; a part of the electron equivalent supplied can end in microbial cell biomass or in unknown/not measured reduction products.





**Figure 3.6:** Cumulative electron equivalents obtained from electric current (blue lines) and electron equivalents accumulated in organic products (red lines) in Batch 1 and Batch 2 operation of CO<sub>2</sub> reducing MES with gas diffusion biocathode. Coulombic efficiencies (CEs) are presented in the secondary axis. Coulombic efficiencies (CEs) based on cumulative electron equivalents seem relatively higher at the beginning of MES operations whereas instantaneously calculated CEs for intervals between two measurement points do not show a clear trend but few high values are seen in the late phase of operation.

The highest instantaneously calculated coulombic efficiency of 72.5% was achieved in the period between day 100 and 102. The instantaneous efficiencies of electron capture from electric current were higher at the late phase of batch 1 with 20% CO<sub>2</sub>. The wide fluctuations in momentarily calculated CE values are due to fall and rise of acetate concentration during the MES operation. The multiple interfering processes of conversion and degradation of acetate and other products had resulted in the rise and fall of acetate concentration. In contrary, accumulated product based efficiencies were higher at the initial phase than at the late phase which indicates that acetate production at the initial phase captured the reducing equivalents more efficiently from the electricity. However, acetate production might also be partly contributed by electron equivalents available from biomass or other sources. The presence of both the suspended biomaterial and cathode based biomass in the reactor might be the reason of this extra source of electron equivalents in the reactor as the suspended biomass will decay when there was no available electron source in the solution. The scanning electron microscope (SEM) images of the activated carbon layer of the GDE in Figure 3.7 shows the coverage of bacterial biomass on the GDE. The SEM images at various magnification show bacterial biofilm attachment to the electrode and also in aggregated form. A turbid appearance of catholyte in each batch also confirmed the suspended biomass.



**Figure 3.7:** SEM images of a piece of an activated carbon (AC) layer from GDE showing the microbial biomass on the AC layer. Full coverage of the AC layer by bacterial biofilm (A). Clumped biofilm on AC layer of GDE clung on the AC layer (B). Rod shaped bacteria scattered on AC layer (C) and individual bacterium attached in the micro-pore of AC layer (D).

---

The acetate production rates were lower during the 80% CO<sub>2</sub> feeding Batch 1 operation than the previous 20% CO<sub>2</sub> fed operation. Only 0.6 g L<sup>-1</sup> extra acetate accumulated during the 80% CO<sub>2</sub> fed operation of Batch 1. Thus the coulombic efficiency based on accumulated product remained only 25%. In this period of operation, though the maximum instantaneous CE of 68.2% was calculated between day 137 and 140, there was no clear trend of acetate production, except the increasing trend in butyrate. The accumulated concentrations of butyrate were low which accounted for hardly 5-7% of coulombic efficiency. In batch 2 there was a clear trend of increasing acetate concentration to 2.89 g L<sup>-1</sup> which accounts for 35% of coulombic efficiency for the batch. The efficiency based on product accumulation was also high at the beginning (64%) and remained stable around 30-35% at the later stage. The CE measured from two consecutive acetate measurements increased at the late stage reaching the highest of 61% between day 235 and 236.

### ***3.4.3 Comparative overview of GDE over submerged cathodes' performance for bioelectrochemical CO<sub>2</sub> reduction***

Batch operations of MES from gaseous CO<sub>2</sub> feed using gas diffusion biocathode repeatedly produce acetate at -1.1 to -1.2 V; butyrate and ethanol were also produced as secondary products. Similar literature on MES from CO<sub>2</sub> also reported the production of acetate where the biocathodes were commonly submerged in the catholyte and gaseous CO<sub>2</sub> was sparged into the catholyte or HCO<sub>3</sub><sup>-</sup> salts were provided as the carbon source. This study uniquely used gas diffusion biocathode and gaseous CO<sub>2</sub> was provided directly to the biocathode. In batch 1 with 20% CO<sub>2</sub> feed through the gas diffusion biocathode, acetate production rate of 32 mg L<sup>-1</sup> d<sup>-1</sup> was achieved which corresponds to 42% current efficiency whereas in case of 80% CO<sub>2</sub> feed in batch 2, the rate of production was 61 mg L<sup>-1</sup> d<sup>-1</sup> with 35% overall current recovery. Several performance parameters have been tabulated in Table 3.3 in order to provide a comparative overview of this gas diffusion biocathode MES experiment with selected submerged-biocathode MES studies using mixed cultures. The selected literature also reported MES from CO<sub>2</sub> between -1 to -1.1 V cathode potential with homoacetogenic activity enriched mixed culture.

**Table 3.3** Production rates and CE from gas diffusion biocathode in comparison to submerged cathodes

| Batch operation   | Gas diffusion biocathode   |  |   | Submerged cathodes                     |   |                                 |  |
|---|--|--|---|--|---|---------------------------------|--|
|   | Batch 1  | Batch 2  | Chapter 2                                 | Jourdin et al. [17]                    | Patil et al. [16]   | Ganigué et al. [11]             |  |
| Feed gas composition (CO <sub>2</sub> :N <sub>2</sub> )                     | 20:80  | 80:20  | 4 g L <sup>-1</sup> NaHCO <sub>3</sub>    | 2 g L <sup>-1</sup> NaHCO <sub>3</sub> | HCO <sub>3</sub> <sup>-</sup> & CO <sub>2</sub> :N <sub>2</sub> (10:90) | 100% CO <sub>2</sub>            |  |
| Cathode potential V vs Ag/AgCl  | -1.1   | -1.1 to -1.3   | -1.1                                      | -1.05                                  | -1.26 ± 0.08 (5 A m <sup>-2</sup> fixed current)                        | -0.997                          |  |
| Acetate production rate at max. titer (mg L <sup>-1</sup> d <sup>-1</sup> ) | 32   | 61   | 14  | 11.49                                  | 60  | 63.16                           |  |
| Acetate production rate at max. titer (g m <sup>-2</sup> d <sup>-1</sup> )  | 16   | 36.6   | 40  | 195±30                                 | 19±1.7  | 16.84 <sup>§</sup>              |  |
| Fastest production rate observed (mg L <sup>-1</sup> d <sup>-1</sup> )      | 238  | 166  | 81  | 24.6                                   | -   | -                               |  |
| Max. acetate Titer (g L <sup>-1</sup> )                                     | 1.8  | 2.89   | 0.63                                      | 1.23                                   | 1.5   | 1.2                             |  |
| Additional products   | <0.1 g L <sup>-1</sup> ethanol<br><0.05 g L <sup>-1</sup> butyrate | 0.1 g L <sup>-1</sup> butyrate<br>0.05 g L <sup>-1</sup> ethanol | CH <sub>4</sub> (10-38% v/v in headspace) | -                                      | Other VFAs (< 0.06 g L <sup>-1</sup> )                                  | 0.33 g L <sup>-1</sup> butyrate |  |
| CE at max. organic products (%)   | 42   | 35   | 26.9                                      | 46.15                                  | 77.2  | 38.87                           |  |
| Max. CE calculated between two nearby readings (%)                          | 72.5   | 66.1   | 49.9                                      | 92.31                                  | -   | -                               |  |

<sup>§</sup>Calculated based on reported 9 cm<sup>2</sup> electrode and 240 mL catholyte

In comparison to our previous study [18] in which the cathode was submerged and bicarbonate was used as the carbon source with same experimental setup, the rate of acetate production with GDE was improved by at least 2 times with 20% CO<sub>2</sub> feed through GDE and 4 times with 80% CO<sub>2</sub> feed. The overall coulombic efficiency of MES was also improved with GDE. In this present work, avoidance of CH<sub>4</sub> with microbial enrichment and treatments had been achieved simultaneously with the improvement in mass transfer rates and pH controlled at acidic level, which resulted into higher rates and titers with GDE as biocathode. Most significantly, suppression of the methanogenic activities can be important for improvement of MES from CO<sub>2</sub>. In comparison to the performance parameters reported in [17], which also used 2 g L<sup>-1</sup> HCO<sub>3</sub><sup>-</sup> as CO<sub>2</sub> source with repeated addition, the production rate of acetate with GDE achieved in the presented work was at least three times higher but energetically relatively less efficient on the basis of CE values. MES process reported in [17] were more efficient in capturing the electrons from the cathode with the majority of electrode-attached bacteria and hence a higher surface based productions were reported in this study. In case of volume based production of acetate from CO<sub>2</sub> reduction using enriched mixed culture, use of gaseous CO<sub>2</sub> via gas diffusion electrode appeared to predominate the production rates and titers compared to using HCO<sub>3</sub><sup>-</sup> as substrate. It could be most likely related to the acidifying effect of gaseous CO<sub>2</sub> on the cathode overpotentials and also on the microbial activity.

Patil et al. [16] and Ganigué et al. [11] used gaseous CO<sub>2</sub> as substrate in MES with submerged cathode and reported acetate production rates of 60 and 63.1 mg L<sup>-1</sup> d<sup>-1</sup> which comes close to the production rate achieved in this work with 80% CO<sub>2</sub> feeding through the GDE. These volume-based production rates were certainly higher than the rates reported with HCO<sub>3</sub><sup>-</sup> in [18] and [17]. Remarkably, butyrate production and CE values reported by [11] with continuous CO<sub>2</sub> sparging have made the MES systems more comparable with our present work. The improvement in the production rates from MES with GDEs in this study was not clearly distinct from the performance of submerged cathode in Ganigué et al. [11]. Nonetheless, when pure CO<sub>2</sub> or high percent of CO<sub>2</sub> containing gas mixture is used as carbon source, the amount of dissolved CO<sub>2</sub> will remain abundant to support relatively slower the biological process. Consequently, mass transfer of CO<sub>2</sub> will not be limiting at high CO<sub>2</sub> partial pressures. Moreover, even sparging 10% CO<sub>2</sub> containing N<sub>2</sub>:CO<sub>2</sub> gas mixture in bulk solution along with 2.5 g L<sup>-1</sup> bicarbonate, Patil et al. [16] showed 60 mg L<sup>-1</sup> d<sup>-1</sup> of acetate production rate with 77% of CE in submerged cathode MES system. A tentative CO<sub>2</sub> mass balance for MES systems with 10%, 20% and 80% CO<sub>2</sub> feeding via GDE can be proposed (Supplementary information Chapter 3 Table SI-3), considering the respective acetate production rates from Patil et al. [16] and from this work. In our study with 20% CO<sub>2</sub> feed through gas diffusion biocathode, although the average acetate production rate was only 31 mg L<sup>-1</sup> d<sup>-1</sup>, there was also a moment with the maximum production rate of 238 mg L<sup>-1</sup> d<sup>-1</sup>.

Estimation of CO<sub>2</sub> mass balance in MES with GDE is presented in Supplementary information-Chapter 3 Table SI-3 and these values of possible production rates from MES system, support the claim that dissolved CO<sub>2</sub> will not be limiting for a bioelectrochemical CO<sub>2</sub> reduction using gas diffusion biocathode. In a steady-state situation, the continuous supply of CO<sub>2</sub> was expected to maintain the maximum CO<sub>2</sub> availability based on the partial pressure of CO<sub>2</sub>. Hence higher production rates and titers could be achievable in the bioelectrochemical CO<sub>2</sub> reduction by optimizing other potentially limiting parameters such as reducing equivalents and microbial activity etc. Not only improving the mass transfer of CO<sub>2</sub>, gas diffusion biocathodes are also useful in capturing CO<sub>2</sub> in aqueous solution, as GDE can adsorb CO<sub>2</sub> [CO<sub>2</sub>(ad)] on the activated carbon catalyst layer. In submerged cathodes with conventional sparging in bulk, CO<sub>2</sub> would be distributed directly as CO<sub>2</sub>(g) → CO<sub>2</sub>(aq) → CO<sub>2</sub>(ad) whereas when CO<sub>2</sub> was fed via GDE, CO<sub>2</sub> would be distributed as GDE, CO<sub>2</sub> (g) → CO<sub>2</sub>(ad). In case of CO<sub>2</sub> sparging in bulk, the fraction of adsorbed CO<sub>2</sub> would be much less than dissolved CO<sub>2</sub> but with GDE direct adsorption increases CO<sub>2</sub>(ad) contributing into more carbon capture. This will effectively increase the

---

CO<sub>2</sub>(ad) at the bioelectrochemically active site. Furthermore, the diffusion layer in GDE can allow CO<sub>2</sub> diffusion in harmony with the bioelectrochemical reduction kinetic to minimize CO<sub>2</sub> wastage.

### 3.5 Conclusions

Bioelectrochemical CO<sub>2</sub> reduction to produce multi-carbon organic compounds was repeatedly performed using gas diffusion biocathode with homoacetogenic activity dominated mixed culture. Gaseous CO<sub>2</sub> feeding in MES system with gas diffusion biocathode produced acetate as the main product and ethanol and butyrate as secondary products. Suppression of methanogenic activity and enrichment of homoacetogenic activity in the mixed culture originating from wastewater significantly improved the production from CO<sub>2</sub> reduction. Gas diffusion electrode enhanced the mass-transfer of gaseous substrates compared to the supply through conventional spargers in submerged electrode. GDE appeared to be potentially effective in delivering gaseous CO<sub>2</sub> faster so that higher rates of production in MES can be expected by using GDE. Gas diffusion biocathodes also provides adsorbed CO<sub>2</sub> at the electrochemically active sites. Apparently, gas diffusion biocathodes will be appropriate in MES from the dilute CO<sub>2</sub> waste stream for continuous operation with efficient CO<sub>2</sub> capture.

### Acknowledgements

The work was supported by a PhD grant to Suman Bajracharya from VITO's strategic research funds. The authors acknowledge Mr. Shishir Kanti Pramanik for conducting the gas-transfer experiments and taking samples from the reactor.

### References

1. Le Quéré C, Peters GP, Andres RJ, et al (2014) Global carbon budget 2013. *Earth Syst Sci Data* 6:235–263. doi: 10.5194/essd-6-235-2014
2. IPCC (2014) *Climate Change 2014: Synthesis Report. Contribution of Working Groups I, II and III to the Fifth Assessment Report of the Intergovernmental Panel on Climate Change*. IPCC, Geneva, Switzerland
3. Chu S (2009) Carbon capture and sequestration. *Science* 325:1599. doi: 10.1126/science.1181637
4. CAST (2006) *Convergence of Agriculture and Energy: Implications for Research and Policy*. Ames, Iowa
5. Naik SN, Goud V V., Rout PK, Dalai AK (2010) Production of first and second generation biofuels: A comprehensive review. *Renew Sustain Energy Rev* 14:578–597.
6. Cassman KG, Liska AJ (2007) Food and fuel for all: realistic or foolish? *Biofuels, Bioprod Biorefining* 1:18–23. doi: 10.1002/bbb.3
7. Rabaey K, Rozendal RA (2010) Microbial electrosynthesis — revisiting the electrical route for microbial production.pdf. *Nat Rev Microbiol* 8:706–16. doi: 10.1038/nrmicro2422
8. Lovley DR, Nevin KP (2013) Electrobiocommodities: powering microbial production of fuels and commodity chemicals from carbon dioxide with electricity. *Curr Opin Biotechnol* 1–6. doi: 10.1016/j.copbio.2013.02.012
9. Nevin KP, Woodard TL, Franks AE, et al (2010) Microbial Electrosynthesis: Feeding Microbes Electricity To Convert Carbon Dioxide and Water to Multicarbon Extracellular Organic. *MBio* 1:e00103–10-. doi: 10.1128/mBio.00103-10.Editor
10. Nevin KP, Hensley SA, Franks AE, et al (2011) Electrosynthesis of organic compounds from carbon dioxide is catalyzed by a diversity of acetogenic microorganisms. *Appl Environ Microbiol* 77:2882–6. doi: 10.1128/AEM.02642-10
11. Ganigué R, Puig S, Batlle-Vilanova P, et al (2015) Microbial electrosynthesis of butyrate from carbon dioxide. *Chem Commun* 51:3235–3238. doi: 10.1039/C4CC10121A
12. Marshall CW, Ross DE, Fichot EB, et al (2012) Electrosynthesis of commodity chemicals by an autotrophic microbial community. *Appl Environ Microbiol* 78:8412–20. doi: 10.1128/AEM.02401-12
13. Drake HL, Gößner AS, Daniel SL (2008) Old Acetogens, New Light. *Ann N Y Acad Sci* 1125:100. doi: 10.1196/annals.1419.016

- 
14. Marshall CW, Ross DE, Fichot EB, et al (2013) Long-term operation of microbial electrosynthesis systems improves acetate production by autotrophic microbiomes. *Environ Sci Technol* 47:6023–9. doi: 10.1021/es400341b
  15. Su M, Jiang Y, Li D (2013) Production of acetate from carbon dioxide in bioelectrochemical systems based on autotrophic mixed culture. *J Microbiol Biotechnol* 23:1140–6.
  16. Patil SA, Arends JBA, Vanwonterghem I, et al (2015) Selective Enrichment Establishes a Stable Performing Community for Microbial Electrosynthesis of Acetate from CO<sub>2</sub>. *Environ Sci Technol* 150701101446004. doi: 10.1021/es506149d
  17. Jourdin L, Freguia S, Donose BC, et al (2014) A novel carbon nanotube modified scaffold as an efficient biocathode material for improved microbial electrosynthesis. *J Mater Chem A* 2:13093–13102. doi: 10.1039/C4TA03101F
  18. Bajracharya S, ter Heijne A, Dominguez X, et al (2015) CO<sub>2</sub> reduction by mixed and pure cultures in microbial electrosynthesis using an assembly of graphite felt and stainless steel as a cathode. *Bioresour Technol*. doi: 10.1016/j.biortech.2015.05.081
  19. Modestra JA, Navaneeth B, Venkata Mohan S (2015) Bio-electrocatalytic reduction of CO<sub>2</sub>: Enrichment of homoacetogens and pH optimization towards enhancement of carboxylic acids biosynthesis. *J CO<sub>2</sub> Util* 10:78–87. doi: 10.1016/j.jcou.2015.04.001
  20. González-López C V, Acién Fernández FG, Fernández-Sevilla JM, et al (2012) Development of a process for efficient use of CO<sub>2</sub> from flue gases in the production of photosynthetic microorganisms. *Biotechnol Bioeng* 109:1637–50. doi: 10.1002/bit.24446
  21. Zhang K, Miyachi S, Kurano N (2001) Photosynthetic performance of a cyanobacterium in a vertical flat-plate photobioreactor for outdoor microalgal production and fixation of CO<sub>2</sub>. *Biotechnol Lett* 23:21–26. doi: 10.1023/A:1026737000160
  22. Gabriel Acien Fernandez F, Gonzalez-Lopez CV, Fernandez Sevilla JM, Molina Grima E (2012) Conversion of CO<sub>2</sub> into biomass by microalgae: How realistic a contribution may it be to significant CO<sub>2</sub> removal? *Appl Microbiol Biotechnol* 96:577–586. doi: 10.1007/s00253-012-4362-z
  23. Doucha J, Straka F, Lívanský K (2005) Utilization of flue gas for cultivation of microalgae (*Chlorella* sp.) in an outdoor open thin-layer photobioreactor. *J Appl Phycol* 17:403–412. doi: 10.1007/s10811-005-8701-7
  24. Fernández FGA, Grima EM, Sevilla JMF, et al (2011) Liquid-phase gas collection. *US2011015957 A1*
  25. Fan Y, Hongqiang H, Liu H, Fan, Y.; Hu, H. & Liu H (2007) Sustainable power generation in microbial fuel cells using bicarbonate buffer and proton transfer mechanisms. *Environ Sci Technol* 41:8154–8158. doi: 10.1021/es071739c
  26. Fornero JJ, Rosenbaum M, Cotta M a, Angenent LT (2010) Carbon dioxide addition to microbial fuel cell cathodes maintains sustainable catholyte pH and improves anolyte pH, alkalinity, and conductivity. *Environ Sci Technol* 44:2728–34. doi: 10.1021/es9031985
  27. Pant D, Van Bogaert G, De Smet M, et al (2010) Use of novel permeable membrane and air cathodes in acetate microbial fuel cells. *Electrochim Acta* 55:7710–7716. doi: 10.1016/j.electacta.2009.11.086
  28. HaoYu E, Cheng S, Scott K, Logan B (2007) Microbial fuel cell performance with non-Pt cathode catalysts. *J Power Sources* 171:275–281. doi: 10.1016/j.jpowsour.2007.07.010
  29. Alvarez-Gallego Y, Dominguez-Benetton X, Pant D, et al (2012) Development of gas diffusion electrodes for cogeneration of chemicals and electricity. *Electrochim Acta* 82:415–426. doi: 10.1016/j.electacta.2012.06.096
  30. Mahmood MN, Masheder D, Harty CJ (1987) Use of gas-diffusion electrodes for high-rate electrochemical reduction of carbon dioxide. I. Reduction at lead, indium- and tin-impregnated electrodes. *J Appl Electrochem* 17:1159–1170. doi: 10.1007/BF01023599
  31. Zhang X, Pant D, Zhang F, et al (2014) Long-Term Performance of Chemically and Physically Modified Activated Carbons in Air Cathodes of Microbial Fuel Cells. *ChemElectroChem* 1:1859–1866. doi: 10.1002/celc.201402123
  32. Kopljar D, Inan A, Vindayer P, et al (2014) Electrochemical reduction of CO<sub>2</sub> to formate at high current density using gas diffusion electrodes. *J Appl Electrochem* 44:1107–1116. doi: 10.1007/s10800-014-0731-x
  33. Zhang F, Cheng S, Pant D, et al (2009) Power generation using an activated carbon and metal mesh cathode in a microbial fuel cell. *Electrochem commun* 11:2177–2179. doi: 10.1016/j.elecom.2009.09.024
  34. Hu P, Rismani-yazdi H, Gregory S (2013) Anaerobic CO<sub>2</sub> fixation by the Acetogenic Bacterium *Morrella thermoacetica*. *AIChE J* 59:3176–3183. doi: 10.1002/aic.14127
  35. Mohanakrishna G, Seelam JS, Vanbroekhoven K, Pant D (2015) An enriched electroactive homoacetogenic biocathode for the microbial electrosynthesis of acetate through carbon dioxide
-

- 
- reduction. *Faraday Discuss.* doi: 10.1039/C5FD00041F
36. Oh S-E, Van Ginkel S, Logan BE (2003) The relative effectiveness of pH control and heat treatment for enhancing biohydrogen gas production. *Environ Sci Technol* 37:5186–90. doi: 10.1021/Es034291y
  37. Pasupuleti SB, Srikanth S, Venkata Mohan S, Pant D (2015) Continuous mode operation of microbial fuel cell (MFC) stack with dual gas diffusion cathode design for the treatment of dark fermentation effluent. *Int J Hydrogen Energy* 40:12424–12435. doi: 10.1016/j.ijhydene.2015.07.049
  38. Lee J, Little B (2015) Electrochemical and Chemical Complications Resulting from Yeast Extract Addition to Stimulate Microbial Growth. *Corrosion.* doi: 10.5006/1833
  39. Liu Z, Liu J, Zhang S, et al (2011) Microbial fuel cell based biosensor for in situ monitoring of anaerobic digestion process. *Bioresour Technol* 102:10221–10229.
  40. Talbot P, Gortares MP, Lencki RW, de la Nouë J (1991) Absorption of CO<sub>2</sub> in algal mass culture systems: a different characterization approach. *Biotechnol Bioeng* 37:834–42. doi: 10.1002/bit.260370907
  41. Cussler EL (1997) *Diffusion: Mass Transfer in Fluid Systems*, 2nd ed. Cambridge University Press, New York
  42. Patil SA, Gildemyn S, Pant D, et al (2015) A logical data representation framework for electricity-driven bioproduction processes. *Biotechnol Adv* 33:736–744. doi: 10.1016/j.biotechadv.2015.03.002
  43. Fast AG, Papoutsakis ET (2012) Stoichiometric and energetic analyses of non-photosynthetic CO<sub>2</sub>-fixation pathways to support synthetic biology strategies for production of fuels and chemicals. *Curr Opin Chem Eng* 1:380–395. doi: 10.1016/j.coche.2012.07.005
  44. Tracy BP, Jones SW, Fast AG, et al (2012) Clostridia: the importance of their exceptional substrate and metabolite diversity for biofuel and biorefinery applications. *Curr Opin Biotechnol* 23:364–81. doi: 10.1016/j.copbio.2011.10.008
  45. Sakai S, Nakashimada Y, Yoshimoto H, et al (2004) Ethanol production from H<sub>2</sub> and CO<sub>2</sub> by a newly isolated thermophilic bacterium, *Moorella* sp. HUC22-1. *Biotechnol Lett* 26:1607–1612. doi: 10.1023/B:BILE.0000045661.03366.f2
  46. Ying K, Al-mashhadani MKH, Hanotu JO, et al (2013) Enhanced Mass Transfer in Microbubble Driven Airlift Bioreactor for Microalgal Culture. *Engineering* 2013:735–743. doi: 10.4236/eng.2013.59088
  47. Hill GA (2006) Measurement of overall volumetric mass transfer coefficients for carbon dioxide in a well-mixed reactor using a pH probe. *Ind Eng Chem Res* 45:5796–5800. doi: 10.1021/ie060242t
  48. Treybal RE (1981) *Mass-transfer operations*, Third. McGraw-Hill, Inc.
  49. Blanchet EM, Duquenne F, Rafrafi Y, et al (2015) Importance of the hydrogen route in up-scaling electrosynthesis for microbial CO<sub>2</sub> reduction. *Energy Environ Sci* 8:3731–3744. doi: 10.1039/C5EE03088A
  50. Jourdin L, Lu Y, Flexer V, et al (2015) Biologically-induced hydrogen production drives high rate / high efficiency microbial electrosynthesis of acetate from carbon dioxide. *ChemElectroChem* n/a–n/a. doi: 10.1002/celec.201500530
  51. Stams AJM, Plugge CM, De Bok FAM, et al (2005) Metabolic interactions in methanogenic and sulfate-reducing bioreactors. *Water Sci Technol* 52:13–20.
  52. Whipple DT, Finke EC, Kenis PJ a. (2010) Microfluidic Reactor for the Electrochemical Reduction of Carbon Dioxide: The Effect of pH. *Electrochem Solid-State Lett* 13:B109. doi: 10.1149/1.3456590
  53. LaBelle E V, Marshall CW, Gilbert JA, May HD (2014) Influence of Acidic pH on Hydrogen and Acetate Production by an Electrosynthetic Microbiome. *PLoS One* 9:e109935.
  54. Steinbusch KJJ, Hamelers HVM, Schaap JD, et al (2010) Bioelectrochemical ethanol production through mediated acetate reduction by mixed cultures. *Environ Sci Technol* 44:513–7. doi: 10.1021/es902371e
  55. Vega JL, Prieto S, Elmore BB, et al (1989) The Biological production of ethanol from synthesis gas. *Appl Biochem Biotechnol* 20-21:781–797. doi: 10.1007/BF02936525
  56. Agler MT, Wrenn B a, Zinder SH, Angenent LT (2011) Waste to bioproduct conversion with undefined mixed cultures: the carboxylate platform. *Trends Biotechnol* 29:70–8. doi: 10.1016/j.tibtech.2010.11.006
-



---

C  
H  
A  
P  
T  
E  
R

4

**Long-term operation of bioelectrochemical CO<sub>2</sub> reduction to multi-carbon chemicals with a mixed culture avoiding methanogenesis**

This chapter is *accepted* for publication as

Bajracharya S, Yuliasni R, Vanbroekhoven K, Buisman CJN, Strik DPBTB, Pant D (2016). *Long-term operation of microbial electrosynthesis cell reducing CO<sub>2</sub> to multi-carbon chemicals with a mixed culture avoiding methanogenesis*. *Bioelectrochemistry* (Accepted).

---

---

**Abstract**

Avoidance of methane production during the long-term operation of Microbial electrosynthesis (MES) secured a high acetate accumulation without the addition of chemical inhibitors by the support of specific culture enrichment and operation procedures. In MES, carbon dioxide (CO<sub>2</sub>) is reduced preferably to multi-carbon chemicals by a biocathode-based process which uses electrochemically active bacteria as catalysts and electrons or other reducing equivalents produced at an electrically-polarized cathode. When a mixed anaerobic consortium from biological origin is used for CO<sub>2</sub> reduction, methane production typically occurs. This methane production needs to be circumvented to allow the production of multi-carbon products. This study aimed at the development of a stable and robust CO<sub>2</sub> reducing biocathode in MES from a mixed culture inocula while avoiding methane production. An effective approach for a robust CO<sub>2</sub> reducing biocathode development was demonstrated based on: (i) a microbial community enrichment procedure involving inoculum pre-treatment and several culture transfers in H<sub>2</sub> & CO<sub>2</sub> growth media, (ii) a transfer of heterotrophic to autotrophic growth and (iii) a sequential batch operation. Biomass growth and gradual acclimation to CO<sub>2</sub> electro-reduction accomplished a maximum acetate production rate of 400 mg L<sub>catholyte</sub><sup>-1</sup> d<sup>-1</sup> at -1 V<sub>Ag/AgCl</sub> cathode potential. Methane was never detected during the long-term operation of CO<sub>2</sub> reducing MES in several sequential batches operated for more than 300 days. Accumulation of acetate up to 7-10 g L<sup>-1</sup> was repeatedly attained in a sequential batch operation of MES by supplying (80: 20) CO<sub>2</sub>:N<sub>2</sub> gas mixture at -0.9 to -1 V<sub>Ag/AgCl</sub> cathode potential. In addition, the products of bioelectrochemical CO<sub>2</sub> reduction diversified to ethanol and butyrate. Overall, the MES reactors displayed robust CO<sub>2</sub> reducing biocathode avoiding methane production during long-term operation which secured a high acetate accumulation without the addition of chemical inhibitors.

Keywords: Microbial electrosynthesis, CO<sub>2</sub> reduction, Biocathode, Wood-Ljungdahl pathway, Autotrophic bioproduction

---

## 4.1 Introduction

Synthesis of organic chemicals at a cathode by applying electrical energy and using microorganisms as catalysts for the electrochemical reduction of low-grade compounds is termed as microbial electrosynthesis (MES) [1, 2]. In MES, water oxidation at the anode generates electrons and protons by the application of an external electric potential, which are transported towards the cathode where the electroactive microbes utilize them in the reduction reactions. Bioelectrochemical CO<sub>2</sub> reduction is one of the attractive applications of MES to generate valuable multi-carbon chemicals. MES of acetate from CO<sub>2</sub> has been reported by using homoacetogenic bacteria as biocatalyst [1, 3]. Homoacetogens such as *Clostridium* spp. and *Sporomusa* spp. are known to reduce CO<sub>2</sub> biologically to acetate according to Wood-Ljungdahl (WL) pathway [4] and a number of *Clostridium* spp. are even reported to produce ethanol from the mixture of H<sub>2</sub>, CO and CO<sub>2</sub> [5]. The concept of electricity-driven process of CO<sub>2</sub> reduction using homoacetogens in MES could provide sustainable chemical feedstocks and biofuels. Moreover, MES could serve as an electricity storage technology for the excess or intermittently produced electricity [2].

Acetate is the main product of CO<sub>2</sub> reduction till date reported but a few recent studies have shown the simultaneous reduction of CO<sub>2</sub> to the mixture of acetate, butyrate, and ethanol using mixed microbial cultures is possible [6, 7]. Acetate is an intermediate extracellular product of bioelectrochemical CO<sub>2</sub> reduction. Further reduction and conversion of acetate can result into valuable fuels and chemicals such as ethanol and butanol [8, 9]. MES of CO<sub>2</sub> is an attractive technology for the renewable fuel and chemicals production and at the same time, is interesting for on-site conversion of CO<sub>2</sub> from industrial exhaust [10].

Bioelectrochemical CO<sub>2</sub> reduction has been studied using pure as well as selectively enriched mixed cultures with methane-inhibitor and both studies resulted in high acetate production rates [11, 12]. However, stable biocathode establishment is still a challenge for the development of MES from CO<sub>2</sub> without the usage of chemical methane-inhibitors [7, 13]. Electroactive biofilm formation enables energetically efficient direct electron-transfer for CO<sub>2</sub> reduction and/or conversion of electron equivalents to reducing species such as H<sub>2</sub> which is theoretically less energetic efficient. Furthermore, recent studies have revealed more about the electron transfer and reduction pathways involved in biocathodes [14, 15]. Different electron transfer and reduction pathways possibly require different cathode overpotentials. It is well known for both acetate-oxidizing bioanodes and oxygen-reducing biocathodes in microbial fuel cells, that both the anode and cathode potentials determine the performance of the bioelectrochemical system [16, 17]. As such, cathode potential is an important parameter which can be used to steer bioelectrochemical systems and, as hypothesized, can steer to diverse electron transfer and reduction pathways in MES [18]. A dynamic cathode polarization approach can allow the development of multiple electron transfer mechanisms to stabilize CO<sub>2</sub> reducing biocathode. For scaling-up and practical application of MES for instance, the industrial CO<sub>2</sub> capture and conversion requires optimization of MES in terms of CO<sub>2</sub> uptake, chemical production rates and also electrical energy requirement [19]. However, the process and microbial electrochemistry at the cathode still need to be investigated. Homoacetogens enrichment in the inoculum from the anaerobic sludge have shown a sustained CO<sub>2</sub> reduction to acetate [13, 20]. However, these studies were not successful in preventing complete avoidance of methane formation on the long term. These studies were performed using a culture enrichment based selection method which resulted to an undefined mixed culture containing uncultured biocatalysts. Addition of methanogenic activity inhibitor—Sodium bromoethanesulfonate (NaBES) [21]—in the MES catholyte avoided methane production for short time operation of these MES (60 days)[13]. However, the establishment of sustained MES system avoiding methanogenesis remained uncertain for the long-term operation of such undefined mixed culture.

---

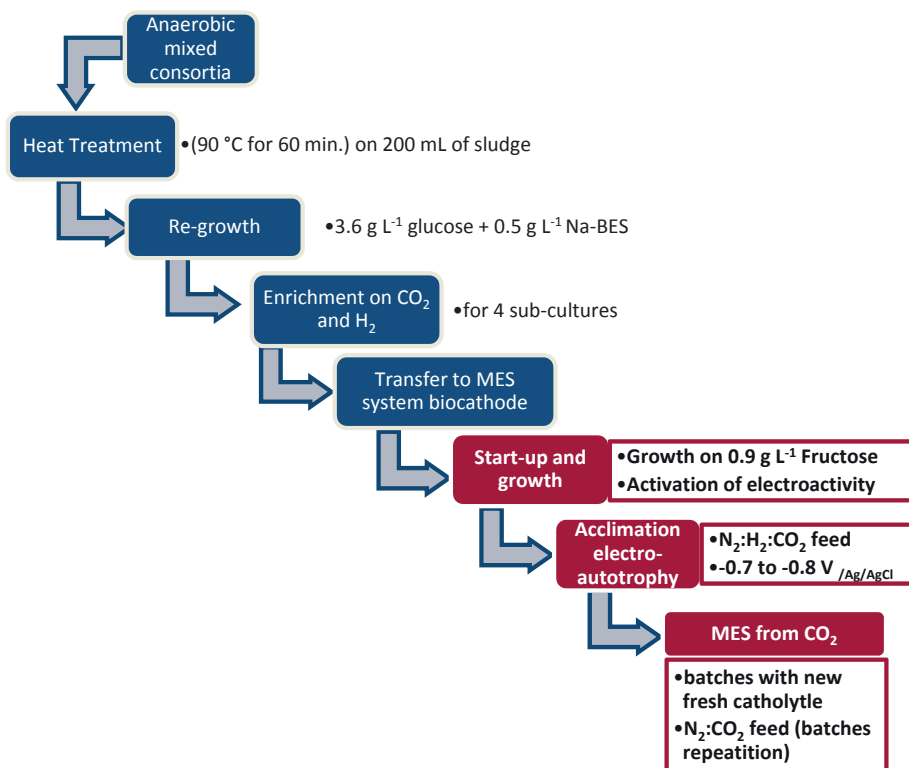
The objective of this study was to develop a stable and robust CO<sub>2</sub> reducing biocathode in MES from a mixed culture inoculum while avoiding methane production. A selective pre-treatment and culture enrichment of inoculum from biological sludge is presented in this study. Additionally, a supplementation of *Clostridium ljungdahlii*, previously reported electro-active CO<sub>2</sub> reducer [3], was done to guarantee the abundance of CO<sub>2</sub> reducers in the selectively enriched mixed culture for the formation of a stable CO<sub>2</sub> reducing biocathode. A long-term operation of MES from CO<sub>2</sub> is investigated for more than 300 days under repetitive batch operations towards extractable product titers. Hereby a variable cathode potential control strategy was applied to support the multiple electron transfer mechanisms for the development of electro-active biofilms. The evolution of biocathode on long-term operation and the effect of cathode polarization on CO<sub>2</sub> reduction were discussed.

## 4.2 Methods and materials

### 4.2.1 Pre-treatment and selective enrichment of inoculum to avoid methanogenesis

A selective enrichment was applied to a sample of an anaerobic sludge to favor homoacetogenic activity suppressing the methanogens as shown in Figure 1. First, 200 mL of wet sludge in a glass bottle was heated over a hot plate to 90 °C for 1 hour in order to eliminate the heat-intolerant methanogens [20, 22]. In the second stage, the heat treated sludge inoculum was regrown in a sealed glass bottle using glucose containing DSMZ medium 879 with 2 mM of Sodium 2-bromoethanesulfonate (Na-BES) at 37 °C to reactivate the spore-forming/heat-tolerant bacteria. The heterotrophically grown culture was shifted to autotrophic condition by transferring to DSMZ medium 879 (fructose omitted) providing a gas mixture of CO<sub>2</sub> (20%) and H<sub>2</sub> (80%) which proliferated the homoacetogenic activity under the repeated transferring and growing under H<sub>2</sub>:CO<sub>2</sub> (80:20) in four culture transfer. Methane production was absent in all the sub-cultures. The culture after four transfers was used as an inoculum for the bioelectrochemical CO<sub>2</sub> reduction in the cathode chamber of the reactor.

During the start-up of biocathode in MES reactor, the enriched mixed culture inoculum was additionally supplemented (1:1 vol/vol) by *Clostridium ljungdahlii* culture (purchased from DSMZ, Germany) to ensure the presence of homoacetogens. This way the biocathode remained homoacetogen enriched mixed culture which did not need highly aseptic treatment. The pure culture of *C. ljungdahlii* was grown anaerobically in serum bottles at 37 °C in DSMZ 879 medium.



**Figure 4.1:** Step-wise representation of pre-treatment and selection procedure (blue text boxes) to avoid methanogens in mixed culture. Subsequent steps for biocathode development in MES reactor (red text boxes).

#### 4.2.2 Electrolytes

The media used for the start-up and growth phase in the study was a mineral solution containing (in g L<sup>-1</sup>): 0.33 KH<sub>2</sub>PO<sub>4</sub>, 0.45 K<sub>2</sub>HPO<sub>4</sub>, 1 NH<sub>4</sub>Cl, 0.1 KCl, 0.8 NaCl, 0.2 MgSO<sub>4</sub>·7H<sub>2</sub>O, and 0.1 yeast extract, which was later supplemented with 20 mL L<sup>-1</sup> vitamin solution (DSMZ 141), 20 mL L<sup>-1</sup> trace element solution (DSMZ 141) and 4 g L<sup>-1</sup> sodium bicarbonate prior to operation. The media was prepared anaerobically by heating it just to boil and then immediately cooled on ice under N<sub>2</sub>:CO<sub>2</sub> (80:20) gas purging. This media is referred to as mineral media henceforth. During the bacterial growth phase, 5 mM fructose as substrate and 2 mL L<sup>-1</sup> of 1 M Na<sub>2</sub>S·9H<sub>2</sub>O solution (as an oxygen scavenger to maintain anaerobic condition) were injected in the mineral media. In the acclimation and autotrophic production phase, the mineral media was used omitting fructose and yeast extract. The anolyte was the yeast extract, bicarbonate, vitamin, and trace element omitted mineral media which remained acidic (pH between 3 and 4) during the operation. The pH of the catholyte was adjusted to 7 at the beginning and temperature was maintained at 30 °C by using a thermocouple-controlled heater.

#### 4.2.3 Electrodes and MES reactor setup

A hermetically closed H-type glass reactor was fabricated by combining two 500 mL glass bottles (see Supplementary Information-Chapter 4 Table SI-1). A pretreated proton

---

exchange membrane (Ion power Nafion 117, Germany) was used to separate the two anode and cathode compartments in this reactor. The anode and cathode chambers were of equal volume and each chamber was isolated and hermetically closed by using butyl rubber stoppers. For the connection to an electrical power source, the electrodes were provided with a short platinum wire extruded through a butyl rubber cap on the top openings of each chamber.

A rectangular piece of Titanium with an Iridium coated dimensionally stable anode (DSA) (Magneto special anodes B. V.) was used as an anode. The cathode was an assembly of two pieces of graphite felts with a graphite stick sandwiched between them. Three H-type reactors were constructed and named MES-1, MES-2 and MES-3 for convenience. The reactors MES-2 and MES-3 were assembled by using 250 mL glass bottles. The electrodes in MES-2 and MES-3 were reduced in size to maintain same electrode-catholyte area-volume ratio. The specification of reactors with dimensions of electrodes used in each reactor is provided in Supplementary information-Chapter 4 Table SI-1.

For the electrochemical measurement, MES-1 and MES-2 were connected to VersaSTAT 4 (Princeton Applied Research) potentiostat and MES-3 to VMP3 (Biologic Science Instruments, France) potentiostat using three electrode configuration, cathode as a working electrode while anode as a counter electrode. The reference electrode used in all the setups was Ag/AgCl, 3 M KCl (+ 0.205 V vs SHE; ref 321, Radiometer Analytical). Catholyte was continuously stirred by using a magnetic stirrer revolving at 400 –500 rpm.

#### 4.2.4 Start-up and Acclimation

Biocathode was started-up by inoculating 5% (v/v) of enriched mixed culture and 5% (v/v) of *Clostridium ljungdahlii* culture as seed culture in the catholyte containing 2 mM fructose, which was maintained anaerobic by sparging N<sub>2</sub> gas and the cathode potential of -0.6 V<sub>/Ag/AgCl</sub> was applied. The cathode potential was maintained through potentiostat using Chronoamperometry (CA), an electrochemical technique to measure the reductive current at constant applied potential. Optical density at 600 nm (OD<sub>600</sub>) was monitored every 2 days. This growth experiment was continued until the OD<sub>600</sub> value reached a stable value (0.6-0.8). Temperature was adjusted to 37 °C and the catholyte was continuously stirred using magnetic stirrer.

After the microbial growth phase, the next stage was adjustment and adaptation of the microbial cultures to CO<sub>2</sub> reduction. This phase was started with the replacement of 30 % of catholyte with new mineral medium containing 32 mM bicarbonate and the cathode potential was maintained for long duration at -0.8 V<sub>/Ag/AgCl</sub>, though MES operation at dynamic cathode potential were also carried out as described later in polarization test. Catholyte replacements with a fresh mineral medium were done to replenish the nutrients and also to remove suspended biomass. A gas mixture of N<sub>2</sub>:H<sub>2</sub>:CO<sub>2</sub> (80:7:13) was continuously sparged in the acclimation phase at 8- 9 L d<sup>-1</sup> but after every 15-20 days, N<sub>2</sub>:CO<sub>2</sub> (80:20) mixture was also sparged for the duration of 5-7 days to check the production of acetate without external H<sub>2</sub> supply. The experimental phases and changes made in the operation MES reactors are indicated with days count in Table 4.1.

Volatile fatty acids (VFAs) from C1 to C4 and ethanol produced in the MES reactor were measured in catholyte samples taken at regular intervals using HPLC measurement as described earlier in Bajracharya et al. [19]. Besides these, OD<sub>600</sub>, Chemical oxygen demand (COD), pH and reduction current were also monitored during the operation. COD was analyzed using HACH Lange COD kit. OD<sub>600</sub> was measured using spectrophotometer UV 1800 (model CPS-240A, Shimadzu, Japan). Headspace gas in the MES reactors was sampled through a gas-tight syringe with needle and analyzed in a GC (Trace GC Ultra, Thermo Scientific) equipped with a thermal conductivity detector (TCD) as described previously [7].

### 4.2.5 Polarization test

Theoretical reduction potential for H<sub>2</sub> evolution is -0.614 V<sub>/Ag/AgCl</sub> at pH 7 and that of HCO<sub>3</sub><sup>-</sup> to acetate is -0.48 V<sub>/Ag/AgCl</sub> at pH 7 but much lower cathode potential had to be applied to overcome the electrode overpotentials. Polarization tests were performed by applying a series of chronoamperometry techniques in order to characterize the biocathode at various cathode potentials. Polarization tests were performed by applying dynamic potential from -0.3 to -1.0 V<sub>/Ag/AgCl</sub> with the step of 0.1 V, each step polarization lasting at least 0.5 to 1 day at each cathode potential (particularly between -0.8 and -1 V<sub>/Ag/AgCl</sub>), then similarly changed from -1.0 to -0.3 V<sub>/Ag/AgCl</sub>. But the duration of cathode polarization at potential between -0.6 to -0.3 V<sub>/Ag/AgCl</sub> was kept short (utmost 2-3 hours) due to the quick stabilization of reductive currents. Reduction current was recorded for every 300 seconds and then the last 20-30 data points at each cathodes potential were averaged to plot the polarization curves.

### 4.2.6 Long-term batch operations of MES with CO<sub>2</sub> feed

After the observation of acetate production in acclimation phase solely from CO<sub>2</sub> reduction, MES reactors were operated by continuously supplying N<sub>2</sub>:CO<sub>2</sub> (80:20) in the reactor without any external supply of H<sub>2</sub>. In the long-term batch operations, cathode potentials of -0.9 to -1 V<sub>/Ag/AgCl</sub> were applied, also considering the voltage losses, to facilitate both direct CO<sub>2</sub> reduction or via H<sub>2</sub> evolution mediated CO<sub>2</sub> reduction.

The subsequent operations of MES with intermittent N<sub>2</sub>:CO<sub>2</sub> (20:80) bubbling were performed in batches, namely Batch 1, Batch 2, Batch 3 and so on. 80 % CO<sub>2</sub> gas mixture bubbling in the catholyte was done for ~15-30 minutes at each time. For starting a new batch, around 10-20 % (v/v) of catholyte from previous batch was retained as microbial inoculum unless otherwise stated. The potentiostatic operation was programmed such that the cathodic potential was shifted periodically between -0.9 and -1 V<sub>/Ag/AgCl</sub> to observe the polarization response on the current densities and facilitation of CO<sub>2</sub> reduction with ample supply of reducing equivalents.

## 4.3. Calculations

### 4.3.1 Production rate

Various reduction products i.e. hydrogen, acetate, propionate, butyrate and ethanol are produced in MES. In batch mode, production of any reduced compound *i* (in mmol) during a time period between *t*<sub>1</sub> and *t*<sub>2</sub> was calculated as per equation 4.1:

$$n_{i,t} = V_{cat} \times (C_{i,t2} - C_{i,t1}) / M_i \quad (4.1)$$

Here subscripts *i* refer to any reduced compound, subscripts *t*<sub>1</sub> and *t*<sub>2</sub> refer to two subsequent samples, *n* is number of moles of reduced compound produced, *V*<sub>cat</sub> is total volume of the catholyte (L), *C* is the concentration of the compound (mg L<sup>-1</sup>), whereas *M* is its molecular weight (g mol<sup>-1</sup>). The rate of production of reduced compound in mg L<sup>-1</sup> d<sup>-1</sup> is given by equation 4.2:

$$P_{i,t} = (C_{i,t2} - C_{i,t1}) / (t_2 - t_1) \quad (4.2)$$

### 4.3.2 Coulombic efficiency

Coulombic efficiency (CE), also named current efficiency, is the efficiency of capturing the electron from the electric current to the product and was calculated using equation 4.3 based on [23]:

$$CE \text{ in } \%, \eta_e = \frac{N_{i,t} \times f_{e,i} \times F}{\int_0^t I dt} \times 100 \quad (4.3)$$

Here  $N_{i,t}$  is the number of moles of the product 'i' analyzed at time t,  $f_{e,i}$  represent the molar conversion factor (e.g. 8 electron equivalent per mol for acetate), F is faraday constant (96,485 C mol<sup>-1</sup> of electron) and I refers the current (A). In this study, mainly the acetate production was considered for coulombic efficiency calculations. Coulombic efficiencies at every measurement of organic compounds were calculated based on the accumulating product concentrations from the beginning of the MES operation as well as intermittently calculated from the difference of concentrations between two consecutive measurements.

**Table 4.1:** operational schemes and phases of MESs experiment

| Experimental phases  | MES-1<br>(days of<br>experiment) | MES-2<br>(days of experiment) | MES-3<br>(days of experiment) |
|--|----------------------------------|-------------------------------|-------------------------------|
| Microbes inoculation   | 7 days prior<br>polarization     | 12 days prior<br>polarization | 0 days prior<br>polarization  |
| Start polarizing cathode $E_{cat} = -0.6 \text{ V}_{/Ag/AgCl}$   | Day 0                            |                               |                               |
| Start sparging $N_2 : H_2 : CO_2$ (80:7:13) $E_{cat} = -0.6 \text{ V}_{/Ag/AgCl}$                        | Day 13                           | Day 9                         | Day 10                        |
| 30 % catholyte replaced $E_{cat} = -0.8 \text{ V}_{/Ag/AgCl}$ ,<br>$N_2 : H_2 : CO_2$ (80:7:13)          | 23                               | 17                            | 11                            |
| 30 % catholyte replaced $E_{cat} = -0.8 \text{ V}_{/Ag/AgCl}$ ,<br>$N_2 : H_2 : CO_2$ (80:7:13) sparging | 41                               | 38                            | 27                            |
| 30 % catholyte replaced $N_2 : H_2 : CO_2$ (80:7:13)   | 64                               | -                             | 48                            |
| Production phase 20% $CO_2$ mixture sparging   | 85                               | 61                            | 92                            |
| Batch 1- $N_2 : CO_2$ (20:80) sparging   | 127                              | 102                           | 120                           |
| Batch 2 – New medium replaced $N_2 : CO_2$ (20:80)<br>sparging   | 205                              | 179                           | 189                           |
| Batch 3 - Full catholyte replaced with new medium<br>$N_2 : CO_2$ (20:80) sparging                       | 246                              | 239                           | 377                           |

## 4.4 Results and Discussions

### 4.4.1 Pretreatment and long-term acclimation lead to the autotrophic production of acetate

#### Start-up and acclimation in sequential batches created selection pressure and supplied nutrients

An effective approach for a robust  $CO_2$  reducing biocathode development was demonstrated based on a pre-treatment of the inoculum and specific operation procedures of the MES. For the avoidance of methanogenesis, the inoculum sludge was initially heat-treated at 90°C for an hour and then treated with 0.5 g L<sup>-1</sup> of Na-BES



---

(chemical methanogens inhibitor) during the revival growth with fructose. The inoculum from pre-treated sludge was used for start-up and acclimation toward the bioelectrochemical CO<sub>2</sub> reduction in MES reactors. Here, the start-up, acclimation and operation procedure are particularly discussed for MES-1

At first, the microbes were pre-grown in the cathode chamber of MES-1 reactor in a fructose supplemented medium for 7 days prior to the cathode polarization in order to grow the bacterial biomass quickly in the cathode. Pre-enrichment in heterotrophic mode also enhanced the start-up for facultative autotrophic biocathode [24]. Microbial growth was measured by OD<sub>600</sub> which was increased to 0.6 in the first 21 days. The cathode was polarized at -0.6 V<sub>/Ag/AgCl</sub> (day 0 to 24) at the beginning and at -0.8 V from day 24. In order to remove the products of heterotrophic growth, 30% of the previous catholyte was replaced by the fresh mineral medium. During the start-up and acclimation period, the catholyte replacement was done on day 22, day 41 and day 64. After the sequential replacement of catholyte, the OD<sub>600</sub> dropped to ca. 0.2 on day 43 and then remained stable at 0.2 afterward. In the batch operation after day 43, a gas mixture of N<sub>2</sub>:CO<sub>2</sub>:H<sub>2</sub> (80:13:7) was fed to provide the additional hydrogen as reducing equivalent. Removal of previous catholyte and replenishment by fresh medium excluded a large fraction of suspended biomass in the reactor and as such selected towards electrode-attached species. The fresh new catholyte also replenished essential vitamins and minerals which vitalized the microbes on the cathode.

#### Successful switch from heterotrophic to autotrophic mode

In order to allow a complete degradation of organic substrates from the start-up phase of the MES-1 reactor, a long-term acclimation (64 days) was adopted. This measure reduced the interference of heterotrophy in the autotrophic bioproduction period. The current densities and product titers are as shown in the production profile of MES-1 operation in Figure 4.2.

The decreasing butyrate concentration and fluctuating ethanol most likely indicate that the acetate production until day 64 might be contributed by the degradation of butyrate and ethanol (Figure 4.2). After replacement of catholyte on day 64, butyrate and ethanol were removed from the catholyte (concentrations were below detection limit). However, acetate production was first observed in new batch under the feeding of N<sub>2</sub>:CO<sub>2</sub>:H<sub>2</sub> (80:13:7), notably on day 79-85 in Figure 4.2, when the cathode polarization was temporally varied from -0.8 to -1 V<sub>/Ag/AgCl</sub> and the current density increased to -2 A m<sup>-2</sup> (here, the minus prefix implies the cathodic nature of the current regardless of the value) at -1 V<sub>/Ag/AgCl</sub>. No significant amounts of other organic compounds except acetate was measured in the catholyte during that phase and the OD<sub>600</sub> remained constant at 0.2 indicating no biomass degradation. During this period (day 77 to 87), the total COD of catholyte increased from 1435 to 1716 mg L<sup>-1</sup>. Thus, the production of acetate from this moment was expected to proceed via the autotrophic metabolism of the microbes utilizing the available reducing equivalents, obtained either from the polarized cathode or from the available H<sub>2</sub>. The electron equivalents were not only available from the electric current for the CO<sub>2</sub> reduction to acetate during day 79-85 but also from H<sub>2</sub> supplied by sparging a mixture (80:13:7 % v/v N<sub>2</sub>:CO<sub>2</sub>:H<sub>2</sub>). A balance-chart of electron equivalents is provided in the Supplementary information-Chapter 4 Figure SI-2 for the CO<sub>2</sub> reduction to acetate from the day 79 to 85 and an overall coulombic efficiency of 24% was calculated from the 273 mg of acetate produced during that period.

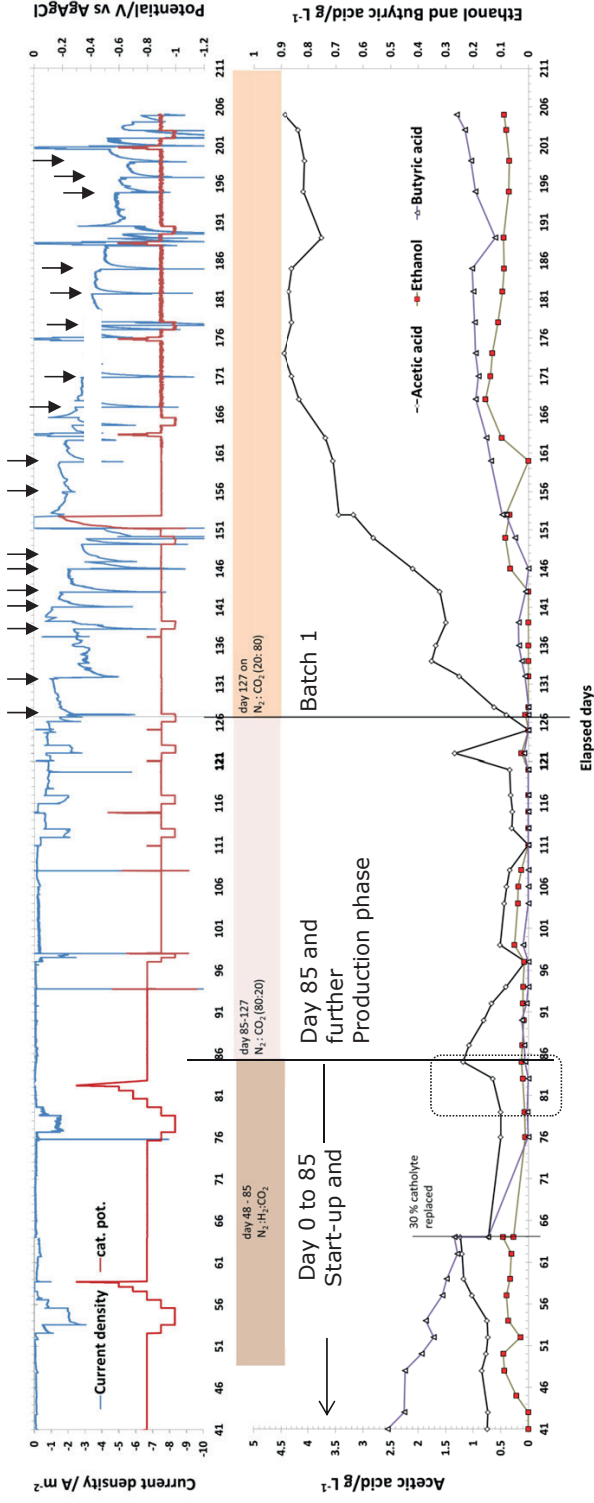
---

#### **4.4.2 Lower cathode potentials stimulated acetate production with 20% CO<sub>2</sub> gas mixture**

From day 85, MES-1 was operated under N<sub>2</sub>: CO<sub>2</sub> (80:20 v/v) gas mixture sparging without H<sub>2</sub> and the potentiostatically controlled cathode was the only source of supplied reducing equivalents. Initially, when the cathode of MES-1 reactor was constantly polarized at -0.8 V from day 85 to day 97, the previously produced acetate declined instead of a further accumulating. Later on, a temporal polarization of cathode to -0.9 and -1 V (dynamic cathode potential) increased the acetate level to ~0.5 mg L<sup>-1</sup>. This indicated that -0.8 V might not be providing sufficient reducing power for CO<sub>2</sub> reduction. Lower potentials did stimulate the production of electrons (equivalents) and acetate. From day 99, the cathode was continuously polarized at -0.9 V<sub>/Ag/AgCl</sub> and even lower potentials (-1 V<sub>/Ag/AgCl</sub>) for short durations for further operation of batch 1 with continuous N<sub>2</sub>:CO<sub>2</sub> (80:20 v/v) gas mixture sparging till day 127. In this period acetate was produced sporadically but did not accumulate to higher concentrations. The period between day 97 and day 127 was the start of production phase from CO<sub>2</sub> reduction solely driven by the electrical input. Figure 4.2 shows that after each temporal lowering of cathode polarization from -0.8 V to -1 V, particularly on day 99 and on day 122, acetate concentration increased, but when the cathode potential remained fixed at -0.9 V, acetate level did not increase. During the stepwise lowering of the cathode potential, the current density reached -2 A m<sup>-2</sup> at -1 V, which might be associated with the observed hydrogen production in the reactor and consequently acetate was produced from CO<sub>2</sub>. Most probably, hydrogen evolution had mediated the CO<sub>2</sub> reduction. Since bioelectrochemical CO<sub>2</sub> reduction in MES has been reported mainly under hydrogen mediated condition [11, 25, 7], the sufficiently low cathode potential of -1 V<sub>/Ag/AgCl</sub> might have been a prerequisite for the bioelectrochemical CO<sub>2</sub> reduction in this MES reactor.

#### **4.4.3 High acetate concentration with 80% CO<sub>2</sub> gas mixture feeding (Batch 1)**

Starting from day 127, the gas feed was replaced with N<sub>2</sub>:CO<sub>2</sub> (20:80 v/v) and the cathode potential was fixed at -0.9 V<sub>/Ag/AgCl</sub>. The current densities and product concentrations in the catholyte of MES-1 during the Batch 1 operation are included in Figure 4.2. The quick jumps in current density during a constant cathode potential are due to the temporal CO<sub>2</sub> gas spargings (indicated by arrows in Figure 4.2). The gas bubbling was frequently done for 15-30 minutes at each time. The current density increased abruptly reaching -6 A m<sup>-2</sup> on 80% CO<sub>2</sub> sparging in the catholyte which gradually stabilized to -2 to -3 A m<sup>-2</sup> after stopping the gas sparging. Under N<sub>2</sub>:CO<sub>2</sub> (20:80) feed, the acetate production accelerated and reached a maximum production rate of 248 mg L<sup>-1</sup> d<sup>-1</sup> and accumulated 1.7 g L<sup>-1</sup> of acetate in the catholyte to from day 126-134. Acetate production continued at slower rates and at the end of the batch, acetate accumulated up to 4.45 g L<sup>-1</sup> which is one order of magnitude higher than during the supply of 20% CO<sub>2</sub>. This remarkable increase in acetate production with 80% CO<sub>2</sub> gas mixture (compared to the 20% CO<sub>2</sub> mixture) inferred that the system was CO<sub>2</sub> limited previously. Furthermore, the pH lowering effect of 80% CO<sub>2</sub> gas mixture sparging also increased the current density and indeed provided thermodynamically more reducing power to the biocatalysts for CO<sub>2</sub> reduction. Sparging of CO<sub>2</sub> gas also can lower the electrode overpotential as a result of buffering effect [26].



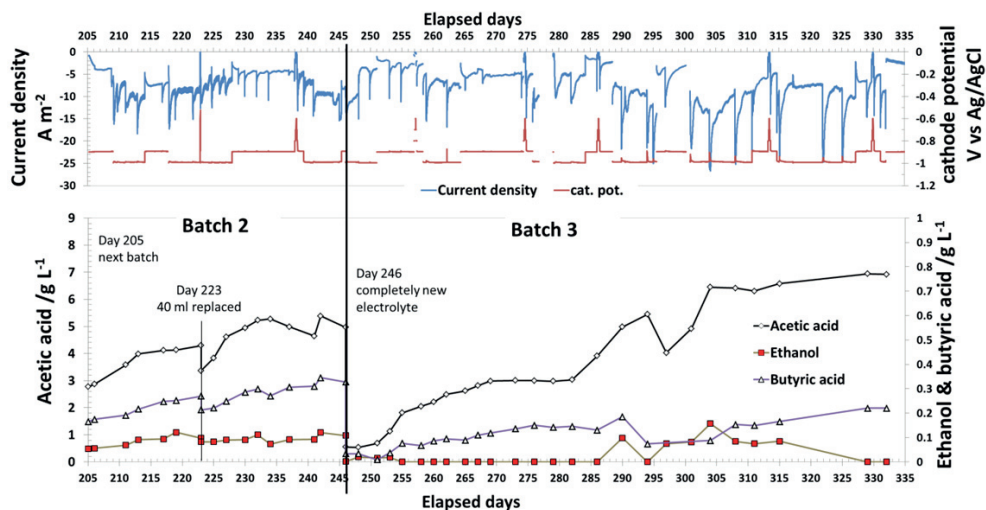
**Figure 4.2:** Current densities at the corresponding cathode potentials and product concentrations observed in MES-1 operation during the acclimation phase (until day 85), production phase with continuous 20% CO<sub>2</sub> gas mixture feed (day 85-126) and Batch 1 with intermittent 80% CO<sub>2</sub> gas mixture feed (day 127-206). The small box between day 76-86 in the lower graph indicates the acetate production solely from CO<sub>2</sub> reduction. The arrows on the top of the figure indicate the sparging of CO<sub>2</sub>:N<sub>2</sub> (80:20) gas mixture.

---

**4.4.4 Acetate was reproduced and higher concentrations were achieved at prolonged batch times (Batch 2 and 3)**

Repetitive batch operation of CO<sub>2</sub> reduction in MES-1 was carried out on day 205 (batch 2) and on day 246 (batch 3) by replacing the previous catholyte with fresh new catholyte (70% replacement for Batch 2). The production profile of MES 1 operation in Batch 2 and Batch 3 are as shown in Figure 4.3. A gradual increase of acetate concentration starting at ~3 g L<sup>-1</sup> reached 6 g L<sup>-1</sup> during the 40 days of operation in Batch 2, whereas in Batch 3, up to 7 g L<sup>-1</sup> acetate was achieved with the intermittent sparging of 80% CO<sub>2</sub> gas mixture at -0.9 and -1 V<sub>/Ag/AgCl</sub> cathode potentials. For the reproducibility of these results, other two independent reactors (namely, MES-2 and MES-3) were also experimented with intermittent N<sub>2</sub>:CO<sub>2</sub> (20:80) bubbling and cathode polarization up to -1 V<sub>/Ag/AgCl</sub>. Long-term (almost 100 days) operation of MES-2 and MES-3 reactors in CO<sub>2</sub> fed-batch mode also produced acetate and accumulated up to 8-10 g L<sup>-1</sup>. Production profiles of acetate and other organic compounds along with current densities and cathode potentials are provided in Supplementary information–Chapter 4 Figure SI-4 and Figure SI-5.

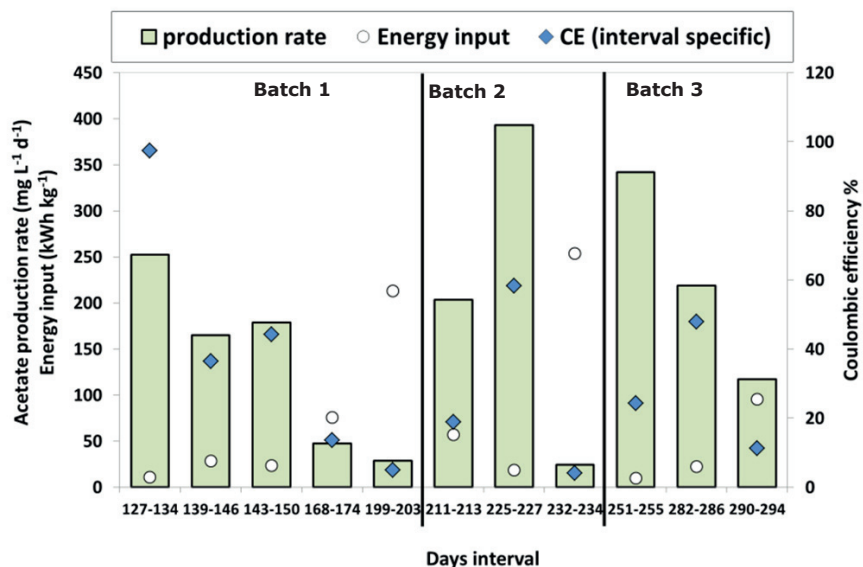
Bioelectrochemical CO<sub>2</sub> reduction was most possibly mediated with H<sub>2</sub> (biocatalytically or electrochemically produced) because acetate production was observed only when the cathode potentials were lower than -0.9 V<sub>/Ag/AgCl</sub> and H<sub>2</sub> was detected in the headspace, specifically 59% H<sub>2</sub> was measured on day 178 (data in supporting information Table SI 5). The roles of biologically catalyzed or electrolytically produced H<sub>2</sub> in MES from CO<sub>2</sub> has already been emphasized in recent literature [27, 15]. H<sub>2</sub> evolution at graphite electrode comprises large electrode overpotential, but microbial electrocatalysis reduces the electrode overpotential significantly. The cathode overpotential for H<sub>2</sub> production with biocathode in microbial electrolysis cell was reported at -0.28 V i.e. at the cathode potential of -0.9 V<sub>/Ag/AgCl</sub> [28]. Hence, both biocatalytically and electrochemically H<sub>2</sub> production is possible in our CO<sub>2</sub> reducing MES systems. The headspace composition of MES-1 during Batch 3 operation repeatedly shows CO<sub>2</sub> filled up in headspace with N<sub>2</sub>:CO<sub>2</sub> (20:80) bubbling and attained 70-80% CO<sub>2</sub> (see supporting information Table SI 5). After stopping the gas bubbling within 1-4 days, CO<sub>2</sub> declined to an undetectable level and H<sub>2</sub> accumulated under -0.9 to -1 V cathode polarization in batch 3. H<sub>2</sub> gas in the headspace of MES-1 reached up to 96% in some recordings when the reduction current densities were higher than 10 A m<sup>-2</sup>. However, the volumetric measurement of H<sub>2</sub> production was not done. Considerable increase in reduction current densities reaching higher than 10 A m<sup>-2</sup> was a remarkable demonstration of the electrocatalytical activity of biocathode. The increase in current densities was more pronounced especially after the stepwise change in cathode potentials (dynamic cathode polarization e.g. in day 238-242 in batch 2 and day 286-293 in batch 3). Cathode polarization at -0.9 and -1 V (upper graph in Figure 4.3) appears to facilitate CO<sub>2</sub> reduction with ample supply of reducing equivalents at high current densities.



**Figure 4.3:** Operation of MES-1 in Batch 2 and 3 under intermittent (20:80)  $N_2:CO_2$  bubbling. Repeated accumulation of acetate in MES to high titer indicates a consistently  $CO_2$  reducing and robust biocathode.

#### 4.4.5 Changing acetate production rates, coulombic efficiencies and energy inputs in MES-1 over time

The acetate production in MES from  $CO_2$  did not remain steady within a batch operation due to dynamic conditions created by the intermittent  $CO_2$  sparging and also likely due to the changing pH, nutrient availability and accumulating of products in the catholyte. There were also trends of decreasing acetate in some intervals in the long-term operation. An overview of acetate production rates along with coulombic efficiencies and electric energy input at various production periods in the three batches of MES-1 operation are provided in Figure 4.4. At the beginning of Batch 1 with fresh catholyte, the acetate production rate was higher during day 126 to 134 and the production corresponds to nearly 97% coulombic efficiency (CE). But after reaching  $1.7 \text{ g L}^{-1}$ , acetate level declined even at  $-1 \text{ V}$  cathode potential (day 134-139) but small amount of butyrate was produced reaching  $0.1 \text{ g L}^{-1}$  (Figure 4.2). Acetate production in MES-1 continued at  $178 \text{ mg L}^{-1} \text{ d}^{-1}$  from day 143 to 153 and further on, acetate produced at slower rate ( $49.8 \text{ mg L}^{-1} \text{ d}^{-1}$ ) in Batch 1. The highest production rate of ca.  $400 \text{ mg L}^{-1} \text{ d}^{-1}$  was obtained between day 225-227 in Batch 2 operation of MES 2 and at this period, the CE registered 53 %. In the late stage, the acetate production rate and also the CE declined. In Batch 3, acetate production rate attained from  $340 \text{ mg L}^{-1} \text{ d}^{-1}$  (day 251-255) to  $219 \text{ mg L}^{-1} \text{ d}^{-1}$  (day 282-286) with maximum CE of 48% during Batch 3.



**Figure 4.4:** Performance of acetate production from  $\text{CO}_2$  reduction in three batches of MES-1 at various time periods. Declining acetate production rates and coulombic efficiencies along a long-term batch operation is visible in concert with an increase in energy requirement for production.

In Batch 1, the production of acetate at the initial days of a batch attributed higher rates and higher coulombic efficiencies than in the late phase (Figure 4.4). Likewise, high initial acetate production rate at the beginning of batch and lower production rate at the late phase of batch was repeatedly observed in Batch 2 and Batch 3 of MES-1. Opposite tendency in electric energy input for electrosynthesis was observed in both batch 1 and 3. High production rates obtained might be linked with the availability of fresh medium replaced for the previous catholyte which can bring a new dose of micronutrients. Electric energy input of as low as 10–18 kWh per kg acetate was calculated at the early stage of a batch whereas as high as 200–250 kWh per kg acetate electric energy input was required during the long-term operation of  $\text{CO}_2$  reducing MES. This means that the reducing equivalents from current densities were more effectively used for  $\text{CO}_2$  reduction at the early phase of the batch. The electrode overpotentials might decrease at the late stage of a batch due to the acidification effect of  $\text{CO}_2$  as well as the accumulation of acetic acid. Overpotentials of MES-1 at different current densities on day 75 and day 163 are calculated and provided in Supplementary information-Chapter 4 Figure SI-3. The overpotential at the current density of  $1.5 \text{ A m}^{-2}$  was lowered by almost 0.2 V in the late stages due to the bubbling of 80%  $\text{CO}_2$ .

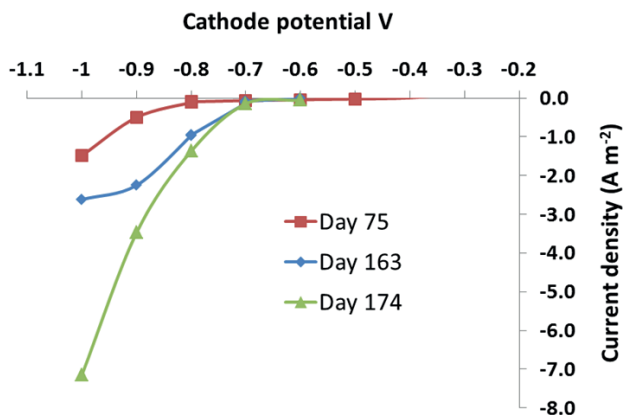
Higher current densities observed at the late stage of batches imply more reducing equivalents including electrolytic  $\text{H}_2$  were available. Evidently, as discussed in the previous section, headspace gas analysis of MES-1 also showed faster accumulation of  $\text{H}_2$  in the late phase. However, acetate production rates were declining at those time periods. Possibly, accumulation of acetic acid in the catholyte could also impose an inhibition effect to the biocatalysts [29]. Similar effects were observed in fermentation studies which did lead to in-situ removal approaches [30]. Additionally, micro-nutrient limitation might also be expected after a long-term operation. Blanchet et al. [27] also pointed out the nutrient limitation in  $\text{H}_2$  &  $\text{CO}_2$  growth of *Sporomusa ovata* when no bioproduction was obtained without yeast extract supplementation. Acetate production rates and efficiencies went down at the late phase of a batch run. Ultimately, the product of MES

---

after higher level of acetate accumulation at the late stage of long-term operation appeared to be mainly H<sub>2</sub>. To support this, Jourdin et al. [31] also demonstrated an autotrophic biocathode only producing H<sub>2</sub> sustained by a cathode as the only electron source. A short batch time may enhance the overall energy efficiency (electric energy input and coulombic efficiency) of the MES; though this will reduce the acetate concentration which will make separation more challenging.

#### **4.4.6 Evolution in biocathode in response to the polarization performance**

The response of MES-1 biocathode at acclimation phase and in Batch 1 production phase showed biocatalytic effect towards the reduction reactions. The standard redox potential for CO<sub>2</sub> reduction to acetate is -0.48 V<sub>/Ag/AgCl</sub> at the biological condition (pH 7) but the energy losses due to the overpotentials demands even lower cathode potential. Likewise, H<sub>2</sub> evolution occurs at -0.6 V<sub>/Ag/AgCl</sub> at biological condition (pH 7) but due to the overpotentials involved, fairly low cathode potentials (< -1 V<sub>/Ag/AgCl</sub>) are required for H<sub>2</sub> evolution in carbon electrodes [28]. In the mixed culture biocathode, the equilibrium potential becomes complex due to the possibility of multiple unknown reactions in addition to the CO<sub>2</sub> reduction. It is known that the chosen applied potential affects the performance of MES [18]. Since there are possibilities for various known and likely unknown electron transfer mechanisms at the biocathode [32], a dynamic cathode potential control can stimulate electron transfer at the biocathodes. In order to set the cathode potential for effective CO<sub>2</sub> reduction, dynamic cathode polarizations were performed during the operation of MES-1 by applying a series of chronoamperometry techniques. Polarization curves (Figure 4.5) are made for MES-1 from the stable current densities recorded during the dynamic cathode polarization from -0.3 V to -1 V, maintaining at least an hour at each cathode potential. The dynamic polarization performed on day 75, day 163 and day 174 are considered for the biocathode evolution analysis. The polarization curves on day 163 and day 174 (at batch 1 with 80 % CO<sub>2</sub> gas mixture sparging) showed higher current densities between the cathode potential -0.7 to -1 V<sub>/Ag/AgCl</sub> than those in the polarization curve of day 75 (13% CO<sub>2</sub> gas mixture sparging period). When the average current density at a certain cathode potential increases along the elapsed time, an increase in electrochemical activity of biocathode can be inferred, given that the physical parameters like pH, temperature and etc. remain the same. As such, the evolution of higher current densities observed during the batch 1 of production phase shows a favorable interaction among the microbes, the polarized electrode and available CO<sub>2</sub>. Furthermore, the dynamic cathode polarization might also stimulate biocatalytical H<sub>2</sub> formation which in turn, favors the biological CO<sub>2</sub> reduction. Ultimately, the rise in current densities in the polarization curves and also during the long-term polarization at -0.9 to -1 V<sub>/Ag/AgCl</sub> in the batch 1 is the indication of the electrocatalytic effect of the biocatalyst striving on the CO<sub>2</sub> reduction by using the reducing equivalents produced at the polarized cathode. Nowadays, several methods to start-up biocathodes are developed. To elucidate the effectiveness of these methods further comparable experiments must be done. Hereby, the knowledge on the electron transfer mechanisms is needed to further clarify the performances.



**Figure 4.5:** Polarization curves obtained from the dynamic cathode polarization performed on day 75, day 163 and day 174 of MES-1 operation.

#### 4.4.7 Methanogenesis was avoided in long-term operating robust biocathode

Remarkably, CH<sub>4</sub> was never detected in the whole operation of MES-1 reactor for more than 300 days (headspace gas composition provided in Supplementary information-Chapter 4 Table SI-6) and methanogenesis inhibiting chemical (Na-BES) was not added directly in the catholyte during microbial electrosynthesis. Heat shock and methanogenesis inhibitor (Na-BES) treatment to the anaerobic sludge and enrichment of resulted mixed culture in H<sub>2</sub> & CO<sub>2</sub> appeared to be an effective procedure for the selective inoculum preparation. Patil et al. [13] also demonstrated a selective enrichment procedure to avoid methanogenic activity but the revival of methanogenesis was mentioned in the long time operation (~60 days) of CO<sub>2</sub> reducing MES. In contrast, a long-term operations of MES from CO<sub>2</sub> were conducted in our experiments, eliminating methanogenesis without direct supplementation of any chemical inhibitor in the catholyte. These findings were repeatedly observed over the whole experiment by analyzing the headspace gas composition in between the intermittent CO<sub>2</sub>:N<sub>2</sub> spargings. As such, it was confirmed that the potentially produced methane was not flushed out of the cathode chamber. The time period between two CO<sub>2</sub>:N<sub>2</sub> mixture flushings was 1 to 4 days and did not result in any methane detection in between (Limit of detection 0.01 %). So, in our study, an extended pre-treatment and sequential batch operation likely resulted in an effective exclusion of methanogens. By microscopic analysis, it was confirmed that a variety of microorganisms was present. But, further microbial analysis is needed to confirm the absence of methanogens. These results promise that the innovative selection procedure of biocatalyst adopted in this study can be applied to the other biological inocula as well for the application in MES. As such the development of the CO<sub>2</sub> reducing biocatalyst for the mixed culture MES processes can be realized also from other anaerobic inocula.

#### 4.4.8 Production of more reduced products than acetate in MES

Acetate was main the organic product of bioelectrochemical CO<sub>2</sub> reduction during the operation of MES-1 reactor in all batches. Besides acetate, formate, propionate, ethanol and butyrate were also detected in the catholyte samples. Particularly, ethanol and butyrate were detected in the catholyte sample constantly above 0.05 g L<sup>-1</sup>. Production of ethanol from syngas fermentation using homoacetogens such as *Clostridium ljungdahlii* has been extensively investigated [33, 34]. Likewise, chain elongation



mechanism along with Wood-Ljungdahl pathway supports acetate conversion to butyrate and other fatty acids [35, 36]. Notably, in the MES from CO<sub>2</sub>, ethanol and butyrate were produced after the accumulation of more than 1.5 g L<sup>-1</sup> acetate and acidifying effect of CO<sub>2</sub> gas sparging may support the production of further reduced products. Ethanol was sporadically measured in the sample of MES-1 (as seen in Figure 4.2 and Figure 4.3) whereas butyrate was more frequently detected and the concentration followed an accumulating trend but the highest butyrate concentrations remained below 0.5 g L<sup>-1</sup>. Further supporting data on butyrate product in MES-3 reactor illustrates that when the current densities were higher than 10 A m<sup>-2</sup> and pH was maintained acidic mostly below 6, butyrate production accumulated up to 1 g L<sup>-1</sup> (MES-3 production profile in Supplementary information-Chapter 4 Figure SI-5). A further study at defined conditions is needed to actually confirm on this mechanism. Ganigué et al. [6] reported MES of butyrate from CO<sub>2</sub> depending on the favoring reactor condition for chain elongation. Ethanol production in MES from CO<sub>2</sub> was evident for *Clostridium ljungdahlii* as biocatalyst in Bajracharya et al. [7]. Moreover, ethanol and butyrate production was independently repeated in different reactor set-up previously [19]. Highly reduced products in MES are attractive in terms of cost-benefits and applicability of product as fuel and chemical feedstocks [37]. Still, the production rates for butyrate and medium chain fatty acids are higher in conventional chain elongation fermentations [38] which gives directions to enhance production rates and concentration within mixed culture systems.

## 4.5 Conclusions

This study illustrates that the inoculum pre-treatment and a number of culture transfers in H<sub>2</sub> & CO<sub>2</sub> growth media is an effective approach for selecting CO<sub>2</sub> reducing biocatalyst during sequence batch operation in MES. Avoidance of methanogenesis without direct addition of inhibitors in long-term operation of MES from CO<sub>2</sub> did result in higher product titers. MES from CO<sub>2</sub> at -1 V<sub>/Ag/AgCl</sub> by using the enriched and acclimated mixed culture repeatedly produced acetate along with hydrogen and also diversified the products to ethanol and butyrate. Apparently, the approach of biocathode development through the selective pre-treatments and the results of long-term operation presented in this study will advance MES from CO<sub>2</sub> toward attractive implications of electricity-driven bioproduction. For a long term operation of MES from CO<sub>2</sub> with high rate production, separation of accumulated product and prevention of potential nutrient limitation could be required.

## Acknowledgments

The work was supported by a PhD grant to Suman Bajracharya from VITO's strategic research funds (project no. 1310225). The authors thank Dr. Mohanakrishna Gunda for carrying out sludge pretreatment.

## References

1. Nevin KP, Woodard TL, Franks AE, et al (2010) Microbial Electrosynthesis : Feeding Microbes Electricity To Convert Carbon Dioxide and Water to Multicarbon Extracellular Organic. MBio 1:e00103-10-. doi: 10.1128/mBio.00103-10.Editor
2. Rabaey K, Rozendal RA (2010) Microbial electrosynthesis — revisiting the electrical route for microbial production.pdf. Nat Rev Microbiol 8:706–16. doi: 10.1038/nrmicro2422
3. Nevin KP, Hensley SA, Franks AE, et al (2011) Electrosynthesis of organic compounds from carbon dioxide is catalyzed by a diversity of acetogenic microorganisms. Appl Environ Microbiol 77:2882–6. doi: 10.1128/AEM.02642-10
4. Schuchmann K, Müller V (2014) Autotrophy at the thermodynamic limit of life: a model for energy conservation in acetogenic bacteria. Nat Rev Microbiol 12:809–821. doi: 10.1038/nrmicro3365
5. Liew FM, Köpke M, Simpson SD (2013) Gas Fermentation for Commercial Biofuels Production.

- 
6. Ganigüé R, Puig S, Batlle-Vilanova P, et al (2015) Microbial electrosynthesis of butyrate from carbon dioxide. *Chem Commun* 51:3235–3238. doi: 10.1039/C4CC10121A
  7. Bajracharya S, ter Heijne A, Dominguez X, et al (2015) CO<sub>2</sub> reduction by mixed and pure cultures in microbial electrosynthesis using an assembly of graphite felt and stainless steel as a cathode. *Bioresour Technol*. doi: 10.1016/j.biortech.2015.05.081
  8. Sharma M, Aryal N, Sarma PM, et al (2013) Bioelectrocatalyzed reduction of acetic and butyric acids via direct electron transfer using a mixed culture of sulfate-reducers drives electrosynthesis of alcohols and acetone. *Chem Commun (Camb)* 49:6495–7. doi: 10.1039/c3cc42570c
  9. Steinbusch KJJ, Hamelers HVM, Schaap JD, et al (2010) Bioelectrochemical ethanol production through mediated acetate reduction by mixed cultures. *Environ Sci Technol* 44:513–7. doi: 10.1021/es902371e
  10. ElMekawy A, Hegab HM, Mohanakrishna G, et al (2016) Technological advances in CO<sub>2</sub> conversion electro-biorefinery: A step towards commercialization. *Bioresour Technol*. doi: 10.1016/j.biortech.2016.03.023
  11. Marshall CW, Ross DE, Fichot EB, et al (2013) Long-term operation of microbial electrosynthesis systems improves acetate production by autotrophic microbiomes. *Environ Sci Technol* 47:6023–9. doi: 10.1021/es400341b
  12. Jourdin L, Grieger T, Monetti J, et al (2015) High Acetic Acid Production Rate Obtained by Microbial Electrosynthesis from Carbon Dioxide. *Environ Sci Technol* 49:13566–13574. doi: 10.1021/acs.est.5b03821
  13. Patil SA, Arends JBA, Vanwonterghem I, et al (2015) Selective Enrichment Establishes a Stable Performing Community for Microbial Electrosynthesis of Acetate from CO<sub>2</sub>. *Environ Sci Technol* 150701101446004. doi: 10.1021/es506149d
  14. van Eerten-Jansen MCAA, Jansen NC, Plugge CM, et al (2015) Analysis of the mechanisms of bioelectrochemical methane production by mixed cultures. *J Chem Technol Biotechnol* 90:963–970. doi: 10.1002/jctb.4413
  15. Jourdin L, Lu Y, Flexer V, et al (2015) Biologically-induced hydrogen production drives high rate / high efficiency microbial electrosynthesis of acetate from carbon dioxide. *ChemElectroChem* n/a–n/a. doi: 10.1002/celec.201500530
  16. Ter Heijne A, Strik DPBTB, Hamelers HVM, Buisman CJN (2010) Cathode potential and mass transfer determine performance of oxygen reducing biocathodes in microbial fuel cells. *Environ Sci Technol* 44:7151–7156. doi: 10.1021/es100950t
  17. Aelterman P, Freguia S, Keller J, et al (2008) The anode potential regulates bacterial activity in microbial fuel cells. *Appl Microbiol Biotechnol* 78:409–418. doi: 10.1007/s00253-007-1327-8
  18. Mohanakrishna G, Vanbroekhoven K, Pant D (2016) Imperative role of applied potential and inorganic carbon source on acetate production through microbial electrosynthesis. *J CO<sub>2</sub> Util*. doi: 10.1016/j.jcou.2016.03.003
  19. Bajracharya S, Vanbroekhoven K, Buisman CJN, et al (2016) Application of Gas Diffusion Biocathode in Microbial Electrosynthesis from Carbon dioxide. *Environ. Sci. Pollut. Res*. doi: 10.1007/s11356-016-7196-x
  20. Mohanakrishna G, Seelam JS, Vanbroekhoven K, Pant D (2015) An enriched electroactive homoacetogenic biocathode for the microbial electrosynthesis of acetate through carbon dioxide reduction. *Faraday Discuss*. doi: 10.1039/C5FD00041F
  21. Zinder SH, Anguish T, Cardwell SC (1984) Selective Inhibition by 2-Bromoethanesulfonate of Methanogenesis from Acetate in a Thermophilic Anaerobic Digester. *Appl Environ Microbiol* 47 :1343–1345.
  22. Oh S-E, Van Ginkel S, Logan BE (2003) The relative effectiveness of pH control and heat treatment for enhancing biohydrogen gas production. *Environ Sci Technol* 37:5186–90. doi: Doi 10.1021/Es034291y
  23. Patil SA, Gildemyn S, Pant D, et al (2015) A logical data representation framework for electricity-driven bioproduction processes. *Biotechnol Adv* 33:736–744. doi: 10.1016/j.biotechadv.2015.03.002
  24. Zaybak Z, Pisciotta JM, Tokash JC, Logan BE (2013) Enhanced start-up of anaerobic facultatively autotrophic biocathodes in bioelectrochemical systems. *J Biotechnol* 168:478–485. doi: 10.1016/j.jbiotec.2013.10.001
  25. Su M, Jiang Y, Li D (2013) Production of acetate from carbon dioxide in bioelectrochemical systems based on autotrophic mixed culture. *J Microbiol Biotechnol* 23:1140–6.
  26. Ki D, Popat SC, Torres CI (2016) Reduced overpotentials in microbial electrolysis cells through improved design, operation, and electrochemical characterization. *Chem Eng J* 287:181–188. doi: 10.1016/j.cej.2015.11.022
  27. Blanchet EM, Duquenne F, Rafrafi Y, et al (2015) Importance of the hydrogen route in up-scaling electrosynthesis for microbial CO<sub>2</sub> reduction. *Energy Environ Sci* 8:3731–3744. doi:
-

- 10.1039/C5EE03088A
28. Jeremiassé AW, Hamelers HVM, Buisman CJN (2010) Microbial electrolysis cell with a microbial biocathode. *Bioelectrochemistry* 78:39–43. doi: 10.1016/j.bioelechem.2009.05.005
  29. Baronofsky JJ, Schreurs WJA, Kashket ER (1984) Uncoupling by acetic acid limits growth of and acetogenesis by *Clostridium thermoaceticum*. *Appl Environ Microbiol* 48:1134–1139.
  30. Lye GJ, Woodley JM (1999) Application of in situ product-removal techniques to biocatalytic processes. *Trends Biotechnol* 17:395–402. doi: 10.1016/S0167-7799(99)01351-7
  31. Jourdin L, Freguia S, Donose BC, Keller J (2015) Autotrophic hydrogen-producing biofilm growth sustained by a cathode as the sole electron and energy source. *Bioelectrochemistry* 102:56–63. doi: 10.1016/j.bioelechem.2014.12.001
  32. Deutzmann J, Sahin M, Spormann A (2015) Extracellular Enzymes Facilitate Electron Uptake in Biocorrosion and. *MBio* 6:1–8. doi: 10.1128/mBio.00496-15.Editor
  33. Phillips JR, Klasson KT, Clausen EC, Gaddy JL (1993) Biological production of ethanol from coal synthesis gas. *Appl Biochem Biotechnol* 39-40:559–571. doi: 10.1007/BF02919018
  34. Köpke M, Mihalcea C, Bromley JC, Simpson SD (2011) Fermentative production of ethanol from carbon monoxide.pdf. *Curr Opin Biotechnol* 22:320–325. doi: 10.1016/j.copbio.2011.01.005
  35. Agler MT, Wrenn B a, Zinder SH, Angenent LT (2011) Waste to bioproduct conversion with undefined mixed cultures: the carboxylate platform. *Trends Biotechnol* 29:70–8. doi: 10.1016/j.tibtech.2010.11.006
  36. Steinbusch KJJ, Hamelers HVM, Plugge CM, Buisman CJN (2011) Biological formation of caproate and caprylate from acetate: fuel and chemical production from low grade biomass. *Energy Environ Sci* 4:216–224. doi: 10.1039/C0EE00282H
  37. Desloover J, Arends JB a, Hennebel T, Rabaey K (2012) Operational and technical considerations for microbial electrosynthesis. *Biochem Soc Trans* 40:1233–8. doi: 10.1042/BST20120111
  38. Grootcholten TIM, Strik DPBTB, Steinbusch KJJ, et al (2014) Two-stage medium chain fatty acid (MCFA) production from municipal solid waste and ethanol. *Appl Energy* 116:223–229. doi: 10.1016/j.apenergy.2013.11.061



---

C  
H  
A  
P  
T  
E  
R

5

***In situ* acetate separation in microbial electrosynthesis  
(MES) from CO<sub>2</sub> using ion-exchange resin**

---

**Abstract**

Bioelectrochemical reduction of carbon dioxide (CO<sub>2</sub>) to multi-carbon organic compounds particularly acetate has been achieved in microbial electrosynthesis (MES) using the reducing equivalents produced at the electrically polarized cathode. MES has evolved considerably as a platform technology for CO<sub>2</sub> utilization and excess electricity storage. In our previous studies on MES from CO<sub>2</sub> reduction, 7–10 g L<sup>-1</sup> acetate was produced in the fed-batch operations using homoacetogenic activity enriched biocatalyst. The accumulation of acetic acid to higher concentrations may lead to product inhibition, especially at acidic pH. In such case, an MES with integrated extraction is interesting, firstly to reduce product inhibition and secondly, for the advancement of product recovery in the large-scale MES applications. We investigated acetate production from CO<sub>2</sub> in MES in combination with a batch-wise extraction of acetate from the broth using a commercially available anion-exchange resin (Amberlite™ FPA53). Acetate absorption of 10–20 mg g<sup>-1</sup> resin was observed at the catholytic conditions. The production of acetate in MES was maintained after the extraction. Overall, an MES system for the production and separation of acetate from CO<sub>2</sub> reduction was technically feasible through the integration of MES with an anion exchange resin extraction.

Keywords: Ion-exchange resin, In situ separation, Adsorption, Microbial electrosynthesis, CO<sub>2</sub> reduction

---

## 5.1 Introduction

World economy still relies greatly on the non-renewable petroleum resources for the production of bulk chemicals and liquid fuels. Because fossil resources are available in a finite stock and the emissions from the combustion of which are the causes of pollution and global warming [1, 2], alternatives are desired to secure our long-term need for energy, fuels and chemicals and to reduce our carbon footprint. In recent decades, advances were made in the field of production of value-added compounds, especially via electricity-driven bioprocesses [3–6]. It has been demonstrated that microorganisms are able to use electricity as the source of energy to reduce oxidized molecules, such as CO<sub>2</sub> into suitable building block chemicals such as volatile fatty acids (VFAs) [3, 7], in a process referred to as microbial electrosynthesis (MES). MES is a promising technology to produce bio-commodities from CO<sub>2</sub> with the input of electricity from renewable sources. In fact, MES can be presented as an excess energy-storing system for an intermittently produced renewable electricity [6]. MES of biochemicals from CO<sub>2</sub> reduction can reduce our dependency on fossil fuel and also utilize CO<sub>2</sub> to mitigate climate change issues [6, 8].

Several studies have shown the use of a mixed culture as biocatalyst in MES to form a robust biocathode for CO<sub>2</sub> reduction with high product yield (i.e. electron recovery) and acetate accumulating up to 10 g L<sup>-1</sup> [9] and 11 g L<sup>-1</sup> [10] at cathode potential  $\leq -0.59$  V versus standard hydrogen electrode ( $V_{/SHE}$ ). Here, the acetate complies the sum-up of acetate and acetic acid; and as such, we use acetate as the collective name for both forms hereafter, unless specifically stated. It has been repeatedly observed that long-term operation of CO<sub>2</sub> reduction in MES (> 300 days) using a homoacetogenic activity enriched mixed biocatalyst produced up to 7–10 g L<sup>-1</sup> of acetate during fed-batch operation [11]. These concentrations of acetate in MES are likely not sufficient for economically sound extraction, for instance, 20–200 g L<sup>-1</sup> of organic acids were produced in industrial fermentations [12]. To achieve these concentrations in MES, (potential) product inhibition must be circumvented or a further conversion of CO<sub>2</sub> to higher concentrations of acetic acid is needed. It is indeed known that the undissociated form of acetic acid can pass through the cytoplasmic membrane of the microorganisms and disrupt the proton-motive force [13]. Hence it could hamper further acetate production from CO<sub>2</sub> reduction. We investigated acetate production from CO<sub>2</sub> in MES, in combination with a batch-wise extraction, by using commercially available anion-exchange resins. An integration of acetate extraction in MES is desirable to reduce the potential product inhibition and also to complete the production with a recovery process.

*In situ* separation of acetate by using ion-exchange membrane electrolysis has already been shown by integrating it to the CO<sub>2</sub> reducing MES [14]. The membrane electrolysis technique is attractive, but the application requires more electric power. On the contrary, the ion-exchange resin based adsorption (sorption) technique is a common method of separation in industry. Adsorption technology has been used in separating organic acids *in situ* from the aqueous fermentation medium with less/no energy input [15, 16]. Ion-exchange resins have charged groups which adsorb counter ions from a solution based on the ion-exchange phenomenon. Such separation techniques are often applied in industrial water treatment, i.e. heavy metal removal [17, 18], nutrient removal [19] or drinking-water softening [20]. The operating pH levels of MES are at near neutral pH, which means that the acetate ion form predominates over the undissociated acetic acid form and can support a charge interaction with the resin. The objective of this study is to obtain a proof-of-principle for the application of an ion-exchange resin to recover acetate from MES process.

---

## 5.2 MATERIALS AND METHODS

### 5.2.1 MES set-up & operation

CO<sub>2</sub> reduction to acetate experiments were performed in a double chamber H-shaped reactor as described earlier [21]. The MES reactor consists of two compartments, each 250 ml, separated by a cation exchange membrane. A dimensionally stable anode (DSA), i.e. a ruthenium/iridium oxide coated titanium mesh, served as an anode. The cathode was a graphite stick with two graphite felts wrapped around it and an exposed surface area of 30 cm<sup>2</sup>. An Ag/AgCl in 3 M KCl reference electrode was positioned close to the cathode. This MES cell was operated with the similar analyte and catholyte buffer solutions as described in Bajracharya et al. [21]. The reactor was closed with airtight stoppers and continuously stirred maintaining a temperature of 35–37 °C with an electric heater. The headspace was intermittently flushed with N<sub>2</sub>:CO<sub>2</sub> (20:80) to render anaerobic condition as well as to provide CO<sub>2</sub> for reduction. The cathode potential was controlled by applying chronoamperometry in a potentiostat (Biologic VMP3).

The MES reactor had been previously operated for long-term (367 days) with a selectively enriched mixed seed culture from a biological sludge which was additionally supplemented with *Clostridium ljungdahlii* [11]. The biocathode had already been producing 7–10 g L<sup>-1</sup> of acetate from CO<sub>2</sub> reduction at -1 V<sub>/Ag/AgCl</sub>. A new batch was started on day 367 by replacing the reactor medium with fresh buffer medium. The MES reactor was operated in a fed-batch mode with intermittent N<sub>2</sub>:CO<sub>2</sub> (20:80) bubbling. Samples were taken at least twice a week for the analyses of VFAs (C1-C4) plus ethanol in Agilent 1200 series HPLC with Agilent Hi-Plex H column and Agilent 1260 infinity refractive index detector (Agilent Technologies) as described previously [22]. Each time the samples were taken, the reactor was sparged with N<sub>2</sub>:CO<sub>2</sub> (20:80) for at least 20–30 minutes and 2–4 mL of mineral medium was added to replace the sample volume.

### 5.2.2 Anion exchange resins and Pre-treatments

A commercially available anion exchange resin was used to investigate the uptake of acetate. This resin was selected (from around 10 types of resins) based on the pre-screening tests of adsorption capacity for carboxylic acids (data not shown). The selected resin Amberlite™ FPA53 (Rohm and Haas France S. A. S., Dow Chemicals) has a tertiary amine as an active group to which an OH<sup>-</sup> group was ionically attached. It is a weak base anion exchange resin with bead size 0.5 - 0.75 mm, a total exchange capacity of ≥ 1.6 eq L<sup>-1</sup> and has a cross-linked acrylic gel structure.

As a pre-treatment, the ion-exchange resins were washed several times with demineralized water to remove external matters on the resin. The washed resins were kept soaked in demineralized water for at least 12 h to remove any remaining residues. The resins were kept soaked in demineralized water until they were used for experiments. Before using in the experiments, the wet resins were washed with demineralized water by using a Whatman® 589/1 blackband filter and air-dried for a few minutes.

### 5.2.3 Ex situ acetate adsorption experiments

#### 5.2.3.1 Effect of pH and catholyte medium on acetate adsorption

For the investigation of adsorption of acetate from MES catholyte at different pH, the MES reactor's catholyte from previous batch operation [11] was used. The catholyte (i.e. medium broth) contained VFAs mainly acetate (~10 g L<sup>-1</sup> [11]). A series of 15 ml centrifuge tubes each containing a mixture of 8 ml of filtered catholyte sample (via a syringe filter; 0.45 µm) and 0.8 g of pretreated anion exchange resins (10 % w/v) were taken. The pH levels of the medium were adjusted to approximately 2, 3, 4, 5, 7 and 8 in different tubes in duplicates by using 3M HCl. The tubes were shaken using a tube rotator



for 24 h. Samples of catholyte were taken at the start and after 24 h of shaking and pH was measured simultaneously. The samples were analyzed for acetate, butyrate and ethanol in Agilent 1200 series HPLC (Agilent Technologies) as described earlier [22].

### 5.2.3.2 Effect of concentrations on acetate adsorption experiments

Acetic acid uptake by anion-exchange resins was examined by suspending 10% w/v resin to a series of increasing concentrations of acetic acid solutions. The acetic acid solutions containing 4, 6, 8, 10, 15 and 20 g L<sup>-1</sup> acetic acid were used in duplicates for concentration effect test. To ensure mixing over a large surface area of the resin, the tubes were rotated head-over-head for 24 h. The pH measurement and HPLC analysis was performed before and after the experiment.

### 5.2.4 In situ acetate separation applying anion exchange resins column on MES reactor

A glass column (diameter 3 cm; height 12 cm) was filled with 35 g FPA53 resin. The MES catholyte was circulated through the column *in situ* using a Watson-Marlow 323 peristaltic pump (Watson-Marlow Fluid Technology Group) at the rate of 50 ml min<sup>-1</sup>. A spacer (100 μm mesh) was applied in a column to prevent the flow of resin into the MES. A set-up for the application of resins to the operating MES cells is illustrated in Supplementary information-Chapter 5 Figure SI-1.

The reactor medium was circulated through the column for two days for the adsorption (sorption) of acetate. Then the adsorbed acetate in the column was eluted by circulating 50 ml of regenerant (eluent) (1 M NaOH) for two days. This regeneration cycle was repeated at least two times to remove any remaining acetate from the column. Then the column was washed with demineralized water to remove eluent from the column so that column can be reused again. An HPLC sample was taken each day to check any uptake or desorption of acetic acid from the reactor medium and resin respectively.

## 5.3 Calculations

### 5.3.1 Acetate production rate in CO<sub>2</sub> reduction

In the batch mode operation of MES, acetate production rate in g L<sup>-1</sup> d<sup>-1</sup> was calculated according to the following equation.

$$P_{\text{acetate}} = \frac{(C_{\text{acetate},t} - C_{\text{acetate},t_0})}{t - t_0} \quad (5.1)$$

Here,  $t_0$  and  $t$  refer to two subsequent samples,  $P$  is the production rate in g L<sup>-1</sup> d<sup>-1</sup> and  $C_{\text{acetate}}$  is the concentration of acetate (g L<sup>-1</sup>).

The number of moles of acetate produced at any time  $t$  was calculated according to the following equation.

$$N_{\text{acetate},t} = \frac{V_{\text{cat}} \times (C_{\text{acetate},t} - C_{\text{acetate},t_0})}{M_{\text{acetate}}} \quad (5.2)$$

Here,  $t_0$  and  $t$  refer to two subsequent samples,  $N$  is the number of moles acetate produced during the time period,  $V_{\text{cat}}$  is the total volume of catholyte,  $C_{\text{acetate}}$  is the concentration of acetate (g L<sup>-1</sup>) and  $M_{\text{acetate}}$  refers to the molar conversion of acetate (g mol<sup>-1</sup>).

### 5.3.2 Coulombic efficiency (CE) of production

Coulombic efficiency (CE) is calculated by using the equation 5.3

$$CE \text{ in } \% = \frac{n_{e,acetate} \times F \times N_{acetate,t}}{\int_{t_0}^t I dt} \times 100 \% \quad (5.3)$$

Here  $N_{acetate,t}$  is the moles of acetate produced between time  $t_0$  and  $t$ ,  $n_{e,acetate}$  represents the molar electron equivalent conversion factor (8 electron equivalent per mole for acetate),  $F$  is Faraday constant ( $96,485 \text{ C mol}^{-1}$  of electron equivalent) and  $I$  is electric current (A).

### 5.3.3 Specific acetate adsorption capacity

Specific acetate adsorption capacity or uptake by the resin, expressed as uptake per gram of resin, is calculated using the following equation:

$$\text{specific acetate uptake (mg g}^{-1}\text{)} = \frac{V \times (C_{acetate,start} - C_{acetate,end})}{m_{resin}} \quad (5.4)$$

Here  $C_{acetate}$  is the concentration of acetate ( $\text{mg L}^{-1}$ ) in the liquid sample at the start and at the end of experiment,  $V$  is volume of liquid (L) and  $m_{resin}$  is the amount of resin used (g).

### 5.3.4 Acetate recovery from resin

For the online application tests, the acetate is extracted from the column with eluent/regenerant solution. The amount of acetate extracted from the column is calculated by multiplying the acetate concentration obtained from the HPLC analysis with the volume of regenerant solution. Next, the efficiency of the removal was calculated by dividing the acetate uptake by the resin with the eluted acetate by the regenerant. These calculations combined are shown in the following equation.

$$\eta_{acetate \text{ recovery}} (\%) = \frac{m_{acetate \text{ in regenerant}}}{m_{acetate \text{ in resin}}} \times 100 \quad (5.5)$$

$$m_{acetate \text{ in regenerant}} = V_{regenerant} \times (C_{acetate,t} - C_{acetate,t_0}) \quad (5.6)$$

$$m_{acetate \text{ in resin}} = m_{resin} \times \text{specific acetate uptake} \quad (5.7)$$

Here  $\eta$  denotes the recovery percentage,  $m_{acetate \text{ in regenerant}}$  is the amount of acetate present in the regenerant (mg) and  $m_{acetate \text{ in column}}$  is the amount of acetate adsorbed in the resin (mg).

## 5.4 Results and discussions

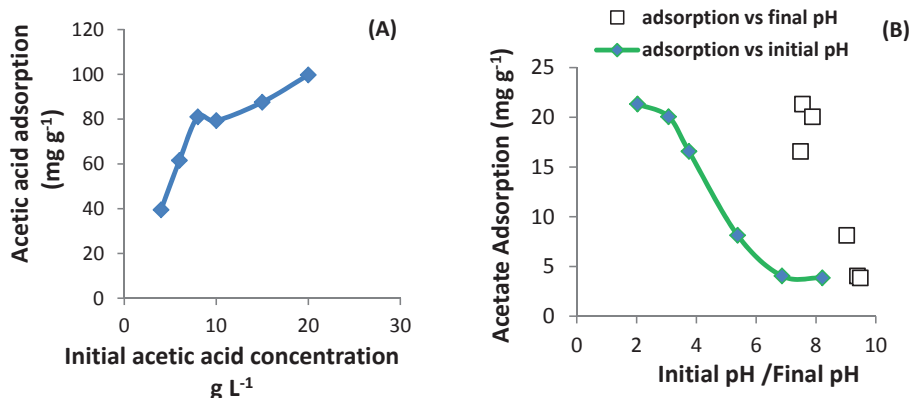
### 5.4.1 Ex situ acetate/acetic acid adsorption on FPA resins was feasible with MES catholyte

Acetic acid adsorption in FPA53 anion-exchange resin from acetic acid solutions of various concentrations, after fluidizing for 24 h, is shown in Figure 5.1A. The FPA53 resin adsorbed more acetic acid with increasing concentration from 4–20  $\text{g L}^{-1}$ . However, these acetic acid concentrations are considerable for extraction from the reactor broths. So far

acetate concentrations in MES from CO<sub>2</sub> reached typical concentrations of 10 g L<sup>-1</sup> [9–11]. Generally, the higher availability of ions gives higher ion-exchange [23]. Thus, the adsorption of acetic acid was maximum at higher concentrations. For 20 g L<sup>-1</sup> acetic acid the achieved adsorption was 100 mg g<sup>-1</sup> (Figure 5.1A). According to adsorption isotherms, there would be an optimum anion concentration in the medium, depending on the ion-exchange capacity of the resin [24]. However, in the current experimental setting, the optimum acetic acid concentration for maximum adsorption might be beyond 20 g L<sup>-1</sup>. Since the concentration of acetate in the catholyte of MES reactor reached only up to 10–15 g L<sup>-1</sup>, the optimum concentrations for FPA53 were not further investigated.

Another test with filtered reactor medium (catholyte) was performed to investigate the effect of pH on anion adsorption. pH affects the adsorption because it determines the fraction of charge species of organic acids and also the charge density of exchangeable ions adsorbed on the surface of the adsorbent [25]. The distribution of acetic acid or acetate is governed by pH. At a pH lower than the pKa (4.75), the majority of acetate remains as undissociated acetic acid. Figure 5.1B shows acetate/acetic acid adsorption to FPA53 from MES catholyte at various initial pH from 2 to 8. The results in Figure 5.1B show that at a lower pH, more acetic acid was adsorbed up to a maximum of 22 mg.g<sup>-1</sup> at pH 2. i.e. adsorption of acetic acid was higher than that for acetate although acetic acid is not charged.

Because the anion-exchange resins have previously adsorbed alkaline groups (OH<sup>-</sup>) that are exchanged with the acetate during absorption, it makes the medium less acidic after the acetate exchange. The resin exchanges previously adsorbed OH<sup>-</sup> for acetate ions and the OH<sup>-</sup> ions released into the solution, turning it more alkaline. Indeed, it was shown that pH increased during adsorption; although low to high pH range was maintained (Figure 5.1B).



**Figure 5.1** (A) Acetic acid uptake by the resin as a function of the solution concentration. Acetic acid adsorption by FPA53 at different starting concentrations of acetic acid (initial pH 2.6 to 2.9). (B) Acetate uptake by FPA53 resin when suspended in MES catholyte for 24 h at different starting pH values. Lower pH has positive influence on the adsorption (exchange) capacity of the resin. The pH rise after 24 h is higher at acidic pH.

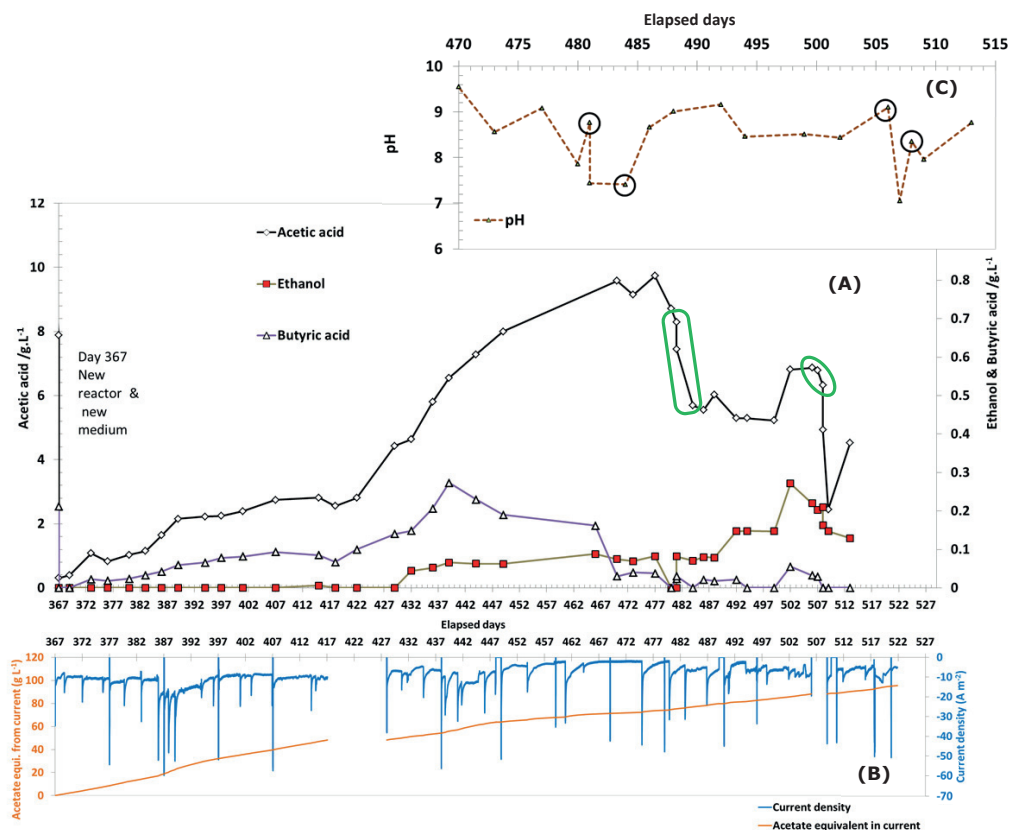
The acetate adsorption from the reactor medium was lower than the pure acetic acid uptake (Figure 5.1A), most probably due to competition with other charged volatile fatty acids molecules (e.g. butyrate), that were also adsorbed on the resins. When the pH is

---

low, more acetate was adsorbed on the resin. However, at a pH lower than the pKa of acetate (4.75), the majority of acetate should be undissociated acetic acid and doesn't have a charge with which it can adsorb on the resin. According to Magalhaes et al. [24] and Shi et al. [26], the uptake of carboxylic acids depends on the pH of the matrix wherein the resins reside. In the ion-exchange process, static interactions occur with the positively charged exchange sites on the resin and the charged counter ions. The dissociated acetate has a negative charge and the resin exchanges the competing counter ions such as  $\text{OH}^-$ ,  $\text{CO}_3^{2-}$  etc. for acetate. However, at a close range, there is a repulsion force created due to the crowding of previously adsorbed negatively charged groups around the ion-exchange site of the resin. When the solution is acidic, the acetate is predominantly in its undissociated form and there is less acetate available to bind to the resin. The uptake of acetate was higher at lower pH which is the indication for the existence of some other mechanisms. Yang et al. (1991) described that tertiary amine groups have a tendency for acetic acid uptake because acetic acid can dimerize with acetate [27]. Accordingly, acetate molecules that were present in the catholyte solution bind to the resin and dimerize with another acetic acid molecule via hydrogen bonds. This phenomenon could lead to the higher uptake at lower pH. At low pH, acetate is present at very low concentrations which should limit the adsorption, even via dimerization. As such it is explained that at high pH, ion exclusion mechanisms take place and acetate anions are repulsed (excluded) from the positively charged resin due to high surface charge density of previously adsorbed alkaline anions ( $\text{OH}^-$ ), thereby the adsorption of acetate remains low at high pH. In acidic condition, the non-ionic acetic acid molecules can easily enter the resin network and the surface charge density of resin decrease due to the neutralization of  $\text{OH}^-$  groups. As such, a higher acetic acid fraction at low pH stimulates the reformation of acetate that will be consequently adsorbed to the resin. Because the acetate uptake in the experiments decreases at higher pH, it is most evident that dimerization and exclusion mechanisms do play a role. For application within MES, this could be attractive while MES typically are operated at slightly acidic pH. Moreover, if MES biocathodes can be developed at more extreme pH [28], the efficiency of the used resins could be enhanced.

#### ***5.4.2 In situ acetate/acetic acid separation from MES catholyte was feasible***

During the MES experiment,  $\text{CO}_2$  reduction at the cathodes of the MES resulted mainly in acetate production and a minor amount of butyrate and ethanol at the cathode potential of  $-1 \text{ V}_{\text{Ag}/\text{AgCl}}$ . Intermittent bubbling of 20:80 mixture of  $\text{N}_2:\text{CO}_2$  steadily resulted in acetate accumulation up to  $10 \text{ g L}^{-1}$  after 100 days of operation. The product profiles in MES are shown in Figure 5.2A. The accumulated concentration of acetate can favor the extraction as indicated by the resin tests. The production rates ( $100 \text{ mg.L}^{-1}.\text{d}^{-1}$ ) and CE (40 to 50%) showed similar profiles as during the previous batches of this MES reactor [11]. The equivalent acetate concentration potentially obtainable from electric current is the indication that yet more electron equivalents were available for higher concentrations. Therefore another electrode designs or materials or operating conditions might be required which could result up to a 100% electron recovery.



**Figure 5.2:** Products of CO<sub>2</sub> reduction at the cathode of MES-1 at -1 V<sub>Ag/AgCl</sub>. (A) The concentration of acetate, ethanol and butyrate in the catholyte over time. (B) Current densities and equivalent acetate concentration (g L<sup>-1</sup>) derived from electric current in MES-1 operation. (C) pH of catholyte over the elapsed days. In situ extractions were performed during day 481-484 and day 506-508 with FPA resins filled in a column. The acetate extraction test points are indicated within the green shapes.

The column filled with FPA53 resins was integrated into the experimental setting when the amount of acetate in the reactor started to fall after reaching ~10 g L<sup>-1</sup>. The acetate profile in the MES reactor showing the days of extraction, pH over time and the current densities are illustrated in Figure 5.2. After the first extraction run with FPA53 column, the acetate concentration in the MES reactor decreased from 8.2 g L<sup>-1</sup> to 6 g L<sup>-1</sup> and remained stable for about two weeks after which it started to rise again reaching 6.8 g L<sup>-1</sup>. The production of acetate resumed after the application of ion exchange resin. During the extraction period, 80% CO<sub>2</sub> gas mixture was continuously bubbled in the MES reactor to neutralize ion-exchange induced pH rise effect. The second test of acetate extraction was performed with the same FPA53 column after the ion-exchange regeneration using 1 M NaOH washing. However, the treatment during the second run was slightly different from the first run. For the second run, the column was pre-treated by a 0.5 M HCl solution to decrease the alkaline groups adsorbed in the resin so that it could take up more acetate and decrease the pH rise in the reactor. An overview of the results of the acetate extraction by FPA53 in MES reactor is shown in Table 5.1.

**Table 5.1:** Results from the acetate removal by FPA53 resin from MES reactor's catholyte

| Parameters   | First run | Second run<br>(HCl pre-treated) |
|--|-----------|---------------------------------|
| pH of catholyte after extraction                           | 7.44      | 7.05                            |
| Total acetate in the catholyte at start of column run (mg) | 2071      | 1717                            |
| Acetate adsorbed on the resin (mg)                         | 649       | 137                             |
| Specific acetate adsorbed by resin (mg g <sup>-1</sup> )   | 18.3      | 3.9                             |

The acetate uptake in the first run was higher than the uptake from the reactor medium in the *ex situ* extraction tests at same pH (shown in Figure 5.1B). At a pH of around 7, the acetate uptake according to the *ex situ* catholyte separation was expected to be around 4–5 mg g<sup>-1</sup> instead of 18 mg g<sup>-1</sup> in the *in situ* extraction. When compared with the values obtained from the pure acetic acid test, this acetate uptake is 22–23% of the maximum observed acetic acid exchanged (adsorbed) from the acetic acid solution at the same concentration in the *ex situ* test.

In the second *in situ* acetate extraction test (after the regeneration process of resins, as would be discussed later), pre-washing of resin column with HCl resulted in a lower acetate-exchange capacity of the resin and also decreased the subsequent elution with NaOH (Table 5.1). Nevertheless, the pH change patterns in the first and second tests were similar (Figure 5.2 C). The lower uptake capacity in the second *in situ* extraction could be caused by the absorption of Cl<sup>-</sup> ions on the resins from HCl which might not be easily exchanged with acetate. This explains why the uptake of acetate in the second run was much lower than the first run, although the uptake values were more or less similar with the acetate exchanged from the reactor medium in the *ex situ* tests. Moreover, the electrolyte-derived microorganisms could attach and foul the resins in the column, after getting deactivated and denatured by the action of alkaline eluent. These live and denatured microbial commodities could have contributed to the column clogging, thereby decreasing the efficiency of acetate adsorption, especially in the second run. The specific acetic acid uptake in the *ex situ* test was 80 mg g<sup>-1</sup> for 8–10 g L<sup>-1</sup> acetic acid solution (Figure 5.1A), which was stimulated by the lower pH compared to the conditions during desorption of the MES derived catholyte. The resins in the *ex situ* tests were submerged and actively mixed in the sample catholyte while in the *in situ* tests, the resins were packed in a column, thereby triggering possible differences in mass transfer as well as surface availability.

#### 5.4.3 High acetate recovery (~70%) with NaOH solution as eluent

After integration of the resins in the MES, the acetate was desorbed from the column by recirculating 50 ml of 1 M NaOH through the column in two consecutive tests and a washing step. For the first test, the initial washing was performed with 30 ml demineralized water for two hours. However, significant amounts of acetate (almost 23% of adsorbed acetate) were washed out during this washing. The amounts of acetate recovery from the ion-exchange column in a number of resin regeneration steps are given in Table 5.2. Washing with water was not performed in the second test of *in situ* acetate extraction. The concentration of acetate within the used eluents was up to 5 g L<sup>-1</sup>.

**Table 5.2:** Results from resin regeneration with NaOH solution and percentages of acetate recovered in both runs

| Eluent used and acetate recovered during desorption steps |            |              |              |                         |
|---|------------|--------------|--------------|-------------------------|
| # run   | Wash water | NaOH cycle 1 | NaOH cycle 2 | Recovery from resin (%) |
| 1   | 150 mg     | 245 mg       | 59 mg        | 72%                     |
| 2   | -          | 21 mg        | 81 mg        | 74%                     |

Desorption of acetate in the first run by the NaOH solution was effective. Approximately 72% of acetate adsorbed in the ion-exchange column was recovered during the two cycles of elution. The first run of elution recovered ca. 40% of adsorbed acetate, since a fraction of acetate would have been lost during the washing step. However, the water used in washing step could itself be considered as eluent and as such acetate was recovered by using demineralized water.

For the second test of acetate extraction and recovery, the first elution cycle with NaOH was less effective compared to the first extraction run, as the amount of acetate desorbed was only 21 mg. As explained earlier, this might be caused by the HCl treatment prior to the column integration. The HCl treatment might cause the binding of Cl<sup>-</sup> ions to the resins which were more easily desorbed than the acetate molecules. The second elution cycle gave a better acetate desorption of acetate ca. 60%. Overall, the acetate recovery percentage from the resin column in the second test was higher as compared to that recovered in the first test (ca.70%). Moreover, the selectivity of recovered acetate was not 100%, since other trace amounts of VFAs and alcohol such as butyrate and ethanol could also be adsorbed on the resin-column. Besides this, the eluate could comprise a part of microorganisms and other elements from the electrolyte. Due to the high pH of the eluent, microorganisms attached to the column are likely to be deactivated and lysed. Hence, a proper technology is desirable to remove these impurities for high-end application of the separated acetate.

#### 5.4.4 Further improvements for ion exchange application on MES cells

The uptake of the FPA resin from 8–10 g L<sup>-1</sup> acetate solution was around 80 mg g<sup>-1</sup> (Figure 5.1A) which was more than the uptakes achieved during the experiments with real catholyte from the reactor. Higher adsorption capacity for acetate can be achieved by increasing the concentration of the acetate in the catholyte and by lowering the pH (Figure 5.1). This could be done with a concentrating step such as *in situ* electrodialysis as performed by Gildemyn et al [14], after which the acetate could be removed with the resin. Further acclimatization of a biocathode under more extreme conditions could enhance the effectiveness of the resin.

There might be no actual issue with the microorganisms that enter the column and adsorbed/positioned there at the beginning. Nevertheless, the long-term operation may lower the adsorption capacity due to the fouling of ion-exchange sites by microorganisms, blocking of the resin and cell lysis during the elution of the column with NaOH solution. However, during the desorption with the eluents, microorganisms are likely to be removed to some extent. To prevent microbial fouling, a suitable filter or membrane can be included in the system. In this study, *in situ* separation was performed to decrease product inhibition and to acquire the concentrated acetate. The effect of acetate removal on CO<sub>2</sub> reduction on MES reactor and an enhanced production could not be observed.

---

Additional studies, using other resins should be performed for a better product yield and to acquire improvements on the ion exchange phenomenon.

## 5.5 Conclusions

An MES system for the production and separation of acetate from CO<sub>2</sub> was feasible through the integration of MES with anion exchange resin extraction. The Amberlite™ FPA53 resin is able to extract acetate and other VFAs from the reactor medium without hindering biochemical production. Both the *ex situ* as well as *in situ* resin applications were shown to be repetitively feasible technically. Acetate absorption of 10–20 mg g<sup>-1</sup> resin was observed at catholyte conditions. The production of acetate in MES retained after the extraction. Acetate desorption from the FPA53 resin resulted up to 74% recovery and up to a final concentration of 5 g L<sup>-1</sup> of acetate in the eluent. Moreover, butyrate and other compounds are adsorbed on the resins and therefore the resin has the potential to be used for different organic acids.

### Acknowledgements

Suman Bajracharya is funded by VITO'S strategic research fund. Authors would like to thank Dr. Heleen De Wever for providing the ion-exchange resins.

## References

1. Shafiee S, Topal E (2009) When will fossil fuel reserves be diminished? *Energy Policy* 37:181–189. doi: 10.1016/j.enpol.2008.08.016
2. Hoel Snorre Kverndokk M, Hoel M, Kverndokk S (1996) Depletion of fossil fuels and the impacts of global warming. *Resour Energy Econ* 18:115–136. doi: 10.1016/0928-7655(96)00005-X
3. Nevin KP, Woodard TL, Franks AE, et al (2010) Microbial Electrosynthesis: Feeding Microbes Electricity To Convert Carbon Dioxide and Water to Multicarbon Extracellular Organic. *MBio* 1:e00103–10-. doi: 10.1128/mBio.00103-10.Editor
4. Steinbusch KJJ, Hamelers HVM, Schaap JD, et al (2010) Bioelectrochemical ethanol production through mediated acetate reduction by mixed cultures. *Environ Sci Technol* 44:513–7. doi: 10.1021/es902371e
5. Van Eerten-Jansen MCAA, Ter Heijne A, Grootsholten TIM, et al (2013) Bioelectrochemical Production of Caproate and Caprylate from Acetate by Mixed Cultures. *ACS Sustain Chem Eng* 1:513–518. doi: 10.1021/sc300168z
6. Rabaey K, Rozendal RA (2010) Microbial electrosynthesis — revisiting the electrical route for microbial production.pdf. *Nat Rev Microbiol* 8:706–16. doi: 10.1038/nrmicro2422
7. Nevin KP, Hensley SA, Franks AE, et al (2011) Electrosynthesis of organic compounds from carbon dioxide is catalyzed by a diversity of acetogenic microorganisms. *Appl Environ Microbiol* 77:2882–6. doi: 10.1128/AEM.02642-10
8. Marshall CW, LaBelle E V, May HD (2013) Production of fuels and chemicals from waste by microbiomes. *Curr Opin Biotechnol* 24:1–7. doi: 10.1016/j.copbio.2013.03.016
9. Marshall CW, Ross DE, Fichot EB, et al (2013) Long-term operation of microbial electrosynthesis systems improves acetate production by autotrophic microbiomes. *Environ Sci Technol* 47:6023–9. doi: 10.1021/es400341b
10. Jourdin L, Grieger T, Monetti J, et al (2015) High Acetic Acid Production Rate Obtained by Microbial Electrosynthesis from Carbon Dioxide. *Environ Sci Technol* 49:13566–13574. doi: 10.1021/acs.est.5b03821
11. Bajracharya S, Yuliasni R, Vanbroekhoven K, et al (2016) Long-term operation of bioelectrochemical CO<sub>2</sub> reduction to multi-carbon chemicals with a mixed culture avoiding methanogenesis. *Bioelectrochemistry* (Accepted)
12. López-Garzón CS, Straathof AJJ (2014) Recovery of carboxylic acids produced by fermentation. *Biotechnol Adv* 32:873–904. doi: 10.1016/j.biotechadv.2014.04.002
13. Baronofsky JJ, Schreurs WJA, Kashket ER (1984) Uncoupling by acetic acid limits growth of and acetogenesis by *Clostridium thermoaceticum*. *Appl Environ Microbiol* 48:1134–1139.



- 
14. Gildemyn S, Verbeeck K, Slabbinck R, et al (2015) Integrated Production, Extraction, and Concentration of Acetic Acid from CO<sub>2</sub> through Microbial Electrosynthesis. *Environ Sci Technol Lett*. doi: 10.1021/acs.estlett.5b00212
  15. Cao X, Yun HS, Koo Y (2002) Recovery of L- (+) -lactic acid by anion exchange resin Amberlite IRA-400. 11:189–196.
  16. Davison BH, Nghiem NP, Richardson GL (2004) Succinic acid adsorption from fermentation broth and regeneration. *Appl Biochem Biotechnol* 113-116:653–669. doi: 10.1385/ABAB:114:1-3:653
  17. Rengaraj S, Joo CK, Kim Y, Yi J (2003) Kinetics of removal of chromium from water and electronic process wastewater by ion exchange resins: 1200H, 1500H and IRN97H. *J Hazard Mater* 102:257–275. doi: 10.1016/S0304-3894(03)00209-7
  18. Chiarle S, Ratto M, Rovatt M, Rovatti M (2000) Mercury removal from water by ion exchange resins adsorption. *Water Res* 34:2971–2978. doi: 10.1016/S0043-1354(00)00044-0
  19. Zheng SK, Chen JJ, Jiang XM, Li XF (2011) A comprehensive assessment on commercially available standard anion resins for tertiary treatment of municipal wastewater. *Chem Eng J* 169:194–199. doi: 10.1016/j.cej.2011.03.005
  20. Berrios M, Siles JA, Martín MA, Martín A (2013) Ion Exchange. In: Ramaswamy S, Huang H-J, Ramarao B V. (eds) *Sep. Purif. Technol. Biorefineries*. John Wiley & Sons, Ltd, pp 149–165
  21. Bajracharya S, ter Heijne A, Dominguez X, et al (2015) CO<sub>2</sub> reduction by mixed and pure cultures in microbial electrosynthesis using an assembly of graphite felt and stainless steel as a cathode. *Bioresour Technol*. doi: 10.1016/j.biortech.2015.05.081
  22. Bajracharya S, Vanbroekhoven K, Buisman CJN, et al (2016) Application of Gas Diffusion Biocathode in Microbial Electrosynthesis from Carbon dioxide. *Environ Sci Pollut Res*. doi: 10.1007/s11356-016-7196-x
  23. Uslu H, Inci I, Bayazit ŞS (2010) Adsorption equilibrium data for acetic acid and glycolic acid onto amberlite IRA-67. *J Chem Eng Data* 55:1295–1299. doi: 10.1021/je900635z
  24. Magalhães AI, de Carvalho JC, Ramírez ENM, et al (2015) Separation of Itaconic Acid from Aqueous Solution onto Ion-Exchange Resins. *J Chem Eng Data* acs.jced.5b00620. doi: 10.1021/acs.jced.5b00620
  25. Xiao F, Pignatello JJ (2014) Effect of Adsorption Nonlinearity on the pH-Adsorption Profile of Ionizable Organic Compounds. *Langmuir* 30:1994–2001. doi: 10.1021/la403859u
  26. Shi T, Wang Z, Liu Y, et al (2009) Removal of hexavalent chromium from aqueous solutions by D301, D314 and D354 anion-exchange resins. *J Hazard Mater* 161:900–906. doi: 10.1016/j.jhazmat.2008.04.041
  27. Yang ST, White S a., Hsu ST (1991) Extraction of carboxylic acids with tertiary and quaternary amines: effect of pH. *Ind Eng Chem Res* 30:1335–1342. doi: 10.1021/ie00054a040
  28. Dopson M, Ni G, Sleutels THJA (2016) Possibilities for extremophilic microorganisms in microbial electrochemical systems. *FEMS Microbiol Rev* 40:164–181. doi: 10.1093/femsre/fuv044
-



---

C  
H  
A  
P  
T  
E  
R

6

**An overview on emerging bioelectrochemical systems (BESs): Technology for sustainable electricity, waste remediation, resource recovery, chemical production and beyond**

This chapter is *published as*

Bajracharya S, Sharma M, Mohanakrishna G, Dominguez X, Strik DPBTB, Sarma PM, Pant D (2016). *An overview on emerging bioelectrochemical systems (BESs): Technology for sustainable electricity, waste remediation, resource recovery, chemical production and beyond*. *Renewable Energy*. doi: 10.1016/j.renene.2016.03.002.

---

**Abstract**

Bioelectrochemical systems (BESs) are unique systems capable of converting chemical energy into electrical energy (and vice-versa) while employing microbes as catalysts. As such organic wastes including low-strength wastewaters and lignocellulosic biomass were converted into electricity with microbial fuel cells (MFCs). Likewise, electrical energy was used to produce hydrogen in microbial electrolysis cells (MECs) or other products including caustic and peroxide. BESs were also designed to recover nutrients, metals or removal of recalcitrant compounds. Moreover, photosynthetic micro-organisms, as well as higher plants were implemented to use solar energy for electricity generation. The diversity on microbial and enzymatic catalysts offered by nature allows a plurality of potential applications. As compared to conventional fuel cells, BESs operate under relatively mild conditions and do not use expensive precious metals as catalysts. The recently discovered microbial electrosynthesis (MES) of high-value chemicals has greatly expanded the horizon for BES. Newer concepts in the application, as well as the development of alternative materials for electrodes, separators, catalysts along with innovative designs, have made BES very promising technology. This article discusses the recent developments that have been made in BESs so far, with the emphasis on their various applications beyond electricity generation and resulting performances as well as existing limitations.

**Keywords:** Recalcitrant removal; Microbial electrocatalysis; CO<sub>2</sub> sequestration; Biosensors; Value-added chemicals production

---

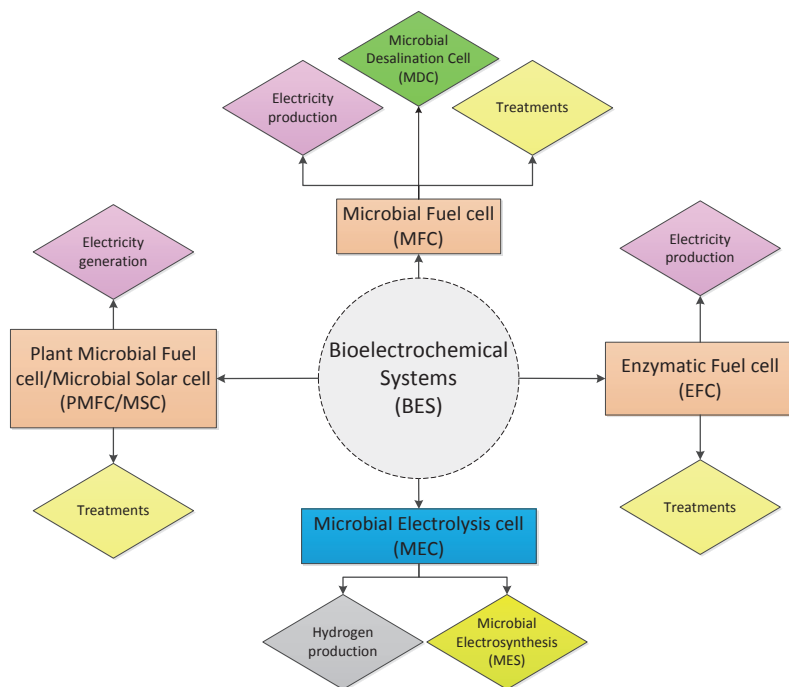
## 6.1 Introduction

There is a growing demand for new energy sources due to the limited accessibility and pollution caused by the use of fossil fuels. At present, the annual energy demand is approximately 13 terawatts (TW) worldwide and it is estimated to reach around 23 TW by the year 2050 [1]. Meanwhile, intensive resource utilization in municipal, industrial and agricultural activities will continue the process of environmental degradation creating environmental threats of global warming and related consequences. In this context, the development of renewable energy sources has become crucial for a sustainable landscape, especially by decreasing the dependency on energy import and by diversifying energy production sources [2]. Bioelectrochemical systems (BESs) have considerably boomed over the past decade for their contribution as an emerging sustainable technology for concurrent electricity production and wastewater treatment [3]. In addition, BESs also offer unique possibilities for the clean and efficient production of fuels and high-value chemicals using microorganisms [4]. As the BES functions in a completely multi-disciplinary approach, a large number of researches have been conducted worldwide in the fields of microbiology, electrochemistry, bioelectrochemistry, biotechnology, environmental science, materials science, etc. In these electrochemical systems, the redox potentials of an oxidation reaction at the anode and a reduction reaction at the cathode create a potential difference which is the driving force for electrons to flow from a low potential to high potential, spontaneously [5]. This flow of electrons through an external circuit is measured as an electric current. Whenever, microbes or enzymes are involved in the oxidation or reduction or both reactions, the system is termed as a microbial electrochemical system (MXC) or in a broader term BES [6]. If microbes catalyze the anodic reaction, they are applied as bioanode and if microbes catalyze the cathodic reactions, they are applied as biocathode. Microbial fuel cells (MFCs) are a type of MXC that generate electricity from the degradation of organic matter in anode chamber. A low redox potential for the oxidation of organic matter at the anode and a high redox potential for the oxygen reduction reaction (ORR) at the cathode, typically results into bioelectricity generation. In the case of microbial electrolysis cells (MECs), an external voltage is applied to subject the cathode potentials driving the production of valuable chemicals [7]. The BES in which CO<sub>2</sub> or organic molecules are cathodically reduced to higher value organic molecules is called microbial electrosynthesis (MES) [8]. In addition, BESs have also emerged with other applications such as microbial desalination cells (MDCs) for the desalination of water, and sediment or plant microbial fuel cells wherein microbes are intermingled with plant roots for the electricity generation [9–11]. Moreover, BESs are also identified as efficient bioreactors for the treatment of recalcitrant pollutants and toxic wastewaters; the process is termed as bioelectrochemical treatment (BET) or microbial electroremediation [12].

In this direction, the present review provides the overview of (i) all types of BESs and their applications, (ii) the basic working principles involved, (iii) substrate utilization, (iv) synthesis of targeted chemicals and (v) the recent concepts and developments made in BES. This review emphasizes the recent advances in BES that were developed beyond electricity generation. This review also helps to attract the young researchers from the allied disciplines of BES to advance the technology with multiple applications.

## 6.2 Types of Bioelectrochemical Systems

Based on the desired end objectives, BESs can be broadly classified into electrogenesis systems, electrohydrogenesis systems, microbial desalination systems, microbial electrosynthesis systems and bioelectrochemical treatment systems. Each type of BES with specific name as shown in Figure 6.1 are discussed in the following sections.



**Figure 6.1:** Schematic overview of various types of bioelectrochemical systems (BESs).

### 6.2.1 Microbial Fuel Cells (MFC)

MFCs harness electrical current from the microbial oxidation of organic matter using a solid electrode as an electron acceptor [13]. The anode surface of MFCs facilitates microbial attachment and oxidation of organics, thereby generating electrons which are then simultaneously transferred to the cathode compartment via an external circuit containing an external load. Electroneutrality is warranted by ions transport through an ion-permeable medium or a membrane while electricity is produced in the process. The first of such systems was demonstrated by M.C. Potter in 1911, which achieved a maximum voltage of 0.3–0.5 V [14]. Electroactive bacterial biofilms developed on the anode of BES function as the electrocatalytic unit for electricity generation. Production of bioelectricity in MFC is directly dependent on the capacity of exoelectrogens (microbes generating electricity) present on the anode, which facilitate the transfer of electrons from the reduced substrate to the anode. Oxidation of complex organic matter in wastewater requires diverse microbial communities. Dozens of bacterial species have been found of being able to produce electric current. The *Shewanella* and *Geobacter* spp were earlier identified as the electron-transferring microbes and as such well-studied. However, stable and higher currents have been recorded more often in MFCs with mixed cultures in bioanodes, rather than with pure cultures. The presence of *Geobacteraceae* in the bioanode community often showed high power densities registered in MFCs [15, 16]. The highest current density reported so far in MFC was 390 A m<sup>-2</sup> obtained using mixed culture at the layered-corrugated carbon anode with high surface area [17]. The nature of substrate, anode potential, and electrolyte chemistry affect the microbial activity and electron transfer [18, 19]. Higher electrolyte conductivity ascertains the better performance of microbial electrochemical systems but the electrolyte conductivity should not go beyond the tolerance level of bacteria [20]. However, it was identified that the application of halophilic bacteria in BESs have reported to produce the current densities

up to  $85 \text{ A m}^{-2}$  with bioanodes formed from a salt-marsh inoculum and cultivated in a 1.5 times more saline electrolyte than seawater [21]. Significant current densities and power densities obtained from MFCs, as reported in various studies, are listed in Table 6.1 and 6.2 respectively. The performance of MFCs also relies on the electrode material used and its structure. Graphite electrodes with a roughened surface have shown to produce higher power densities than flat graphite electrodes [22]. Likewise, increasing the surface area of MFC anodes using porous materials such as graphite brush, carbon felt and carbon nanotubes, have shown a considerable increase in current density [23–25]. Higher surface area of electrodes provides a larger surface for bacterial adhesion and electron transfer between the bacteria and electrode, thereby demonstrating noteworthy improvement in current densities. Direct electron transfer phenomenon of microbes with metal electrodes has also been demonstrated including dimensionally stable anodes (DSA, titanium over iridium and tantalum oxide), stainless steel and platinum electrodes [26]. Current densities obtained with porous carbon anodes are typically higher than those reported with metals except for platinum [27]. A switch from planar electrodes to three-dimensional electrodes—having optimized microstructures—was correlated to a considerable increase in bioelectrode performance [28]. Macrostructure modification in the anode, with multi-layered corrugated carbon configuration evidenced a huge rise in current densities [17]. Especially once mass transport limitations are tackled by flow-through electrodes, higher current and power densities can be achieved as a result of low internal resistances [29]. Materials used for MFC construction, design and configuration influence the internal resistance, which in turn govern the total performance of the system.

**Table 6.1:** Overview of current densities reported in MFCs in connection to the type of microbial culture used and anode material

| Source inoculum   | Type of MFC and anode material/specifications  | Current density (A m <sup>-2</sup> ) | Reference |
|---|--|--------------------------------------|-----------|
| <i>Geobacter</i> spp.   | Two chamber /graphite sticks   | 0.065                                | [30]      |
| <i>Geobacter</i> spp.   | Two chamber/ graphite anodes at 0.2 V <sub>/AgAgCl</sub>   | 0.16–1.14                            | [30]      |
| Anaerobic culture of <i>Escherichia coli</i> K12                        | Two-chambered MFC / platinum paddle electrodes (5 cm <sup>2</sup> ) and ethanol as substrate   | 5                                    | [31]      |
| Anaerobic culture of <i>Escherichia coli</i> K12                        | Two-chambered MFC / platinum paddle electrodes (5 cm <sup>2</sup> ) and formate as substrate   | 50                                   | [31]      |
| Pre-acclimated bacteria from MFC  | Cube shaped single-chamber MFC / graphite fiber brush anode (7170 m <sup>2</sup> m <sup>-3</sup> brush volume)                       | 8                                    | [32]      |
| Mixed culture   | 2.5 ml anode chamber, bicarbonate buffer / Double cloth electrode assemblies (CEAs); (2x7 cm <sup>2</sup> projected electrode area), | 9.9                                  | [33]      |
| <i>Klebsiella pneumoniae</i> L17  | Two chamber / Carbon felt  | 1.2                                  | [34]      |
| <i>Rhodospseudomonas palustris</i> DX-1                                 | Single chamber / graphite brush  | 9.9                                  | [35]      |
| <i>Geobacter sulfurreducens</i>   | Single chamber / DSA at 0.2 V <sub>/AgAgCl</sub>   | 5                                    | [36]      |
| <i>Geobacter sulfurreducens</i>   | Single chamber / solid graphite at 0.2 V <sub>/AgAgCl</sub>  | 8                                    | [36]      |
| <i>Geobacter sulfurreducens</i>   | Single chamber / multiple stainless steel anode at +0.2 V <sub>/AgAgCl</sub>   | 2.4                                  | [37]      |
| Mixed culture   | Single chamber / Graphite plates projected surface area of 70 cm <sup>2</sup>  | 0.27 to 0.35                         | [12]      |
| Mixed culture   | 3D carbon fiber anode prepared by gas assisted electrospinning ; anode polarized at 0.2 V <sub>/AgAgCl</sub>                         | 30                                   | [23]      |
| Mixed culture   | Half-cell semi batch reactor / Layered corrugated Carbon anode / polarized at 0.2 V <sub>/AgAgCl</sub>                               | 70 - 400                             | [17]      |
| Mixed culture from air cathode MFC                                      | 30 ml anode chamber / Double cloth electrode assemblies (CEAs); (2x100 cm <sup>2</sup> projected area);                              | 16.4                                 | [38]      |
| <i>Geokalibacter subterraneus</i>                                       | Planar graphite electrode poised at 0.2 V/SCE; Saline electrolyte 3.5% NaCl  | 4.68 ± 0.54                          | [39]      |
| Mixed culture   | 3D scaffold-NanoWeb reticulated vitreous carbon electrode at 0 V <sub>/AgAgCl</sub>  | 68±30                                | [40]      |
| Garden compost  | Carbon cloth, -0.2 V/SCE   | 33.5                                 | [41]      |
| Garden compost  | Stainless steel foam at 0 V <sub>/SCE</sub>  | 100                                  | [41]      |
| <i>Geobacteraceae</i> dominated secondary mixed culture from wastewater | Ag sheet anode at 0.2 V <sub>/AgAgCl</sub>   | 11                                   | [42]      |
| <i>Geobacteraceae</i> dominated secondary mixed culture from wastewater | Cu sheet anode at -0.2 V <sub>/AgAgCl</sub>  | 15                                   | [42]      |
| <i>Geobacter sulfurreducens</i>   | Ice-templated titanium based ceramic anode, 88% porosity   | 128.7                                | [43]      |
| Mixed culture   | Carbonized corn stem   | 31.2                                 | [44]      |

DSA: Dimensionally stable anode; SCE: Standard calomel electrode



**Table 6.2:** An overview of power densities reported in MFCs in connection to cathode material

| MFC Design  | Anode   | Cathode   | Maximum power density (mW m <sup>-2</sup> projected cathode) | Reference |
|---|---|---|--|-----------|
| <b>MFCs carbon paper, carbon cloth and similar anodes</b> |   |   |  |           |
| Single chamber  | Toray carbon paper (without wet proofing; E-TEK)    | MEA with Pt catalyst; PEM-carbon clothes assemblies                       | 262±10   | [45]      |
| Dual chamber  | Plain carbon paper                                  | Aqueous air-cathode; Carbon paper with platinum catalyst                  | 33 (anode area based)  | [46]      |
| Single chamber  | Carbon cloth (type A, E-TEK)                        | Air-cathode; Carbon clothes, PTFE (diffusion layer)                       | 766  | [47]      |
| Single chamber air-cathode                                | Carbon cloth  | Double Cloth Electrode Assemblies (CEA)                                   | 4300   | [38]      |
| Miniatured tubular MFCs                                   | Untreated carbon veil                               | Air cathode; untreated carbon veil;                                       | 9.8 W m <sup>-3</sup>  | [48]      |
| <b>MFCs with granular graphite and similar anodes</b>     |   |   |  |           |
| Open air biocathode with tubular MFC configuration        | granular graphite                                   | Sludge biocathode; graphite felt with MnO <sub>2</sub>                    | 83±11 W m <sup>-3</sup> total electrolyte                    | [49]      |
| Dual chamber  | Graphite granules                                   | Aqueous air cathode without catalyst; granular graphite with nano pores   | 5.88 (nominal cathode surface area based)                    | [50]      |
| Dual chamber  | Graphite granules                                   | Sludge biocathode; graphite fiber brush                                   | 68.4 W m <sup>-3</sup> anolyte                               | [51]      |
| Tubular air-chamber MFC                                   | Graphite felt and graphite granules                 | MEA; Canvas cloth with Ni and MnO <sub>2</sub> coating                    | 86.03  | [52]      |
| Tubular air-chamber MFC                                   | Graphite felt and graphite granules                 | MEA/Canvas cloth with graphite and MnO <sub>2</sub> coating               | 24.67  | [52]      |
| Tubular air-chamber MFC                                   | Graphite felt and graphite granules                 | β-MnO <sub>2</sub> catalyzed air cathode                                  | 172±7  | [53]      |
| Two chambered MFC   | Carbon granules anode; acetate fed mixed culture    | Activated nitrogen-doped carbon fiber cathode                             | 1377±46  | [54]      |
| <b>MFCs with carbon and graphite brush anodes</b>         |   |   |  |           |
| Tubular cathode in single chamber configuration           | Plain graphite fiber brush                          | MEA/ ultrafiltration membrane; graphite coating with CoTMPP catalyst      | 18 W m <sup>-3</sup> total electrolyte                       | [55]      |
| Single chamber MFC  | Graphite fiber brush                                | MEA; Ion exchange membrane-graphite coating and CoTMPP catalyst; AEM      | 449±35   | [56]      |
| Single chamber  | Graphite fiber brush treated with ammonia gas       | Air cathode; stainless steel mesh and Nafion binder with diffusion layer  | 1610±56  | [57]      |
| Two chamber MFC   | Carbon brush anode                                  | Crumpled graphene cathode   | 3.3 W m <sup>-3</sup>  | [58]      |
| Single chamber MFC  | carbon fiber brush anode                            | Goretex diffusion layered carbon cloth cathode                            | 1330±30  | [59]      |
| Single chamber MFC  | carbon fiber brush anode; acetate fed mixed culture | PTFE diffusion layered carbon cloth cathode                               | 1390±70  | [59]      |
| <b>MFCs with carbon felt anodes</b>                       |   |   |  |           |
| Two chamber upflow MFC                                    | Carbon felt   | Aqueous air cathode; activated carbon fiber felt                          | 315 (vs Area of separator)                                   | [60]      |
| Tubular air-cathode MFC                                   | Graphite felt                                       | A tubular air-cathode; non-Pt; continuous MFC stack with swine wastewater | 175.7  | [61]      |

| MFC Design                              | Anode   | Cathode   | Maximum power density (mW m <sup>-2</sup> projected cathode) | Reference |
|---|---|---|--|-----------|
| Single chamber MFC                      | carbon felt anode   | Manganese dioxide-graphene nano sheet (MnO <sub>2</sub> /GNS) air cathode | 2083   | [62]      |
| <b>MFCs with graphene coated anodes</b> |   |   |  |           |
| Two chamber MFC                         | Crumpled graphene anode   | Carbon brush cathode;   | 3.6 W m <sup>-3</sup>  | [58]      |
| Two-chamber MFC                         | Graphene coated stainless steel fiber felt anode; Acetate fed mixed culture | with Carbon cloth cathode with ferricyanide catholyte                     | 2143   | [63]      |
| Two-chamber MFC                         | Graphene coated carbon cloth anode (acetate fed mixed culture )             | Carbon cloth cathode with ferricyanide catholyte                          | 1018   | [63]      |

CoTMPP: Cobalt tetramethylphenylporphyrin; MEA: Membrane electrode assembly

### 6.2.2 Microbial Electrolysis Cells (MEC)

MECs utilize the property of bacteria to convert chemical energy to electrical energy and allow electrolysis of water [64]. External electric power applied through the electrical circuit of BES drives electrons from anode to the cathode and supports the hydrogen generation at the cathode [65]. On the contrary to MFCs, the cathode of MECs operates under anaerobic conditions that facilitate hydrogen production. However the anoxic environment in MECs, along with high concentrations of hydrogen production, can also promote methane production once CO<sub>2</sub> and methanogens are available. A few of the methods to mitigate methane production includes the aeration of the cathode chamber between batches, lowering of the pH, operation at short retention times and giving a heat shock to the inoculum, or adding chemicals that inhibit the growth of methanogens [66]. Hydrogen production in MECs, according to their configurations and the substrates treated, were listed in Table 6.3. Higher electric currents are typically observed in MECs, when compared to MFCs, which is due to the additionally applied voltage that helps to overcome the cathode limitations in MEC [29]. The energy required for MEC operation can also be provided by another separate MFC as a power source [67]. This study reported a hydrogen production rate of 0.24 m<sup>3</sup>-H<sub>2</sub> m<sup>-3</sup>d<sup>-1</sup> and energy recovery of 23 % using a fermentation effluent as substrate. However, for the supply of a stipulated voltage that allows for maximal hydrogen production in MEC, efficiently connected multiple MFCs are required [67]. In an MEC with bioanode and biocathode, expensive metals like platinum are not required as catalysts and preferably, the enrichment of microbes on the carbon cathode decreases the start-up time and produces comparable current densities to those of bioanode [65]. Furthermore, the hydrogen synthesized in MECs can also drive the biochemical production of other chemicals [8]. Most common examples of reduction reactions at the cathode are proton reduction to hydrogen, oxygen reduction to H<sub>2</sub>O<sub>2</sub> and CO<sub>2</sub> reduction to methane (CH<sub>4</sub>) and acetate [66, 68, 69]. These recently developed BESs for the production of valuable chemicals and biofuels such as organic acids, or alcohols from low-value compounds or CO<sub>2</sub> [8, 70, 71] are deliberated in the next paragraph.

**Table 6.3:** An overview of experimental conditions and results from hydrogen producing MEC with mixed culture biocatalyst

| BES specifications and anode/cathode material  | H <sub>2</sub> production rate (m <sup>3</sup> H <sub>2</sub> m <sup>-3</sup> d <sup>-1</sup> ) | Current density (A m <sup>-2</sup> ) | Electric energy input (kWh m <sup>-3</sup> H <sub>2</sub> ) | Efficiencies and recovery in %                                 | Reference |
|--|---|--------------------------------------|---|--|-----------|
| <b>A) Bioanode and abiotic cathode</b>   |   |                                      |   |  |           |
| Two chamber; Graphite felt anode; Ti -Pt cathode; 0.5 V applied voltage  | 0.1   | 0.447                                | NA  | 53±3.5 % overall efficiency                                    | [72]      |
| Single chamber; Graphite brush anode; carbon cloth with Pt coating cathode; 0.8 V applied voltage  | 3.12  | 11.6                                 | NA  | 78% overall efficiency   | [73]      |
| Two chamber; graphite felt forced flow through anode; Pt-Ti mesh cathode; 1 V applied voltage  | 5.6   | 16.4                                 | NA  | 43% overall, 71% cathodic H <sub>2</sub> recovery              | [74]      |
| Cloth separator; carbon felt anode; carbon cloth cathode with Pt coating; 1 V applied voltage  | 6.3   | 4.7                                  | NA  | 90 % COD recovery  | [75]      |
| Two chamber; graphite felt; nickel foam; 1 V applied voltage   | 50  | 22.8                                 | 2.62  | 90% cathodic H <sub>2</sub> recovery                           | [76]      |
| Single chambered cube MEC; Graphite brush anode at 0.2 V <sub>/AgAgCl</sub> ; Pt coated carbon cloth cathode   | 7.9±0.3   | 33.28                                | 4.7 ±0.5  | 40±1% overall efficiency                                       | [77]      |
| Single chambered cube MEC; graphite brush anode at 0 V <sub>/AgAgCl</sub>  | 6.9±0.8   | 26.08                                | 2.9 ±0.4  | 54±5% overall efficiency                                       | [77]      |
| Single chambered cube MEC; graphite brush anode at -0.2 V <sub>/AgAgCl</sub>   | 3.6±0.6   | 14.6                                 | 2.3±0.3   | 58±6% overall efficiency                                       | [77]      |
| Single chamber; graphite fiber brush anode; Pt coated carbon cloth; 1 V applied voltage  | 17.8  | 26.14                                | NA  | ~80 % overall efficiency, 93% cathodic H <sub>2</sub> recovery | [78]      |
| Two chamber MEC with AEM; Carbon felt anode; 1 V applied voltage   | NA  | 10.2                                 | 2.62  | 90% cathodic H <sub>2</sub> recovery                           | [79]      |
| Wastewater feed 100 L reactor with 6 MEC cassettes; 2 carbon felt anodes in each cassette; stainless steel wool cathode; 1.1 V applied voltage                                   | 0.006   | NA                                   | NA  | 48.7 % energy recovery; 41.2 % CE                              | [80]      |
| Glycerol, milk and starch feed single chamber MEC; graphite fiber brush anode; Pt coated graphite fiber cloth cathode; 0.8 V applied voltage; enriched anaerobic sludge inoculum | 0.94  | 150 A m <sup>-3</sup>                | NA  | 91 % cathodic H <sub>2</sub> recovery                          | [81]      |
| H-type reactor; Spent yeast and ethanol fed MEC; ; Graphite fiber brush anode at -0.3 V <sub>/AgAgCl</sub> ; Stainless steel mesh cathode; pig manure inoculum                   | 2.18±0.66   | 222±31.3 A m <sup>-3</sup>           | NA  | 87±2 % COD recovery, 71±4 % CE                                 | [82]      |

| BES specifications and anode/cathode material   | H <sub>2</sub> production rate (m <sup>3</sup> H <sub>2</sub> m <sup>-3</sup> d <sup>-1</sup> ) | Current density (A m <sup>-2</sup> ) | Electric energy input (kWh m <sup>-3</sup> H <sub>2</sub> ) | Efficiencies and recovery in %                               | Reference |
|---|---|--------------------------------------|---|--|-----------|
| <b>B) Biocathodes and abiotic anodes</b>  |   |                                      |   |  |           |
| Continuous mode double chamber reactor; graphite felt cathode at -0.7 V <sub>SHE</sub>                            | 0.63  | -1.2                                 | NA  | 49 % H <sub>2</sub> recovery                                 | [83]      |
| Continuous mode double chamber reactor; graphite felt cathode at -0.7 V <sub>SHE</sub>                            | 2.2   | 2.7                                  |   | 50 % H <sub>2</sub> recovery                                 | [84]      |
| Double chamber reactor; graphite granules cathode at -0.59 V <sub>SHE</sub> ; autotrophic biocathode              | 2.5   | NA                                   | NA  | 2.5 % H <sub>2</sub> recovery                                | [85]      |
| Double chamber reactor; plain carbon cloth cathode at -0.8 V <sub>SHE</sub> ; autotrophic thermophilic biocathode | 376.5 mmol m <sup>-2</sup> d <sup>-1</sup>  | -1.28                                | NA  | 70 % H <sub>2</sub> recovery                                 | [86]      |
| Double chamber reactor; graphite plate cathode; autotrophic biocathode at -0.75 V <sub>SHE</sub>                  | 9.2 L H <sub>2</sub> m <sup>-2</sup> d <sup>-1</sup>  | 1.88                                 | NA  | 39.4 % electron recovery as H <sub>2</sub>                   | [87]      |
| Single chamber PANI/MWCNT modified carbon cloth biocathode; 0.9 V applied voltage                                 | 0.67  | 205 A m <sup>-3</sup>                | NA  | 81 % energy efficiency, 42 % H <sub>2</sub> recovery, 72% CE | [88]      |

NA: Information not available; PANI: Polyaniline; MWCNT: Multi-walled carbon nanotube; CE: Coulombic efficiency; COD: Chemical oxygen demand

### 6.2.3 Microbial Electrosynthesis (MES)

MES, also known as bioelectrosynthesis, is a new-fangled perspective of BES which utilizes the reducing power generated from the anodic oxidation to produce value added products at the cathode. Cathodic biocatalysts (with attached cathodic biofilms) reduce the available terminal electron acceptor to produce value-added products [8, 89, 90]. The bioelectrosynthesis process can be highly specific, depending on the biocatalyst catalyzing the redox reaction and the terminal electron acceptor involved in the process, along with the electrochemically active redox mediators or suitable reducing equivalents. Biocathodes are the key components of microbial electrosynthesis, where the electrode oxidizing microorganisms are involved in the formation of reduced value-added product such as acetate, ethanol, butyrate [91]. MES refers to the production of chemical compounds in an electrochemical cell by electricity-driven CO<sub>2</sub> reduction as well as reduction/oxidation of other organic feedstocks using microbes as biocatalyst [8]. As a proof of concept, Nevin et al. [70] presented MES as a microbial catalysis of CO<sub>2</sub> reduction to multi-carbon organic compounds using electrical current at the cathode. As such, MES is also prospected as an alternative strategy to capture electrical energy in the covalent chemical bonds of organic products. Several studies have reviewed and highlighted different aspects of MES including microbiology, technology, and economics, as well as the understandings on the metabolic routes involved, electron transfer mechanisms and practical considerations [8, 13, 92].

---

### 6.2.4 Enzymatic Fuel Cells (EFC)

Enzymatic fuel cells (EFCs) make use of specific enzymes on the electrode surface (or in electrolyte suspension) that facilitate the catalytic oxidation of fuel and drive specific reactions desired for various applications. Davis and Yabrough [93] demonstrated the use of microbes and enzymes in biofuel cells using glucose oxidase. Glucose oxidase has been widely used in pacemakers, indicator lights, small actuators, micro pumps, and other glucose electro-oxidizing anode-based systems, because of its thermostability and high selectivity [94]. Several enzymes are used on anode and cathodes, based on their specific redox function. If highly selective enzymes are used at the anode and cathode, this eliminates the need for any membrane between the anode and cathode compartments. However, enzymatic catalysts are usually reported to oxidize the fuel partially and heat generation occurs as a result of side reactions, which might be detrimental to the enzymatic activity [95, 96]. The shelf life of these enzyme-based systems has been extended through encapsulation in micelle polymers that provide a buffering capacity for pH control and a hydrophobic niche to prevent enzymatic degradation [95]. The flavin adenine dinucleotide-dependent glucose dehydrogenases (FADGDH) /Osmium (Os)-polymer-based electrodes showed high sensitivity towards glucose and also reported higher current densities, which made them suitable for use as bioanodes in glucose-based EFCs [97]. The Pyrroquinolinequinone-dependent alcohol dehydrogenase (PQQ-ADH), enzyme originating from acetic acid bacteria, has been reported for the development of EFCs and biosensors, as it can undergo quasi-reversible electrochemistry at an exposed carbon surface [97, 98]. This enzyme was reported to be capable of using different redox mediators and also has a good electron transfer kinetics [97, 98]. Higher energy densities in combination with lower power outputs make EFCs suitable for independently powering the wireless sensor applications such as video monitoring and also for the development of other portable power devices [99, 100]. The use of FAD-dependent fructose dehydrogenase, obtained from *Gluconobacter*, as an anodic catalyst, and copper containing laccase from mushrooms, have been evaluated as cathodes, showing a high turnover rate, good stability and high selectivity [97, 101]. Multi-enzyme based EFCs are generally preferred over single enzyme systems so as to increase the substrate conversion and the performance of the system as a whole [95]. Many studies are now focusing on the cascading of enzymes in EFCs to facilitate complex mechanisms and 3-D electrode configurations to provide ample surface area for enzymatic reactions. However, due to the utilization of purified enzymes with catalytic capacity, the cost for EFCs is still high.

### 6.2.5 Microbial Solar Cells (MSC)

Microbial solar cells (MSCs) make use of photoautotrophic microbes or higher plants to entrap solar energy which is further utilized by electroactive bacteria to perform electrode-driven reactions. These reactions include generation of electric current or compounds like hydrogen, methane, ethanol, hydrogen peroxide etc. Primarily photosynthesis leads to the generation of organic compounds, which are subsequently fed into the anode compartment where they are oxidized by electroactive microbes to produce electrons. These electrons are then transferred to the cathodic side where reduction of oxygen leads to the formation of water [102]. The phototrophic biofilms developed on the anode contain species of cyanophyta including *Synechocystis*, chlorophyta and other electroactive microbes [103]. A system for treatment of algal blooms in lakes has been reported based on MSC principles, where algal biomass provided by *Microcystis aeruginosa* and *Chlorella vulgaris* was fed as a substrate in MFCs along with lake water, for concomitant power production and water treatment [104]. The algal biomass from photobioreactor—after the treatment in an anaerobic digester, can be used as a feed for the fuel cell [105]. An MSC with a photobioreactor using *Chlorella* at the anode, reached a light to electricity conversion efficiency of 0.04% resulting in 14 mW m<sup>-2</sup> of average power density [103]. Without mediator or carbon source in the anolyte, *Synechocystis* PCC6803 was reported to produce 539 mA m<sup>-2</sup>, under higher light intensity (10,000 lux) and resulted on effective CO<sub>2</sub> sequestration (625 mmol CO<sub>2</sub> m<sup>-3</sup>)

---

[106]. Improvement of performance is possible by photobioreactor optimization, improved chemical energy transfer from algae to bioanode, higher surface electrode area, and enriched electroactive biofilm [107]. The advantages of this system lie on simultaneous CO<sub>2</sub> sequestration and direct conversion of light to electricity [106].

### **6.2.6 Plant Microbial Fuel Cell (PMFC)**

Plant microbial fuel cells (PMFC) incorporate the living plant's root system into the MFC anode so that the organic products, called as rhizodeposits, released to the soil by the roots, can be used as the substrates for electricity production by electroactive microbes [108]. Hence, in a broader sense, PMFCs harness solar radiation by transforming it into green electricity in a clean and efficient manner. The rhizodeposits from the roots mainly comprise exudates (sugars, organic acids), secretions (polymeric carbohydrates and enzymes), lysates (dead cell materials) and gases [108]. The choice of a plant for PMFC is crucial, as it directly controls the amount of rhizodeposits for bioelectricity generation. Reed manna grass [108], rice plants [109] and *Spartina anglica* [110] have been utilized in separate studies. PMFCs from *Pennisetum setaceum* have been reported to be the most sustainable in terms of power production so far, with a maximum power generation of 163 mW m<sup>-2</sup> [9]. *Spartina anglica* PMFCs with integrated oxygen reducing biocathodes reached the highest long-term (2 weeks) power output of 240 mW m<sup>-2</sup> [111]. PMFCs along with MSCs with phototrophic biofilms are considered a promising and novel energy harvesting systems. It was also identified that the total amount of rhizodeposits available for oxidation at the anode is directly proportional to bioelectricity generation, rather than the photosynthesis process occurring in the plant [112].

### **6.2.7 Microbial Desalination Cell (MDC)**

Microbial desalination cells (MDCs) utilize the electric potential difference developed across the anode and the cathode via MFC technology to operate *in situ* desalination. Cao et al. [10] reported the first water desalination system in combination with MFC technology. MDCs comprise an additional middle compartment in between the anode and cathode compartments, for water desalination. The middle compartment is partitioned by an anion exchange membrane (AEM) towards the anode and a cation exchange membrane (CEM) towards the cathode. Bacteria on the anode oxidize biodegradable substrates and generate electrons and protons; the electrons are externally transferred to cathode whereas the anions (e.g., SO<sub>4</sub><sup>2-</sup>, Cl<sup>-</sup>) in the desalination compartment migrate to the anode and the cations (e.g., K<sup>+</sup>, Na<sup>+</sup>) are transferred to the cathode to maintain charge neutrality, thereby, desalination of the middle chamber solution occurs [10, 113, 114]. In MDC, the migration of ions from the saline water in the middle chamber towards the anode and cathode increases the conductivity of the anolyte and catholyte. Thus, electrical power production in MDC has been improved due to higher conductivity and mass transfer. However, the increased salinity of water could adversely affect the anodic/cathodic bacteria as well as the effluent water quality from MDC [113]. The MDC can be operated for simultaneous organic and salt removal with power production or can be combined with the conventional reverse osmosis (RO) process as a pretreatment for lowering the salinity of feed solution, and to decrease energy consumption. Studies have estimated that an MDC can generate up to 58% of the electrical energy needed by downstream RO systems [115]. Jacobson et al. [115] compared RO systems that use 2.2 kWh energy to desalinate 1 m<sup>3</sup> of seawater with MDCs, that can produce 1.8 kWh of electric energy, with a net benefit of 4 kWh by treating 1 m<sup>3</sup> of seawater. When an MDC is operated in electrolysis mode for hydrogen production at the cathode, 180–231% surplus energy than the input electricity can be recovered as H<sub>2</sub>, with the added advantage of water desalination [114, 116].

---

### 6.3 Wastewater Treatment in BES

Bioelectricity generation has been the primary outcome from the MFC technology. Apart from this, several other advantages are associated with BES technology. Wastewater treatment is one of the most important applications of BES. Current processes for biological treatment of low concentrated wastewaters are based on the energy-intensive conventional technologies which are not environmentally friendly. New approaches to wastewater treatment by enabling substantial energy recovery are the most effective way to compensate the huge amount of energy consumed in conventional wastewater treatments. BES associates the benefit of wastewater treatment from diverse origin and energy and resource recovery through the production of bioelectricity or other valuable products [117]. Conventional activated sludge process in domestic wastewater treatment needs  $0.3 \text{ kWh m}^{-3}$  for aeration and about twice of this amount of energy for the pumping and other purposes [118]. Energy can be recovered from domestic wastewaters via anaerobic conversion of organic components to methane. But only a portion of the potentially available energy is recovered through the combined anaerobic digestion and conventional aerobic wastewater treatment. The energy contained in the dissolved organic fraction is lost in the aerobic oxidation processes. If anaerobic digestion is used in place of an aerobic process (activated sludge treatment), energy recovery as methane is possible but still the requirement of concentrated waste stream  $>3 \text{ kg m}^{-3}$  organic load and the maintenance of warmer temperatures  $>20 \text{ }^\circ\text{C}$  are the main limitations [119]. Also, very large digesters are required to make the process economical. Due to these reasons, anaerobic digestion is applied only to treat the sludge from wastewater and high strength wastewaters, but not low strength wastewater. When BESs are used for treating the wastewater, only small amounts of solids (sludge) are produced. Therefore, there is no need of additional sludge management and treatment strategies. Direct electricity generation from wastewaters in MFC can attain high energy efficiencies due to the absence of Carnot cycle limitations in power generation unlike in combustion processes [119]. However, the energy recovery from BES still remains low. Power densities produced in MFCs using only domestic wastewater has attained up to  $12 \text{ W m}^{-3}$  [120] which is equivalent to  $0.07 \text{ kWh m}^{-3}$  produced over 6 hours (6 hours is typical activated sludge treatment time). However, this energy recovery is still low as the organic waste in domestic wastewater can potentially produce up to around  $2 \text{ kWh m}^{-3}$  based on the methane gas that could be generated in anaerobic digestion.

A prediction of the economic gain from the scaled up MFCs treating wastewater concluded that although electricity generation will not rationalize the MFC operation, the organic waste removal is more attractive with this more sustainable technology [121]. In this context, it is more realistic to utilize wastewaters as the source of energy and materials for valuable chemical production in-situ in MEC/MESs [119]. Production of hydrogen or hydrogen peroxide in MECs with wastewaters as the source of electrons is energetically beneficial as compared to the production via conventional electrolysis or other means because the energy contained in wastewater is further used in the production of chemicals [119]. But as an exception, in a comparative experimental study between MFC and MEC, Cusick et al. [122] showed that the treatment efficiency in terms of chemical oxygen demand (COD) removal and the energy recoveries in terms of  $\text{kWh kg}^{-1}\text{-COD}$  were higher for MFCs than MECs with winery and domestic wastewaters. Albeit, utilization of BES technology for the treatment and recovery of energy and chemicals from lower value wastes may become environmentally and economically beneficial. An estimate of hydrogen production cost of  $\$4.51/\text{kg-H}_2$  from winery wastewater and  $\$3.01/\text{kg-H}_2$  from domestic wastewater was reported when both wastewaters were treated in MEC; these costs of hydrogen production were less than the estimated market value of hydrogen ( $\$6 \text{ kg}^{-1}\text{-H}_2$ ) [122].

---

## **6.4 Recalcitrant Pollutants Degradation in BES**

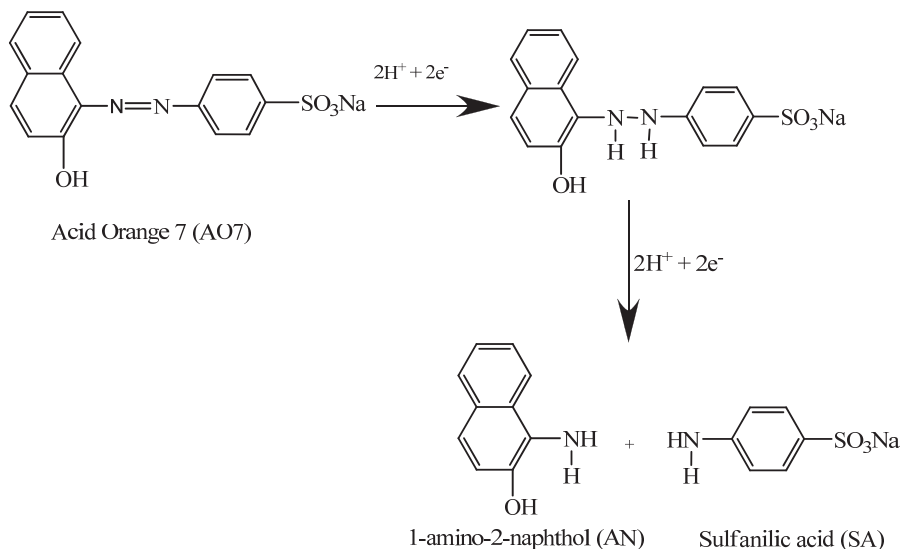
### **6.4.1 Dye decolorization and removal**

Azo dyes, most of which are xenobiotics, contain one or more azo groups (-N=N-), and are the most widely used synthetic dyes in textile, leather, cosmetics, plastics and food industries. Industrial wastewaters containing dyes creates environmental problems due to their persistent colors which spoil the aesthetic values and causality to toxic effects [123, 124]. The contamination of azo dyes in surface water hampers light penetration and decreases the amounts of dissolved oxygen, thereby threatening the aquatic life. Studies have shown that azo dyes are toxic and mutagenic [125, 126]. Dyes are designed to be chemically and photolytically stable and are also not easily degradable to natural microbial action. Due to their complex chemical structures, the decolorization of these wastes is a challenging task. A range of physicochemical treatments exists to decolorize effluents containing dyes. Namely, (i) chemical treatments like ozonation [127], alkalization etc.; (ii) physical treatments like adsorption, flocculation-coagulation etc.; (iii) photo degradation; (iv) membrane processes [128] and (v) a few biological treatments [129] can effectively decolorize the industrial wastewaters. But these techniques are generally very expensive because they require large amounts of chemicals and additionally produce considerable amounts of sludge.

Bioelectrochemical systems are successfully proven to decolorize the dyes [124, 130, 131]. The range of the half-cell potentials for the reduction of azo dyes to their constituent aromatic amines was reported to be between -530 and -180 mV versus the standard hydrogen electrode (vs SHE) [132]. Sun et al. [131] carried out the decolorization of active brilliant red X-3B (ABRX3) utilizing the electrons generated from the biodegradation of readily biodegradable organic matter at the anode of air-cathode single-chamber MFC with concurrent bioelectricity generation. Glucose and confectionery wastewaters were found to be suitable co-substrates for ABRX3 decolorization. ABRX3 decolorization was significantly improved in MFCs as compared to conventional anaerobic treatment. Mu et al. [124] used BES to decolorize acid orange 7 (AO7) abiotically in the cathode, using acetate as the electron donor at the bioanode. AO7 decolorization rates up to  $2.64 \pm 0.03$  mol m<sup>-3</sup> d<sup>-1</sup> were achieved with simultaneous power generation, whereas the decolorization rate was enhanced five times when power was supplied to the BES maintaining the cathode potential at -400 mV (vs SHE). The identification of decolorization products suggests the cathodic reaction mechanism depicted in Figure 6.2.

Alizarin yellow R (AYR) was decolorized in a dual-chamber BES with a biocathode of enriched autotrophic biodegrading inoculum [130]. Within 48 hours of operation under the optimized condition of pH 5.2, and 0.5 V of supplied voltage, the decolorization efficiency was as high as 99.2% (from an initial concentration of 100 mg L<sup>-1</sup>), which was higher than the efficiency obtained from abiotic and mixed sludge-inoculated biocathode operations.





**Figure 6.2:** Possible mechanism of Acid Orange 7 reduction in bioelectrochemical systems. "Adapted with permission from Mu et al. [124] Copyright (2009) American Chemical Society".

#### 6.4.2 Organochlorine removal

Organochlorines are organic compounds containing at least one covalently bonded chlorine atom. Many derivatives of organochlorines persist in the environment and have been found toxic to plants and animals, including humans. Industrial chlorinated solvents, bleaching and preservative agents and chlorine-containing pesticides are the main anthropogenic source of recalcitrant organochlorines. Improper handling and disposal of industrial solvents and degreasing agents such as perchloroethene (PCE) and trichloroethene (TCE) contaminate the soil and groundwater. The physico-chemical technologies to treat these subsurface pollutants are normally very expensive. Naturally existing anaerobic microorganisms can decay and detoxify the chlorinated pollutants via *in situ* bioremediation processes and restore the contaminated soil and groundwater effectively and inexpensively [133]. A brief list of the removal of organochlorines through different types of BESes is overviewed in Table 6.4. Anaerobic bacteria can dechlorinate chlorinated aliphatic hydrocarbons (CAHs) in groundwater, by using them as a terminal electron acceptor for microbial respiration [134]. Incomplete dechlorination of PCE and TCE to the intermediate *cis*-dichloroethene (*cis*-DCE) and then to vinyl chloride (VC) generally occurs in halorespiration. VC is a singly chlorinated ethene and a known carcinogen. Chlorinated compounds (PCE, TCE and *cis*-DCE) reducing microorganisms compete for electrons in acetate and hydrogen intermediates with sulfate, iron (III), and  $CO_2$  reducers [134]. Generally, hydrogen ( $H_2$ ) is considered as an ultimate electron donor for reductive dechlorination by *Desulfitobacterium* spp and *Dehalococcoides* spp [135–137]. But acetate and  $H_2$ , solely or in combination, were identified as key electron donors to stimulate the anaerobic microbial dechlorination of chloroethenes to ethene at the chloroethene-contaminated site [138]. When acetate or  $H_2$  alone was the electron donor, syntrophic acetate-oxidizing species or  $H_2/CO_2$  acetogens respectively were present as the co-culture. Certain dechlorinating bacteria were discovered to be able to accept electrons directly from polarized graphite electrodes to sustain the dechlorination process [139, 140]. These findings have led to the development of BESes for groundwater remediation. TCE-dechlorinating bacteria can directly gain the required electrons from a

negatively polarized carbon paper electrode [139]. Aulenta et al.[141] investigated the performance of TCE dechlorination in bioelectrochemical reactor operating for about 570 days at different cathode potentials ranging from -250 mV to -750 mV vs SHE. At a cathode potential of -250 mV vs SHE, methanogenesis was almost suppressed and 94.7 % of available electrons were accounted for dechlorination, whereas at the cathode potential below -450 mV vs SHE, a higher TCE dechlorination rate up to  $64 \pm 2 \mu\text{mol L}^{-1}\text{d}^{-1}$  was achieved—but simultaneous methanogenesis was reported consuming about 60% of electric current [141]. BES for dechlorination has shown stable and reproducible performance even in the absence of organic carbon sources confirming long-term direct exocellular electron transfer [139, 141] Studies have also been carried out to demonstrate the dechlorination of other chlorinated compounds in the BES including the dechlorination of chlorophenols and 1,2-dichloroethane [142].

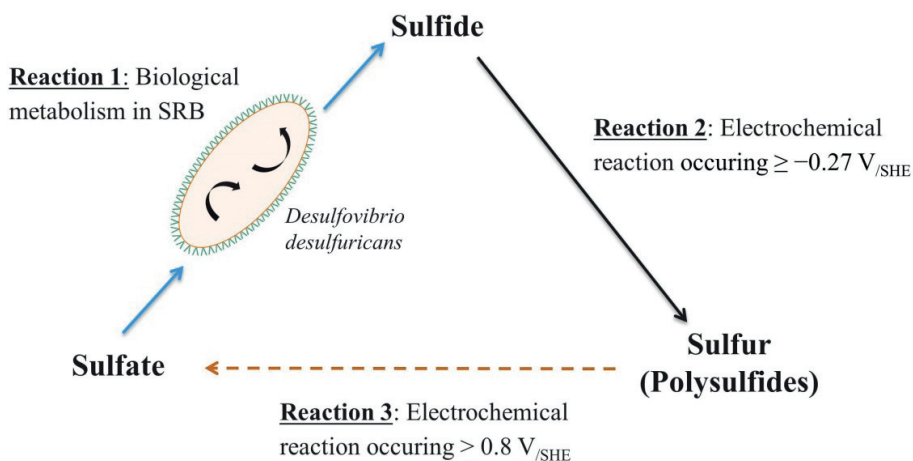
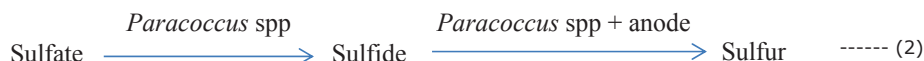
**Table 6.4:** BESs for dechlorination of trichloroethene and other chlorinated compounds

| Compound           | BES   | Electrode   | Operating mode                           | Removal rate<br>( $\text{mol m}^{-3}\text{d}^{-1}$ ) | Reference |
|--------------------|---|---|--|--|-----------|
| Trichloroethene    | Mediator-Methyl Viologen                                    | Glassy carbon cathode, platinum disk anode        | Batch fed                                | 0.001  | [143]     |
| Trichloroethene    | Direct  | graphite electrodes                               | Batch                                    | $25 \mu\text{mol d}^{-1}$                            | [144]     |
| Trichloroethene    | Direct  | Carbon paper                                      |  |  | [139]     |
| Trichloroethene    | Undetectable mediator                                       | Glassy carbon cathode, platinum disk anode        | Batch fed                                | 0.002-0.004  | [145]     |
| Trichloroethene    | Direct  | Graphite cathode                                  |  | $64 \pm 2 \mu\text{mol L}^{-1}\text{d}^{-1}$         | [141]     |
| 4-chlorophenol     | MFC; acetate in anode, 4-chlorophenol in abiotic cathode    | Carbon fiber anode and cathode                    | Batch fed                                | 0.3  | [146]     |
| 1,2-dichloroethane | MFC; Dichloroethane in anode<br><br>Ferricyanide in cathode | Graphite plate anode and graphite granule cathode | Recirculated anode and batch fed cathode | 0.061-0.068  | [147]     |
| 2-chlorophenol     | MEC acetate in anode, 2-chlorophenol in biocathode          | Graphite granule anode and cathode                | Batch fed                                | 0.04   | [148]     |

### 6.4.3 Sulfide Removal

Organic wastes and wastewaters generated from many processes ubiquitously contain sulfur compounds. Biological conversion of sulfur compounds in the wastewaters by sulfate reducing bacteria releases sulfides, which are toxic, odorous and corrosive. Sulfate reducing bacteria like *Desulfovibrio desulfuricans* are commonly found in the wastewaters containing high organic load. Treatment of sulfate-rich wastewaters with biological sulfate reduction processes is a well-known effective method but the treatment process is limited due to the generation of sulfides and other sulfur-based gases which inhibit the bacterial metabolism and even cause the failure of the process, associated to the corrosive and toxic nature of the sulfides [149]. MFCs can be used to remove sulfides

by oxidizing them electrochemically at the anode and, in parallel, power can be generated [150, 151]. As per the reactions mentioned below and according to Figure 6.3, sulfide was biologically reduced to sulfate which was then catalytically oxidized to sulfate using different anodes such as a metal hydroxide-modified graphite [150], charcoal [152], graphite foil, carbon fiber veil and activated carbon cloth [149]. In these studies, oxygen was reduced at the air-cathode to maintain the electron flow through the external circuit.



**Figure 6.3:** Pathways of sulfide/sulfate removal in MFCs. Reaction 1 is biological metabolism in sulfur reducing bacteria (SRB); Reactions 2 and 3 are chemical in nature.

Rabaey et al. [151] reported sulfide and sulfate removal from the wastewater, as solid sulfur accumulation on the granular graphite anode of the MFC, with the ferricyanide redox couple for the cathodic reaction. The biocatalysts identified in this anaerobic oxidation of sulfide were *Paracoccus* species. In this process, sulfide was shuttling the electrons between the bacteria and anode, undergoing an oxidation to insoluble elemental sulfur. In the tubular MFC with air-cathode, at most  $514 \text{ mg sulfide L}^{-1} \text{ day}^{-1}$  (unit normalized to net anodic compartment volume, NAC) was removed via biocatalytic oxidation to elemental sulfur that resulted in electricity generation which accounted maximum power outputs of  $101 \text{ mW L}^{-1} \text{ NAC}$  [151]. Activated carbon cloth was identified as a superior anode material for sulfide oxidation to sulfate when compared to the graphite foil and carbon fiber, and it enabled to extract higher electric power density ( $0.51 \text{ mW cm}^{-2}$ ) in the batch mode operation of a single-chambered, air-cathode MFCs, using sulfate-rich solutions [149]. Oxidation of solid sulfur to sulfate requires a high positive overpotential, whereas sulfide can be oxidized to elemental sulfur when the

---

anode potential is controlled at or above  $-0.27$  V in aqueous solutions at neutral pH (Figure 6.3). In the sulfide removing MFCs, elemental sulfur and/or soluble polysulfide species were the dominant sulfide oxidation products in the anode chamber [149].

#### 6.4.4 Chromium Removal

Reduction of hexavalent chromium Cr(VI) at the cathode of MFCs has high utility in the bioremediation of Cr(VI) contaminated sites, as the technology has low cost of operation, self-regenerating ability and also provides a sustainable power supply [142]. Cr(VI) can be electrochemically or biocatalytically reduced to less toxic, less soluble and less mobile trivalent chromium Cr(III). An acidic environment is required at the cathode for the electrochemical Cr(VI) reduction in abiotic condition [153]. Several bacterial species of *Bacilli* and *Clostridia* as well as a number of proteobacter species such as *Pseudomonas dechromaticans*, *Escherichia coli*, *Desulfovibrio vulgaris*, *Shewanella oneidensis*, *Aeromonas dechromatica* and *Enterobacter cloacae* were reported to catalyze Cr(VI) reduction whenever a suitable carbon source like acetate was available to the biocatalysts [154, 155]. The reduction of Cr(VI) was also attained in an air-bubbling-cathode MFC in which the electrochemical reduction of oxygen to  $H_2O_2$  strongly favored the reduction of Cr(VI) [156]. Improvement to the biocathode for Cr(VI) reduction and electricity generation was reported by Huang et al. [157] using tubular MFCs in which the cathode to anode surface area ratio of 3:1 was maintained. Specific rates of Cr(VI) reduction between  $12.4$  to  $20.6$   $mg\ g^{-1}$  volatile suspended solid(VSS)  $h^{-1}$  were achieved with power generation from  $6.8$  to  $15$   $W\ m^{-3}$  using a graphite-fiber as cathode support for the biocatalyst. The graphite fiber biocathode showed better performance for chromium reduction when compared to graphite felt or graphite granules [157]. The rate of Cr(VI) reduction and electricity generation in MFCs were affected by various physicochemical and biological conditions, like pH, redox mediators, and the bacterial electrochemical activity and etc.. In addition, the anode potential, electrode materials, and reactor configurations also influenced the efficiency of the Cr(VI) reducing biocathode [142].

### 6.5 Metal and nutrient recovery in BES

Application of MFCs has not been limited only to the wastewater treatment and electricity generation, it has also expanded to the electricity-driven production of a number of value-added compounds such as  $H_2$ , acetate, etc. at the cathode [158]. MFCs have also been applied for the removal and recovery of metals from leachates and effluents from mining and metallurgical processes that would preferably result in the recovery of metals especially copper for (re-)use in industries [158]. A subsequent study by Ter Heijne et al. [159] demonstrated the electrochemical reduction of copper at the cathode, using bioelectrochemical acetate oxidation at the anode. In this bioelectrochemical process, a bipolar membrane (BPM) was used for simultaneous bioelectricity generation along with copper reduction/removal at the cathode. The reduced copper was plated onto a flat plate graphite electrode at a current density of  $3.2$   $A\ m^{-2}$ . Further studies accomplished higher current densities in the range of  $0.9$  to  $7$   $A\ m^{-2}$  along with copper removal by using a larger anode surface than the cathode surface [160, 161]. Zhang et al. [162] validated the recovery of vanadium (V) and chromium (Cr) in dual chambered MFCs by employing vanadium and chromium-containing wastewater as the cathodic electron acceptor with simultaneous bioelectricity generation. The maximum power density of these MFCs was  $970$   $mW\ m^{-2}$  and showed enhanced electrode reduction efficiency by using the two electron acceptors  $V^{5+}$  and  $Cr^{6+}$  together [162].

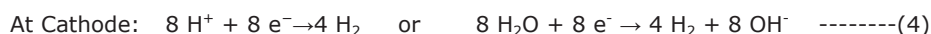
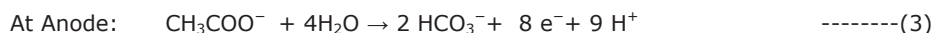
Apart from metals, nutrient recovery was also observed with MFCs. Particularly, successful ammonium ( $NH_4^+$ ) recovery from urine was demonstrated by Kuntke et al. [163]. The electrons required for the migration of  $NH_4^+$  from anode to cathode are generated by the anodic bacteria from the oxidation of organic matter. At the cathode,

diffusion of ammonia (NH<sub>3</sub>) promotes the total ammonium transported to the cathode. Due to the localized high pH prevailing in the cathode, NH<sub>3</sub> stripping occurs and thus improves the transport of ammonium. The ammonium recovery rate and current density were registered as 3.29 g-N d<sup>-1</sup> m<sup>-2</sup> (vs membrane surface area) and 0.50 A m<sup>-2</sup> (vs membrane surface area), respectively. The process produced a surplus energy of 3.46 kJ gN<sup>-1</sup> which was more than the required energy for the ammonium recovery by stripping [163].

## 6.6 Production of Chemicals in BES

### 6.6.1 Hydrogen

Wastewaters from industrial, agricultural and municipal sources contain large amounts of dissolved organic matter that are a potential resource for chemical and fuel production [164]. Biological treatment technologies are known for the production of energy from wastewaters. Methanogenic anaerobic digestion has already been used worldwide for the production of biogas (a mixture of methane and CO<sub>2</sub>). Hydrogen production from wastewaters by acetogenic fermentation is another method of utilization of wastewaters [165, 166]. However, low yields and thermodynamical limitations in microbial metabolism exist in the fermentation process. BESs offer an alternative technology to upgrade the hydrogen yield at a relatively low electric energy input when compared to conventional water electrolysis; more specifically, MEC mode of operation has shown promising rates of hydrogen production. This technology is also termed as bio-electrohydrogenesis [167–170]. Hydrogen is extensively used both as chemical and fuel, in various industrial processes such as upgrading fossil fuels and saturating fats, hence H<sub>2</sub> has unique values compared to methane. On COD basis, H<sub>2</sub> production from wastewater is 7 times more valuable than methane produced from the same amount of wastewater [164]. H<sub>2</sub> production in MEC can be done from various organic sources, including waste materials as well as non-fermentable substrates [66]. Principally, bacteria oxidize organic compounds typically, acetate and generate CO<sub>2</sub>, electrons, and protons at the anode of an MEC. The electrochemical interaction of bacteria transfers the electrons to the solid anode. With an external voltage, the electrons flow to the cathode where they combine with protons to form hydrogen gas (reactions 3 and 4) [171]. For charge neutrality, the protons migrate from anode to cathode in the solution. In practice, a voltage difference of >0.2 V is required for H<sub>2</sub> production in MEC, which is less than the typical voltage (>1.6 V) required for water electrolysis [66, 171]. A membrane separates the anode and cathode chamber to avoid the mixing of the substrate and product. The reactions that occur in an MEC with acetate as substrate are as below.



Theoretically, hydrogen formation at the cathode occurs after overcoming the endothermic barrier of -0.414 V vs SHE by applying only a small external voltage difference of 0.14 V to the MEC, the oxidation reaction carried out by the anodic bacteria can supply the remaining overpotential (-0.279 V) [66, 72]. Concomitant wastewater treatment and H<sub>2</sub> production in MEC is an efficient approach to generate clean energy. The utilization of a wide range of organic compounds by exoelectrogens in MECs makes it sustainable and economically advantageous. However, the hydrogen evolution reaction (HER) occurs very slowly on carbon cathodes of MEC and need to overcome a high endothermic potential barrier (overpotential). To reduce the overpotentials, platinum (Pt) has been used as the catalyst. Electrodes with different amounts of platinum loadings are commercially available and also prepared in the laboratory. Titanium with platinum coating is used as a cathode to avoid the overpotentials. However, platinum based electrodes are very expensive. Cathodes made from cheap non-noble metals like

stainless steel, nickel (Ni) or nickel alloys have also been tested for H<sub>2</sub> production in MEC [172–175]. Nickel and Nickel Molybdenum (NiMo) electrocatalysts have shown good results with only a slightly larger overpotential than platinum [170, 176]. By increasing the specific surface area of the Ni cathodes, the cathode overpotential was lowered and high hydrogen production over 50 m<sup>3</sup> m<sup>-3</sup> MEC d<sup>-1</sup> was attained [76].

It has been shown that bacteria can also catalyze the HER at biocathodes [65, 83]. Studies have focused on the upscaling and improvement of H<sub>2</sub> production in MEC by finding good performing cathodes materials. A bench scale 4 L MEC reactor using stainless steel as cathode produced 0.9 m<sup>3</sup> H<sub>2</sub> m<sup>-3</sup>-MEC d<sup>-1</sup> which had graphite felt as an anode to treat acetate-containing saline wastewater [177]. An overview of the performances of H<sub>2</sub> producing MECs along with their operating conditions is presented in Table 6.3. Although the applied voltage controls the electric current, the current densities reported in MECs increased with the specific surface area of electrodes. Higher current densities are reported with larger specific surface anodes like carbon felt and graphite brush anodes (Table 6.3). Likewise, the production at the cathode of MEC is also enhanced by increasing the cathode surface area. Generally, metal catalysts, like Pt and Ni are used for higher hydrogen production.

### 6.6.2 Acetate

MES took another approach to fix CO<sub>2</sub> in multi-carbon compounds such as liquid fuels or chemicals by electricity-driven reduction reactions. This application is considered as a technology for the storage of electrical energy in the Carbon-Carbon bond of value-added chemicals. Nevin et al. [70] demonstrated the first proof of microbial electrosynthesis using the acetogen *Sporomusa ovata* that could use electrons directly derived from a graphite cathode for the reduction of CO<sub>2</sub> to produce acetate and small quantities of 2-oxobutyrate [70]. Electron recovery in these products was more than 85% of the electrons transferred at the cathodes. Subsequent studies demonstrated the process of CO<sub>2</sub> reduction using MES with a wider range of microorganisms [178]. These studies showed the ability of other acetogenic bacteria, including *S. silvacetica*, *S. sphaeroides*, *Clostridium ljungdahlii*, *C. acetium* and *Moorella thermoacetica* to reduce CO<sub>2</sub> to acetate, 2-oxobutyrate and formate. Electron recoveries in acetate and 2-oxobutyrate were accounted for 84%, 48±6%, 82±10% and 53±4% in *S. silvacetica*, *S. sphaeroides*, *C. ljungdahlii* and *C. acetium* respectively. Gong et al. [179] showed that sulfide can be used as an electron donor at the anode for microbial electrosynthesis. The study used a sulfur oxidizer, *Desulfobulbus propionicus*, at anode as a biocatalyst to oxidize elemental sulfur to sulfate. The electrons generated in biotic anode were used for CO<sub>2</sub> reduction to acetate growing *S. ovata* on a graphite cathode. Marshall et al. [180] showed the improvements in the rate of acetate production by CO<sub>2</sub> reduction using mixed microbial communities termed as microbiomes. Jiang et al. [181] used a biocathode of mixed culture of that accepts electrons from the anode and produced H<sub>2</sub> abiotically to fix CO<sub>2</sub> into methane and acetate. Bioelectrochemical CO<sub>2</sub> reduction with electron capture efficiency of 97% was reported controlling the cathode potential below -950 mV vs NHE [181]. Marshall et al. [85] demonstrated the improved performance of microbial electrosynthesis for acetate production at the highest rate of 1 g L<sup>-1</sup> d<sup>-1</sup> by autotrophic microbiomes when operated for long-term. Furthermore, the long-term adaptation resulted into a stable and resilient biocathode.

The conditions of the MES process must be created to allow the optimal metabolism of biocatalyst present at the biocathode. A suitable terminal electron acceptor should be available for the reduction reaction. In addition, the cathodic or applied potential that breaks the thermodynamic barrier of a biological reaction should be applied for a successful reduction reaction in MES. Homoacetogenic bacteria can efficiently convert CO<sub>2</sub> to acetate, which is a major intermediate molecule for the production of biochemicals [182]. Thermodynamically, the conversion of CO<sub>2</sub> to acetate requires -280 mV vs SHE cathodic potential. However, under practical conditions, a much lower potential is required to overcome the potential losses due to the microbial energy uptake and mass &

charge transfer resistances involved in the bioelectrochemical system. Apart from the above factors, several other underlying factors such as electrode materials, reactor design, mediators in electron transfer influence the overall process efficiency [92]. At present the MES technology is in its infancy, therefore current studies are mainly focused on fabricating new proofs of concept.

### 6.6.3 Methane

Methane generation from anaerobic digestion of organic substrates has long been in practice and it is considered as a renewable process. Still, to improve the sustainability of the methane generation process, recycling of the CO<sub>2</sub> generated from various biological processes can be integrated to produce more methane through microbial electrosynthesis. Microbial electrosynthesis of methane, also known as electromethanogenesis, can proceed at lower temperatures than anaerobic digestion. The specialty of electromethanogenesis through MEC is that the organic matter present in wastewater can be treated and at the same time methane production is achieved. This process provides more advantages than traditional methanogenesis in terms of higher methane yield and utilization of the effluents issued from anaerobic digestion processes [183, 184].

Clauwaert and Verstraete [184] showed bioelectrochemical methane production using a single chamber configuration in MEC mode, using plain graphite electrodes. An applied potential of -0.8 V (vs SHE) was employed, reporting a maximum methane production rate of  $0.75 \pm 0.12 \text{ L L}^{-1}\text{-MEC d}^{-1}$  from  $4.13 \text{ kg m}^{-3}\text{-MEC d}^{-1}$  COD loading with  $86 \pm 14 \%$  of acetate to methane conversion, whereas without voltage application only  $0.17 \pm 0.06 \text{ L L}^{-1}\text{-MEC d}^{-1}$  of methane were generated at a COD feeding of  $1.38 \text{ kg m}^{-3}\text{-MEC d}^{-1}$  with  $47 \pm 17\%$  of acetate to methane conversion. Treatment of anaerobic digestion effluents in a single chamber MEC with methane production was prospected as a viable technology for efficient waste treatment [184]. Sasaki et al. [185] focused on the use of a membrane-less configuration under a working potential of -0.395 or -0.595 V (vs SHE) at neutral pH and demonstrated efficient methane production. It was observed that the dominating methanogens on the cathode were different from those grown in control reactors with no electrochemical reactions [185].

In the scalability studies on MEC with multi-electrode configuration for H<sub>2</sub> production using acetate as a substrate, Rader and Logan [186] reported that the methanogenesis rates increased gradually with time. After 16 days of operation, the system showed little H<sub>2</sub> production but a subsequent CH<sub>4</sub> production with good substrate conversion efficiency, showing that electromethanogenesis is the predominant process at the biocathode, when operated with effluents from dark fermentation and anaerobic digestion processes [186].

A biocathode dominated by *Methanobacterium palustre* was shown to successfully reduce CO<sub>2</sub> to methane, in combination with an abiotic graphite anode through a mediator-less mechanism (kind of direct electron transfer) [68]. The thermodynamic constraints of methane production from CO<sub>2</sub> reduction predict the requirement of -0.244 V vs SHE cathodic potential at standard biological conditions. Practically, a wide range of applied cathode potentials (i.e. between -0.5 to -1.0 V vs SHE) has been reported for the electromethanogenesis [68, 187, 188]. Cheng et al. [68] demonstrated the electromethanogenesis in the BESs with abiotic and biotic anodes and also in dual chamber and single chamber combinations. Methane production with 80% overall efficiency (electrical energy + substrate enthalpy) at -0.8 V vs SHE cathode in a single-chamber MEC was reported, with an anodic biofilm growing on acetate. In a double-chamber BES with an abiotic anode, Cheng et al. [68] achieved  $4.5 \text{ L m}^{-2} \text{ d}^{-1}$  of methane production with 96% energy/coulombic efficiency, controlling the cathode at -0.8 V vs SHE. Compared to conventional methanogenesis, the advantage of bioelectrosynthesis is the physical separation of the oxidation of organic waste from methane production, which protects the methanogenic consortia from the inhibitory compounds that can be present in the waste stream, and CO<sub>2</sub> can be recycled for methane production. Villano et al. [188, 189] worked with mixed methanogenic cultures as cathodic biocatalysts in dual

---

chambered configurations with an applied voltage changing within a range of -0.5 V and -1.0 V vs SHE.

#### **6.6.4 Other Chemicals**

In recent studies on BESs, the production of value-added chemicals and fuels other than acetate, methane and hydrogen has been highlighted [8, 119]. Valuable products such as hydrogen peroxide and caustic soda were produced at the metallic cathode of MEC by applying external electric potential and at the concomitantly achieved improved performance efficiency for wastewater treatment [69, 78, 190]. Electrosynthesis of fuels such as methanol has long been reported from the electrochemical reduction of CO<sub>2</sub> using metal catalysts like copper [191] but the process is energy intensive and not sustainable. In this context, microbial electrosynthesis could be a less energy intensive and sustainable solution for electricity-driven fuel and chemical production. In recent studies, small amounts of ethanol and butyrate production have been reported as secondary products in MES, from CO<sub>2</sub> reduction using lithoautotrophs [91] whereas the heterotrophic production of ethanol from acetate as the substrate has been demonstrated at the cathode of BES [192]. Most of the MES studies on CO<sub>2</sub> reduction reported H<sub>2</sub> evolution at the cathode as a mediator for the microbial CO<sub>2</sub> reduction [85, 91, 181]. As an alternative to H<sub>2</sub>-driven MES for CO<sub>2</sub> fixation, an innovative strategy has been suggested that uses formic acid (HCOOH) as an energy carrier [193]. Formic acid production from CO<sub>2</sub> and water by bioelectrochemical reactions and its further conversion to isobutanol by engineered *Ralstonia eutropha* was demonstrated [194]). The *R. eutropha* strain was engineered to divert the usual poly-hydroxybutyrate synthesis pathway to produce liquid fuel and also made it able to withstand electric current. The metabolically engineered strain was also used for the conversion of CO<sub>2</sub> to ethanol [195]. Xafenias et al. [196] showed increased 1,3-propanediol titers using a mixed-culture as biocatalyst, with glycerol as a substrate. Along with all the above-discussed products, a few reports are available on the production of butanol, acetone and succinate through MES processes [8, 71, 197].

### **6.7 BES based Biosensors**

MFC technology can be applied for the easy and fast testing of the water quality. MFC based biosensors have been proposed in recent studies for the detection of toxic compounds and for the measurement of biochemical oxygen demand (BOD) of water samples. MFCs have the potential advantage for on-site and real-time monitoring of water quality [198, 199]. MFC technology can also be highly cost-effective in comparison with the conventional sensors, as it can be built on low-cost carbon-based materials. In MFC based biosensors, oxidation of organic matter in the inflow feed was catalyzed by the bacteria growing on the anode and produce electrons giving an electrical signal. The electrical signal generated by the MFC is associated with the rate of metabolic activity of the biofilm at the anode [200]. Any disturbance in the bacterial activity is interpreted into a change in the electric current. When toxic compounds are present in the feed water, the bacterial activities will be affected, which can be detected in the variation in electrical signal. This extent of change in electric current was shown to be directly associated to the specific disturbance imposed to the bioanode when other operational parameters of MFC such as pH, temperature, and conductivity of the feeding solution were kept constant [201]. MFCs were highly sensitive with regards to many compounds present in the feed water. Hence, it can be used as an early warning signal. In MFC based biosensors, transducers were not required to translate the signals to a readable ones as the bacterial growth on the anode directly produces measurable electrical signals from the sensing element. The application of MFC as a biosensor for BOD and toxic contaminants in water has been separately discussed as in the following sections.



### 6.7.1 BOD Sensors

BOD has been used as a basic parameter to quantify the extent of organic contamination in the water systems. The electronic charge generated from a mediator-less MFC is in good positive correlation to the concentration of organic matters. So, MFCs have been investigated as BOD sensors [198, 199, 202]. Chang et al. [198] continuously monitored the BOD of sample water on-line using an MFC, by measuring the electric current in amperometric mode. BOD values of up to  $100 \text{ mg L}^{-1}$  were in good linear fit with the electric current generated. An extrapolation of the fitted model can be used to measure higher BOD values [198, 199]. MFC as a BOD sensor can operate with stable performance for over 5 years with minimum maintenance service [198]. A performance overview of MFC-based BOD sensors is presented in Table 6.5, along with the operational characteristics of the MFCs. In all of the literature mentioned in Table 6.5, inoculation of the anode with mixed bacterial cultures issued from wastewater was carried out to widen the variety of usable substrates and also for long-term performance stability. The quickest response time of MFC-based BOD sensors was 2.8 minutes for a scaled-down single chamber MFC and the response time varied with the reactor design [200]. Table 6.5 shows that the most recent studies have improved the BOD detection range and response time of MFC-based sensors.

**Table 6.5:** Overview of performance, design and functional characteristics of MFCs used as BOD sensors

| Source of inoculum                | Anode         | Configuration                          | Detection Range ( $\text{BOD}_5$ , $\text{mg}\cdot\text{L}^{-1}$ ) | Saturation Signal                  | Response Time | References |
|-----------------------------------|---------------|--|--|------------------------------------|---------------|------------|
| Enriched consortium (waste water) | Graphite felt | Two chamber                            | 2.58–206 (based charge) on   | 1.1 mA                             | 0.5–10 h      | [202]      |
| Consortium (activated sludge)     | Graphite felt | Two chamber                            | 23–100   | 6 mA                               | 1 h           | [198]      |
| Consortium (primary clarifier)    | Carbon paper  | Two chamber                            | 10–250   | $233 \text{ mA}\cdot\text{m}^{-2}$ | 40 min        | [203]      |
| Consortium (from an active MFC)   | Carbon cloth  | Single chamber (air breathing cathode) | 3–164  | $35 \mu\text{A}$                   | 2.8–8.7 min   | [200]      |

### 6.7.2 Toxicity Sensors

MFC-based toxicity sensors was first demonstrated by Kim et al. [204] which showed the variation in the electrical current in response to the presence of contaminants such as heavy metals, like Pb and Hg, organophosphorus pesticides (e.g. Diazinon) and polychlorinated biphenyls (PCBs) in the water samples. Principally, the substrate consumption rate and the microbial activity in MFC biosensors are directly linked to the electric current generated. A decrement in electric current under the exposure to a toxin, when all of the operational conditions remain same, is an indication of toxic inhibition. An effect of toxic components on the electrochemically-active bacteria has been shown by a shift in the polarization curves, specifically, a dose-response relationship for nickel was visualized in the polarization curves [205]. A higher concentration of contaminant leads to a lower current at all overpotentials [205, 206]. The MFC-based biosensors studied for the detection of toxic components in water are summarized in Table 6.6. Table 6 shows that the lowest detection limit of the MFC biosensors was  $1 \text{ mg}\cdot\text{L}^{-1}$  for heavy metals like Pb, Hg, Cr and even  $100 \mu\text{g}\cdot\text{L}^{-1}$  for Cd, while the upper limits of detection were not assessed within the short range of concentrations employed.

**Table 6.6:** Overview of the reactor, performance and functional characteristics of MFCs used as toxicant sensors

| Source of inoculum               | Anode material     | Toxicant-Detection Range (mg·L <sup>-1</sup> )   | Baseline Signal        | Response Time | References |
|----------------------------------|--------------------|--|------------------------|---------------|------------|
| Mixed culture (Activated sludge) | Graphite felt      | Diazinon: 1–10<br>Pb: 1–10<br>Hg: 1–10<br>PCBs: 1–10   | 0.04 mA                | 20 min–2 h    | [204]      |
| Mixed culture (active MFC)       | Graphite plate     | Cu <sup>2+</sup> : 85  | 1.37 A·m <sup>-2</sup> | 50–100 min    | [207]      |
| <i>Geobacter sulfurreducens</i>  | Ti/Ni/Au tri-layer | Formaldehyde 0.1%–4%   | 4 μA·cm <sup>-2</sup>  | <5 min        | [208]      |
| Mixed culture (active MFC)       | Graphite plate     | Ni: 10   | 2.25 mA                | 30 min        | [206]      |
| Mixed culture (waste-water)      | Carbon cloth       | Cr <sup>6+</sup> : 1–8<br>Fe <sup>3+</sup> : 1, 8, 48<br>NO <sub>3</sub> <sup>-</sup> : 1, 8, 48 | 0.10–0.12 V            | 5 min         | [209]      |
| Mixed culture (active MFC)       | Carbon cloth       | Cd <sup>2+</sup> 0.1–100 μg·L <sup>-1</sup>  | 32.2 μA                | 12 min        | [200]      |

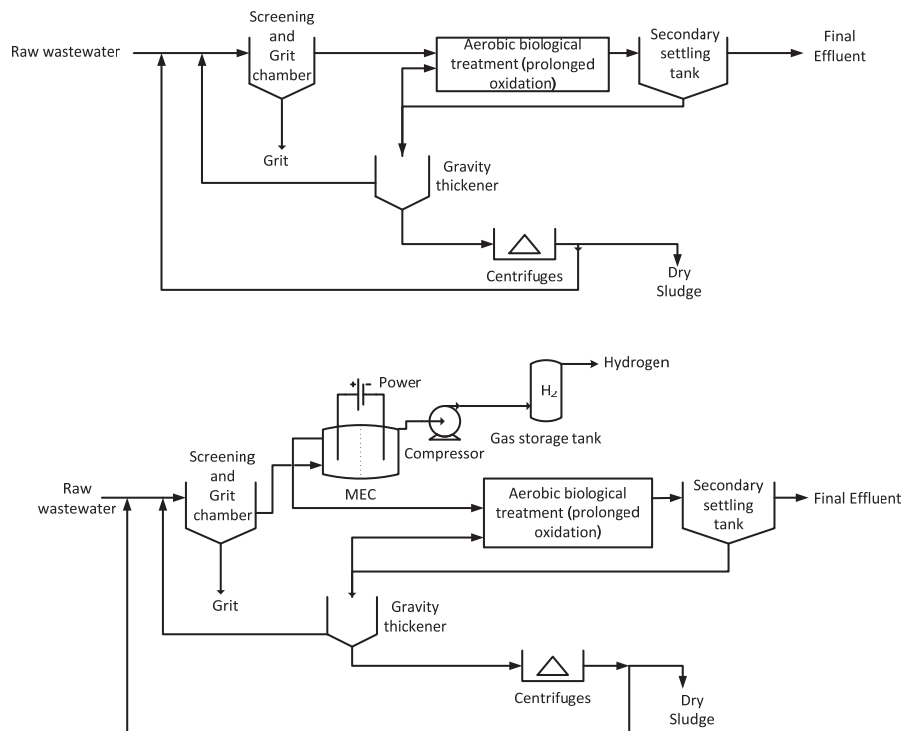
It has been established that MFC based sensors could be sensitive to the target compounds with the detection limits lower than 1 ppm, and can be operated for a long time with stable performance. However, a few key constraints of MFC-based biosensors have to be addressed for a full-scale installation of this technology. These constraints are low selectivity, lower detection limit, the risk of other microbial infections and mass-transfer limitations concerning substrates and products [210]. Recent advances made in MFC-based biosensors have broadened the perspective for simple, on-site and cost-effective water quality monitoring. The use of highly acid/base tolerant and halo-tolerant microbes in MFC biosensors will be highly attractive for industrial wastewater monitoring [210].

## 6.8 Future prospects and conclusions

BESs are versatile systems designed for converting chemical energy into electrical energy (and vice-versa) while employing microbes as catalysts. MES is the most recent application of BESs utilized for the electricity-driven chemical and fuel production. However, the understanding of the multi-disciplinary aspects involved in MES processes is still in its infancy. Compared to conventional industrial microbiology, MES requires more expertise from other disciplines such as electrochemistry, bioelectrochemistry and materials sciences. Generally, the performance of any biological system is dependent on the substrate conversion, biocatalyst activity, specificity of the enzymes involved in the conversion process and redox conditions. In the case of electrochemical processes, it also depends on the conductivity of the electrolyte (either anolyte or catholyte), the mediators involved, anode and cathode potentials, overpotentials (voltage losses), mass and charge transfer etc. Since MES result from a combination of these two processes, the overall limitations are especially complex and difficult to identify.

The above-stated limitations were generally established for MFC technologies in which only one biological component is present, whereas, in the case of biocathodes, plenty of limitations are typically associated than the anodes. Reduction of overpotentials and high coulombic efficiencies often remain the main technological challenges of BES to solve in future applications. Upscaling the production at industrial scale is also found as the major step for BES technologies. Stacking up of a number of MFCs and integration of multiple electrodes in a single system have been reported in the literature. Even though these attempts were providing promising results, the upscaling of BES still need to address the overpotentials and other associated design aspects. Reproducibility of bench scale performances in the large scale systems will certainly make the process economically and environmentally feasible. Studies have also proposed the possible way to incorporate the BES technology in existing wastewater treatment plants. It has been projected more

technically feasible to incorporate MEC for simultaneous waste treatment and hydrogen production than running MFC for electricity generation from wastewater. The possible and appropriate scheme to incorporate MEC to produce hydrogen gas in existing wastewater treatment plant as proposed by Escapa et al. [211] is shown in Figure 6.4.



**Figure 6.4:** Possible scheme to incorporate BES in wastewater treatment plant [adapted from Escapa et al [211]]. The flowcharts show the processes in an existing wastewater treatment plant (top) and the proposed plant (bottom) incorporating the Microbial Electrolysis Cell for wastewater treatment and hydrogen production.

In anodic mechanism of MFCs, mixed cultures are considered to be as effective biocatalysts with wastewaters as substrate. In MES, less is known about the behavior of cathodic biofilms, planktonic cells and electron transfer mechanism involved. It is also necessary to understand the interface of both biofilms and planktonic cells. Conceptually, mixed as well as pure homoacetogenic bacterial cultures could effectively carry out  $\text{CO}_2$  reduction. The electron transfer efficiency and mechanism, the sustainability of biofilms in the electrochemical system and the biochemistry of microorganisms command the selection procedure of the type of biocatalyst to be chosen. Selection of biocatalyst is also influenced by the terminal electron acceptor to be used for reduction process. To take the full advantage of MES, it is very important to understand which intracellular and extracellular factors influence the metabolic rate.

The combination of BES technology with the fermentation technology termed as Electro-fermentation (EF) has added a new prospect of versatility of BES application. The concept is to use electrical energy as a source of reducing power for microbial fermentation and also to provide the required electrons for the generation of the product of interest. Researchers from the BES and fermentation disciplines are focusing on EF as a potential technology to overcome many biological, electrochemical, logistical and economical challenges incorporated in the production of value-added products in BES.

---

## Acknowledgements

Suman Bajracharya is supported by a PhD grant from VITO's strategic research funds. Mohita Sharma acknowledges Indo-Belgian scholarship from the Flemish Government (Vlaamse Gemeenschap) for supporting her stay at VITO. G. Mohanakrishna gratefully acknowledges the Marie-Curie Intra-European Fellowship (IEF) supported project BIO-ELECTRO-ETHYLENE (Grant No: 626959) from the European Commission.

## References

1. Chae K-J, Choi M-J, Kim K-Y, et al (2009) A solar-powered microbial electrolysis cell with a platinum catalyst-free cathode to produce hydrogen. *Environ Sci Technol* 43:9525–30. doi: 10.1021/es9022317
2. Resch G, Held A, Faber T, et al (2008) Potentials and prospects for renewable energies at global scale. *Energy Policy* 36:4048–4056. doi: 10.1016/j.enpol.2008.06.029
3. Venkata Mohan S, Mohanakrishna G, Velvizhi G, et al (2010) Bio-catalyzed electrochemical treatment of real field dairy wastewater with simultaneous power generation. *Biochem Eng J* 51:32–39. doi: 10.1016/j.bej.2010.04.012
4. ElMekawy A, Srikanth S, Bajracharya S, et al (2015) Food and Agricultural Wastes as Substrates for Bioelectrochemical System (BES): The Synchronized Recovery of Sustainable Energy and Waste Treatment. *Food Res Int* 73:213–225. doi: 10.1016/j.foodres.2014.11.045
5. Patil SA, Gildemyn S, Pant D, et al (2015) A logical data representation framework for electricity-driven bioproduction processes. *Biotechnol Adv* 33:736–744. doi: 10.1016/j.biotechadv.2015.03.002
6. Harnisch F, Schröder U (2010) From MFC to MXC: chemical and biological cathodes and their potential for microbial bioelectrochemical systems. *Chem Soc Rev* 39:4433–4448. doi: 10.1039/c003068f
7. Singh A, Sevda S, Abu Reesh I, et al (2015) Biohydrogen Production from Lignocellulosic Biomass: Technology and Sustainability. *Energies* 8:13062–13080. doi: 10.3390/en8112357
8. Rabaey K, Rozendal RA (2010) Microbial electrosynthesis — revisiting the electrical route for microbial production.pdf. *Nat Rev Microbiol* 8:706–16. doi: 10.1038/nrmicro2422
9. Chiranjeevi P, Mohanakrishna G, Mohan SV (2012) Rhizosphere mediated electrogenesis with the function of anode placement for harnessing bioenergy through CO<sub>2</sub> sequestration. *Bioresour Technol* 124:364–70. doi: 10.1016/j.biortech.2012.08.020
10. Cao X, Huang X, Liang P, et al (2009) A New Method for Water Desalination Using Microbial Desalination Cells. *Environ Sci Technol* 43:7148–7152. doi: 10.1021/es901950j
11. ElMekawy A, Hegab HM, Vanbroekhoven K, Pant D (2014) Techno-productive potential of photosynthetic microbial fuel cells through different configurations. *Renew Sustain Energy Rev* 39:617–627. doi: http://dx.doi.org/10.1016/j.rser.2014.07.116
12. Mohanakrishna G, Venkata Mohan S, Sarma PN (2010) Bio-electrochemical treatment of distillery wastewater in microbial fuel cell facilitating decolorization and desalination along with power generation. *J Hazard Mater* 177:487–94. doi: 10.1016/j.jhazmat.2009.12.059
13. Rabaey K, Girguis P, Nielsen LK (2011) Metabolic and practical considerations on microbial electrosynthesis. *Curr Opin Biotechnol* 22:371–7.
14. Potter AMC (2010) Electrical Effects Accompanying the Decomposition of Organic Compounds . II . Ionisation of the Gases Produced during Fermentation Decomposition of Organic Compounds . 91:465–480.
15. Kiely PD, Regan JM, Logan BE (2011) The electric picnic: synergistic requirements for exoelectrogenic microbial communities. *Curr Opin Biotechnol* 22:378–85. doi: 10.1016/j.copbio.2011.03.003
16. Logan BE (2009) Exoelectrogenic bacteria that power microbial fuel cells. *Nat Rev Microbiol* 7:375–81. doi: 10.1038/nrmicro2113
17. Chen S, He G, Liu Q, et al (2012) Layered corrugated electrode macrostructures boost microbial bioelectrocatalysis. *Energy Environ Sci* 5:9769. doi: 10.1039/c2ee23344d
18. Pant D, Van Bogaert G, Diels L, Vanbroekhoven K (2010) A review of the substrates used in microbial fuel cells (MFCs) for sustainable energy production. *Bioresour Technol* 101:1533–43. doi: 10.1016/j.biortech.2009.10.017
19. Fan Y, Sharbrough E, Liu H (2008) Quantification of the Internal Resistance Distribution of Microbial Fuel Cells. *Environ Sci Technol* 42:8101–8107. doi: 10.1021/es801229j

- 
20. Sharma M, Sarma PM, Pant D, Dominguez-Benetton X (2015) Optimization of electrochemical parameters for sulfate-reducing bacteria (SRB) based biocathode. *RSC Adv* 5:39601–39611. doi: 10.1039/C5RA04120A
  21. Rousseau R, Dominguez-Benetton X, Délia M-L, Bergel A (2013) Microbial bioanodes with high salinity tolerance for microbial fuel cells and microbial electrolysis cells. *Electrochem commun* 33:1–4. doi: 10.1016/j.elecom.2013.04.002
  22. ter Heijne A, Hamelers HVM, Saakes M, Buisman CJN (2008) Performance of non-porous graphite and titanium-based anodes in microbial fuel cells. *Electrochim Acta* 53:5697–5703. doi: 10.1016/j.electacta.2008.03.032
  23. Chen S, Hou H, Harnisch F, et al (2011) Electrospun and solution blown three-dimensional carbon fiber nonwovens for application as electrodes in microbial fuel cells. *Energy Environ Sci* 4:1417. doi: 10.1039/c0ee00446d
  24. Feng Y, Yang Q, Wang X, Logan BE (2010) Treatment of carbon fiber brush anodes for improving power generation in air–cathode microbial fuel cells. *J Power Sources* 195:1841–1844.
  25. Mohanakrishna G, Krishna Mohan S, Venkata Mohan S (2012) Carbon based nanotubes and nanopowder as impregnated electrode structures for enhanced power generation: Evaluation with real field wastewater. *Appl Energy* 95:31–37. doi: <http://dx.doi.org/10.1016/j.apenergy.2012.01.058>
  26. Pocaznoi D, Erable B, Delia M-L, Bergel A (2012) Ultra microelectrodes increase the current density provided by electroactive biofilms by improving their electron transport ability. *Energy Environ Sci* 5:5287. doi: 10.1039/c1ee01469b
  27. Zhang X, Pant D, Zhang F, et al (2014) Long-Term Performance of Chemically and Physically Modified Activated Carbons in Air Cathodes of Microbial Fuel Cells. *ChemElectroChem* 1:1859–1866. doi: 10.1002/celc.201402123
  28. Sharma M, Bajracharya S, Gildemyn S, et al (2014) A critical revisit of the key parameters used to describe microbial electrochemical systems. *Electrochim Acta* 140:191–208. doi: 10.1016/j.electacta.2014.02.111
  29. Sleutels THJ a, Ter Heijne A, Buisman CJN, Hamelers HVM (2012) Bioelectrochemical systems: an outlook for practical applications. *ChemSusChem* 5:1012–9.
  30. Bond DR, Lovley DR (2003) Electricity Production by *Geobacter sulfurreducens* Attached to Electrodes. doi: 10.1128/AEM.69.3.1548
  31. Rosenbaum M, Schröder U, Scholz F (2006) Investigation of the electrocatalytic oxidation of formate and ethanol at platinum black under microbial fuel cell conditions. *J Solid State Electrochem* 10:872–878. doi: 10.1007/s10008-006-0167-2
  32. Logan B, Cheng S, Watson V, Estadt G (2007) Graphite Fiber Brush Anodes for Increased Power Production in Air–Cathode Microbial Fuel Cells. *Environ Sci Technol* 41:3341–3346. doi: 10.1021/es062644y
  33. Fan Y, Hongqiang H, Liu H, Fan, Y.; Hu, H. & Liu H (2007) Sustainable power generation in microbial fuel cells using bicarbonate buffer and proton transfer mechanisms. *Environ Sci Technol* 41:8154–8158. doi: 10.1021/es071739c
  34. Zhang L, Zhou S, Zhuang L, et al (2008) Microbial fuel cell based on *Klebsiella pneumoniae* biofilm. *Electrochem commun* 10:1641–1643. doi: 10.1016/j.elecom.2008.08.030
  35. Xing D, Zuo Y, Cheng S, et al (2008) Electricity generation by *Rhodospseudomonas palustris* DX-1. *Environ Sci Technol* 42:4146–51.
  36. Dumas C, Basseguy R, Bergel A (2008) DSA to grow electrochemically active biofilms of *Geobacter sulfurreducens*. *Electrochim Acta* 53:3200–3209. doi: 10.1016/j.electacta.2007.10.066
  37. Dumas C, Basseguy R, Bergel A (2008) Electrochemical activity of *Geobacter sulfurreducens* biofilms on stainless steel anodes. *Electrochim Acta* 53:5235–5241. doi: 10.1016/j.electacta.2008.02.056
  38. Fan Y, Han S-K, Liu H (2012) Improved performance of CEA microbial fuel cells with increased reactor size. *Energy Environ Sci* 5:8273. doi: 10.1039/c2ee21964f
  39. Carmona-Martinez AA, Pierra M, Trably E, Bernet N (2013) High current density via direct electron transfer by the halophilic andoe respiring bacterium *Geoalkalibacter subterraneus*. *Phys Chem Chem Phys*. doi: 10.1039/C3CP54045F
  40. Flexer V, Chen J, Donose BC, et al (2013) The nanostructure of three-dimensional scaffolds enhances the current density of microbial bioelectrochemical systems. *Energy Environ Sci* 6:1291–1298. doi: 10.1039/C3EE00052D
  41. Ketep SF, Bergel A, Calmet A, Erable B (2014) Stainless steel foam increases the current produced by microbial bioanodes in bioelectrochemical systems. *Energy Environ Sci* 7:1633–1637. doi: 10.1039/C3EE44114H
-

- 
42. Baudler A, Schmidt I, Langner M, et al (2015) Does it have to be carbon? Metal anodes in microbial fuel cells and related bioelectrochemical systems. *Energy Environ Sci* 8:2048–2055. doi: 10.1039/C5EE00866B
  43. Massazza D, Parra R, Busalmen JP, Romeo HE (2015) New ceramic electrodes allow reaching the target current density in bioelectrochemical systems. *Energy Environ Sci* 8:2707–2712. doi: 10.1039/C5EE01498K
  44. Karthikeyan R, Wang B, Xuan J, et al (2015) Interfacial electron transfer and bioelectrocatalysis of carbonized plant material as effective anode of microbial fuel cell. *Electrochim Acta* 157:314–323. doi: 10.1016/j.electacta.2015.01.029
  45. Liu H, Logan BE (2004) Electricity generation using an air-cathode single chamber microbial fuel cell in the presence and absence of a proton exchange membrane. *Environ Sci Technol* 38:4040–6.
  46. Logan BE, Murano C, Scott K, et al (2005) Electricity generation from cysteine in a microbial fuel cell. *Water Res* 39:942–52. doi: 10.1016/j.watres.2004.11.019
  47. Cheng S, Liu H, Logan BE (2006) Increased performance of single-chamber microbial fuel cells using an improved cathode structure. *Electrochem Commun* 8:489–494. doi: 10.1016/j.elecom.2006.01.010
  48. Winfield J, Teropoulos I, Greenman J (2012) Investigating a cascade of seven hydraulically connected microbial fuel cells. *Bioresour Technol* 110:245–50. doi: 10.1016/j.biortech.2012.01.095
  49. Clauwaert P, van der Ha D, Boon N, et al (2007) Open air biocathode enables effective electricity generation with microbial fuel cells. *Environ Sci Technol* 41:7564–9.
  50. Freguia S, Rabaey K, Yuan Z, Keller J (2007) Non-catalyzed cathodic oxygen reduction at graphite granules in microbial fuel cells. *Electrochim Acta* 53:598–603. doi: 10.1016/j.electacta.2007.07.037
  51. You S-J, Ren N-Q, Zhao Q-L, et al (2009) Power Generation and Electrochemical Analysis of Biocathode Microbial Fuel Cell Using Graphite Fibre Brush as Cathode Material. *Fuel Cells* 9:588–596.
  52. Zhuang L, Zhou S, Wang Y, et al (2009) Membrane-less cloth cathode assembly (CCA) for scalable microbial fuel cells. *Biosens Bioelectron* 24:3652–6. doi: 10.1016/j.bios.2009.05.032
  53. Zhang L, Liu C, Zhuang L, et al (2009) Manganese dioxide as an alternative cathodic catalyst to platinum in microbial fuel cells. *Biosens Bioelectron* 24:2825–9. doi: 10.1016/j.bios.2009.02.010
  54. Yang X, Zou W, Su Y, et al (2014) Activated nitrogen-doped carbon nanofibers with hierarchical pore as efficient oxygen reduction reaction catalyst for microbial fuel cells. *J Power Sources* 266:36–42. doi: 10.1016/j.jpowsour.2014.04.126
  55. Zuo Y, Cheng S, Call D, Logan BE (2007) Tubular membrane cathodes for scalable power generation in microbial fuel cells. *Environ Sci Technol* 41:3347–53.
  56. Zuo Y, Cheng S, Logan BE (2008) Ion exchange membrane cathodes for scalable microbial fuel cells. *Environ Sci Technol* 42:6967–72.
  57. Zhang F, Saito T, Cheng S, et al (2010) Microbial fuel cell cathodes with poly(dimethylsiloxane) diffusion layers constructed around stainless steel mesh current collectors. *Environ Sci Technol* 44:1490–5. doi: 10.1021/es903009d
  58. Xiao L, Damien J, Luo J, et al (2012) Crumpled graphene particles for microbial fuel cell electrodes. *J Power Sources* 208:187–192. doi: 10.1016/j.jpowsour.2012.02.036
  59. Luo Y, Zhang F, Wei B, et al (2013) The use of cloth fabric diffusion layers for scalable microbial fuel cells. *Biochem Eng J* 73:49–52. doi: 10.1016/j.bej.2013.01.011
  60. Deng Q, Li X, Zuo J, et al (2010) Power generation using an activated carbon fiber felt cathode in an upflow microbial fuel cell. *J Power Sources* 195:1130–1135. doi: 10.1016/j.jpowsour.2009.08.092
  61. Zhuang L, Zheng Y, Zhou S, et al (2012) Scalable microbial fuel cell (MFC) stack for continuous real wastewater treatment. *Bioresour Technol* 106:82–8. doi: 10.1016/j.biortech.2011.11.019
  62. Wen Q, Wang S, Yan J, et al (2012) MnO<sub>2</sub>-graphene hybrid as an alternative cathodic catalyst to platinum in microbial fuel cells. *J Power Sources* 216:187–191. doi: 10.1016/j.jpowsour.2012.05.023
  63. Hou J, Liu Z, Li Y, et al (2015) A comparative study of graphene-coated stainless steel fiber felt and carbon cloth as anodes in MFCs. *Bioprocess Biosyst Eng* 38:881–888. doi: 10.1007/s00449-014-1332-0
  64. Verstraete W, Rabaey K (2006) Critical Review Microbial Fuel Cells: Methodology and Technology †. *40:5181–5192*.
  65. Jeremiasse AW, Hamelers HVM, Buisman CJN (2010) Microbial electrolysis cell with a microbial biocathode. *Bioelectrochemistry* 78:39–43. doi: 10.1016/j.bioelechem.2009.05.005
  66. Logan BE, Call DF, Cheng S, et al (2008) Critical Review Microbial Electrolysis Cells for High Yield Hydrogen Gas Production from Organic Matter. *Environ Sci Technol* 42:8630–8640.
  67. Wang A, Sun D, Cao G, et al (2011) Integrated hydrogen production process from cellulose by
-

- 
- combining dark fermentation , microbial fuel cells , and a microbial electrolysis cell. *Bioresour Technol* 102:4137–4143.
68. Cheng S, Xing D, Call DF, Logan BE (2009) Direct biological conversion of electrical current into methane by electromethanogenesis. *Environ Sci Technol* 43:3953–8.
69. Rozendal R a., Leone E, Keller J, Rabaey K (2009) Efficient hydrogen peroxide generation from organic matter in a bioelectrochemical system. *Electrochem Commun* 11:1752–1755. doi: 10.1016/j.elecom.2009.07.008
70. Nevin KP, Woodard TL, Franks AE, et al (2010) Microbial Electrosynthesis : Feeding Microbes Electricity To Convert Carbon Dioxide and Water to Multicarbon Extracellular Organic. *MBio* 1:e00103–10-. doi: 10.1128/mBio.00103-10.Editor
71. Sharma M, Aryal N, Sarma PM, et al (2013) Bioelectrocatalyzed reduction of acetic and butyric acids via direct electron transfer using a mixed culture of sulfate-reducers drives electrosynthesis of alcohols and acetone. *Chem Commun (Camb)* 49:6495–7. doi: 10.1039/c3cc42570c
72. Rozendal R, Hamelers H, Euverink G, et al (2006) Principle and perspectives of hydrogen production through biocatalyzed electrolysis. *Int J Hydrogen Energy* 31:1632–1640. doi: 10.1016/j.ijhydene.2005.12.006
73. Call D, Logan BE (2008) Hydrogen production in a single chamber microbial electrolysis cell lacking a membrane. *Environ Sci Technol* 42:3401–6.
74. Sleutels THJ a., Lodder R, Hamelers HVM, Buisman CJN (2009) Improved performance of porous bio-anodes in microbial electrolysis cells by enhancing mass and charge transport. *Int J Hydrogen Energy* 34:9655–9661. doi: 10.1016/j.ijhydene.2009.09.089
75. Tartakovskiy B, Manuel M, Wang H, Guiot S (2009) High rate membrane-less microbial electrolysis cell for continuous hydrogen production. *Int J Hydrogen Energy* 34:672–677. doi: 10.1016/j.ijhydene.2008.11.003
76. Jeremiassé AW, Hamelers HVM, Saakes M, Buisman CJN (2010) Ni foam cathode enables high volumetric H<sub>2</sub> production in a microbial electrolysis cell. *Int J Hydrogen Energy* 35:12716–12723. doi: 10.1016/j.ijhydene.2010.08.131
77. Nam J-Y, Tokash JC, Logan BE (2011) Comparison of microbial electrolysis cells operated with added voltage or by setting the anode potential. *Int J Hydrogen Energy* 36:10550–10556. doi: 10.1016/j.ijhydene.2011.05.148
78. Cheng S, Logan BE (2011) High hydrogen production rate of microbial electrolysis cell (MEC) with reduced electrode spacing. *Bioresour Technol* 102:3571–4. doi: 10.1016/j.biortech.2010.10.025
79. Sleutels THJ a., Heijne A Ter, Buisman CJN, Hamelers HVM (2013) Steady-state performance and chemical efficiency of Microbial Electrolysis Cells. *Int J Hydrogen Energy* 38:7201–7208. doi: 10.1016/j.ijhydene.2013.04.067
80. Heidrich ES, Edwards SR, Dolfig J, et al (2014) Performance of a pilot scale microbial electrolysis cell fed on domestic wastewater at ambient temperatures for a 12 month period. *Bioresour Technol* 173:87–95. doi: 10.1016/j.biortech.2014.09.083
81. Montpart N, Rago L, Baeza JA, Guisasaola A (2015) Hydrogen production in single chamber microbial electrolysis cells with different complex substrates. *Water Res* 68:601–615. doi: 10.1016/j.watres.2014.10.026
82. Sosa-Hernández O, Papat SC, Parameswaran P, et al (2016) Application of microbial electrolysis cells to treat spent yeast from an alcoholic fermentation. *Bioresour Technol* 200:342–349. doi: 10.1016/j.biortech.2015.10.053
83. Rozendal R a., Jeremiassé AW, Hamelers HVM, Buisman CJN (2008) Hydrogen Production with a Microbial Biocathode. *Environ Sci Technol* 42:629–634. doi: 10.1021/es071720+
84. Jeremiassé AW, Hamelers HVM, Croese E, Buisman CJN (2012) Acetate enhances startup of a H<sub>2</sub> producing microbial biocathode. *Biotechnol Bioeng* 109:657–64. doi: 10.1002/bit.24338
85. Marshall CW, Ross DE, Fichot EB, et al (2013) Long-term operation of microbial electrosynthesis systems improves acetate production by autotrophic microbiomes. *Environ Sci Technol* 47:6023–9. doi: 10.1021/es400341b
86. Fu Q, Kobayashi H, Kuramochi Y, et al (2013) Bioelectrochemical analyses of a thermophilic biocathode catalyzing sustainable hydrogen production. *Int J Hydrogen Energy* 38:15638–15645. doi: 10.1016/j.ijhydene.2013.04.116
87. Jourdin L, Freguía S, Donose BC, Keller J (2015) Autotrophic hydrogen-producing biofilm growth sustained by a cathode as the sole electron and energy source. *Bioelectrochemistry* 102:56–63. doi: 10.1016/j.bioelechem.2014.12.001
88. Chen Y, Xu Y, Chen L, et al (2015) Microbial electrolysis cells with polyaniline/multi-walled carbon nanotube-modified biocathodes. *Energy* 88:377–384. doi: 10.1016/j.energy.2015.05.057
-

- 
89. Marshall CW, Ross DE, Fichot EB, et al (2012) Electrosynthesis of commodity chemicals by an autotrophic microbial community. *Appl Environ Microbiol* 78:8412–20. doi: 10.1128/AEM.02401-12
  90. Mohanakrishna G, Seelam JS, Vanbroekhoven K, Pant D (2015) An enriched electroactive homoacetogenic biocathode for the microbial electrosynthesis of acetate through carbon dioxide reduction. *Faraday Discuss.* doi: 10.1039/C5FD00041F
  91. Bajracharya S, ter Heijne A, Dominguez X, et al (2015) CO<sub>2</sub> reduction by mixed and pure cultures in microbial electrosynthesis using an assembly of graphite felt and stainless steel as a cathode. *Bioresour Technol.* doi: 10.1016/j.biortech.2015.05.081
  92. Desloover J, Arends JB a, Hennebel T, Rabaey K (2012) Operational and technical considerations for microbial electrosynthesis. *Biochem Soc Trans* 40:1233–8. doi: 10.1042/BST20120111
  93. Davis JB, Yarbrough HF (1962) Preliminary Experiments on a Microbial Fuel Cell. *Science (80- )* 137:615–616.
  94. Ieropoulos I, Greenman J, Melhuish C (2008) Microbial fuel cells based on carbon veil electrodes: Stack configuration and scalability. *Int J Energy Res* 32:1228–1240. doi: 10.1002/er.1419
  95. Minteer SD, Liaw BY, Cooney MJ (2007) Enzyme-based biofuel cells. *Curr Opin Biotechnol* 18:228–34. doi: 10.1016/j.copbio.2007.03.007
  96. Palmore R. G, Tayhas, Whitesides M. G, et al (1994) Microbial and Enzymatic Biofuel Cells. *Enzym Convers Biomass Fuels Prod* 271–290. doi: 10.1021/bk-1994-0566.ch014
  97. Zafar MN, Beden N, Leech D, et al (2012) Characterization of different FAD-dependent glucose dehydrogenases for possible use in glucose-based biosensors and biofuel cells. *Anal Bioanal Chem* 402:2069–77. doi: 10.1007/s00216-011-5650-7
  98. Yakushi T, Matsushita K (2010) Alcohol dehydrogenase of acetic acid bacteria: structure, mode of action, and applications in biotechnology. *Appl Microbiol Biotechnol* 86:1257–65.
  99. Barton SC, Gallaway J, Atanassov P, et al (2004) Enzymatic biofuel cells for implantable and microscale devices. *Chem Rev* 104:4867–86. doi: 10.1021/cr020719k
  100. Gellert W, Kesmez M, Schumacher J, et al (2010) Biofuel Cells for Portable Power. *Electroanalysis* 22:727–731.
  101. Kamitaka Y, Tsujimura S, Setoyama N, et al (2007) Fructose/dioxygen biofuel cell based on direct electron transfer-type bioelectrocatalysis. *Phys chem chem phys* 9:1793–801. doi: 10.1039/b617650j
  102. ElMekawy A, Hegab HM, Pant D (2014) The near-future integration of microbial desalination cells with reverse osmosis technology. *Energy Environ Sci* 7:3921–3933. doi: 10.1039/C4EE02208D
  103. Strik DPBTB, Timmers R a, Helder M, et al (2011) Microbial solar cells: applying photosynthetic and electrochemically active organisms. *Trends Biotechnol* 29:41–9. doi: 10.1016/j.tibtech.2010.10.001
  104. Wang H, Liu D, Lu L, et al (2012) Degradation of algal organic matter using microbial fuel cells and its association with trihalomethane precursor removal. *Bioresour Technol* 116:80–5.
  105. De Schampelaire L, Verstraete W (2009) Revival of the biological sunlight-to-biogas energy conversion system. *Biotechnol Bioeng* 103:296–304. doi: 10.1002/bit.22257
  106. Madiraju KS, Lyew D, Kok R, Raghavan V (2012) Carbon neutral electricity production by *Synechocystis* sp. PCC6803 in a microbial fuel cell. *Bioresour Technol* 110:214–8. doi: 10.1016/j.biortech.2012.01.065
  107. Strik DPBTB, Terlouw H, Hamelers HVM, Buisman CJN (2008) Renewable sustainable biocatalyzed electricity production in a photosynthetic algal microbial fuel cell (PAMFC). *Appl Microbiol Biotechnol* 81:659–68. doi: 10.1007/s00253-008-1679-8
  108. Strik DPBTB, Bert HVMH, Snel JFH, Buisman CJN (2008) Green electricity production with living plants and bacteria in a fuel cell. *Int J Energy Res.* doi: 10.1002/er
  109. De Schampelaire L, Cabezas A, Marzorati M, et al (2010) Microbial community analysis of anodes from sediment microbial fuel cells powered by rhizodeposits of living rice plants. *Appl Environ Microbiol* 76:2002–8.
  110. Helder M, Strik DP, Hamelers HV, Buisman CJ (2012) The flat-plate plant-microbial fuel cell: the effect of a new design on internal resistances. *Biotechnol Biofuels* 5:70. doi: 10.1186/1754-6834-5-70
  111. Wetsler K, Sudirjo E, Buisman CJN, Strik DPBTB (2015) Electricity generation by a plant microbial fuel cell with an integrated oxygen reducing biocathode. *Appl Energy* 137:151–157. doi: 10.1016/j.apenergy.2014.10.006
  112. Timmers R a, Strik DPBTB, Arampatzoglou C, et al (2012) Rhizosphere anode model explains high oxygen levels during operation of a *Glyceria maxima* PMFC. *Bioresour Technol* 108:60–7.
  113. Luo H, Xu P, Roane TM, et al (2012) Microbial desalination cells for improved performance in wastewater treatment, electricity production, and desalination. *Bioresour Technol* 105:60–6. doi: 10.1016/j.biortech.2011.11.098
-



- 
114. Luo H, Jenkins PE, Ren Z (2011) Concurrent Desalination and Hydrogen Generation Using Microbial Electrolysis and Desalination Cells. *Environ Sci Technol* 45:340–344. doi: 10.1021/es1022202
  115. Jacobson KS, Drew DM, He Z (2011) Use of a Liter-Scale Microbial Desalination Cell As a Platform to Study Bioelectrochemical Desalination with Salt Solution or Artificial Seawater. *Environ Sci Technol* 45:4652–4657. doi: 10.1021/es200127p
  116. Mehanna M, Kiely PD, Call DF, Logan BE (2010) Microbial Electrodesalination Cell for Simultaneous Water Desalination and Hydrogen Gas Production. *Environ Sci Technol* 44:9578–9583. doi: 10.1021/es1025646
  117. Pandey P, Shinde VN, Deopurkar RL, et al (2016) Recent advances in the use of different substrates in microbial fuel cells toward wastewater treatment and simultaneous energy recovery. *Appl Energy* 168:706–723. doi: 10.1016/j.apenergy.2016.01.056
  118. McCarty PL, Bae J, Kim J (2011) Domestic wastewater treatment as a net energy producer--can this be achieved? *Environ Sci Technol* 45:7100–6. doi: 10.1021/es2014264
  119. Logan BE, Rabaey K (2012) Conversion of wastes into bioelectricity and chemicals by using microbial electrochemical technologies. *Science* 337:686–90. doi: 10.1126/science.1217412
  120. Hays S, Zhang F, Logan BE (2011) Performance of two different types of anodes in membrane electrode assembly microbial fuel cells for power generation from domestic wastewater. *J Power Sources* 196:8293–8300. doi: 10.1016/j.jpowsour.2011.06.027
  121. Fornero JJ, Rosenbaum M, Angenent LT (2010) Electric Power Generation from Municipal, Food, and Animal Wastewaters Using Microbial Fuel Cells. *Electroanalysis* 22:832–843. doi: 10.1002/elan.200980011
  122. Cusick RD, Kiely PD, Logan BE (2010) A monetary comparison of energy recovered from microbial fuel cells and microbial electrolysis cells fed winery or domestic wastewaters. *Int J Hydrogen Energy* 35:8855–8861. doi: 10.1016/j.ijhydene.2010.06.077
  123. Van der Zee FP (2002) Anaerobic azo dye reduction. Wageningen University
  124. Mu Y, Rabaey K, Rozendal RA, et al (2009) Decolorization of Azo Dyes in Bioelectrochemical Systems. *Environ Sci Technol* 43:5137–5143. doi: 10.1021/es900057f
  125. Selvam K, Swaminathan K, Chae K-S (2003) Microbial decolorization of azo dyes and dye industry effluent by *Fomes lividus*. *World J Microbiol Biotechnol* 19:591–593.
  126. Umbuzeiro G de A, Freeman HS, Warren SH, et al (2005) The contribution of azo dyes to the mutagenic activity of the Cristais River. *Chemosphere* 60:55–64.
  127. Colindres P, Yee-Madeira H, Reguera E (2010) Removal of Reactive Black 5 from aqueous solution by ozone for water reuse in textile dyeing processes. *Desalination* 258:154–158.
  128. Marcucci M, Ciardelli G, Matteucci A, et al (2002) Experimental campaigns on textile wastewater for reuse by means of different membrane processes. *Desalination* 149:137–143.
  129. Naresh Kumar A, Nagendranatha Reddy C, Venkata Mohan S (2015) Biomineralization of azo dye bearing wastewater in periodic discontinuous batch reactor: Effect of microaerophilic conditions on treatment efficiency. *Bioresour Technol* 188:56–64. doi: 10.1016/j.biortech.2015.01.098
  130. Cui D, Kong F-Y, Liang B, et al (2011) Decolorization of Azo dyes in dual-chamber biocatalyzed electrolysis systems seeding with enriched inoculum. *J. Environ. Anal. Toxicol.* S3:001:
  131. Sun J, Hu Y, Bi Z, Cao Y (2009) Simultaneous decolorization of azo dye and bioelectricity generation using a microfiltration membrane air-cathode single-chamber microbial fuel cell. *Bioresour Technol* 100:3185–3192.
  132. van der Zee FP, Bisschops IAE, Lettinga G, Field JA (2002) Activated Carbon as an Electron Acceptor and Redox Mediator during the Anaerobic Biotransformation of Azo Dyes. *Environ Sci Technol* 37:402–408.
  133. Lovley DR (2001) Anaerobes to the Rescue. *Science* (80- ) 293:1444–1446.
  134. Seshadri R, Adrian L, Fouts DE, et al (2005) Genome sequence of the PCE-dechlorinating bacterium *Dehalococcoides ethenogenes*. *Science* 307:105–8. doi: 10.1126/science.1102226
  135. DiStefano TD, Gossett JM, Zinder SH (1991) Reductive dechlorination of high concentrations of tetrachloroethene to ethene by an anaerobic enrichment culture in the absence of methanogenesis. *Appl Environ Microbiol* 57:2287–2292.
  136. Löffler Sun, Qing, Li, Jieran, Tiedje, James M. FE (2000) 16S rRNA Gene-Based Detection of Tetrachloroethene-Dechlorinating *Desulfuromonas* and *Dehalococcoides* Species. *Appl Environ Microbiol* 66:1369–1374.
  137. Yang Y, McCarty PL (1998) Competition for Hydrogen within a Chlorinated Solvent Dehalogenating Anaerobic Mixed Culture. *Environ Sci Technol* 32:3591–3597.
-

- 
138. He J, Sung Y, Dollhopf ME, et al (2002) Acetate versus Hydrogen as Direct Electron Donors To Stimulate the Microbial Reductive Dechlorination Process at Chloroethene-Contaminated Sites†. *Environ Sci Technol* 36:3945–3952.
  139. Aulenta F, Canosa A, Reale P, et al (2009) Microbial reductive dechlorination of trichloroethene to ethene with electrodes serving as electron donors without the external addition of redox mediators. *Biotechnol Bioeng* 103:85–91.
  140. Strycharz SM, Woodard TL, Johnson JP, et al (2008) Graphite electrode as a sole electron donor for reductive dechlorination of tetrachloroethene by *Geobacter lovleyi*. *Appl Environ Microbiol* 74:5943–7. doi: 10.1128/AEM.00961-08
  141. Aulenta F, Tocca L, Verdini R, et al (2011) Dechlorination of Trichloroethene in a Continuous-Flow Bioelectrochemical Reactor: Effect of Cathode Potential on Rate, Selectivity, and Electron Transfer Mechanisms. *Environ Sci Technol* 45:8444–8451. doi: 10.1021/es202262y
  142. Huang L, Cheng S, Chen G (2011) Bioelectrochemical systems for efficient recalcitrant wastes treatment. *J Chem Technol Biotechnol* 86:481–491. doi: 10.1002/jctb.2551
  143. Aulenta F, Catervi A, Majone M, et al (2007) Electron transfer from a solid-state electrode assisted by methyl viologen sustains efficient microbial reductive dechlorination of TCE. *Environ Sci Technol* 41:2554–9.
  144. Strycharz SM, Woodard TL, Johnson JP, et al (2008) Graphite electrode as a sole electron donor for reductive dechlorination of tetrachloroethene by *Geobacter lovleyi*. *Appl Environ Microbiol* 74:5943–5947.
  145. Aulenta F, Reale P, Canosa A, et al (2010) Characterization of an electro-active biocathode capable of dechlorinating trichloroethene and cis-dichloroethene to ethene. *Biosens Bioelectron* 25:1796–802. doi: 10.1016/j.bios.2009.12.033
  146. Gu H, Zhang X, Li Z, Lei L (2007) Studies on treatment of chlorophenol-containing wastewater by microbial fuel cell. *Chinese Sci Bull* 52:3448–3451. doi: 10.1007/s11434-007-0503-7
  147. Pham H, Boon N, Marzorati M, Verstraete W (2009) Enhanced removal of 1,2-dichloroethane by anodophilic microbial consortia. *Water Res* 43:2936–46. doi: 10.1016/j.watres.2009.04.004
  148. Strycharz SM, Gannon SM, Boles AR, et al (2010) Reductive dechlorination of 2-chlorophenol by *Anaeromyxobacter dehalogenans* with an electrode serving as the electron donor. *Environ Microbiol Rep* 2:289–94. doi: 10.1111/j.1758-2229.2009.00118.x
  149. Zhao F, Rahunen N, Varcoe JR, et al (2008) Activated carbon cloth as anode for sulfate removal in a microbial fuel cell. *Environ Sci Technol* 42:4971–6. doi: 10.1021/es8003766
  150. Habermann W, Pommer EH (1991) Biological fuel cells with sulphide storage capacity. *Appl Microbiol Biotechnol* 35:128–133. doi: 10.1007/bf00180650
  151. Rabaey K, Van de Sompel K, Maignien L, et al (2006) Microbial Fuel Cells for Sulfide Removal†. *Environ Sci Technol* 40:5218–5224.
  152. Cooney MJ, Svoboda V, Lau C, et al (2008) Enzyme catalysed biofuel cells. *Energy Environ Sci* 1:320.
  153. Wang G, Huang L, Zhang Y (2008) Cathodic reduction of hexavalent chromium [Cr(VI)] coupled with electricity generation in microbial fuel cells. *Biotechnol Lett* 30:1959–1966.
  154. Tandukar M, Huber SJ, Onodera T, Pavlostathis SG (2009) Biological Chromium(VI) Reduction in the Cathode of a Microbial Fuel Cell. *Environ Sci Technol* 43:8159–8165.
  155. Chen JM, Hao OJ (1998) Microbial Chromium (VI) Reduction. *Crit Rev Environ Sci Technol* 28:219–251.
  156. Liu L, Yuan Y, Li F, Feng C (2011) In-situ Cr(VI) reduction with electrogenerated hydrogen peroxide driven by iron-reducing bacteria. *Bioresour Technol* 102:2468–2473.
  157. Huang L, Chai X, Cheng S, Chen G (2011) Evaluation of carbon-based materials in tubular biocathode microbial fuel cells in terms of hexavalent chromium reduction and electricity generation. *Chem Eng J* 166:652–661.
  158. Hamelers HVM, Ter Heijne A, Sleutels THJ a, et al (2010) New applications and performance of bioelectrochemical systems. *Appl Microbiol Biotechnol* 85:1673–85. doi: 10.1007/s00253-009-2357-1
  159. Heijne A Ter, Liu F, Weijden R Van Der, et al (2010) Copper recovery combined with electricity production in a microbial fuel cell. *Environ Sci Technol* 44:4376–81. doi: 10.1021/es100526g
  160. Modin O, Wang X, Wu X, et al (2012) Bioelectrochemical recovery of Cu, Pb, Cd, and Zn from dilute solutions. *J Hazard Mater* 235–236:291–7. doi: 10.1016/j.jhazmat.2012.07.058
  161. Zhang B, Feng C, Ni J, et al (2012) Simultaneous reduction of vanadium (V) and chromium (VI) with enhanced energy recovery based on microbial fuel cell technology. *J Power Sources* 204:34–39. doi: <http://dx.doi.org/10.1016/j.jpowsour.2012.01.013>
  162. Zhang L-J, Tao H-C, Wei X-Y, et al (2012) Bioelectrochemical recovery of ammonia–copper(II)
-

- 
- complexes from wastewater using a dual chamber microbial fuel cell. *Chemosphere* 89:1177–1182. doi: <http://dx.doi.org/10.1016/j.chemosphere.2012.08.011>
163. Kuntke P, Śmiech KM, Bruning H, et al (2012) Ammonium recovery and energy production from urine by a microbial fuel cell. *Water Res* 46:2627–2636.
164. Rozendal RA, Hamelers HVM, Molenkamp RJ, Buisman CJN (2007) Performance of single chamber biocatalyzed electrolysis with different types of ion exchange membranes. *Water Res* 41:1984–94. doi: [10.1016/j.watres.2007.01.019](http://dx.doi.org/10.1016/j.watres.2007.01.019)
165. Venkata Mohan S, Lenin Babu M, Venkateswar Reddy M, et al (2009) Harnessing of biohydrogen by acidogenic fermentation of Citrus limetta peelings: Effect of extraction procedure and pretreatment of biocatalyst. *Int J Hydrogen Energy* 34:6149–6156. doi: <http://dx.doi.org/10.1016/j.ijhydene.2009.05.056>
166. Mohan SV, Chiranjeevi P, Mohanakrishna G (2012) A rapid and simple protocol for evaluating biohydrogen production potential (BHP) of wastewater with simultaneous process optimization. *Int J Hydrogen Energy* 37:3130–3141. doi: <http://dx.doi.org/10.1016/j.ijhydene.2011.10.109>
167. Logan BE (2004) Peer Reviewed: Extracting Hydrogen and Electricity from Renewable Resources. *Environ Sci Technol* 38:160A–167A. doi: [10.1021/es040468s](http://dx.doi.org/10.1021/es040468s)
168. Pasupuleti SB, Srikanth S, Venkata Mohan S, Pant D (2015) Development of exoelectrogenic bioanode and study on feasibility of hydrogen production using abiotic VITO-CoRE™ and VITO-CASE™ electrodes in a single chamber microbial electrolysis cell (MEC) at low current densities. *Bioresour Technol* 195:131–138. doi: <http://dx.doi.org/10.1016/j.biortech.2015.06.145>
169. R.A. Rozendal, Buisman CJ. (2005) Bio-Electrochemical Process for Producing Hydrogen. Pat. WO/2005/005981
170. Rozendal RA, Harnisch F, Jeremiassi AW, Schroder U (2010) Chemically catalyzed cathodes in bioelectrochemical systems. In: *Bioelectrochemical Syst. from Extracell. electron Transf. to Biotechnol. Appl.* IWA Publishing, London, UK, pp 263–284
171. Logan BE, Hamelers B, Rozendal R, et al (2006) Microbial Fuel Cells: Methodology and Technology†. *Environ Sci Technol* 40:5181–5192.
172. Hu H, Fan Y, Liu H (2009) Hydrogen production in single-chamber tubular microbial electrolysis cells using non-precious-metal catalysts. *Int J Hydrogen Energy* 34:8535–8542. doi: <http://dx.doi.org/10.1016/j.ijhydene.2009.08.011>
173. Manuel M-F, Neburchilov V, Wang H, et al (2010) Hydrogen production in a microbial electrolysis cell with nickel-based gas diffusion cathodes. *J Power Sources* 195:5514–5519. doi: <http://dx.doi.org/10.1016/j.jpowsour.2010.03.061>
174. Selembo PA, Merrill MD, Logan BE (2009) The use of stainless steel and nickel alloys as low-cost cathodes in microbial electrolysis cells. *J Power Sources* 190:271–278. doi: [10.1016/j.jpowsour.2008.12.144](http://dx.doi.org/10.1016/j.jpowsour.2008.12.144)
175. Selembo PA, Merrill MD, Logan BE (2010) Hydrogen production with nickel powder cathode catalysts in microbial electrolysis cells. *Int J Hydrogen Energy* 35:428–437. doi: <http://dx.doi.org/10.1016/j.ijhydene.2009.11.014>
176. Hu H, Fan Y, Liu H (2010) Optimization of NiMo catalyst for hydrogen production in microbial electrolysis cells. *Int J Hydrogen Energy* 35:3227–3233. doi: <http://dx.doi.org/10.1016/j.ijhydene.2010.01.131>
177. Carmona-Martínez AA, Trably E, Milferstedt K, et al (2015) Long-term continuous production of H<sub>2</sub> in a microbial electrolysis cell (MEC) treating saline wastewater. *Water Res* 81:149–156. doi: <http://dx.doi.org/10.1016/j.watres.2015.05.041>
178. Nevin KP, Hensley SA, Franks AE, et al (2011) Electrosynthesis of organic compounds from carbon dioxide is catalyzed by a diversity of acetogenic microorganisms. *Appl Environ Microbiol* 77:2882–6. doi: [10.1128/AEM.02642-10](http://dx.doi.org/10.1128/AEM.02642-10)
179. Gong Y, Ebrahim A, Feist AM, et al (2013) Sulfide-driven microbial electrosynthesis. *Environ Sci Technol* 47:568–73. doi: [10.1021/es303837j](http://dx.doi.org/10.1021/es303837j)
180. Marshall CW, LaBelle E V, May HD (2013) Production of fuels and chemicals from waste by microbiomes. *Curr Opin Biotechnol* 24:1–7. doi: [10.1016/j.copbio.2013.03.016](http://dx.doi.org/10.1016/j.copbio.2013.03.016)
181. Jiang Y, Su M, Zhang Y, et al (2013) Bioelectrochemical systems for simultaneously production of methane and acetate from carbon dioxide at relatively high rate. *Int J Hydrogen Energy* 38:3497–3502. doi: [10.1016/j.ijhydene.2012.12.107](http://dx.doi.org/10.1016/j.ijhydene.2012.12.107)
182. Battle-Vilanova P, Puig S, Gonzalez-Olmos R, et al (2015) Continuous acetate production through microbial electrosynthesis from CO<sub>2</sub> with microbial mixed culture. *J Chem Technol Biotechnol* n/a–n/a. doi: [10.1002/jctb.4657](http://dx.doi.org/10.1002/jctb.4657)
183. Wagner RC, Regan JM, Oh S-E, et al (2009) Hydrogen and methane production from swine wastewater
-

- 
- using microbial electrolysis cells. *Water Res* 43:1480–8. doi: 10.1016/j.watres.2008.12.037
184. Clauwaert P, Verstraete W (2009) Methanogenesis in membraneless microbial electrolysis cells. *Appl Microbiol Biotechnol* 82:829–836. doi: 10.1007/s00253-008-1796-4
185. Sasaki K, Hirano S, Morita M, et al (2011) Bioelectrochemical system accelerates microbial growth and degradation of filter paper. *Appl Microbiol Biotechnol* 89:449–455. doi: 10.1007/s00253-010-2972-x
186. Rader GK, Logan BE (2010) Multi-electrode continuous flow microbial electrolysis cell for biogas production from acetate. *Int J Hydrogen Energy* 35:8848–8854. doi: 10.1016/j.ijhydene.2010.06.033
187. Cheng KY, Ho G, Cord-Ruwisch R (2011) Novel methanogenic rotatable bioelectrochemical system operated with polarity inversion. *Environ Sci Technol* 45:796–802. doi: 10.1021/es102482j
188. Villano M, Monaco G, Aulenta F, Majone M (2011) Electrochemically assisted methane production in a biofilm reactor. *J Power Sources* 196:9467–9472. doi: 10.1016/j.jpowsour.2011.07.016
189. Villano M, Aulenta F, Ciucci C, et al (2010) Bioelectrochemical reduction of CO<sub>2</sub> to CH<sub>4</sub> via direct and indirect extracellular electron transfer by a hydrogenophilic methanogenic culture. *Bioresour Technol* 101:3085–90. doi: 10.1016/j.biortech.2009.12.077
190. Rabaey K, Bützer S, Brown S, et al (2010) High current generation coupled to caustic production using a lamellar bioelectrochemical system. *Environ Sci Technol* 44:4315–21. doi: 10.1021/es9037963
191. Azuma M, Watanabe M (1990) Electrochemical Reduction of Carbon Dioxide on Various Metal Electrodes in Low-Temperature Aqueous KHC<sub>3</sub> Media. *J Electrochem Soc* 137:1772–1778.
192. Steinbusch KJJ, Hamelers HVM, Schaap JD, et al (2010) Bioelectrochemical ethanol production through mediated acetate reduction by mixed cultures. *Environ Sci Technol* 44:513–7. doi: 10.1021/es902371e
193. Srikanth S, Maesen M, Dominguez-Benetton X, et al (2014) Enzymatic electrosynthesis of formate through CO<sub>2</sub> sequestration/reduction in a bioelectrochemical system (BES). *Bioresour Technol* 165:350–4. doi: 10.1016/j.biortech.2014.01.129
194. Li H, Opgenorth PH, Wernick DG, et al (2012) Integrated electromicrobial conversion of CO<sub>2</sub> to higher alcohols. *Science* 335:1596. doi: 10.1126/science.1217643
195. Nybo SE, Khan NE, Woolston BM, Curtis WR (2015) Metabolic engineering in chemolithoautotrophic hosts for the production of fuels and chemicals. *Metab Eng* 30:105–120. doi: <http://dx.doi.org/10.1016/j.ymben.2015.04.008>
196. Xafenias N, Anunobi MO, Mapelli V (2015) Electrochemical startup increases 1,3-propanediol titers in mixed-culture glycerol fermentations. *Process Biochem* 50:1499–1508. doi: <http://dx.doi.org/10.1016/j.procbio.2015.06.020>
197. Ganigué R, Puig S, Batlle-Vilanova P, et al (2015) Microbial electrosynthesis of butyrate from carbon dioxide. *Chem Commun* 51:3235–3238. doi: 10.1039/C4CC10121A
198. Chang IS, Jang JK, Gil GC, et al (2004) Continuous determination of biochemical oxygen demand using microbial fuel cell type biosensor. *Biosens Bioelectron* 19:607–613. doi: 10.1016/S0956-5663(03)00272-0
199. Chang IS, Moon H, Jang JK, Kim BH (2005) Improvement of a microbial fuel cell performance as a BOD sensor using respiratory inhibitors. *Biosens Bioelectron* 20:1856–1859. doi: <http://dx.doi.org/10.1016/j.bios.2004.06.003>
200. Di Lorenzo M, Thomson AR, Schneider K, et al (2014) A small-scale air-cathode microbial fuel cell for on-line monitoring of water quality. *Biosens Bioelectron* 62:182–8. doi: 10.1016/j.bios.2014.06.050
201. Su L, Jia W, Hou C, Lei Y (2011) Microbial biosensors: a review. *Biosens Bioelectron* 26:1788–99. doi: 10.1016/j.bios.2010.09.005
202. Kim BH, Chang IS, Gil GC, et al (2003) Novel BOD (biological oxygen demand) sensor using mediator-less microbial fuel cell. *Biotechnol Lett* 25:541–545. doi: 10.1023/A:1022891231369
203. Zhang Y, Angelidaki I (2011) Submersible microbial fuel cell sensor for monitoring microbial activity and BOD in groundwater: focusing on impact of anodic biofilm on sensor applicability. *Biotechnol Bioeng* 108:2339–47. doi: 10.1002/bit.23204
204. Kim M, Sik Hyun M, Gadd GM, Joo Kim H (2007) A novel biomonitoring system using microbial fuel cells. *J Environ Monit* 9:1323–1328. doi: 10.1039/B713114C
205. Stein NE, Hamelers HVM, van Straten G, Keesman KJ (2012) Effect of Toxic Components on Microbial Fuel Cell-Polarization Curves and Estimation of the Type of Toxic Inhibition. *Biosensors* 2:255–268.
206. Stein NE, Hamelers HVM, Buisman CNJ (2012) The effect of different control mechanisms on the sensitivity and recovery time of a microbial fuel cell based biosensor. *Sensors Actuators B Chem* 171–172:816–821.
207. Stein NE, Hamelers HVM, Buisman CNJ (2010) Stabilizing the baseline current of a microbial fuel cell-based biosensor through overpotential control under non-toxic conditions. *Bioelectrochemistry* 78:87–
-

91. doi: 10.1016/j.bioelechem.2009.09.009
208. Dávila D, Esquivel JP, Sabaté N, Mas J (2011) Silicon-based microfabricated microbial fuel cell toxicity sensor. *Biosens Bioelectron* 26:2426–30. doi: 10.1016/j.bios.2010.10.025
209. Liu B, Lei Y, Li B (2014) A batch-mode cube microbial fuel cell based “shock” biosensor for wastewater quality monitoring. *Biosens Bioelectron* 62:308–14. doi: 10.1016/j.bios.2014.06.051
210. D’Souza SF (2001) Microbial biosensors. *Biosens Bioelectron* 16:337–353. doi: 10.1016/S0956-5663(01)00125-7
211. Escapa a., Gómez X, Tartakovsky B, Morán a. (2012) Estimating microbial electrolysis cell (MEC) investment costs in wastewater treatment plants: Case study. *Int J Hydrogen Energy* 37:18641–18653. doi: 10.1016/j.ijhydene.2012.09.157



---

C  
H  
A  
P  
T  
E  
R



7

**Syntheses, discussion and perspectives**

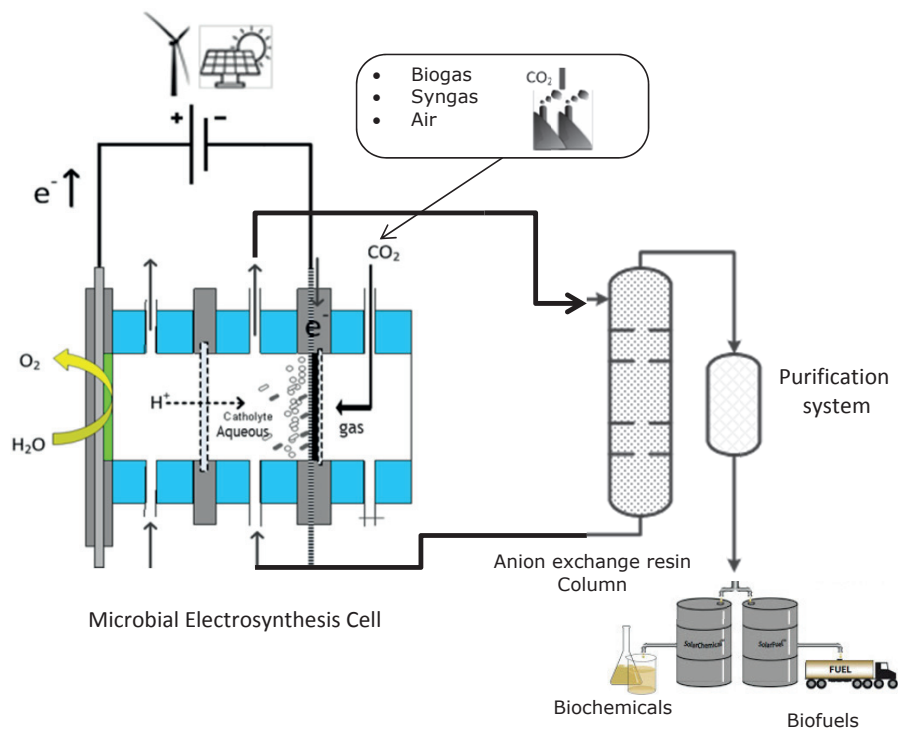
---

This thesis aims to bring insight on the process of microbial electrosynthesis from CO<sub>2</sub> toward the synthesis of platform biochemicals at high concentration by using mixed microbial culture. It sought to innovate the electricity-driven bioproduction system comprising production and extraction of chemical via the modification in CO<sub>2</sub> feeding, biocatalyst, electrode and ion-exchange. In this Chapter, the main outcomes of electricity-driven bioproduction from CO<sub>2</sub> are synthesized based on the results obtained and advancement made in this thesis. The adjustments made on electrode for CO<sub>2</sub> supply and product extraction are envisioned for future applications. The understanding of the process, performance and limiting parameters are discussed further for the comparisons and analyses.

### ***The envisioned integrated microbial electrosynthesis from CO<sub>2</sub>***

Developments reported in recent literature [1, 2] and this thesis have revealed encouraging improvements in the production rates of biochemicals in MES via enhanced microbial electrocatalysis using suitable biocatalysts and electrodes. Indeed, biocompatible electrodes can further boost the process. Thus, the incorporation of surface modified gas diffusion biocathode with enriched biocatalyst will support MES on the technological ground as a realistic and competitive technology for electricity-driven bioproduction. Indeed, integration of product extraction and recovery of the biofuel/biochemicals from CO<sub>2</sub> would establish it as a completely sustainable bioproduction system. This thesis has envisioned MES system from CO<sub>2</sub> into a complete bioproduction system as represented in Figure 7.1. In this context, the developments and insights obtained with this thesis and the practical implementation of MES technology, prospective and scenarios are presented in the following sections based on the CO<sub>2</sub> source, process improvement and product valorization.

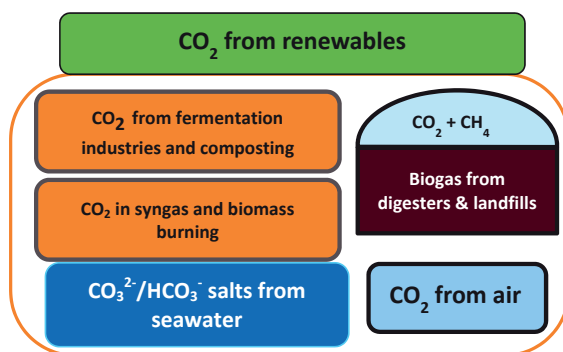




**Figure 7.1:** Envisioned MES system from CO<sub>2</sub> biorefinery based on this thesis.

### CO<sub>2</sub> sources are readily available to produce biochemicals

A crucial concern for the real application of CO<sub>2</sub> based MES technology is the source of CO<sub>2</sub>. i.e. what is/are the appropriate CO<sub>2</sub> source(s) for MES? CO<sub>2</sub> is abundantly available from its natural carbon cycle. CO<sub>2</sub> is also of concern due to its global warming potential as part of anthropogenic activities predominantly related to fossil fuel combustion, industrial pollution and land-use changes. Several point sources/off-gas streams of CO<sub>2</sub> are available for direct utilization and conversion, namely power plants, steel industries and cement production and fermentation processes [3]. At the present trend of growing utilization of renewable energy and resources, various stationary sources of renewable CO<sub>2</sub> emission are available originating from biomass combustion and processes in agriculture/food/biochemical based industries. The sources of CO<sub>2</sub> from renewables are as represented in Figure 7.2. Biogas from anaerobic digesters or from landfill sites and/or CO<sub>2</sub> from other industrial fermentation processes are readily available options of CO<sub>2</sub> sources in MES. Since these systems also employ biological/microbial catalysts (of which some are the same as those present in MES; e.g. in Chapter 2 also methanogens were present in the MES), it is very evident that CO<sub>2</sub> from such sources can be directly used in MES. This is furthermore supported by a number of studies in which the (bio)electrodes were directly introduced in fermentations [4]. Bicarbonate/carbonate salt from seawater source is also an option but the adaptability of microbial process in saline condition could be an issue to tackle. Still, electrochemically active bacteria are found even in extreme conditions which does warrant the development of novel bioelectrodes [5].



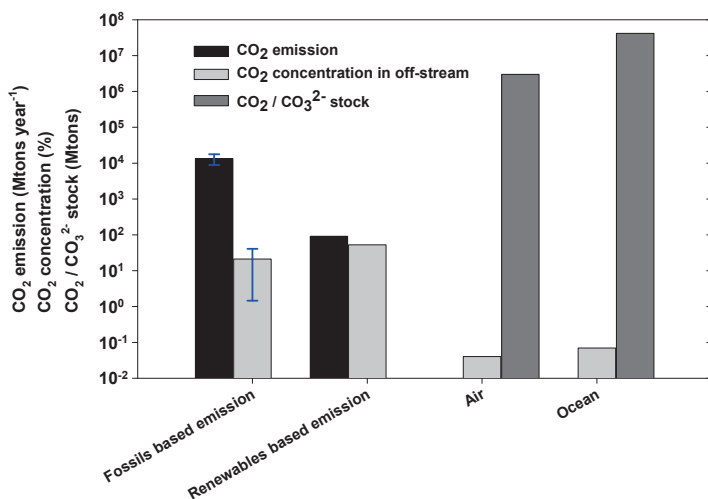
**Figure 7.2:** CO<sub>2</sub> from renewable sources.

Some point sources for CO<sub>2</sub> may on the first-sight not seem to be attractive for MES applications because of the energy requirements in pretreatment/purification of CO<sub>2</sub> from off-gas. Fossil fuel-fired power plants and steel industries emit a large amount of off-gases but only contains 10-20% of CO<sub>2</sub> whereas cement production emits relatively high concentration of CO<sub>2</sub> in the off-gas stream (almost 100%) [3]. The off-gas stream from the combustion of fossil fuels mostly contains other harmful gases or particles and the proportion of CO<sub>2</sub> is relatively low. Still, usage of a mixed microbial population at the biocathodes may be attractive for these off-gases (CO<sub>2</sub> reduction was achieved from only 20% CO<sub>2</sub> containing gas-mixture in MES in Chapter 3), while the microbial population can be robust in handling harmful components. For instance, it is well known that microorganisms can handle and degrade toxic compounds like volatile organic compounds (VOCs), hydrogen sulfide, hydrocyanic acid [6–8]. Other CO<sub>2</sub> to biochemical conversion technologies lack this ability. For example, electrochemical catalysts are easily inactivated by the pollutants in chemical syngas conversions [9, 10]. Furthermore, at the industrial sites where biochemicals are already produced, MES can produce drop-in chemicals from the exhaust CO<sub>2</sub>.

Based on the annual CO<sub>2</sub> emission data and CO<sub>2</sub> concentrations in the off-gases reported by IPCC [3], Figure 7.3 depicts an overview of CO<sub>2</sub> emissions and concentrations from fossil fuel combustion and from the biological processes based industrial emissions, in concert with the CO<sub>2</sub> stock in relatively perpetual CO<sub>2</sub>/carbonate sources. CO<sub>2</sub> emissions from biological processes including fermentation industries are renewable in origin and more interesting to utilize in the MES system or any other CO<sub>2</sub> utilization as the purity of CO<sub>2</sub> is high. The CO<sub>2</sub> utilization in MES also becomes independent of fossil fuels and the process becomes completely CO<sub>2</sub> neutral conceptually. Certainly, a complete life-cycle analysis (LCA) is required to assess such sustainability claims [11].

Atmospheric air is a constant source of CO<sub>2</sub> with a stock of approximately 3 million megatons of CO<sub>2</sub> and represents a potential carbon source for MES [12]. CO<sub>2</sub> concentration currently recorded at ca. 400 ppm (0.04% by volume) [13]. Due to the low concentrations of CO<sub>2</sub>, capture from air is challenging and highly energy intensive and indeed oxygen should be removed from the air before supplying to the anaerobic process. However, aerobic processes for CO<sub>2</sub> conversion have also been included in MES to produce precursors for bioplastics [14]. As such MES could also include oxygen reduction at the cathode. Oxygen-reducing biocathode has been extensively studied in microbial fuel cell [15, 16] but it is unknown whether the synthesis of biochemicals will be possible. Nevertheless, atmospheric air remains an anticipated CO<sub>2</sub> source since CO<sub>2</sub> capture from air provides a real 'GHG sink'. There are several techniques available and under development which capture CO<sub>2</sub> from air [17, 18]. These systems require significant

energy input (0.2 to 0.35 kWh kg<sup>-1</sup> of CO<sub>2</sub> capture from coal plant emission [19] and 2.3 kWh kg<sup>-1</sup> for CO<sub>2</sub> capture from the air [20]). With respect to the energy need in MES for CO<sub>2</sub> reduction [10 to 12 kWh kg<sup>-1</sup> CO<sub>2</sub> (calculated based on energy input mentioned in Chapter 4)], the energy required to capture CO<sub>2</sub> from the air is in the similar range of energy need during MES.



**Figure 7.3:** Overview of CO<sub>2</sub> sources and concentrations in the off-gas based on the figures provided in [3].

When CO<sub>2</sub> off-gas from non-renewables is converted to chemicals, CO<sub>2</sub> is captured only one-time and this concept keeps promoting fossil fuel usage. This concept does not comply with the circular economy concept. CO<sub>2</sub> utilization from fossil fuel's emission can be effective in the transitional stage from linear to the circular economy. To enable CO<sub>2</sub> neutral biochemical production, fossil resource independent economy is being promoted by the governments in countries. Off-gas from renewables such as biogas and fermentation processes would be more attractive for CO<sub>2</sub> utilization via MES which will reduce the CO<sub>2</sub> flux into the atmosphere and also provides biochemical/biofuel for further utilization. Off-gas CO<sub>2</sub> capture from non-renewable resources can also be used in transitional period to capture and store CO<sub>2</sub> in stable biochemicals. This approach is currently practiced by Lanza Tech using fermentation technology [21].

### **Scaling-up of Gas diffusion biocathode is needed to supply CO<sub>2</sub>**

CO<sub>2</sub> is available to the microorganisms in the MES reactor only in the dissolved form which is limited by the gas-liquid mass transfer when gaseous CO<sub>2</sub> is used. The first developed gas diffusing biocathode adapted from gas diffusion electrode (GDE) for microbial electrosynthesis has shown enhancement in the mass-transfer of gaseous substrates compared to the supply through conventional spargers in submerged electrode (Chapter 3). This study uniquely used a gas diffusion biocathode to provide CO<sub>2</sub> directly on the reaction site, creating a three phase (gas-liquid-electrode) interface. The mass transfer rate of CO<sub>2</sub> was found at least double than that with conventional gas sparging. Acetate production from bioelectrochemical CO<sub>2</sub> reduction was demonstrated and acetate production from CO<sub>2</sub> has been improved, accumulating to the concentration of ca. 2.5 g L<sup>-1</sup>. In comparison to the case in Chapter 2, in which cathode was submerged and bicarbonate solution was used keeping the rest of conditions similar, the acetate

production rate with GDE was improved by at least 2 times with 20% CO<sub>2</sub> gas mixture and 4 times with 80% CO<sub>2</sub> gas mixture. This shows that using CO<sub>2</sub> feedstock with higher concentrations do allow more effective use of the GDE. Ethanol fermentation produced a gas stream with typical high CO<sub>2</sub> concentration which would stimulate the performance compared to a dilute stream. The coulombic efficiency in the GDE MES was also improved by 1.5 times than achieved in Chapter 2. However, the coulombic efficiencies were still lower than those reported in similar studies using enriched mixed culture by Jourdin et al. [22] and Patil et al. [23]. CO<sub>2</sub> supply via GDE appeared to outweigh the production rates and titers of acetate than those obtained by using HCO<sub>3</sub><sup>-</sup> which could be most likely related to the acidifying effect of CO<sub>2</sub> on the cathode overpotentials and also on the microbial activity. Suitability of gas diffusion biocathodes in MES from dilute CO<sub>2</sub> waste streams (20 to 80%) was presented for the continuous operation with the efficient CO<sub>2</sub> mass transfer. Still, further studies are needed to confirm on the usage of GDEs with real CO<sub>2</sub> waste stream and also in the scaling-up of the electrodes.

### ***Robust biocathode without toxic inhibitors does warrant easier product separation***

An MES system with mixed culture from wastewater sources, reducing CO<sub>2</sub> at a graphite felt and stainless steel assembly cathode, was presented in Chapter 2. Bioelectrochemical reduction of CO<sub>2</sub> primarily produced acetate with electrochemically produced hydrogen serving as an energy source. Methane production, occurred when anaerobic mixed culture catalyzed CO<sub>2</sub> reduction, should be prevented in order to improve the production of other multi-carbon compounds. CH<sub>4</sub> production, in MES from CO<sub>2</sub>, was also reported in Marshall et al. [24] and Jiang et al. [25]. The volumetric productivities of acetate were relatively low in such MES systems [4 mM d<sup>-1</sup> [24] and 6.57 mM d<sup>-1</sup> [25] and 1.3 mM d<sup>-1</sup> in Chapter 2 ].

An establishment of active and stable biocatalyst at cathode was the main bottleneck for CO<sub>2</sub> reducing biocathode. The operation of MES using a wastewater originated mixed culture without methane production was another major objective. Indeed, the (desired) product yields and production rates should be maximized to make MES from CO<sub>2</sub> useful in terms of cost-benefit analysis. Production of valuable bioproducts at higher concentrations is targeted in order to lower the downstream processing costs. In this aspect, the main challenges are to develop the biocatalysts (microorganisms and enzymes) and electrodes to improve the production (process) rates and product titers of the targeted biochemicals.

Pre-treatment of the inoculum with heat-shock, selective enrichment and acclimation to CO<sub>2</sub> and H<sub>2</sub> resulted in a significant improvement of microbial electrosynthesis of acetate at -1 V<sub>/Ag/AgCl</sub>, with an acetate accumulation up to 8-13 g L<sup>-1</sup>. Acetate accumulation to such level was repeatedly observed in a number of batches. A maximum reduction current density of -10 A m<sup>-2</sup> sustained an acetate production rate of 400 mg L<sup>-1</sup> d<sup>-1</sup> with 60% coulombic efficiency (Chapter 4). Previously, a mixed-culture biocathode produced acetate at the maximum rate of 78 mg L<sup>-1</sup> d<sup>-1</sup> (0.6 g L<sup>-1</sup> accumulation), along with methane and hydrogen at -1.1 V<sub>/Ag/AgCl</sub> (Chapter 2). A stable electricity-driven autotrophic bioproduction system was demonstrated in a long-term operation of more than a year and remarkably, methane production was absent. Avoidance of methanogenic activity and accumulation of acetate to higher levels confirmed a fully adaptive biocathode for bioelectrochemical CO<sub>2</sub> reduction which is very promising for the advancement of MES system because it enables the use of undefined mixed cultures which are probably more robust to the changing conditions and allow a microbiome which could make use of a variety of electron and electron equivalents transfer routes. This means that the microorganisms thriving on direct electrons transfer from the electrode or on hydrogen transfer or those utilizing acetate as the substrate can all co-exists in the MES. Such microbiome, as described in Chapters 3 and 4 of the thesis, resulted in a stable and self-maintaining biocathode capable of reducing CO<sub>2</sub> for a long term (more than a year).

---

Hence, the biocatalyst from mixed culture origin can be effectively shaped toward electricity-driven bioproduction from CO<sub>2</sub>.

Short-term inhibition of methanogen using sodium-2-bromoethanesulfonate (Na-BES) in MES reactor was reported in a number of literature in MES [1, 26–28]. But the continual addition of such inhibitors is not sustainable for long-term and large-scale application [29]. Addition of chemical inhibitor is less preferential because of the added cost, potential toxicity and the difficulties in product separation. A strategy of methanogens elimination with the one-time addition of Na-BES and successive enrichment was also reported recently [23] which showed that the enriched culture grown on H<sub>2</sub>:CO<sub>2</sub> had 77% of the total relative abundance of bacteria belonging to the order *Clostridiales* and only <0.1% relative abundance of methanogens. But during the MES operation, methanogenic activity was avoided for only two to three months with the one-time use of inhibitor and selective enrichment [23]. In this study, methanogen inhibitor was used only once, during the pre-enrichment phase after heat shock and successive culturing on H<sub>2</sub>:CO<sub>2</sub> in serum bottles created a suitable inoculum for MES from CO<sub>2</sub> and avoided methanogen for more than a year in MES operation (Chapter 4). We demonstrated that the inhibition of methanogens in mixed culture MES process no longer required harmful chemicals which would otherwise make product separation more complicated. Indeed, toxic/harmful chemicals are not desirable in the end product. Still, the experimental work was executed within a controlled environment. One must prevent any infection of the system by methanogens to warrant long-term biochemical production without methane formation.

### **Electrode and MES design, operation conditions and biocatalyst do determine efficiency and production rates**

From the first proof of concept of biocathode-driven acetate production from CO<sub>2</sub> reduction using biofilms of *Sporomusa ovata* [30] to the present situation, MES technology is being popularly investigated to understand and improve the process. Mixed-culture biocatalysts have also been explored for MES from CO<sub>2</sub> due to their compatibility concerning growth with minimum need of aseptic conditions in the scaled-up application and eventually lowers the operation costs [23, 29]. Methanogenic activity can be avoided with heat-treatment and selective enrichment of biocatalysts from mixed cultures which enhanced the acetate production rate almost fivefold from 1.3 mM d<sup>-1</sup> in Chapter 2 to 6.3 mM d<sup>-1</sup> in Chapter 4. In literature, methanogen suppressed mixed culture biocathodes were reported to attain higher volumetric acetate production rates e.g. 17.25 mM d<sup>-1</sup> (1 g L<sup>-1</sup> d<sup>-1</sup>) at -0.79 V<sub>Ag/AgCl</sub> [26] and 11.67 mM d<sup>-1</sup> at -1.34 V<sub>Ag/AgCl</sub> [31] with product concentrating system. The acetate production rate in this thesis did not reach as high as reported in Marshall et al. [26] but the highest volumetric rate of 6.3 mM d<sup>-1</sup> was achieved without any electrode modification at -1 V<sub>Ag/AgCl</sub> which is the highest rate for graphite felt electrode. Notably, Marshall et al. [26] used granular graphite bed as the cathode which resulted in an abundant surface for the bacterial adhesion and effective electrode-interaction for the microbiome. Moreover, the granular bed cathode also can adsorb the evolved hydrogen. The volumetric acetate production rates reported in LaBelle et al. [32] and Patil et al. [23] with enriched and methanogens suppressed biocathode for CO<sub>2</sub> reduction are comparable with the results achieved in this thesis [23, 32]. A high current density of -10 A m<sup>-2</sup> was attained at -1 V<sub>Ag/AgCl</sub> which supported an acetate production rate of 550-400 mg L<sup>-1</sup> d<sup>-1</sup> with 60 % coulombic efficiency (Chapter 4). An overview of improvements made in the process of CO<sub>2</sub> reduction in MES system in this thesis and also in the recent literature is presented in Table 7.1.

As the bacterial interaction with the electrode is associated with the electrode coverage of the bacterial biofilm, the production rates are expressed based on the surface area. However, planktonic production is also possible which does not rely on the biofilm

bacteria attached to the electrode. In the study of CO<sub>2</sub> reduction in MES with *Sporomusa ovata* biocathode, surface modifications with positively charge material, metal nanoparticles catalysts and carbon nanoparticles [33] have resulted in at least three times higher acetate production rate than usual graphite stick electrodes [30] at -0.6 V<sub>/Ag/AgCl</sub>. Highest production rate with of 3.38 g m<sup>-2</sup> d<sup>-1</sup> was reported at -0.6 V<sub>/Ag/AgCl</sub> with Ni-coated carbon cloth biocathode of *Sporomusa ovata* for CO<sub>2</sub> reduction [34]. In surface modification aspect, the tremendous improvements in the surface based acetate production rate have been reported for mixed culture biocathode in recent literature with modified cathode surface with carbon-nanotubes reaching 685 ± 30 g m<sup>-2</sup> d<sup>-1</sup> [1] and 1330 g m<sup>-2</sup> d<sup>-1</sup> [2]. In this thesis, projected surface area based production rate reached a fastest rate of 325 g m<sup>-2</sup> d<sup>-1</sup> and 119 g m<sup>-2</sup> d<sup>-1</sup> (Chapter 3) for the gas diffusion biocathode of 10 cm<sup>2</sup> projected surface area whereas 31 g m<sup>-2</sup> d<sup>-1</sup> for graphite felt biocathode with enriched mixed culture (Chapter 4). Although these rates are lower than the latest reported rates in literature [1], these rates are relatively high for an untreated electrode.

In MES research, various normalization (surface area based or volume based) factors are used in the production parameters for measuring the process rate. For example, the production rate of 119 g m<sup>-2</sup> d<sup>-1</sup> for gas diffusion biocathode in Chapter 2 corresponds to a maximum of only 3.39 mM d<sup>-1</sup> volumetric productivity which is lower than the volumetric productivity (6.3 mM d<sup>-1</sup>) achieved with graphite felt cathode in H-type reactor in Chapter 4 but this high volumetric productivity in Chapter 4 corresponds to lower projected area based productivity (31.47 g m<sup>-2</sup> d<sup>-1</sup>). Hence, a single parameter for process performance may not be sufficient to represent and compare the real performance of MES system. The process has to be well represented using a true production parameter.

In the latest development of CO<sub>2</sub> reducing biocathode in this thesis, acetate accumulation of up to 7-10 g L<sup>-1</sup> was repeatedly achieved with CO<sub>2</sub> reduction at -1 V<sub>/Ag/AgCl</sub> in number of batches which is a remarkable acetate accumulation without methanogenesis. Similar concentrations of acetate were achieved only in Marshall et al. [26] with granular cathode, in Jourdin et al. [1] with surface modified cathode and in Gildemyn et al. [31] at much lower cathode potential integrated with acetate concentrating compartment. In the mixed culture environment where multiple interfering processes occurring simultaneously, such a high accumulation of acetate is a major achievement towards active biocatalyst.

The coulombic efficiencies (CEs) of bioelectrochemical CO<sub>2</sub> reduction calculated in the experiments in this thesis ranges between 20% and 60% and were not consistent within a single batch of operation. Most likely, the unstable electrochemical parameters and operational procedure were responsible for such inconsistencies in the CEs. The literature on MES from CO<sub>2</sub> using pure culture biocatalyst consistently reported CE above 80% [30, 33, 34] showing minimum loss of energy and also operated at higher cathode potential (-0.4 V<sub>/SHE</sub>). Whereas the CE values reported in literature for mixed culture biocathode also varies between 40 - 70%. However, recent development has extended it to up to 94% even operating at lower cathode potential of -0.85 V<sub>/SHE</sub> [1]. Within these studies microbial populations, electrode designs/materials and reactor configurations and operations conditions do differ. All these aspects explain the variations on CE. To further improve MES one should continue to work using the best achieved results. Highest CE observed in this thesis was up to 60% and on average the efficiencies were between 30 - 40%. Most of the losses can be credited to the electrode overpotentials and also to the electric current consumed in the side reactions mainly hydrogen evolution if H<sub>2</sub> is not mediating the reduction reaction and it escapes the reactor. But, H<sub>2</sub> can be the ultimate electron donor for CO<sub>2</sub> reduction in MES, so the issue of H<sub>2</sub> evolution becomes insignificant when the cathode biofilm could be made highly effective in scavenging H<sub>2</sub> before it escapes from the reactor.

Gas-liquid mass transfer is one of the limiting factors in CO<sub>2</sub> reduction in MES. The solubilities of H<sub>2</sub> and CO<sub>2</sub> are fairly low—at 298 K, those were recorded around 1.6 mg H<sub>2</sub> L<sup>-1</sup> at 1 atm H<sub>2</sub> [35] and around 1.5 g CO<sub>2</sub> L<sup>-1</sup> at 1 atm CO<sub>2</sub>. Using gas diffusion biocathode in Chapter 3, the mass transfer rate of CO<sub>2</sub> was almost doubled and H<sub>2</sub> was produced on-site biocathodically to maximize the availability. But, H<sub>2</sub> scavenging was not yet optimally effective as the H<sub>2</sub> evolved was escaping from the reactor which accounts a major loss of electrons. Hence, optimum electron or hydrogen transfer to targeted product (here acetate) is still sought for improving coulombic efficiency of MES system. The immediate solution foreseen for such CO<sub>2</sub> based MES systems in addition to the improvements made in this thesis would be to increase the gaseous substrate and energy source (H<sub>2</sub>) confinement in the reactor along with bacterial retention. The bioelectrochemical reactors for MES could be adapted to the existing configurations of bioreactors for the optimization of electrochemical, biological, hydraulic and mass transport requirements. Possible modifications in the reactor shapes, liquid/gas interfaces and electrode configurations for MES were proposed by Roy et al. to maximized gas utilization via effective interaction with the active microbial population [36]. Immobilization of cells to favor biofilm formation on the solid materials has been one of the most applied strategies. Packed bed, fluidized bed and biofilters are the different possible configurations of bioreactors which favor biofilm formation and simultaneously, allow the gas or liquid phase substrates to flow through the solid matrix holding the immobilized cells [36]. Electrically conductive materials, like activated carbon granules can be used in bioelectrochemical reactors as an electrode to create such configurations which would ensure electron transport to/from the active biofilm. Notably, the high volumetric production rate of acetate from CO<sub>2</sub> reduction in MES, reported by Marshall et al. (2013), was indeed achieved by using graphite granules bed as a cathode. High microbial cell retention might have attained with graphite granular bed in MES reactor which further allowed the improvement in CO<sub>2</sub> reduction rate and efficiency.

**Table 7.1:** Comparative overview of MES performances reported in relevant literature

| References                   | Microbial inoculum                       | Cathode material                 | $E_{cat}$ (V <sub>SHE</sub> ) | Current density (A m <sup>-2</sup> ) | Acetate production rate [mM d <sup>-1</sup> ] | Projected Area based acetate production (g m <sup>-2</sup> d <sup>-1</sup> ) | CE for acetate (%) | Max. acetate titer (g L <sup>-1</sup> ) |
|------------------------------|--|----------------------------------|-------------------------------|--------------------------------------|---|--|--------------------|---|
| Chapter 2 (this thesis) [37] | mixed culture WW                         | Carbon felt with SS mesh         | -0.9                          | 10                                   | 1.3   | 40   | 40-50              | 0.6                                     |
| Chapter 3 (this thesis)      | Enriched mixed culture                   | Gas diffusion biocathode         | -0.9                          | 10                                   | 0.12 – 3.96                                   | 10.8 – 119   | 35.46 – 88         | 2.89                                    |
| Chapter 4 (this thesis)      | Enriched mixed culture                   | Carbon felt with graphite stick  | -0.8                          | 10                                   | 1.3 – 6.3                                     | 6.67 – 31.47   | 16.2 – 49.4        | 8-10                                    |
| Nevin et al. (2010) [30]     | <i>Sporomusa ovata</i>                   | graphite stick                   | -0.4                          | -0.208                               | 0.17  | 1.3  | 85                 | 0.063                                   |
| Zhang et al. (2013) [33]     | <i>Sporomusa ovata</i>                   | Carbon cloth chitosan CNT-cotton | -0.4                          | -0.475                               | ng  | 2.7  | 86 ± 12            | 0.118                                   |
| Nie et al. (2013) [34]       | <i>Sporomusa ovata</i>                   | Ni-coated graphite stick         | -0.4                          | -0.63                                | 1.13  | 3.38   | 82 ± 14            | 0.094                                   |
| Giddings et al. (2015) [38]  | <i>Sporomusa ovata</i>                   | graphite stick                   | -0.74                         | -1.7±0.19                            | 4.68±1.27                                     | 9.68±2.65  | 89±12              | ng                                      |
| Marshall et al. (2015) [26]  | adapted brewery WW sludge                | graphite granules                | -0.59                         | ng                                   | 17.25   | ng   | 69                 | 10.5                                    |
| LaBelle et al. (2014) [32]   | adapted brewery WW sludge                | graphite rod                     | -0.6                          | ~1.2                                 | 3.6   | 10.8   | 40                 | 0.35                                    |
| Jourdin et al. (2014) [22]   | pond sediments and anaerobic WWTP sludge | nanoweb RVC                      | -0.85                         | -37 ± 3                              | 0.42 ± 0.06                                   | 195 ± 30   | 78.5               | 1.65                                    |
| Jourdin et al. (2015) [1]    | anaerobic digester WWTP                  | RVC foam with SS wire            | -0.85                         | -102 ± 1                             | ng  | 685 ± 30   | 94 ± 2             | 11                                      |
| Patil et al. (2015) [23]     | enriched culture (UASB sludge)           | Carbon felt                      | -1.26 ± 0.08                  | -5                                   | 1 ± 0.09                                      | 19 ± 1.7   | 58 ± 5             | 1.29 ± 0.15                             |
| Gildemyn et al. (2016) [31]  | Enriched mixed culture                   | Carbon felt                      | -1.14 ± 0.04                  | ng                                   | 11.67   | 23.35  | 61                 | 13.5                                    |
| Jourdin et al. (2016) [2]    | Enriched mixed culture                   | MWCN-RVC                         | -1.1                          | -200                                 | ng  | 1330   | ng                 | 11                                      |

CE- Coulombic efficiency, RVC-Reticulated vitreous carbon; MWCN- Multi-walled carbon nanotubes; SS- Stainless Steel; WW- Wastewater; ng- Not given or cannot be deduced; WWTP- Wastewater treatment plant



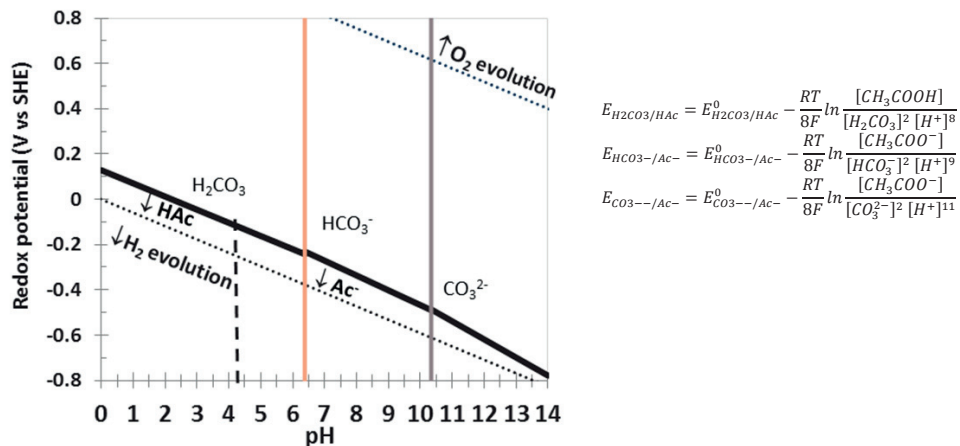
---

**Medium optimization is needed to obtain a fast start-up and allow effective CO<sub>2</sub> use on long term**

The product yield in microbial bioproduction is primarily governed by the metabolic activities of the organisms which is potentially limited by (1) energy source, (2) redox power and (3) carbon source [39]. The energy conserved as Adenosine triphosphate (ATP) in the metabolism and the change in redox power-Nicotinamide adenine dinucleotide (phosphate) [NAD(P)H], is based on the carbon source and product. The Wood-Ljungdahl (WL) pathway of CO<sub>2</sub> reduction to acetate, using H<sub>2</sub> as the electron donor, produces lower energy. However, more than 95% of carbon and electron flow is diverted to the production of extracellular organic end-products, rather than the growth and biomass production [40]. Thus, the WL pathway should be associated with a chemi-osmotic pathway to provide the essential energy. Recent studies have shown the presence of membrane-driven ATP synthesis metabolism in the acetogens. Nevertheless, the WL pathway is the most energetically efficient pathway known for CO<sub>2</sub> reduction [40]. In the WL pathway, two CO<sub>2</sub> molecules are combined to form one molecule of acetyl-CoA at the expense of one ATP. Acetyl kinase converts this acetyl-CoA to acetate and one ATP molecule which is assimilated for the biomass production. There is no net energy gained in CO<sub>2</sub> reduction to acetate hence the bacterial metabolism could be limited in the processes based on the WL pathway including MES from CO<sub>2</sub>. Furthermore, in the autotrophic growth of acetogens utilizing the mineral medium, the cell biomass yield and growth are normally reduced due to the nutritional limitation. Nutritional supplements such as yeast extract were shown to enhance the cell growth of acetogens in H<sub>2</sub>:CO<sub>2</sub> culture [41]. However, the addition of yeast extract and other organic supplements should be avoided to maintain a complete autotrophic bioproduction. So far, in this thesis either yeast extract or fructose on H<sub>2</sub>:CO<sub>2</sub> grown culture was used to stimulate the bacterial growth during the startup. For a fast startup, these strategies can be useful for the long-term operation. But it is worthy to investigate whether the exclusion of nutrients supplements can be achieved to make the MES economically more attractive.

**Electron transfer mechanism must be understood to optimize the energy efficiency and product spectrum**

Electrochemically active bacteria directly use the electrons available from the solid electrode for the reduction reaction, which is termed as direct electron transfer (DET). Several mechanisms of electron transfer has been proposed for biological interaction with the cathode [42]. For the CO<sub>2</sub> reduction, thermodynamically, the reaction can take place at higher potentials than the H<sub>2</sub> evolution with less electric energy input. But when bacteria catalyze the CO<sub>2</sub> reduction reaction, the interaction of bacteria with the electrode for the catalysis has still not been clearly understood. For an undefined mixed culture biocathode, it becomes more complex to understand the mechanism of electron transfer. However, biological pathways of reduction of CO<sub>2</sub> to acetate under H<sub>2</sub> as electron donor have been known. Furthermore, H<sub>2</sub> can be produced electrochemically via water electrolysis at the cathode potential lower than -0.414 V<sub>SHE</sub> (H<sub>2</sub> evolution onset potential at biological condition). So, when the reduction reaction occurs below the hydrogen evolving potential, it is considered that the bacteria are gaining the electrons from the electrochemically produced H<sub>2</sub>. Such type of electron transfer where a potential electron donor such as H<sub>2</sub> or any redox mediator is available is called indirect or mediated electron transfer. In the context of electron transfer mechanisms in CO<sub>2</sub> reduction process, Pourbaix diagram provides the information on the electrochemically stable state of redox species based on the pH and potentials. The Pourbaix diagram for the bioelectrochemical reduction of CO<sub>2</sub> to acetate is given in Figure 7.4. In a quick glance, it can be said that the area in Figure 7.4 above the H<sub>2</sub> evolution and below the CO<sub>2</sub>/HCO<sub>3</sub><sup>-</sup> reduction line represents the region of dominance of DET for bioelectrochemical CO<sub>2</sub> reduction whereas the reduction reaction is said to be H<sub>2</sub> mediated the redox potential and pH conditions falls in the region below the hydrogen evolution line.



**Figure 7.4:** Pourbaix diagram for CO<sub>2</sub> reduction showing the regions of relative predominance of different species in the potential–pH plane. The activities/concentrations of all aqueous CO<sub>2</sub> forms (H<sub>2</sub>CO<sub>3</sub>, HCO<sub>3</sub><sup>-</sup> and CO<sub>3</sub><sup>2-</sup>), acetic acid (HAc) and acetate (Ac<sup>-</sup>) are considered at 1 M.

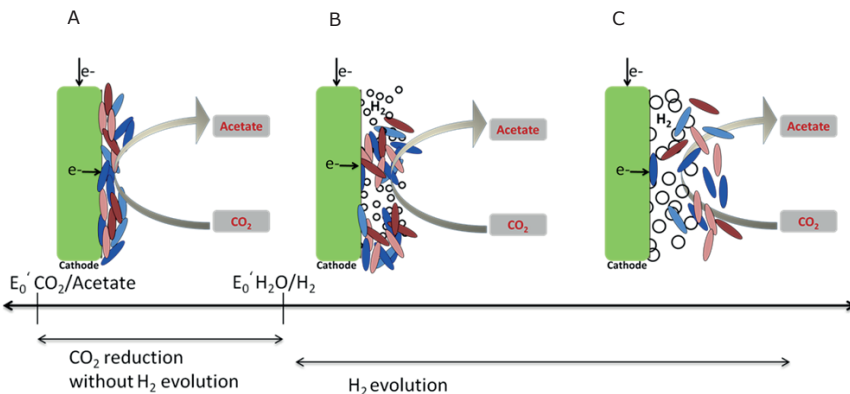
Acetogenic species, including *Sporomusa ovata* and *Clostridium ljungdahlii*, have been reported for catalyzing the CO<sub>2</sub> reduction at -0.4 V<sub>SHE</sub> [30, 43] which is above the H<sub>2</sub> evolution potential and hence it is supposed as DET mechanism of CO<sub>2</sub> reduction. However, it is still unclear how the bacteria interact with the solid electrode for CO<sub>2</sub> reduction. At the actual reactor condition, the overpotential of the electrode has to be overcome for a reaction to take place. The overpotential of -0.28 V was reported for the H<sub>2</sub> producing microbial biocathode on graphite felt electrode at neutral pH [44]. Higher overpotential for CO<sub>2</sub> reduction at graphite felt cathode can shift the actual electrode potential to much lower potential than hydrogen evolution. Moreover, it is equally likely that an undefined mixed culture biocatalyst first catalyzes the hydrogen evolution which can further mediate CO<sub>2</sub> reduction. Reduction via DET is interesting when higher production rates can be achieved at minimum electric power input regardless of the mechanisms of DET or H<sub>2</sub> mediated transfer. Still further studies are needed to completely reveal the electrons transfer mechanisms in both pure as well as mixed cultures. Hereby, studies on enzymes involved in electroreduction can be used to clarify the production of chemicals [36, 45, 46].

An electroactive bacteria biocathode might require studies on the activation of specialized enzymes like cytochrome-c for extracellular electron transfer. In this regards, electrochemical activity studies on homoacetogenic bacteria show that different mechanism of electron transfer might be possible depending on the individual bacterial species. For example, Sydow et al. [47] discussed that, in *Sporomusa ovata* cytochrome-c is present in the outer membrane of the bacteria which might favor the DET whereas another homoacetogen, *C. ljungdahlii*, does not possess the cytochrome-c. However, hydrogenases are reported to carry out the reduction of CO<sub>2</sub> in *C. ljungdahlii*, thus the CO<sub>2</sub> reduction occurs most probably via H<sub>2</sub> in *C. ljungdahlii* biocathode [47].

In all of our experiments, bioelectrochemical reduction of CO<sub>2</sub> was occurring at much lower cathode potentials than the theoretical H<sub>2</sub> evolution potential (-0.414 V<sub>SHE</sub> or -0.61 V<sub>Ag/AgCl</sub>). Bioelectrochemical CO<sub>2</sub> reduction in MES experiments, carried out using

enriched mixed cultures with carbon felt/graphite stick cathodes, showed a considerable production of acetate only when the polarization potentials were more negative than  $-0.8 \text{ V}_{/\text{Ag}/\text{AgCl}}$  (Chapter 4). When the cathode potentials were  $-0.8 \text{ V}_{/\text{Ag}/\text{AgCl}}$  and above, the degradation of acetate and butyrate was observed. For the carbon felt electrode,  $\text{H}_2$  was measured in the headspace at  $\leq -0.9 \text{ V}_{/\text{Ag}/\text{AgCl}}$  and no methane was detected. Since acetate production remained low unless the cathode potential was dropped below  $-0.9 \text{ V}_{/\text{Ag}/\text{AgCl}}$ , it can be indicative that  $\text{H}_2$  was mediating the  $\text{CO}_2$  reduction reaction. Higher current densities (up to  $10 \text{ A m}^{-2}$ ) obtained at  $-0.9$  to  $-1 \text{ V}_{/\text{Ag}/\text{AgCl}}$  with biocathode (Chapter 4) is an indication of microbial electrocatalysis in concert with electrochemical  $\text{H}_2$  evolution. However,  $\text{H}_2$  evolution might be a side reaction that the biocathode catalyzes which can further mediate the bioelectrochemical  $\text{CO}_2$  reduction. But the actual mechanism of electron transfer in biocathode consisting undefined mixed culture is not clearly understood.

In all the experiments of this thesis, the reduction of  $\text{CO}_2$  occurred simultaneously with the  $\text{H}_2$  evolution, hence the reduction process is most likely mediated by the  $\text{H}_2$ , produced at the cathode either electrochemically or bioelectrochemically. Still the direct electron transfer mechanisms can also occur at these hydrogen evolution potentials. Figure 7.5 illustrates the possible bacterial interaction with the cathode, that has been proposed previously by Blanchet et al. [48]. Based on our results from Chapter 4, the  $\text{H}_2$  interaction in our experiments can be resembled to Figure 7.5B. On-site produced  $\text{H}_2$  would be effective for  $\text{CO}_2$  reduction as it might be immediately available to the bacteria on the cathode. Electrochemical or bioelectrochemical  $\text{H}_2$  formation at cathode potentially governs a typical electron transfer to the biocatalysts that can support high rate bioproduction, although the CEs remained low.



**Figure 7.5:** Hydrogen evolution controlling bacterial attachment at the cathode (adapted from Blanchet et al. [48]). Our MES systems most likely resemble Figure B with  $\text{H}_2$  evolution and other cathode-interaction based processes.

### Surface modified electrodes can be integrated with GDE electrodes

Modification/improvement in bioelectrodes should allow enhancement of electronic conductivity, electron transfer and biofilm adhesion which can be possible by (1) increasing porosity for an effective utilization of the electrode surface area (2) improving surface oxygen and nitrogen functional groups; (3) using conductive material and biocompatible materials [49]. Evidently, the studies of  $\text{CO}_2$  reduction in MES with *Sporomusa ovata*, the surface modified biocathodes embedded with either positively

charge materials or Au, Ni nanoparticles or carbon nanoparticles [33] have resulted in at least three times higher acetate production rates than the usual graphite stick electrodes [30] at  $-0.6 \text{ V}_{\text{Ag}/\text{AgCl}}$ . Highest production rate with of  $3.38 \text{ g m}^{-2} \text{ d}^{-1}$  was reported at  $-0.6 \text{ V}_{\text{Ag}/\text{AgCl}}$  with Ni-coated carbon cloth biocathode of *Sporomusa ovata* for  $\text{CO}_2$  reduction [34]. Carbon nanotube scaffold cathodes have been reported to improve the bacterial attachment on the cathodes of  $\text{CO}_2$  reducing MES [22]. Considerably high area-normalized acetate production rates have been reported for mixed culture biocathodes in recent literature with carbon-nanotubes embedded cathodes reaching  $685 \pm 30 \text{ g m}^{-2} \text{ d}^{-1}$  [1] and  $1330 \text{ g m}^{-2} \text{ d}^{-1}$  [2]. These surface modified electrodes can be integrated with the developed GDE electrode with the developed mixed culture biocatalysts. This could further enhance the electron-uptake.

### **Steering biochemical production to ethanol and butyrate production can be improved**

Development of stable and active biocatalyst (suspended or biofilm) at the cathode was attained with significant improvement in the MES setup. Bioelectrochemical  $\text{CO}_2$  reduction with mixed culture biocatalyst, at the cathode potential more negative than  $-0.9 \text{ V}_{\text{Ag}/\text{AgCl}}$ , directed the MES of acetate and additionally ethanol and butyrate were also produced (Chapters 3 and 4). In the fed-batch mode, after the accumulation of acetate reached more than  $1.5 \text{ g/L}$ , the reduction products started to shift towards ethanol and butyrate upon decreasing the pH below 6. The pH of catholyte decreased due to acidifying effect of continuous  $\text{CO}_2$  gas sparging. Homoacetogens e.g. *Clostridium ljungdahlii* and *Clostridium autoethanogenum* are reported to reduce  $\text{CO}_2$  to ethanol along with VFAs at lower pH if sufficient reducing equivalents ( $\text{H}^+$  or  $\text{H}_2$ ) are available [50]. Acetate produced from  $\text{CO}_2$  reduction can be converted to longer chain fatty acids [51, 52]. Butyrate production was also reported by Ganigué et al. in MES from  $\text{CO}_2$  and stated to be related to the chain elongation [53]. Supplying 80%  $\text{CO}_2$  resulted in an increase in butyrate concentration in MES (Chapter 3). Alcohols and medium chain fatty acids not only have higher economic value and also can be easily extracted from the medium [52]. However, MES of ethanol from  $\text{CO}_2$  in this thesis, remained fairly low (up to  $200 \text{ mg L}^{-1}$  in Chapters 3 and 4) but butyrate production was higher than ethanol; accumulated up to  $1 \text{ g L}^{-1}$  (Chapter 4). Ethanol and butyrate production in  $\text{CO}_2$  reducing MES is the breakthrough for the application of MES towards  $\text{CO}_2$  based biorefinery.

Literature on growing bacteria on  $\text{CO}_2$  and  $\text{H}_2$  showed that the product of  $\text{CO}_2$  reduction varies depending on the bacterial species. Along the Wood-Ljungdahl pathway (as in Figure 7.6), ethanol and butyrate are also produced either directly from  $\text{CO}_2$  reduction or by acetate reduction or both  $\text{CO}_2$  and acetate as carbon source. Ethanol is produced from acetate reduction at lower pH where the undissociated acids exist [54]. Reduction of both  $\text{CO}_2$  and acetate together is expected in the mixed culture MES. The thermodynamics of ethanol production by  $\text{CO}_2$  or acetate reduction indicates that lower pH and excess  $\text{H}_2$  can shift the production to ethanol. The selectivity of the products of  $\text{CO}_2$  reduction has been shown to be dependent on micro-elements of trace metal and vitamin components due to their effect on the activity of NADPH/NADP and Acetyl-CoA enzymes [55]. By limiting micronutrient and trace elements (namely pantothenic acid and cobalt), higher concentrations of ethanol were produced rather than acetate [56]. Thus, to enhance production of longer carboxylates or more reduced compounds, strategies from gas fermentations can be used in MES.

### **Integration of product separation and purification is needed**

An integrated system of production and extraction of acetate was investigated in MES integrating a column of commercial anion-exchange resins. An MES with integrated extraction is interesting, firstly to reduce product inhibition and secondly, for the advancement of product recovery in MES process for real application. Acetate absorption of  $10$  to  $18 \text{ mg g-resin}^{-1}$  was observed at the catholyte conditions. Overall, an MES

system for the production and extraction of acetate from CO<sub>2</sub> was demonstrated in Chapter 5 of this thesis via an integration of anion-exchange resin column. Likewise, membrane electrolysis was also used to extract the anionic forms of short/mid-chain fatty acids (e.g. acetate, butyrate, caproate, etc.) from the neutral broth by transferring across an anion exchange membrane (AEM) [57]. *In situ* separation and concentration of acetic acid was demonstrated by integrating membrane electrolysis with CO<sub>2</sub> reducing MES reactor [31]. Acetate produced at the rate of 11.6 mM d<sup>-1</sup> in MES was concentrated up to 13.5 g L<sup>-1</sup> in concentration compartment after transporting through AEM. However, the extraction process requires high electric energy input and the extraction efficiency remain highly proportional to product concentration. In this sense, anion-exchange resin column does not require extra energy input and the regenerants such as sodium hydroxide or carbonate solutions can recover the adsorbed carboxylate anions in concentrated form. Still, the production of the regenerants itself is energy intensive. Development of a continuous reactor with integrated separation system is sought for the practical application of bioproduction and recovery of the products from CO<sub>2</sub> reduction. Hereby specific product purity must be met. Catholyte remains or biocatalysts are likely not desired in the final product. As such a complete system must be evaluated at an industrial site and the product must be tested on its suitability for the eventual application.

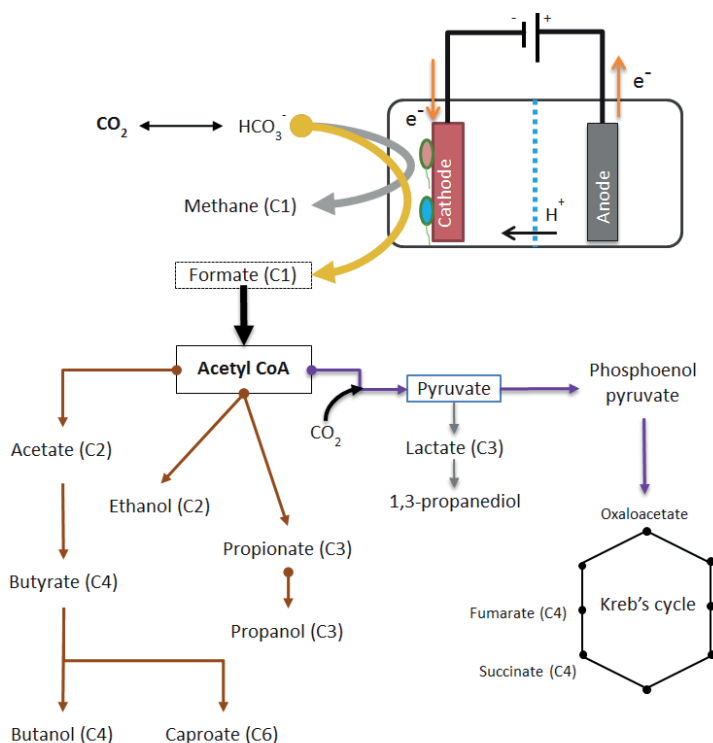
### ***MES can become a new platform technology within biorefineries***

A range of biobased carboxylic acids used in industrial applications can be synthesized in MES from CO<sub>2</sub>. Acetate and methane are the most common biobased products that can be initially derived based on the biocatalyst and operational parameters. Acetate is one of the major precursors and commodities in many chemical synthesis processes [58]. However, more valuable products are sought in MES system to achieve economic advantages and hence the implementation of MES technology will be attractive. The bioproducts derived from CO<sub>2</sub> reducing MES can be directly utilized and/or integrated with other bioprocesses as substrate and/or towards carbon chain-elongation, resulting in a closed-loop system that could be utilized as a sustainable biobased refinery. Acetyl-CoA, a key intermediate in the WL pathway, serves as a building block for the production of various chemical commodities [58]. Under the appropriate conditions some acetogens can produce high titers of ethanol, butyrate and in some instances lactate, 1,3-propanediol and butanol were also produced [58, 59]. Production of ethanol, propionate and butyrate in MES from CO<sub>2</sub> was achieved in the MES experiments of this thesis especially in Chapters 3 and 4. The microbiologically mediated chain elongation of acetate by H<sub>2</sub>/CO<sub>2</sub> produces propionate (C3), butyrate (C4) and caproate (C6) [51, 52]. Further reduction of carboxylic acids to alcohols also occurs depending upon the operational parameters. In addition, lactate (C3) and succinate (C4) can also be electrosynthesized via Krebs cycle. Figure 7.6 presents an overview of possible end products formed in MES from CO<sub>2</sub> reduction via WL pathways. All of these value-added products have direct applications or can be further utilized as substrates or precursors for other processes or for biofuel production. This closed-loop CO<sub>2</sub> MES model appears promising and may represent a model for CO<sub>2</sub> conversion and utilization offering a wider range of platform chemicals. Thus, MES is a key technology to produce arrays of value added products by employing carbon and electron flow. Therefore, this is a promising technology that provides prospects for biobased economy/biorefineries.

### ***MES application can be employed for bioremediation, fermentation and more***

Research and development in MES technology offers excellent future prospects with attractive breakthroughs in converting electrical energy to new chemicals. MES is a technology that can store electricity directly in the form of biofuel or its precursors. This stored chemical can principally also be oxidized in a microbial fuel cell system to produce electricity. Recently a proof-of-principle on this was achieved [60]. Another advantage of this electricity-driven bioproduction method is its non-dependence on fertile land compared to other biomass to biofuel approaches. Commercial photovoltaic (PV) has an

efficiency around 10 - 15%, while net photosynthetic efficiency is around 0.5%. When an MES system is integrated with a photovoltaic system, then even assuming 25% MES efficiency, the overall chemical production efficiency will be 3.75 % which means at least 7.5 times more organic matter is harvested per  $\text{m}^2$  of land. Thus, the land usage will be appreciably lowered, and we do not need fertile land and a large volume of fresh water for the production of biochemicals. Furthermore, the water usage and nutrient consumption are lower in the electricity-driven bioproduction as compared to the agricultural production. This gives remarkable advantages to the microbial electrosynthesis of biochemicals, apart from being a clean technology. MES technology can also be incorporated in bioremediation and in the conventional fermentation process in order to steer the reaction towards electrically-controlled. Chapter 6 of this thesis has presented an overview of bioelectrochemical systems (BESSs) and discussed its potential application mostly emphasizing bioproduction in MES technology. In polluted soils or wastewater streams, *in situ* produced electron donors (like acetate) can be made available to biodegrade soil pollutants. Microbial electrosynthesis and biotransformation of biomass would represent a promising alternative to conventional chemical synthesis which utilizes hazardous and non-renewable raw materials unsustainably (high temperature/pressure, acid/alkaline solutions, etc.). In addition, by electrically-steering the metabolic pathways, it opens the possibilities to promote cell growth, redox states control in fermentation/bioaccumulation processes, and biosynthesis induction from the inexpensive carbon sources including  $\text{CO}_2$  and waste streams. The proof-of-principle of the bioelectrochemical systems within the bio-based conversions has been widely demonstrated in recent MES literature. For the real application, further understanding and, technological advancements are needed upon demonstration. Eventually, finding the right niche market will allow a break-through for MES.



**Figure 7.6:** Possible metabolic end products based on Wood-Ljungdahl pathway of  $\text{CO}_2$  reduction in homoacetogens (Adapted from [61] and [62]).

---

## References

1. Jourdin L, Grieger T, Monetti J, et al (2015) High Acetic Acid Production Rate Obtained by Microbial Electrosynthesis from Carbon Dioxide. *Environ Sci Technol* 49:13566–13574. doi: 10.1021/acs.est.5b03821
2. Jourdin L, Freguia S, Flexer V, Keller J (2016) Bringing High-Rate, CO<sub>2</sub>-Based Microbial Electrosynthesis Closer to Practical Implementation through Improved Electrode Design and Operating Conditions. *Environ Sci Technol* 50:1982–1989. doi: 10.1021/acs.est.5b04431
3. IPCC (2005) IPCC Special Report on Carbon dioxide capture and storage. Cambridge University Press
4. Schievano A, Pepé Sciarria T, Vanbroekhoven K, et al (2016) Electro-Fermentation – Merging Electrochemistry with Fermentation in Industrial Applications. *Trends Biotechnol.* doi: 10.1016/j.tibtech.2016.04.007
5. Dopson M, Ni G, Sleutels THJA (2016) Possibilities for extremophilic microorganisms in microbial electrochemical systems. *FEMS Microbiol Rev* 40:164–181. doi: 10.1093/femsre/fuv044
6. Mirizadeh S, Yaghmaei S, Ghobadi Nejad Z (2014) Biodegradation of cyanide by a new isolated strain under alkaline conditions and optimization by response surface methodology (RSM). *J Environ Heal Sci Eng* 12:1–9. doi: 10.1186/2052-336X-12-85
7. Elías A, Barona A, Ríos FJ, et al (2000) Application of biofiltration to the degradation of hydrogen sulfide in gas effluents. *Biodegradation* 11:423–427. doi: 10.1023/A:1011615906278
8. Civilini M (2006) Multiple Microbial Activities for Volatile Organic Compounds Reduction by Biofiltration. *J Air Waste Manage Assoc* 56:922–930. doi: 10.1080/10473289.2006.10464503
9. Kedzierzawski P, Augustynski J (1994) Poisoning and Activation of the Gold Cathode during Electroreduction of CO<sub>2</sub>. *J Electrochem Soc* 141:L58–L60. doi: 10.1149/1.2054936
10. Dry ME (2002) The Fischer–Tropsch process: 1950–2000. *Catal Today* 71:227–241. doi: 10.1016/S0920-5861(01)00453-9
11. ElMekawy A, Hegab HM, Mohanakrishna G, et al (2016) Technological advances in CO<sub>2</sub> conversion electro-biorefinery: A step towards commercialization. *Bioresour Technol.* doi: 10.1016/j.biortech.2016.03.023
12. Dunsmore HE (1992) A geological perspective on global warming and the possibility of carbon dioxide removal as calcium carbonate mineral. *Energy Convers Manag* 33:565–572. doi: 10.1016/0196-8904(92)90057-4
13. Dlugokencky E, Tans P (2016) Trends in Atmospheric Carbon Dioxide. In: NOAA/ESRL. [www.esrl.noaa.gov/gmd/ccgg/trends/global.html](http://www.esrl.noaa.gov/gmd/ccgg/trends/global.html). Accessed 5 May 2016
14. Liu C, Ziesack M, Silver PA (2016) Water splitting – biosynthetic system with CO<sub>2</sub> reduction efficiencies exceeding photosynthesis. *Science* (80-) 352:1210–3. doi: 10.1126/science.aaf5039
15. Huang L, Regan JM, Quan X (2011) Electron transfer mechanisms, new applications, and performance of biocathode microbial fuel cells. *Bioresour Technol* 102:316–23. doi: 10.1016/j.biortech.2010.06.096
16. Rosenbaum M a, Franks AE (2014) Microbial catalysis in bioelectrochemical technologies: status quo, challenges and perspectives. *Appl Microbiol Biotechnol* 98:509–18. doi: 10.1007/s00253-013-5396-6
17. Yang H, Xu Z, Fan M, et al (2008) Progress in carbon dioxide separation and capture: A review. *J Environ Sci* 20:14–27. doi: 10.1016/S1001-0742(08)60002-9
18. Climeworks (2016) Capturing CO<sub>2</sub> from air. <http://www.climeworks.com/>. Accessed 4 Jun 2016
19. DNV (2011) Carbon Dioxide Utilization: Electrochemical Conversion of CO<sub>2</sub> - Opportunities and Challenges.
20. Climeworks (2016) Climeworks CO<sub>2</sub> Capture Plant. <http://www.climeworks.com/co2-capture-plants/articles/capture-plants.html>. Accessed 5 May 2016
21. ArcelorMittal (2015) ArcelorMittal, LanzaTech and Primetals Technologies announce partnership to construct breakthrough €87m biofuel production facility. In: News Release. <http://corporate.arcelormittal.com/news-and-media/news/2015/july/13-07-2015>. Accessed 5 May 2016
22. Jourdin L, Freguia S, Donose BC, et al (2014) A novel carbon nanotube modified scaffold as an efficient biocathode material for improved microbial electrosynthesis. *J Mater Chem A* 2:13093–13102. doi: 10.1039/C4TA03101F
23. Patil SA, Arends JBA, Vanwonterghem I, et al (2015) Selective Enrichment Establishes a Stable Performing Community for Microbial Electrosynthesis of Acetate from CO<sub>2</sub>. *Environ Sci Technol* 150701101446004. doi: 10.1021/es506149d
24. Marshall CW, Ross DE, Fichot EB, et al (2012) Electrosynthesis of commodity chemicals by an

- autotrophic microbial community. *Appl Environ Microbiol* 78:8412–20. doi: 10.1128/AEM.02401-12
25. Jiang Y, Su M, Zhang Y, et al (2013) Bioelectrochemical systems for simultaneously production of methane and acetate from carbon dioxide at relatively high rate. *Int J Hydrogen Energy* 38:3497–3502. doi: 10.1016/j.ijhydene.2012.12.107
  26. Marshall CW, Ross DE, Fichot EB, et al (2013) Long-term operation of microbial electrosynthesis systems improves acetate production by autotrophic microbiomes. *Environ Sci Technol* 47:6023–9. doi: 10.1021/es400341b
  27. Battle-Vilanova P, Puig S, Gonzalez-Olmos R, et al (2015) Continuous acetate production through microbial electrosynthesis from CO<sub>2</sub> with microbial mixed culture. *J Chem Technol Biotechnol n/a–n/a*. doi: 10.1002/jctb.4657
  28. Su M, Jiang Y, Li D (2013) Production of acetate from carbon dioxide in bioelectrochemical systems based on autotrophic mixed culture. *J Microbiol Biotechnol* 23:1140–6.
  29. Desloover J, Arends JB a, Hennebel T, Rabaey K (2012) Operational and technical considerations for microbial electrosynthesis. *Biochem Soc Trans* 40:1233–8. doi: 10.1042/BST20120111
  30. Nevin KP, Woodard TL, Franks AE, et al (2010) Microbial Electrosynthesis: Feeding Microbes Electricity To Convert Carbon Dioxide and Water to Multicarbon Extracellular Organic. *MBio* 1:e00103–10–. doi: 10.1128/mBio.00103-10.Editor
  31. Gildemyn S, Verbeeck K, Slabbinck R, et al (2015) Integrated Production, Extraction, and Concentration of Acetic Acid from CO<sub>2</sub> through Microbial Electrosynthesis. *Environ Sci Technol Lett*. doi: 10.1021/acs.estlett.5b00212
  32. LaBelle E V, Marshall CW, Gilbert JA, May HD (2014) Influence of Acidic pH on Hydrogen and Acetate Production by an Electrosynthetic Microbiome. *PLoS One* 9:e109935.
  33. Zhang T, Nie H, Bain TS, et al (2013) Improved cathode materials for microbial electrosynthesis. *Energy Environ Sci* 6:217. doi: 10.1039/c2ee23350a
  34. Nie H, Zhang T, Cui M, et al (2013) Improved cathode for high efficient microbial-catalyzed reduction in microbial electrosynthesis cells. *Phys Soc Chem Phys* 15:14290–4. doi: 10.1039/c3cp52697f
  35. Zhang F, Ding J, Zhang Y, et al (2013) Fatty acids production from hydrogen and carbon dioxide by mixed culture in the membrane biofilm reactor. *Water Res* 47:6122–6129. doi: 10.1016/j.watres.2013.07.033
  36. Roy S, Schievano A, Pant D (2016) Electro-stimulated Microbial Factory for value added product synthesis. *Bioresour Technol*. doi: 10.1016/j.biortech.2016.03.052
  37. Bajracharya S, ter Heijne A, Dominguez X, et al (2015) CO<sub>2</sub> reduction by mixed and pure cultures in microbial electrosynthesis using an assembly of graphite felt and stainless steel as a cathode. *Bioresour Technol*. doi: 10.1016/j.biortech.2015.05.081
  38. Giddings CGS, Nevin KP, Woodward T, et al (2015) Simplifying microbial electrosynthesis reactor design. *Front Microbiol* 6:1–6. doi: 10.3389/fmicb.2015.00468
  39. Harnisch F, Rosa LFM, Kracke F, et al (2015) Electrifying white biotechnology: engineering and economic potential of electricity-driven bio-production. *ChemSusChem* 8:739. doi: 10.1002/cssc.201403199
  40. Fast AG, Papoutsakis ET (2012) Stoichiometric and energetic analyses of non-photosynthetic CO<sub>2</sub>-fixation pathways to support synthetic biology strategies for production of fuels and chemicals. *Curr Opin Chem Eng* 1:380–395. doi: 10.1016/j.coche.2012.07.005
  41. Leclerc M, Elfoul-Bensaid L, Bernalier A (1998) Effect of yeast extract on growth and metabolism of H<sub>2</sub>-utilizing acetogenic bacteria from the human colon. *Curr Microbiol* 37:166–171. doi: 10.1007/s002849900358
  42. Rosenbaum M, Aulenta F, Villano M, Angenent LT (2011) Cathodes as electron donors for microbial metabolism: Which extracellular electron transfer mechanisms are involved? *Bioresour Technol* 102:324–333. doi: 10.1016/j.biortech.2010.07.008
  43. Nevin KP, Hensley SA, Franks AE, et al (2011) Electrosynthesis of organic compounds from carbon dioxide is catalyzed by a diversity of acetogenic microorganisms. *Appl Environ Microbiol* 77:2882–6. doi: 10.1128/AEM.02642-10
  44. Jeremiasse AW, Hamelers HVM, Buisman CJN (2010) Microbial electrolysis cell with a microbial biocathode. *Bioelectrochemistry* 78:39–43. doi: 10.1016/j.bioelechem.2009.05.005
  45. Reda T, Plugge CM, Abram NJ, Hirst J (2008) Reversible interconversion of carbon dioxide and formate by an electroactive enzyme. *Proc Natl Acad Sci U S A* 105:10654–8. doi: 10.1073/pnas.0801290105
  46. Kracke F, Vassilev I, Krömer JO (2015) Microbial electron transport and energy conservation – the foundation for optimizing bioelectrochemical systems. *Front Microbiol* 6:1–18. doi: 10.3389/fmicb.2015.00575



47. Sydow A, Krieg T, Mayer F, et al (2014) Electroactive bacteria-molecular mechanisms and genetic tools. *Appl Microbiol Biotechnol* 8481–8495. doi: 10.1007/s00253-014-6005-z
48. Blanchet EM, Duquenne F, Rafrafi Y, et al (2015) Importance of the hydrogen route in up-scaling electrosynthesis for microbial CO<sub>2</sub> reduction. *Energy Environ Sci* 8:3731–3744. doi: 10.1039/C5EE03088A
49. Fiset E, Puig S (2015) Modified Carbon Electrodes: A New Approach for Bioelectrochemical Systems. *J Bioremediation Biodegrad* 6:1–2. doi: 10.4172/2155-6199.1000e16
50. Phillips JR, Klasson KT, Clausen EC, Gaddy JL (1993) Biological production of ethanol from coal synthesis gas. *Appl Biochem Biotechnol* 39-40:559–571. doi: 10.1007/BF02919018
51. Agler MT, Wrenn B a, Zinder SH, Angenent LT (2011) Waste to bioproduct conversion with undefined mixed cultures: the carboxylate platform. *Trends Biotechnol* 29:70–8. doi: 10.1016/j.tibtech.2010.11.006
52. Steinbusch KJJ, Hamelers HVM, Plugge CM, Buisman CJN (2011) Biological formation of caproate and caprylate from acetate: fuel and chemical production from low grade biomass. *Energy Environ Sci* 4:216–224. doi: 10.1039/C0EE00282H
53. Ganigué R, Puig S, Batlle-Vilanova P, et al (2015) Microbial electrosynthesis of butyrate from carbon dioxide. *Chem Commun* 51:3235–3238. doi: 10.1039/C4CC10121A
54. Steinbusch KJJ, Hamelers HVM, Buisman CJN (2008) Alcohol production through volatile fatty acids reduction with hydrogen as electron donor by mixed cultures. *Water Res* 42:4059–66. doi: 10.1016/j.watres.2008.05.032
55. Wilkins MR, Atiyeh HK (2011) Microbial production of ethanol from carbon monoxide. *Curr Opin Biotechnol* 22:326–30. doi: 10.1016/j.copbio.2011.03.005
56. Gaddy JL, Arora DK, Phillips JR, et al (2007) Methods for increasing the production of ethanol from microbial fermentation. 2:
57. Andersen SJ, Hennebel T, Gildemyn S, et al (2014) Electrolytic Membrane Extraction Enables Production of Fine Chemicals from Biorefinery Sidestreams. *Environ Sci Technol* 48:7135–7142. doi: dx.doi.org/10.1021/es500483w
58. Schiel-Bengelsdorf B, Dürre P (2012) Pathway engineering and synthetic biology using acetogens. *FEBS Lett* 586:2191–8. doi: 10.1016/j.febslet.2012.04.043
59. Köpke M, Mihalcea C, Liew F, et al (2011) 2,3-Butanediol Production By Acetogenic Bacteria, an Alternative Route To Chemical Synthesis, Using Industrial Waste Gas. *Appl Environ Microbiol* 77:5467–5475. doi: 10.1128/AEM.00355-11
60. Molenaar SD, Mol AR, Sleutels THJA, Heijne A (2016) Microbial Rechargeable Battery: Energy Storage and Recovery through Acetate. *Environ Sci Technol Lett* 3:144–1. doi: 10.1021/acs.estlett.6b00051
61. Daniell J, Köpke M, Simpson S (2012) Commercial Biomass Syngas Fermentation. *Energies* 5:5372–5417. doi: 10.3390/en5125372
62. Venkata Mohan S, Modestra JA, Amulya K, et al (2016) A Circular Bioeconomy with Biobased Products from CO<sub>2</sub> Sequestration. *Trends Biotechnol* 34:506–519. doi: 10.1016/j.tibtech.2016.02.012





**Summary**

---

---

## Summary

The level of carbon dioxide (CO<sub>2</sub>) in the atmosphere has risen significantly due to the combustion of fossil fuels in the industrial and other anthropogenic activities. It is inevitable that this rise is linked to climate change and its impact is expected to continue in the future. Implementation of policies and technologies that would reduce carbon footprint is a global concern with respect to climate change mitigation.

CO<sub>2</sub> reduction to multi-carbon compounds at the cathode using chemolithoautotrophs is an emerging application of microbial electrosynthesis (MES). Microbial electrosynthesis (MES) from carbon dioxide (CO<sub>2</sub>) comprises bioelectrochemical reduction of CO<sub>2</sub> to multi-carbon organic compounds using the reducing equivalents produced at the electrically-polarized cathode. The recent developments in bioelectrochemical systems (BESs) are gaining significant attention for the electricity-driven production of value-added chemicals/fuels from low-value wastes including CO<sub>2</sub> by employing microbes as catalysts.

This thesis "**Microbial electrosynthesis of biochemicals**" aims to bring innovation and insights on the microbial electrosynthesis biocatalysts, electrodes and ion exchange resins for the supply of CO<sub>2</sub>, production of chemicals and for the eventual extraction of products. Pure and mixed bacterial cultures were used as biocatalysts for CO<sub>2</sub> reduction. Specifically, an enriched mixed culture was developed from the biological sources which could reduce CO<sub>2</sub> effectively. An exploration on CO<sub>2</sub> based MES and its emerging prospects have been presented in this thesis. Adjustment on biocatalyst and electrodes has been sought for the establishment of a complete MES system from CO<sub>2</sub> for the production and separation of organics.

Following are the main highlights and findings of this work summarized in accordance with the chapters outlined in this thesis.

Chapter 2 "**Carbon dioxide reduction by mixed and pure cultures in microbial electrosynthesis using an assembly of graphite felt and stainless steel as a cathode**" sought to elucidate the profiles of bioelectrochemical CO<sub>2</sub> reduction using a mixed culture from biological source and a pure culture of *Clostridium ljungdahlii* in an MES setting comprising of a graphite felt and stainless steel assembly as a cathode. Acetate production was prominently detected as the primary multi-carbon product of CO<sub>2</sub> reduction in these experiments. Beside this, the more valuable products including ethanol, butyrate could also be produced on further reduction. The mixed-culture reactor produced acetate at the maximum rate of 1.3 mM d<sup>-1</sup>, along with methane and hydrogen at -1.1 V<sub>Ag/AgCl</sub>. Over 160 days of run-time in four fed-batches, at the maximum, 26% of supplied bicarbonate was converted to acetate between days 28 to 41, whereas in the late batches, methane production prevailed. Out of 45 days of run-time in the *C. ljungdahlii* reactor, 2.4 mM d<sup>-1</sup> acetate production was achieved at -0.9 V<sub>Ag/AgCl</sub> in batch 1.

Chapter 3 "**Application of gas diffusion biocathode in microbial electrosynthesis from carbon dioxide**" aims to develop a biocompatible electrode capable of CO<sub>2</sub> capturing and reduction. This work featured the innovative approach to supply the gaseous CO<sub>2</sub> to the MES system, by using Gas diffusion electrode (GDE) as a CO<sub>2</sub> diffusing biocathode, for an effective microbial catalysis. The results revealed that the CO<sub>2</sub> mass transfer was doubled with GDE and was also able to utilize CO<sub>2</sub> from the diluted gas mixture (20% CO<sub>2</sub>) to produce acetate at the rate of 240 mg L<sup>-1</sup> d<sup>-1</sup> when the cathode was polarized at -1.1 V<sub>Ag/AgCl</sub>. Compared to conventional submerged technology for biocathodic CO<sub>2</sub> reduction, GDE showed better performance in MES and compatibility for converting CO<sub>2</sub> from industrial sources.

Chapter 4 “**Long-term operation of bioelectrochemical CO<sub>2</sub> reduction to multi-carbon chemicals with a mixed culture avoiding methanogenesis**” aimed to develop stable microbial CO<sub>2</sub> reduction system from mixed culture while avoiding methanogenesis. Improvements and development of a long-term operational biocathode using a mixed culture isolated from an open biological source were discussed in this chapter. This work focussed on the approach to suppress of methanogens and selective enrichment for acetogenesis to improve acetate production. Heat shock and H<sub>2</sub>:CO<sub>2</sub> enrichment was performed to establish an effective CO<sub>2</sub> reducing biocathode. High acetate titer of 7 – 10 g L<sup>-1</sup> was achieved in a sequential batch operation of MES by supplying (80:20) CO<sub>2</sub>:N<sub>2</sub> gas mixture at -0.9 to -1 V<sub>/Ag/AgCl</sub> cathode potential. The MES reactors demonstrated a robust CO<sub>2</sub> reducing biocathode, avoiding methane production, during long-term operation and attaining a high acetate production without the requirement of chemical inhibitors.

Chapter 5 “**In situ acetate separation in microbial electrosynthesis (MES) from CO<sub>2</sub> using ion-exchange resin**” sets the sights on operating an MES system with a special preference on product recovery. This study illustrates an MES reactor integrated with *in situ* anion exchange extraction system. Feasibility of using Amberlite™ FPA53 resins as anion exchanger in MES design for the extraction of acetate was discussed in this chapter. Acetate absorption of 10 – 20 mg g<sup>-1</sup> resin was achieved at the catholyte conditions and the production of acetate in MES was maintained after the extraction.

Chapter 6 “**An overview on emerging bioelectrochemical systems (BESs): Technology for sustainable electricity, waste remediation, resource recovery, chemical production and beyond**” provides an overview of the potential application of BES with new developments in MES. This chapter reviews the trend and mechanism behind the biological electrosynthesis and emphasizes on the potential applications of BES beyond electricity generation. The review also explores the recent innovations made in BESs and the future potentials of these growing ideas in the field of MES.

Finally, the main findings of this thesis are summarized and discussed in Chapter 7, “**Syntheses, discussion and perspectives**”. This chapter provides a platform to discuss and debate on the state-of-art of MES and the requirements for its developments as well as its future applications. This chapter is a compilation of findings of all chapters of this thesis work and envisions a full-scale technology for CO<sub>2</sub> reduction in MES based on the experimental findings in this thesis. Furthermore, it provides an overview of the outcomes, future applications and new perspectives of MES.

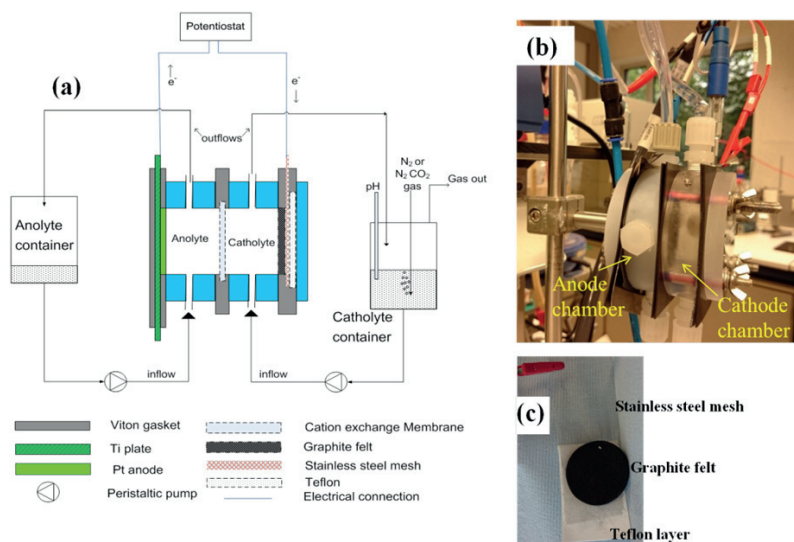




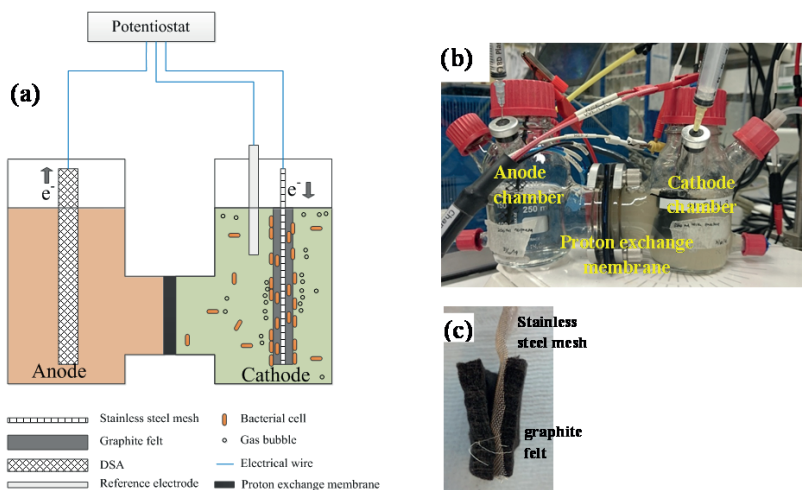
**Supplementary information**

---

## Supplementary information-Chapter 2

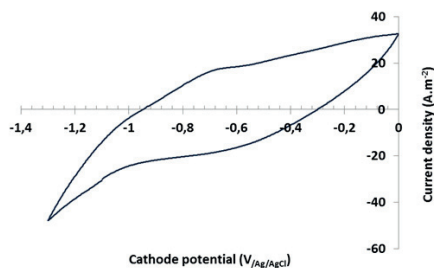


**Figure SI-1:** A circular bioelectrochemical reactor/cell setup for mixed culture MES. (a) Schematic diagram of the experimental setup. (b) Photograph of circular cell. (c) Photograph of the cathode: an assembly of graphite felt and stainless steel mesh (view from catholyte side).

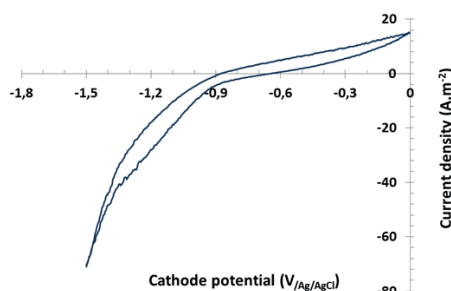


**Figure SI-2:** H-type bioelectrochemical reactor/cell for pure culture MES. (a) Schematic diagram of experimental setup and (b) an H-type reactor photograph (c) Photograph of Cathode- graphite felt and stainless steel mesh assembly.

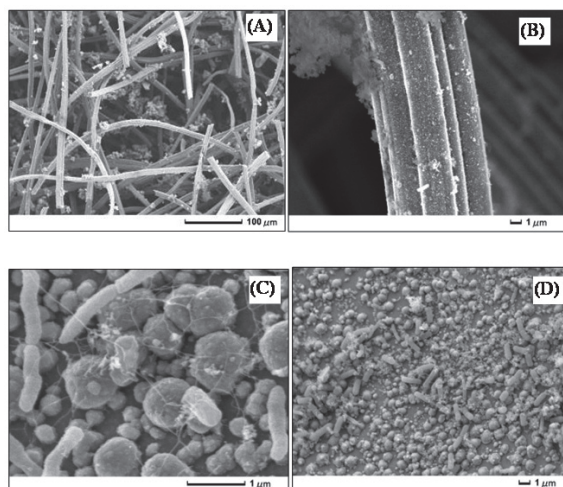




**Figure SI-3:** Cyclic Voltammogram (CV) of mixed culture reactor during the operational stage at  $-1.1 V_{/Ag/AgCl}$ . Cyclic voltammetry was carried out at  $1 mV.s^{-1}$  scan rate. Hydrogen evolution occurring at more negative potential than  $-1 V_{/Ag/AgCl}$ .

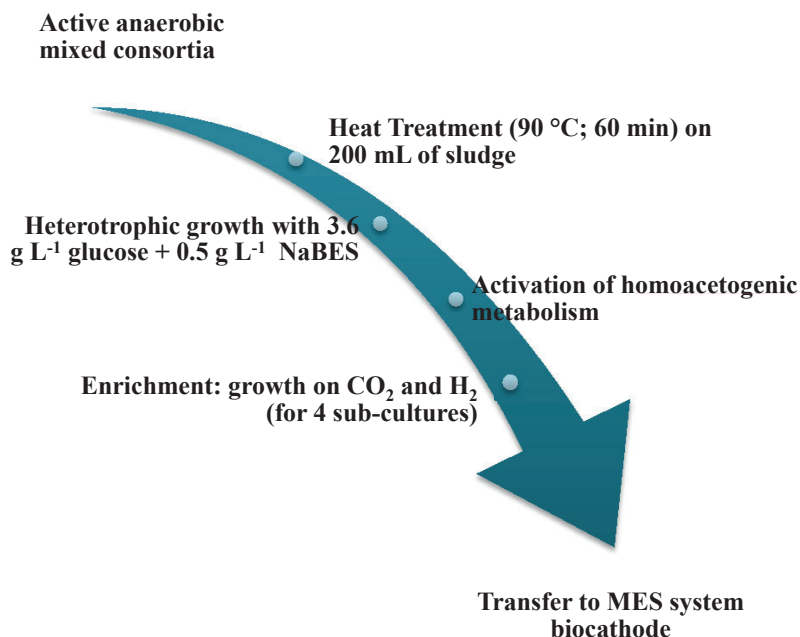


**Figure SI-4:** Cyclic Voltammogram (CV) of *C. ljungdahlii* H-type reactor during the operational stage at  $-0.9 V_{/Ag/AgCl}$ . Cyclic voltammetry was carried out at  $1 mV.s^{-1}$  scan rate. The change of slope at  $-0.9 V_{/Ag/AgCl}$  indicates the start of hydrogen evolution.

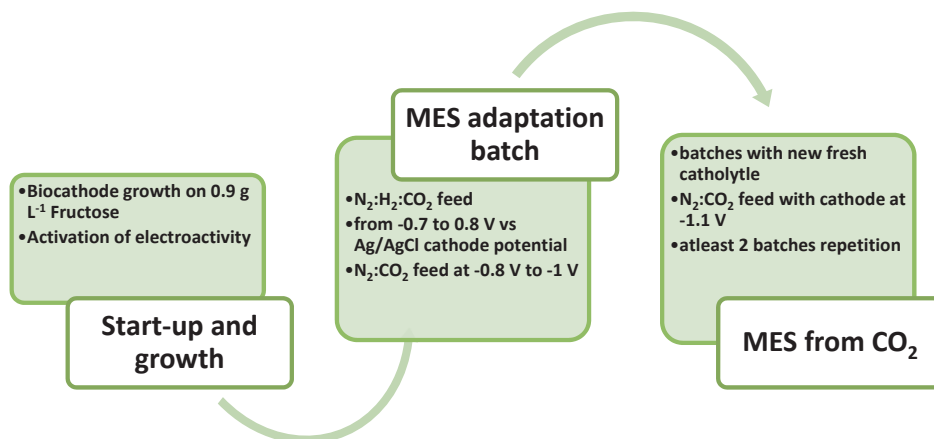


**Figure SI-5:** Scanning electron micrograph of biocathode and proton exchange membrane (PEM) from H-type cell with *C. ljungdahlii* MES taken at the final stage of Batch 3. Carbon felt from the biocathode (A & B). No bacterial attachment on the carbon felt is visible in the image. Rod-shaped bacteria attached to the PEM (C & D). Round globular shapes are the precipitations of salts on PEM.

### **Supplementary information-Chapter 3**



**Figure SI-1:** Biocatalyst development and enrichment steps followed in inoculum preparation for CO<sub>2</sub> reducing MES.

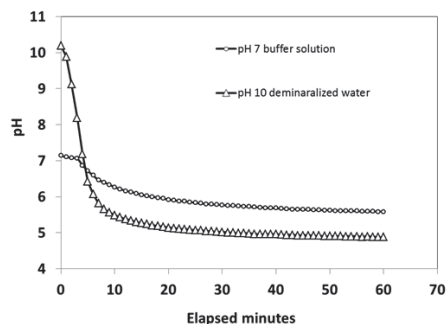


**Figure SI-2:** Scheme for the start-up and operation of MES for CO<sub>2</sub> reduction with GDE.

**Table SI-3:** Estimated mass balance of CO<sub>2</sub> in MES system based on the production rates observed in this study with GDE at various composition of N<sub>2</sub>:CO<sub>2</sub> gas mixture feed

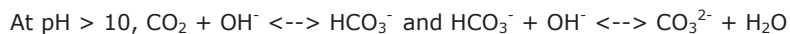
| Feed gas composition (N <sub>2</sub> :CO <sub>2</sub> ) | CO <sub>2</sub> saturation concentration C* (g CO <sub>2</sub> L <sup>-1</sup> ) | Highest mass transfer rate with GDE (g CO <sub>2</sub> L <sup>-1</sup> d <sup>-1</sup> ) <sup>§</sup> | Highest CO <sub>2</sub> assimilation rate measured with GDE (g CO <sub>2</sub> L <sup>-1</sup> d <sup>-1</sup> ) <sup>§</sup> | Remark                          | Maximum acetate production rate supported at CO <sub>2</sub> limiting condition (g acetate L <sup>-1</sup> d <sup>-1</sup> ) |
|---|--|---|---|---------------------------------|--|
| <b>90:10</b>  | 0.14   | 13.19   | 0.088 <sup>£</sup>  | CO <sub>2</sub> is not depleted | 8.98   |
| <b>80:20</b>  | 0.28   | 26.36   | 0.36  | CO <sub>2</sub> is not depleted | 17.97  |
| <b>20:80</b>  | 1.12   | 105.43  | 1.001   | CO <sub>2</sub> is not depleted | 71.88  |

<sup>§</sup>calculated as  $k_{La} \times C^*$  and  $k_{La} = 3.9 \text{ h}^{-1}$ ; <sup>§</sup>calculated from highest production rate + 5% to biomass; <sup>£</sup>production rate from [1]

**CO<sub>2</sub> flushing in aqueous solution maintained acidic pH and CO<sub>2</sub> bioavailability**

**Figure SI-4:** pH change observed during CO<sub>2</sub> flushing in buffer solution and demineralized water.

Dissolution of gases in aqueous solution is governed by Henry's law which states that the saturation concentration of a gas in aqueous solution at equilibrium only depends on the partial pressures when other gas/liquid properties and temperature are constant. The saturation concentration of CO<sub>2</sub> at 25 °C with 1 atm partial pressure is 1.4 g CO<sub>2</sub> L<sup>-1</sup>. When CO<sub>2</sub> dissolves in the aqueous solution, the pH decreases as it forms carbonic acid with water which will be neutralized if OH<sup>-</sup> is available otherwise it will increase the acidity of the solution. The dissolved CO<sub>2</sub> is converted to HCO<sub>3</sub><sup>-</sup>/CO<sub>3</sub><sup>2-</sup> according to the equilibrium condition

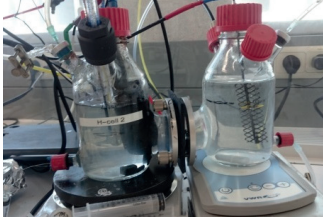



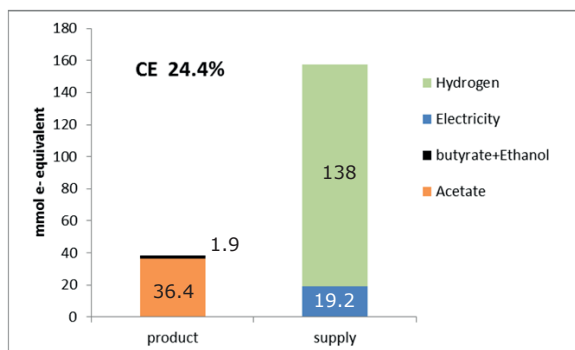
For the biological assimilation of CO<sub>2</sub>, carbonic acid and bicarbonate forms are necessary since carbonic acid can readily diffuse across the cell-membranes whereas the bicarbonate ions cross the membranes via the magnesium/calcium trans-membrane channels [2, 3]. Buffer solutions control the final equilibrium pH of the medium on CO<sub>2</sub> sparging but the amount of dissolved CO<sub>2</sub> (mainly H<sub>2</sub>CO<sub>3</sub>) at saturation remains independent of the pH. When CO<sub>2</sub> was supplied to the aqueous solution at pH > 10, CO<sub>2</sub> reacts with OH<sup>-</sup> to produce CO<sub>3</sub><sup>2-</sup> and thus, the pH decreases. Neutralization and dissolution of CO<sub>2</sub> in alkaline aqueous solution capture CO<sub>2</sub> in the form of carbonate ions rather than dissolved form. At acidic pH, the carbonate/bicarbonate species shifted to readily bioavailable carbonic acid form.

In the CO<sub>2</sub> dissolving tests, when there was no buffering capacity in the aqueous solution (demineralized water) at pH 10, a rapid fall in pH was observed as shown in Fig SI4. and after CO<sub>2</sub> saturation, the solution maintained buffering at pH 4.5-5 and the dissolved CO<sub>2</sub> measured by titration with 1 M NaOH after 1 h test was 1.17 g L<sup>-1</sup>. In the case of CO<sub>2</sub> dissolution in phosphate buffer of pH 7, the decrease in pH was not as drastic as in demineralized water. The final pH remained stabilized at 6 while CO<sub>2</sub> sparging in phosphate buffer solution of pH 7. The dissolved CO<sub>2</sub> measured after 1 h sparging was 1.24 g L<sup>-1</sup> which was fairly close to the measured dissolved CO<sub>2</sub> in demineralized water. Buffer solutions control the equilibrium pH but the concentration of dissolved CO<sub>2</sub> attained under CO<sub>2</sub> flushing was independent of the equilibrium pH. At acidic pH, attained during CO<sub>2</sub> flushing, shifted the carbonate/bicarbonate species shifted to readily bioavailable carbonic acid form.

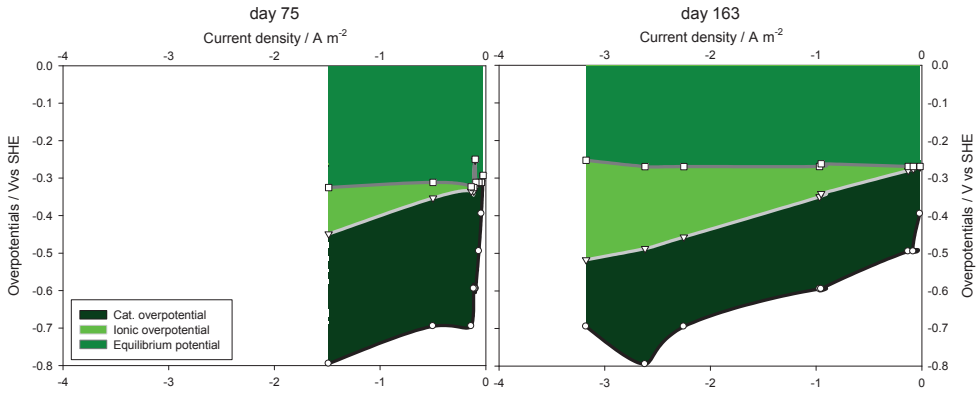
## Supplementary information-Chapter 4

**Table SI-1:** Specifications of H-type dual chamber MES reactors (named MES-1, MES-2 and MES-3 for writing convenience)

| H-type reactors<br>Photograph   | MES - 1  |                     | MES-2 and MES-3     |  |
|---|--|---------------------|---------------------|--|
|   | Cathodes   | Anode               | Anode               | Cathodes   |
|  |        |                     |                     |  |
| <b>Material</b>   | Graphite stick sandwiched between two graphite felts                                     | DSA                 | DSA                 | Graphite stick sandwiched between two graphite felts                                       |
| <b>Dimension</b>  | Graphite stick (13.8 cm x 1.5 cm x 0.5 cm) and 2 x Graphite felts (8 cm x 3 cm x 0.6 cm) | 13.8 cm x 3 cm      | 10.5 cm x 3 cm      | Graphite stick (10.5 cm x 1.5 cm x 0.5 cm) and 2 x Graphite felts (4 cm x 3.3 cm x 0.6 cm) |
| <b>working area of graphite (cm<sup>2</sup>)</b>                                  | 67.2   | -                   | -                   | 36   |
| <b>Total Volume (mL)</b>  | Catholyte volume= 400  | Anolyte volume= 400 | Anolyte volume= 200 | Catholyte volume= 200  |



**Figure SI-2:** Distribution of electron equivalents for day 79 to 85 operation of MES. The cathode was polarized between  $-1$  V and  $-0.4$  V<sub>Ag/AgCl</sub> and N<sub>2</sub>:H<sub>2</sub>:CO<sub>2</sub> (80:7:13) gas mixture was supplied. The number of mole e<sup>-</sup> equivalents from H<sub>2</sub> gas bubbling = moles H<sub>2</sub> supplied x 2.



**Figure SI-3:** Overpotentials involved in  $\text{CO}_2$  reduction at the cathode with and without  $\text{CO}_2$  spargings. Current density increased. At the current density of  $-1.5 \text{ A m}^{-2}$ , the cathode overpotential was calculated to be  $-0.8 \text{ V}$  on day 75 whereas on day 163, it was  $-0.6 \text{ V}$  only, due to the bubbling of 80%  $\text{CO}_2$  gas mixture. Current densities at  $-1 \text{ V}_{\text{Ag/AgCl}}$  cathode potential in the early stage were much lower than the last batch.

### Calculations

#### Equilibrium potential at reactors condition

$$E_{cat,eq} = E_{cat}^0 - \frac{RT}{8F} \ln \frac{[\text{CH}_3\text{COO}^-]}{[\text{H}_2\text{CO}_3]^2 [\text{H}^+]^7}$$

$E_{cat,eq}^0$  is equilibrium cathode potential at reactor condition (V),  $E_{cat}^0$  is the standard reduction potential (V), R is the universal gas constant ( $8.3145 \text{ J mol}^{-1} \text{ K}^{-1}$ ), T is the temperature (303 K) and F is the Faraday's constant ( $96485 \text{ C mol}^{-1}$ ).

On day 75, for 20 %  $\text{CO}_2$  bubbling,  $[\text{H}_2\text{CO}_3] = 50 \text{ mg L}^{-1} = 0.0008 \text{ M}$

On day 163, 80%  $\text{CO}_2$  bubbling,  $[\text{H}_2\text{CO}_3] = 600 \text{ mg L}^{-1} = 0.0097 \text{ M}$

#### Cathode overpotential

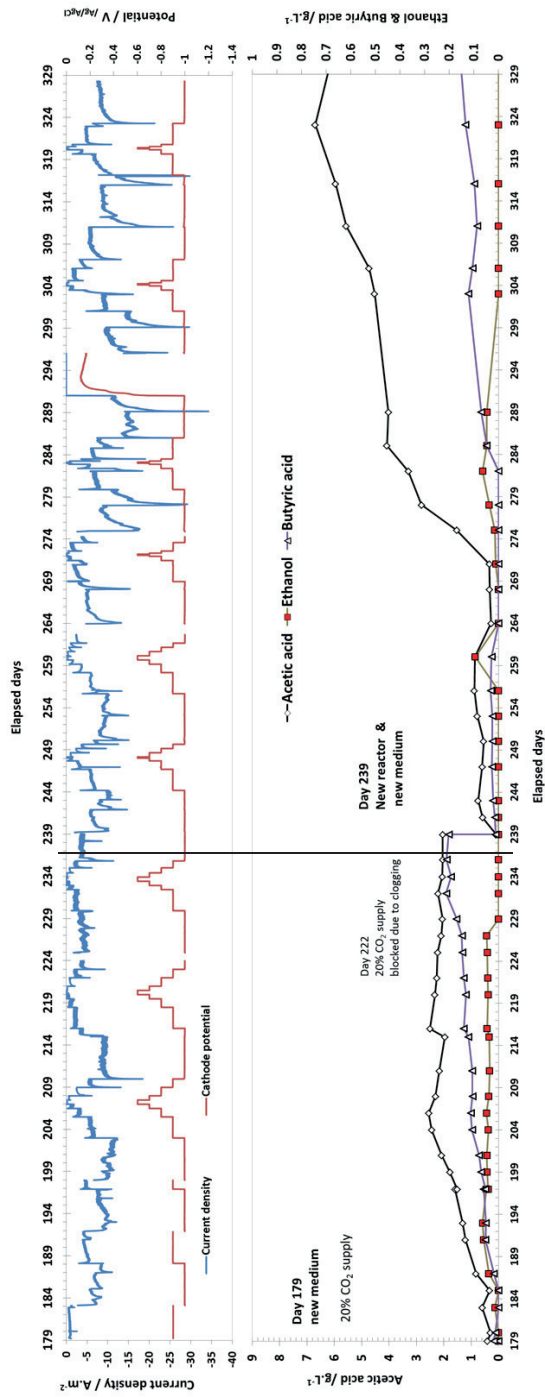
$$E_{cat,overpotential} = E_{measured} - E_{cat,eq}$$

#### Ionic overpotential

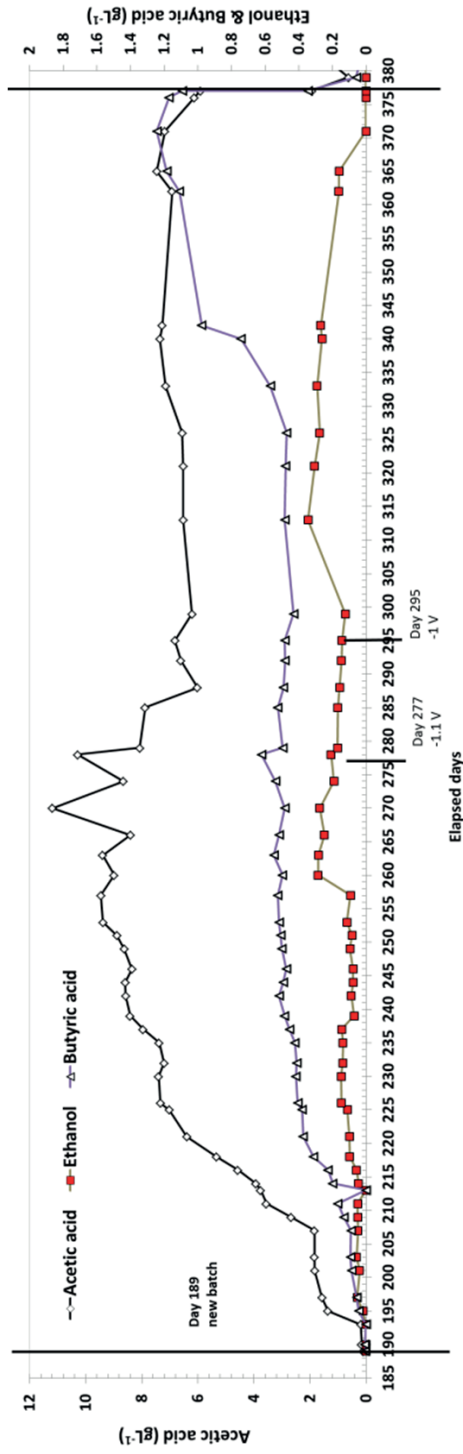
The ionic overpotential for cathode is calculated by using the following equation as referred in Sleutel [4].

$$E_{ionic} = j_{ions} \left( \frac{d_{cat/mem}}{2\sigma_{cat}} \right)$$

where  $j_{ions}$  is the ion current density along the electrolyte which is equal to the current density (A),  $d_{cat/mem}$  is the distance between the cathode and the membrane (m),  $\sigma_{cat}$  is the cathode conductivity ( $\text{S m}^{-1}$ ).



**Figure SI-4:** Products of bioelectrochemical CO<sub>2</sub> reduction in MES-2. A shift to acetate production in 2nd batch in relation to the rise in current density.



**Figure SI-5:** Products of bioelectrochemical CO<sub>2</sub> reduction in MES-3. Production of acetate reached ~10 g L<sup>-1</sup> in between day 207 to 280. Between day 342 to 375, butyrate concentration remained > 1 g L<sup>-1</sup>.

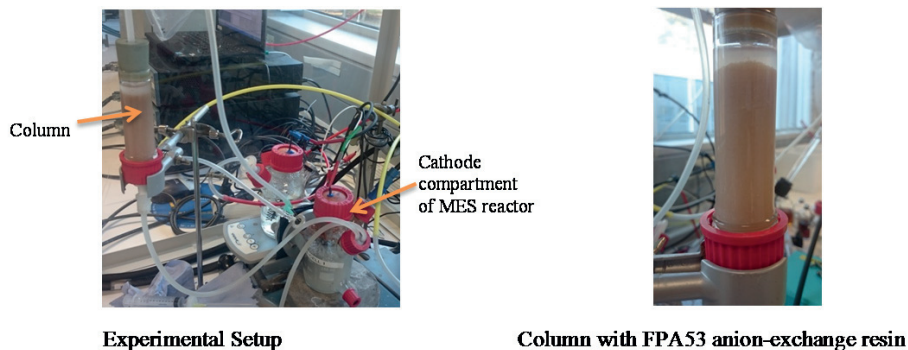


**Table SI-6:** Headspace gas composition of MES-1 during the operation

| Day | Phase in MES-1 operation | Headspace composition |                |                |                 |   | Remarks   |
|-----|--------------------------|-----------------------|----------------|----------------|-----------------|---|---|
|     |                          | CO <sub>2</sub>       | O <sub>2</sub> | N <sub>2</sub> | CH <sub>4</sub> | H <sub>2</sub>                              |   |
| 62  | Acclimation phase        | 11%                   | 1%             | 80%            | 'nd'            | 6%  |   |
| 98  | Batch 1                  | 8%                    | 1%             | 87%            | 'nd'            | 3%  |   |
| 115 |                          | 18%                   | 1%             | 78%            | 'nd'            | 'nd'  |   |
| 178 |                          | 1%                    | 1%             | 41%            | 'nd'            | 59%   |   |
| 227 | Batch 2                  | 73%                   | 1%             | 25%            | 'nd'            | 1%  | Sampled just after gas 80% CO <sub>2</sub> bubbling |
| 229 |                          | 12%                   | 2%             | 80%            | 'nd'            | 'nd'  | 2 days after gas bubbling                           |
| 253 | Batch 3                  | 10%                   | 1%             | 85%            | 'nd'            | 'nd'  | 2 days after gas bubbling                           |
| 260 |                          | 80%                   | 'nd'           | 20%            | 'nd'            | 'nd'  | just after gas 80% CO <sub>2</sub> bubbling         |
| 262 |                          | 1%                    | 1%             | 26%            | 'nd'            | 72%   | 2 days after gas bubbling                           |
| 274 |                          | 1%                    | 'nd'           | 25%            | 'nd'            | 73%   | no CO <sub>2</sub> bubbled for some days            |
| 274 |                          | 80%                   | 'nd'           | 20%            | 'nd'            | 'nd'  | just after gas 80% CO <sub>2</sub> bubbling         |
| 276 |                          | 7%                    | 'nd'           | 16%            | 'nd'            | 76%   | 2 days after gas bubbling                           |
| 276 |                          | 72%                   | 'nd'           | 22%            | 'nd'            | 4%  | just after gas 80% CO <sub>2</sub> bubbling         |
| 279 |                          | 13%                   | 1%             | 74%            | 'nd'            | 'nd'  | not polarized, 3 days after gas bubbling            |
| 279 |                          | 75%                   | 'nd'           | 22%            | 'nd'            | 'nd'  | just after gas 80% CO <sub>2</sub> bubbling         |
| 280 |                          | 20%                   | 'nd'           | 80%            | 'nd'            | 'nd'  | just after 20% CO <sub>2</sub> bubbling             |
| 282 |                          | 1%                    | 1%             | 40%            | 'nd'            | 52%   | 2 days after 20% CO <sub>2</sub> gas bubbling       |
| 282 |                          | 74%                   | 'nd'           | 22%            | 'nd'            | 2%  | just after gas 80% CO <sub>2</sub> bubbling         |
| 286 |                          | 2%                    | 'nd'           | 96%            | 'nd'            | 'nd'  | 4 days after gas bubbling                           |
| 286 |                          | 78%                   | 'nd'           | 24%            | 'nd'            | 'nd'  | just after gas 80% CO <sub>2</sub> bubbling         |
| 290 |                          | 'nd'                  | 'nd'           | 21%            | 'nd'            | 82%   | 4 days after gas bubbling                           |
| 290 | 74%                      | 'nd'                  | 24%            | 'nd'           | 4%              | just after gas 80% CO <sub>2</sub> bubbling |   |
| 294 | 'nd'                     | 'nd'                  | 28%            | 'nd'           | 67%             | 4 days after gas bubbling                   |   |
| 294 | 80%                      | 'nd'                  | 20%            | 'nd'           | 4%              | just after gas 80% CO <sub>2</sub> bubbling |   |
| 295 | 2%                       | 'nd'                  | 3%             | 'nd'           | 96%             | 1 day after gas bubbling                    |   |
| 295 | 69%                      | 'nd'                  | 27%            | 'nd'           | 5%              | during 80% CO <sub>2</sub> bubbling at -1V  |   |
| 296 | 12%                      | 4%                    | 23%            | 'nd'           | 65%             | 1 day after gas bubbling                    |   |
| 298 | 0%                       | 1%                    | 4%             | 'nd'           | 96%             | 2 days after gas bubbling                   |   |
| 298 | 80%                      | 'nd'                  | 20%            | 'nd'           | 4%              | just after gas 80% CO <sub>2</sub> bubbling |   |
| 301 | 25%                      | 1%                    | 21%            | 'nd'           | 54%             | 3 days after gas bubbling                   |   |
| 301 | 80%                      | 'nd'                  | 20%            | 'nd'           | 0%              | just after gas 80% CO <sub>2</sub> bubbling |   |
| 304 | 0%                       | 1%                    | 2%             | 'nd'           | 98%             | 4 days after gas bubbling                   |   |
| 304 | 78%                      | 'nd'                  | 21%            | 'nd'           | 3%              | just after gas 80% CO <sub>2</sub> bubbling |   |
| 308 | 0%                       | 1%                    | 5%             | 'nd'           | 95%             | 4 days after gas bubbling                   |   |
| 308 | 62%                      | 'nd'                  | 16%            | 'nd'           | 25%             | just after gas 80% CO <sub>2</sub> bubbling |   |

'nd': not detected (detection limit 0.01%)

## **Supplementary information-Chapter 5**



**Figure SI-1:** Photographs of MES reactor with *in situ* acetate separation using anion-exchange resins in a column.

### **References**

1. Patil SA, Arends JBA, Vanwonterghem I, et al (2015) Selective Enrichment Establishes a Stable Performing Community for Microbial Electrosynthesis of Acetate from CO<sub>2</sub>. *Environ Sci Technol* 150701101446004. doi: 10.1021/es506149d
2. Gutknecht J, Bisson MA, Tosteson FC (1977) Diffusion of carbon dioxide through lipid bilayer membranes. Effects of carbonic anhydrase, bicarbonate, and unstirred layers. *J Gen Physiol* 69:779–794.
3. Missner A, Kugler P, Saparov SM, et al (2008) Carbon dioxide transport through membranes. *J Biol Chem* 283:25340–25347. doi: 10.1074/jbc.M800096200
4. Sleutels THJA (2010) Microbial Electrolysis, Kinetics and cell design. PhD dissertation, Wageningen University]. Wageningen University

---

## ***Acknowledgements***

At this moment, my PhD journey is almost at the end. Yesss!!! It's a great feeling of accomplishment. This PhD has been truly a life-changing experience for me, yet a long journey full of constant challenges. I do feel fortunate to find guidance and help of several individuals who in one way or another drove me on my way to the successful completion of this study. First and foremost, I would like to express my sincere appreciation and thanks to my promotor and co-promotors. First of all, Cees, thank you very much for your inspiration and valuable time to observe and guide me during the entire period of this research work.

I would like to express my sincere gratitude to Deepak for your whole-hearted support. I am grateful to you for having faith in me to carry out this challenging research. Thank you for all your efforts, contributions and inspirations to make my Ph.D. experience productive. The enthusiasm you have for science and research has always been motivational for me. I am thankful to you and Yamini for providing an amicable and homely environment during my stay in Belgium. I sincerely like to express my profound appreciation to David for your cooperation, encouragement and valuable suggestions throughout the PhD journey. Thank you very much for supporting and guiding me to progress and finalize this PhD research successfully and to prepare this dissertation as accurate and as useful as possible. I thank you for being such a friendly and caring mentor.

I am particularly grateful to Xochitl (VITO) and Annemiek (WUR), who supervised me for the first two years of my PhD. Xoch, thank you very much for your guidance and contributions for providing the knowledge-base for this PhD research. I am grateful to you for making me able to understand the fundamentals of electrochemical techniques. Thank you Annemiek, for helping me out in different phases, from the PhD proposal writing to the guidance for conducting the experiments.

I would like to thank all the leaders and staffs of Separation and Conversion unit, VITO for the supportive contributions. Special thanks go to the project manager, Karolien for providing me this opportunity in VITO as a PhD researcher. I learnt a lot from our discussions. I appreciate your constructive suggestions and direction to systematize and consolidate the research outputs. My deep appreciation goes to the researchers in VITO Heleen, Linsey, Yolanda and Wouter for the fruitful discussions and suggestions.

I would like to express my appreciation to Mohan Krishna, Srikanth and Ahmed for your help in laboratory, constructive discussions and manuscripts. Very special thanks go to the Bachelor and Master thesis/intern students: Kjell,

---

Rustiana, Shishir, Bart and Tim. I am very grateful to Nabin for being always helpful and providing me assistance during various phases of my PhD. I also thank Sunita, Dennis, Doğa, Suraj, Mohita, Suresh, Kuda, Elena and Jai for being supportive. Jai, once again thank you for designing the thesis cover.

This work would not have been possible without the technical support from Christof, Diane, Helmut, Hans, Jef and Rob in my experimental setups. I am particularly indebted to the analytical team of unit SCT, especially Miranda and Carine for providing all the analytical supports. I would like to extend my acknowledgements to Silvia, Queenie, Lieve, Guy, Nicole and Nadine for the technical assistance. I would like to acknowledge the support of Katrien and Sofie, Maurits from VITO for making all necessary arrangements throughout the PhD project.

This PhD study would not have been possible without the corporation and support extended by staffs and members of sub-department of Environmental technology (ETE), Wageningen, the Netherlands. I am also grateful to Monika from Laboratory of microbiology, Wageningen University for demonstrating and teaching me the anaerobic culture techniques.

I would like to thank all of my ETE colleagues for the discussions in bioenergy and fermentation group meetings. Exclusive thanks to Momo, Sam, Sanne, and Dandan for providing the constructive ideas and also for the great company. Special appreciations go to my paranymphs Koen and Indra for supporting me in my defense. I thank Liesbeth from Wageningen for providing administrative support.

I am grateful to all my Nepalese friends in wageningen, especially, Ekaraj, Arun, Puja and Udit for providing me unfailing personal and professional support throughout my Ph.D. experiences. I would also like to thank Andrea, Eurico, Ehiaze, Daniel, Bruno, Naira, Pamela, Veronica, Tomas, Ran, Xavi, Enrique, Salatul, Elias, Poonam, Richa and all others for the wonderful company during my stay in Boeretang 278. Special thanks go to Sailesh and Manila for supporting me, especially during my Denmark trips. And of course, Trishna, thank you very much for being there for me all the time. I highly admire your help and support in the entire PhD .

Last but not the least, I would like to express my deepest thanks to my family who encouraged me in all my pursuits.

Thank you.

Suman Bajracharya

---

## ***Publications***

### **In peer –reviewed journals**

- Sharma, M., S. Bajracharya, S. Gildemyn, S. A. Patil, Y. Alvarez-Gallego, D. Pant, K. Rabaey and X. Dominguez-Benetton (2014). "A critical revisit of the key parameters used to describe microbial electrochemical systems." *Electrochimica Acta* 140: 191-208.
- Bajracharya, S., A. ter Heijne, X. D. Benetton, K. Vanbroekhoven, C. J. Buisman, D. P. Strik and D. Pant (2015). "Carbon dioxide reduction by mixed and pure cultures in microbial electrosynthesis using an assembly of graphite felt and stainless steel as a cathode." *Bioresource technology* 195: 14-24.
- ElMekawy, A., S. Srikanth, S. Bajracharya, H. M. Hegab, P. S. Nigam, A. Singh, S. V. Mohan and D. Pant (2015). "Food and agricultural wastes as substrates for the bioelectrochemical system (BES): the synchronized recovery of sustainable energy and waste treatment." *Food Research International* 73: 213-225.
- Bajracharya, S., M. Sharma, G. Mohanakrishna, X. Dominguez Benetton, D. P. B. T. B. Strik, P. M. Sarma and D. Pant (2016). "An overview on emerging bioelectrochemical systems (BESs): Technology for sustainable electricity, waste remediation, resource recovery, chemical production and beyond." *Renewable Energy* 98: 153-170.
- Bajracharya, S., K. Vanbroekhoven, C. J. Buisman, D. Pant and D. P. Strik (2016). "Application of gas diffusion biocathode in microbial electrosynthesis from carbon dioxide." *Environmental Science and Pollution Research*: 1-17.
- Bajracharya, S., R. Yuliasni, K. Vanbroekhoven, C. J. Buisman, D. P. Strik and D. Pant (2016). "Long-term operation of microbial electrosynthesis cell reducing CO<sub>2</sub> to multi-carbon chemicals with a mixed culture avoiding methanogenesis." *Bioelectrochemistry* Accepted.
- Vermaas, D.A., Bajracharya, S., Sales, B.B., Saakes, M., Hamelers, B. and Nijmeijer, K., (2013). "Clean energy generation using capacitive

---

electrodes in reverse electrodialysis." *Energy & environmental science*, 6(2), pp.643-651.

### **Contributions to book chapters**

- Bajracharya, S., S. Srikanth, et al. (2015). Cathodes for microbial fuel cells. *Microbial Electrochemical and Fuel Cells. Fundamentals and Applications*. K. Scott and E. Hao Yu, Woodhead Publishing: 179-214.

---

## ***About the author***

Suman Bajracharya was born on January 5th, 1980, in Bhaktapur, Nepal. He completed his bachelor degree in environmental science in 2003 from Tri-Chandra campus, Kathmandu and pursue master degree studies in the same field. He obtained M. Sc. from Tribhuvan University, Kathmandu in 2005. After the university education, he started his research career first as a research intern and then as a research associate in 'Biomass Energy and biobriquetting Technologies' at Nepal Academy of Science and Technology, Kathmandu, Nepal. In 2009, Suman was



selected to study masters courses in Wageningen University under Netherlands fellowship program and obtained his second MSc degree in Environmental Science. During his master study in Wageningen University, he carried out his thesis on "Capacitive reverse-electrodialysis" and research internship on "Microbial Electrolysis" within Sub-department of Environmental Technology (ETE), Wageningen. The MSc thesis and the internship works were carried out at Wetsus in Leeuwarden. In 2012, he started PhD research at VITO, Flemish institute for technological research under the promotorship of Prof. Dr Cees Buisman, ETE-department of Wageningen University, which is presented in this thesis.



*Netherlands Research School for the  
Socio-Economic and Natural Sciences of the Environment*

# D I P L O M A

*For specialised PhD training*

The Netherlands Research School for the  
Socio-Economic and Natural Sciences of the Environment  
(SENSE) declares that

***Suman Bajracharya***

born on 5 January 1980 in Bhaktapur, Nepal

has successfully fulfilled all requirements of the  
Educational Programme of SENSE.

Wageningen, 23 September 2016

the Chairman of the SENSE board

Prof. dr. Huub Rijnaarts

the SENSE Director of Education

Dr. Ad van Dommelen

*The SENSE Research School has been accredited by the Royal Netherlands Academy of Arts and Sciences (KNAW)*



K O N I N K L I J K E N E D E R L A N D S E  
A K A D E M I E V A N W E T E N S C H A P P E N





The SENSE Research School declares that **Mr Suman Bajracharya** has successfully fulfilled all requirements of the Educational PhD Programme of SENSE with a work load of 35.5 EC, including the following activities:

#### SENSE PhD Courses

- o Environmental research in context (2012)
- o SENSE summer academy 'Emerging issues in sustainable energy and water systems' (2013)
- o Research in context activity: 'Co-organising a symposium in the 67<sup>th</sup> Annual Meeting of International Society of Electrochemistry Conference', The Hague, The Netherlands (2016)

#### Other PhD and Advanced MSc Courses

- o Summer course Measuring, monitoring, modelling and control (M3C) in biochemical engineering, Technical University of Denmark (2013)
- o Academic writing, University of Antwerp (2014)
- o Summer school Electrochemistry and bioelectrochemistry: fundamentals and applications, University of Antwerp (2014)

#### External training at a foreign research institute

- o Electrochemical Impedance Spectroscopy (EIS) workshop, Flemish Institute for Technological Research (2012)
- o COMSOL Multiphysics, COMSOL BV and Flemish Institute for Technological Research (2013)
- o Workshop on Electrochemical analytical techniques: Electrochemical Impedance Spectroscopy (EIS) and Cyclic Voltammetry (CV), Flemish Institute for Technological Research (2014)
- o Workshop on Microbial electrochemistry, 1<sup>st</sup> and 2<sup>nd</sup> European Meeting, and 5<sup>th</sup> International Meeting of International Society for Microbial Electrochemistry and Technology (2012, 2014-2015)

#### Management and Didactic Skills Training

- o Assisting in the workshop 'Electrochemical Impedance Spectroscopy' (EIS) (2012)
- o Lecturing in MSc course 'BioElectrochemical System (BES)-Basic principles & Applications', University of Antwerp (2013)
- o Teaching in MSc course 'Renewable energy: Source, Technology & Applications', Wageningen University (2013-2015)
- o Supervising two MSc students and one MSc Internship student, Wageningen University (2015-2016)

#### Oral Presentations

- o *Application of Gas Diffusion Cathodes for CO<sub>2</sub> Reduction in Microbial Electrosynthesis*. XXIII International Symposium on Bioelectrochemistry and Bioenergetics, 14-18 June 2015, Malmo, Sweden
- o *Application of Gas Diffusion and Flow-through Cathodes for CO<sub>2</sub> Reduction in Microbial Electrosynthesis*. 5<sup>th</sup> International meeting of the International Society for Microbial Electrochemistry and Technology (ISMET 2015), 1-4 October 2015, Arizona, USA.

SENSE Coordinator PhD Education

Dr. ing. Monique Gulickx

This PhD project was supported by VITO's strategic research funds.

Cover design by Jai Shankar Seelam



